

THE PALEOMAGNETIC INVESTIGATION
OF EARLY PALEOZOIC ROCKS IN
WESTERN NEWFOUNDLAND

CENTRE FOR NEWFOUNDLAND STUDIES

**TOTAL OF 10 PAGES ONLY
MAY BE XEROXED**

(Without Author's Permission)

JAGAT NANDAN PRASAD



National Library
of Canada

Bibliothèque nationale
du Canada

Canadian Theses Service

Services des thèses canadiennes

Ottawa, Canada
K1A 0N4

CANADIAN THESES

THÈSES CANADIENNES

NOTICE

The quality of this microfiche is heavily dependent upon the quality of the original thesis submitted for microfilming. Every effort has been made to ensure the highest quality of reproduction possible.

If pages are missing, contact the university which granted the degree.

Some pages may have indistinct print especially if the original pages were typed with a poor typewriter ribbon or if the university sent us an inferior photocopy.

Previously copyrighted materials (journal articles, published tests, etc.) are not filmed.

Reproduction in full or in part of this film is governed by the Canadian Copyright Act, R.S.C. 1970, c. C-30.

**THIS DISSERTATION
HAS BEEN MICROFILMED
EXACTLY AS RECEIVED**

AVIS

La qualité de cette microfiche dépend grandement de la qualité de la thèse soumise au microfilmage. Nous avons tout fait pour assurer une qualité supérieure de reproduction.

S'il manque des pages, veuillez communiquer avec l'université qui a conféré le grade.

La qualité d'impression de certaines pages peut laisser à désirer, surtout si les pages originales ont été dactylographiées à l'aide d'un ruban usé ou si l'université nous a fait parvenir une photocopie de qualité inférieure.

Les documents qui font déjà l'objet d'un droit d'auteur (articles de revue, examens publiés, etc.) ne sont pas microfilmés.

La reproduction, même partielle, de ce microfilm est soumise à la Loi canadienne sur le droit d'auteur, SRC 1970, c. C-30.

**LA THÈSE A ÉTÉ
MICROFILMÉE TELLE QUE
NOUS L'AVONS REÇUE**

A PALEOMAGNETIC INVESTIGATION OF EARLY PALEOZOIC
ROCKS IN WESTERN NEWFOUNDLAND

BY

Jagat Nandan Prasad, M.Sc.

A thesis submitted to the School of Graduate
Studies in partial fulfillment of the
requirements for the degree of
Doctor of Philosophy

Department of Earth Sciences (Geophysics)
Memorial University of Newfoundland

April 1986

St. John's

Newfoundland

Permission has been granted to the National Library of Canada to microfilm this thesis and to lend or sell copies of the film.

The author (copyright owner) has reserved other publication rights, and neither the thesis nor extensive extracts from it may be printed or otherwise reproduced without his/her written permission.

L'autorisation a été accordée à la Bibliothèque nationale du Canada de microfilmer cette thèse et de prêter ou de vendre des exemplaires du film.

L'auteur (titulaire du droit d'auteur) se réserve les autres droits de publication; ni la thèse ni de longs extraits de celle-ci ne doivent être imprimés ou autrement reproduits sans son autorisation écrite.

ISBN 0-315-31031-6

IN THE MEMORY OF MY FATHER.

ABSTRACT

The results of paleomagnetic studies on carbonate rocks of Cambrian and Ordovician age from the Western Platform of Newfoundland are presented. The study includes tectonically transported Middle Ordovician strata. All the rocks studied are weakly magnetic and so all remanence measurements were made with a cryogenic magnetometer.

Two characteristic components, "A" and "B", both of reverse polarity, were isolated by thermal demagnetization from each of the Port au Port Group (mid-to Upper Cambrian) and St. George Group (Lower Ordovician) on the Port au Port Peninsula. It was concluded that the "A" component represents a primary or early diagenetic magnetization, corresponding to a Cambrian pole at 3.4°N , 145.6°E and a Lower Ordovician pole at 17.5°N , 152.3°E . The respective "B" component poles seem to be Late Paleozoic (Kiaman) overprints. Magnetic mineralogy studies show that the "A" component is carried by magnetite and the "B" component by diagenetic hematite.

In the Port au Choix area, the St. George Group did not show evidence of Late Paleozoic overprinting, but yielded a characteristic direction 40° misaligned in declination with the age-equivalent rocks on the Port au Port Peninsula. The remanence, which resides in magnetite, corresponds to a pole at 20.5°N , 113.3°E and may be a thermoviscous remagnetization related to the Acadian orogeny.

A single characteristic component with pole at 15.9 N, 153.6°E was isolated from the Middle Ordovician Table Head Group on the Port au Port Peninsula. This component predates the probable Acadian deformation. A polarity change between the uppermost Table Head and the lowermost Long Point Group was identified, though the Long Point rocks mostly yielded unstable magnetizations.

A magnetization predating the Acadian(?) folding was isolated from the Middle Ordovician strata of the allochthonous Cow Head Group. The corresponding pole position falls close to the poles from the platformal Ordovician rocks, suggesting that these rocks were not transported far.

The hypothesis of a rotation of western Newfoundland relative to mainland North America is not supported. However, a relative rotation between the Port au Port area and part of the Great Northern Peninsula (north of Cow Head) is possible.

Key Words: Paleomagnetism - Lower Paleozoic - carbonates - western Newfoundland - primary remanence - Kiaman overprints.

ACKNOWLEDGEMENTS

I am grateful to my supervisor, Dr. E. R. Deutsch, for suggesting the topic, for his keen interest and constant guidance in carrying out this research.

Among faculty members in the Department of Earth Sciences, I like to thank Dr. G.S. Murthy and Dr. R.K. Stevens for many fruitful and long sessions of stimulating discussion that led to improvement of the thesis. I also appreciate greatly the help received from Dr. C. R. Barnes, Dr. T. J. Calon, Dr. J. P. Hodych, Dr. R. S. Hyde, and Dr. H. G. Miller, with various aspects of this study.

Many valuable discussions with Dr. K. M. Storetvedt, Visiting Professor from University of Bergen, Norway, while this work was in progress, are gratefully acknowledged.

Thanks are also due to Dr. N. Chow and Dr. M. Coniglio, former graduate students in Earth Sciences, for helpful discussions.

I am indebted to Dr. I. Knight of Mines and Energy, Newfoundland, for his assistance with the geology and the field collection in the Port au Choix area.

It is a pleasure to acknowledge the invaluable help extended by the personnel of the Geomagnetic Research Laboratory of the Department of Earth Sciences; Mr. Ray Patzold and Mr. Mike Tubrett for their assistance in the field and in the laboratory, and Miss Libby Moore for making available her computational expertise. I owe special thanks

to them for their active co-operation at various stages of this work.

Drafting by Mr. Larry Nowlan and Mr. Roger Guest, and photographic work by Mr. Wilf Marsh and Mr. Robert Bradley are thankfully acknowledged.

I also thank Miss Jeannie Hiscock, who typed this thesis.

Throughout my tenure as a graduate student, I held a University Fellowship for which I am thankful to Memorial University of Newfoundland and the Dean of Graduate Studies, Dr. F.A. Aldrich. Additional financial support was received in the form of teaching assistantships from the Physics Department; and research assistantships and a bursary from the Department of Earth Sciences, through operating grants from the Natural Sciences and Engineering Research Council of Canada (NSERC) to Drs. Deutsch and Murthy. All this assistance is gratefully acknowledged.

I also express my appreciation to Ranchi University for granting me leave of absence for my studies abroad.

Finally, I am indebted to my wife, Reena, who has been a constant source of strength and encouragement to me. I also thank my mother and other family members for their understanding and encouragement.

TABLE OF CONTENTS

	Page
Abstract	iii
Acknowledgements	v
Table of Contents	vii
List of Tables	xi
List of Figures	xiv

CHAPTER

1. INTRODUCTION	1
2. REGIONAL GEOLOGY AND SAMPLING	9
3. PORT AU PORT GROUP ,	20
3.1 Geological setting	20
3.2 Paleomagnetic sampling and results	20
3.2.1 Port au Port area	21
3.2.2 Port au Choix area	41
3.3 Magnetic mineralogy	49
3.4 Discussion	53
4. CAMBRIAN PALEOPOLES WITH RESPECT TO CRATONIC NORTH AMERICA	56
5. ST. GEORGE GROUP	72
5.1 Geological setting	72
5.2 Paleomagnetic sampling and results	74
5.2.1 Port au Port area	74
5.2.2 Magnetic mineralogy (Port au Port rocks)	97

CHAPTER	Page
5.2.3 Port au Choix area	103
5.2.4 Magnetic mineralogy (Port au Choix rocks)	123
5.3 Discussion	123
6. TABLE HEAD GROUP	129
6.1 Geological setting	129
6.2 Paleomagnetic sampling and results .	130
6.2.1 Port au Port area	131
6.2.2 Port au Choix area	152
6.3 Magnetic mineralogy	161
6.4 Discussion	162
7. LONG POINT GROUP	164
7.1 Geological setting	164
7.2 Paleomagnetic sampling and results .	164
7.3 Discussion	170
8. COW HEAD GROUP	173
8.1 Geological setting	173
8.2 Paleomagnetic sampling and results .	179
8.3 Fold test	187
8.4 Conglomerate test	188
8.5 Magnetic mineralogy	194
8.6 Discussion	196
9. ORDOVICIAN PALEOPOLES OF NORTH AMERICA AND ROTATION OF NEWFOUNDLAND	199
9.1 Ordovician paleopoles	199
9.2 Rotation of Newfoundland	211

CHAPTER	Page
10. SUMMARY AND CONCLUSIONS	214
REFERENCES	221
 APPENDIX	
A. TECHNIQUES	236
A.1 Sample preparation	236
A.2 Remanence measurement	236
A.3 Alternating field demagnetization	238
A.4 Thermal demagnetization	239
A.5 Statistical analysis	240
B. SAMPLING LOCALITIES AND DIRECTIONS OF MAGNETIZATION - PORT AU PORT GROUP	243
B.1 Sampling localities	243
B.2 Detailed directions of magnetizations.	245
C. SAMPLING LOCALITIES AND DIRECTIONS OF MAGNETIZATION - ST. GEORGE GROUP	265
C.1 Sampling localities	265
C.2 Detailed directions of magnetization	267
D. SAMPLING LOCALITIES AND DIRECTIONS OF MAGNETIZATION - TABLE HEAD GROUP	295
D.1 Sampling localities	295
D.2 Detailed directions of magnetization	297
E. SAMPLING LOCALITY AND DIRECTIONS OF MAGNETIZATION - LONG POINT GROUP	317

CHAPTER	Page
E.1 Sampling locality	317
E.2 Detailed direction of magnetization.	317
F. STRUCTURAL CORRECTIONS AND DIRECTIONS OF MAGNETIZATION - COW HEAD GROUP	321
F.1 Sampling locality	321
F.2 Correction for plunging folds	321
F.3 Detailed directions of magnetization	323

LIST OF TABLES

TABLE	Page
3.1 Thermal demagnetization results from the Port au Port Group for the "A" component, Port au Port area	33
3.2 Thermal demagnetization results from the Port au Port Group for the "B" component, Port au Port area	37
3.3 Mean paleomagnetic data for the "A" and "B" components after thermal demagnetization of the Port au Port Group	38
3.4 Anomalous directions from the Port au Port Group after thermal demagnetization, Port au Port area	48
3.5 Thermal demagnetization results from the Port au Port Group, Port au Choix area . .	48
4.1 Selected paleomagnetic poles from Late Precambrian to Cambrian rocks of North America	58
4.2 Some Late Paleozoic poles of North America .	63
5.1 Thermal demagnetization results from the St. George Group for the "A" component, Port au Port area	84
5.2 Site-level characteristic directions from the St. George Group, "A" component, Port au Port area	86

TABLE	Page
5.3 Thermal demagnetization results from the St. George Group for the "B" component, Port au Port area	95
5.4 Mean paleomagnetic data for the "A" and "B" components after thermal demagnetization of the St. George Group, Port au Port area	96
5.5 Thermal demagnetization results from the St. George Group; Port au Choix area	116
5.6 Mean paleomagnetic data after thermal demagnetization of the St. George Group, Port au Choix area	118
6.1 Thermal demagnetization results from the Table Head Group, Port au Port area	142
6.2 Mean paleomagnetic data from the Table Head Group, Port au Port area	144
6.3 Thermal demagnetization results from the Table Head Group, Port au Choix area	159
7.1 Thermal demagnetization results from the Long Point Group, Port au Port area	169
8.1 Thermal demagnetization results from the Middle Ordovician bedded limestones of the Cow Head Group, Cow Head Peninsula	184
8.2 Site-level characteristic directions of the Cow Head Group, Cow Head Peninsula	185
8.3 Mean paleomagnetic data from the Cow Head Group, Cow Head Peninsula	186

TABLE

Page

8.4	Thermal demagnetization results for pebbles from a breccia bed of the Cow Head Group, Cow Head Peninsula	193
9.1	Selected paleomagnetic pole positions from the Ordovician rocks of North America	201

LIST OF FIGURES

FIGURE	Short Caption	Page
2.1	Generalized map of western Newfoundland	10
2.2	A generalized stratigraphic section of Cambro-Ordovician autochthonous strata and allochthonous packages	14
2.3	Simplified geologic map of the Port au Port Peninsula	16
2.4	Simplified geologic map of the Port au Choix area	18
3.1	NRM directions of the Port au Port Group . . .	22
3.2	Demagnetization characteristics of specimen pairs from 2 Port au Port Group samples . . .	24
3.3	Representative thermal demagnetization results for specimens yielding "A" component from the Port au Port Group	28
3.4	Representative thermal demagnetization results for specimens yielding "A" component from the Port au Port Group	29
3.5	Characteristic sample directions for "A" and "B" components of the Port au Port Group in Port au Port Peninsula	32
3.6	Representative thermal demagnetization results from Port au Port Group specimens yielding "B" component	35

FIGURE	Page
3.7 Representative thermal demagnetization results from Port au Port Group specimens yielding "B" component	36
3.8 Thermal demagnetization results of Port au Port Group specimens showing normal polarity swing of directions at high temperature	40
3.9 Thermal demagnetization results for 2 Port au Port Group specimens from Port au Choix area	43
3.10 Thermal demagnetization results for 2 specimens from Port au Port Group, Port au Choix area	45
3.11 Uncharacteristic stable directions from Port au Port Group	47
3.12 Representative IRM acquisition and back-field characteristics for Port au Port Group specimens	50
4.1 Selected paleopoles from Cambrian rocks of North America	57
5.1 NRM directions of St. George Group samples, Port au Port area	75
5.2 Demagnetization results of specimen pairs from 2 St. George Group samples	77

FIGURE	Page
5.3 Representative thermal demagnetization results of 2 specimens yielding "A" component for the St. George Group	80
5.4 Representative orthogonal vector diagrams of 3 specimens yielding "A" component for the St. George Group	81
5.5 Characteristic sample and site mean directions for the "A" component of the St. George Group	83
5.6 Demagnetization results of 2 St. George specimens yielding "B" component	90
5.7 Thermal demagnetization results of 2 St. George specimens yielding both "A" and "B" components	92
5.8 Sample characteristic directions for the "B" component	94
5.9 IRM acquisition and back-field characteristics for the St. George Group	98
5.10 Demagnetization results of specimen pairs from a St. George sample indicating goethite as the main remanence carrier	101
5.11 NRM directions of St. George Group samples, Port au Choix area	104
5.12 AF demagnetization results for 3 St. George specimens from Port au Choix area	107

FIGURE	Page
5.13 Representative thermal demagnetization results for 2 St. George specimens from Port au Choix area	109
5.14 Representative thermal demagnetization results for 2 St. George specimens from the Port au Choix area	110
5.15 Representative thermal demagnetization results for 4 St. George specimens from Port au Choix area	111
5.16 Sample characteristic directions from the St. George Group, Port au Choix area	113
5.17 Formation means with their 95% confidence circles for the St. George Group in the two main sampling areas	115
5.18 Thermal demagnetization results for 6 St. George specimens from Port au Choix	121
6.1 NRM directions of Table Head Group specimens, Port au Port area	132
6.2 AF demagnetization results for 3 representative specimens of the Table Head Group, Port au Port area	134
6.3 Representative thermal demagnetization results for 2 Table Head Group specimens, Port au Port area	136

FIGURE	Page
6.4 Thermal demagnetization results for 2 Table Head specimens, Port au Port area	137
6.5 Thermal demagnetization results for 2 Table Head Group specimens	139
6.6 Characteristic specimen directions from the Table Head Group, Port au Port area	141
6.7 Thermal demagnetization results for 4 Cape Cormorant specimens	147
6.8 Thermal demagnetization results of specimen pairs from 2 Cape Cormorant samples	149
6.9 NRM sample directions for the Table Head Group, Port au Choix area	153
6.10 Thermal demagnetization results for 2 Table Head specimens, Port au Choix area	155
6.11 Thermal demagnetization results for 4 Table Head specimens } Port au Choix area	156
6.12 Characteristic sample directions from the Table Head Group, Port au Choix area	158
6.13 Unstable thermal demagnetization behaviour of 3 Table Head specimens from the Port au Choix area	160
7.1 Thermal demagnetization results for 4 Long Point Group specimens	166
7.2 Characteristic specimen directions from the Long Point Group	168

FIGURE	Page
8.1 Simplified geologic map of the Cow Head Peninsula	176
8.2 Bedding correction for the plunging fold . . .	178
8.3 Thermal demagnetization results for 2 Cow Head Group specimens	181
8.4 Characteristic sample and site mean directions from Bed 13	183
8.5 Thermal demagnetization results for 2 pebbles from the breccia Bed 14	189
8.6 Thermal demagnetization results for 2 pebbles from the breccia Bed 14	190
8.7 Characteristic pebble directions from breccia Bed 14	192
8.8 IRM acquisition and back-field characteristics of 2 specimens from the Cow Head Group . . .	195
9.1 Paleopoles from the Ordovician rocks of cratonic North America	200

CHAPTER 1

INTRODUCTION

Over the past three decades, paleomagnetism has played a significant role in providing key evidence on continental drift, major tectonic problems and polar wandering.

Methods and techniques of paleomagnetism are primarily concerned with obtaining, from a statistically significant number of rock samples, reliable information about the earth's magnetic field in the geological past relative to the land mass sampled.

It is essential in a paleomagnetic study to express the magnetic field directions obtained from the rocks in geographical co-ordinates. For this purpose, some constant feature associated with the geomagnetic field is required to provide a reference system on a geological time scale. This reference system then forms the basis for comparing the paleomagnetic results obtained from different land masses. The model of the field which provides this common reference is the axial geocentric dipole field. There is strong theoretical and observational evidence that for the past several million years the earth's magnetic field, when averaged over periods of several thousands of years, has been that of a geocentric dipole co-axial with the spin axis. On this model, the magnetic vectors in rocks of any particular age can be used to calculate the position of a paleomagnetic pole which coincides with the ancient

geographic pole. From the magnetic vectors, one obtains also the paleolatitude of the sampling site and its azimuthal orientation with respect to the paleomeridians.

On the assumption of fixed continents, all rocks magnetized at the same time all over the world should yield the same paleomagnetic pole position on this dipole model. But, as the continents move relative to each other, the location of the paleopole as calculated from different continental block differs, although the earth's spin axis remains fixed in space. As continental drift proceeds, the pole position relative to each drifting continent will change, resulting in a so-called "apparent polar wandering" (APW) path, which is constructed by joining the pole positions derived from rocks of different ages from the same continental region. A comparison of pole positions or of APW paths for different continents derived from rocks representing a particular time or a time span provides crucial evidence for continental drift.

Based on worldwide paleomagnetic data, APW paths for major continental blocks have been proposed (e.g., Morel and Irving, 1978; Irving and Irving, 1982). These APW paths provide estimates of changes in latitude and azimuthal orientation of the continents over geological periods of time, but they do not fix the longitude of the continental blocks. Portions of the APW paths are still subject to modifications as earlier data are being revised, even in the case of major crustal blocks, while, the APW

history of some smaller blocks is still in much doubt.

A paleomagnetic investigation of Early Paleozoic rocks, especially the Cambrian-Ordovician sequences of western Newfoundland, is valuable for a number of reasons. First, western Newfoundland is considered to be the eastern margin of cratonic North America in Early Paleozoic times (Williams and Stevens, 1974), and it has a nearly complete stratigraphic record of the Lower Paleozoic which is ideally suited for establishing characteristic Early Paleozoic directions of the earth's magnetic field relative to western Newfoundland. Secondly, if successful, the results can provide useful information in the documentation of the history of the presumed Proto-Atlantic (Iapetus) ocean and the closure that gave rise to the Paleozoic orogenic belts around the Atlantic (Wilson, 1966; Harland, 1967; Dewey, 1969; McKerrow and Ziegler, 1972). This could be accomplished by comparing the western Newfoundland results with the time-equivalent paleomagnetic record from the other side of the presumed ocean (e.g., Avalon Zone and the "European" part of the British-Irish Caledonides). Such a comparison, under favourable circumstances, could lead to an estimate of the width of the Proto-Atlantic. A paleomagnetic comparison across the Proto-Atlantic suture in Ireland was done by Deutsch (1980, 1984) from which he inferred a wide Proto-Atlantic during the Middle Ordovician.

Thirdly, the results could be used for a test of the hypothesis of rotation of western Newfoundland, originally

proposed by Wegener (1929). Such a test requires comparisons with cratonic mainland North America. Black (1964) deduced a 30° anticlockwise rotation of western Newfoundland from a paleomagnetic comparison of Cambrian, Devonian and Permo-Carboniferous rocks between western Newfoundland and the mainland maritimes. He placed this rotation in mid -> to Late Devonian times. Black's conclusion was later questioned because of insufficient demagnetizations and a doubtful choice of paleopoles used in his comparisons. On a reexamination of paleomagnetic data available up to 1977, Deutsch and Rao (1977) demonstrated that the data fail to support a 30° rotation of western Newfoundland relative to North America but would be consistent with a small rotation ($5-10^{\circ}$). Since some of the data used in this comparison have since been discarded, the question of rotation of Newfoundland remains to be settled.

Presented in this study are paleomagnetic investigations of Middle Cambrian to Middle Ordovician rocks from the Western Platform of Newfoundland. It is assumed that the reader is familiar with the standard procedures in paleomagnetism. Hence no attempt was made in the writing of the thesis to explain the well-established techniques. A comprehensive treatment of the subject can be found in Irving (1964), McElhinny (1973), Collinson (1983) and Tarling (1983).

The main objective of this investigation has been to

obtain a reliable Cambrian-Ordovician paleomagnetic record for western Newfoundland. This is needed, first, because of the existence of major gaps in the Lower Paleozoic paleomagnetic record for this region; and secondly, because it has become evident, during the past decade or so, that much of the earlier published work on the subject is in need of revision. The same applies to the paleomagnetic literature on the Lower Paleozoic in other parts of the Appalachians and interior North America. This is in part because, in earlier studies especially, rigorous tests for establishing magnetic stability and for estimating an age of magnetization were not always used. In some of these studies it was assumed without sufficient evidence that the observed stable magnetization had been acquired at, or soon after, the time of formation of the rock. Such an assumption may be often invalid, because of the increasing recognition that Early Paleozoic rocks have been widely subjected to remagnetization in later geologic periods, especially in the Late Paleozoic.

Remagnetization on a wide scale was first proposed by Creer (1968). Its pervasive effect on the magnetization of Appalachian rocks has been pointed out by Roy et. al. (1983). Irving and Strong (1984 a, b; 1985) showed that Devonian and Lower Carboniferous rocks in Newfoundland carry partial magnetic overprints acquired during the Kiaman reverse magnetic interval (Late Carboniferous to Early Permian). They argued further that Kiaman-age

overprinting affected also many Paleozoic rocks in mainland North America. Irving and Strong (op. cit.) used their findings to demonstrate that there had been no post-Devonian sinistral displacement of "Acadia" relative to interior North America as proposed by Kent and Opdyke (1978). The proposition of a displaced terrane was shown to be due to the imperfect resolution of superposed components, particularly the Klamath overprint, in the paleomagnetic data. Thus, in such studies it is important that the superposed components be identified following extensive experimental studies, before giving any tectonic interpretation to the paleomagnetic data.

Much of the Lower Paleozoic stratigraphy of North America, including western Newfoundland, is dominated by carbonates, both in autochthonous and allochthonous rock sequences. The paleomagnetic analysis of Paleozoic carbonates is difficult, chiefly for two reasons. First, the intensity of their natural remanent magnetization (NRM) is normally very low; and secondly, there is evidence of complete Late Paleozoic remagnetization in Lower and Middle Paleozoic carbonates from widely separated localities on the craton (e.g., Scotese et al., 1982; Wisniowiecki et al., 1983; McCabe et al., 1983, 1984; Elmore et al., 1985). As for the first problem of low NRM intensity, the advent of cryogenic magnetometers (e.g., Goree and Fuller, 1976) has made it possible to measure low natural remanence with reasonable accuracy and rapidity, but measuring

extremely weak remanences left after demagnetization treatments may still be a problem. Quite often the magnetic moment either falls to noise level or becomes comparable to the specimen holder moment during demagnetization while a significant proportion of the natural remanence still remains. This can seriously limit the number of samples from which valuable information could be obtained.

Despite evidence of complete remagnetization in some Lower Paleozoic carbonates, as mentioned above, some carbonate bodies have been shown to have escaped remagnetization either partially (e.g., Dunn and Elmore, 1985) or completely (e.g., McCabe et al., 1985; Jackson and Van der Voo, 1985). These authors inferred that the stable magnetizations isolated from their rocks are of depositional or early post-depositional origin. A central task of the present investigation therefore, has been to obtain evidence on the occurrence of partial to complete remagnetization in the western Newfoundland carbonates, or alternatively, to verify the absence of any overprinting in them.

The paleomagnetic results presented in this study reveal that the Lower Paleozoic carbonates of Newfoundland have indeed been subject to remagnetization, and the presence of multicomponents is clearly evident. A detailed analysis has led to the isolation of presumably original magnetizations in some of the rock formations, in addition

to the identification of superposed components. The paleomagnetic results presented in this thesis, which include data for the first time from the allochthonous rock sequence of the Cow Head Group, significantly improve the Lower Paleozoic data base of western Newfoundland and thereby that of cratonic North America.

The results of these investigations are presented in the following sequence. A brief description of the regional geology of western Newfoundland and the sampling localities is given in Chapter 2. Paleomagnetic results from the Cambrian rocks are presented and discussed in Chapters 3-4. Chapters 5-8 are devoted to Ordovician rocks. Results from the Lower and Middle Ordovician autochthonous rocks are described in Chapters 5-7. Chapter 8 deals with the results from the Middle Ordovician allochthonous rocks. All Ordovician results from the present study are further discussed and compared with published results in Chapter 9. Summary and conclusions form the last Chapter (10) of this thesis.

CHAPTER 2

REGIONAL GEOLOGY AND SAMPLING

The island of Newfoundland forms the northern extremity of the Appalachian structural province and occupies a key area in the Appalachian-Caledonian fold belt. Based on stratigraphic and structural contrast between Cambrian-Ordovician and older rocks, the Newfoundland segment of the Appalachian orogen has been divided into four zones (Williams, 1979). From west to east, they are the Humber, Dunnage, Gander and Avalon Zones. Western Newfoundland corresponds to the Humber zone of this subdivision (Figure 2.1).

The Lower Paleozoic sequence of the Humber Zone records the evolution of a platform at the margin of a Proto-Atlantic ocean and its partial subduction under a slab of oceanic lithosphere (Williams and Stevens, 1974). This is recorded in the development of an autochthonous sequence near the continental margin. Subsequently there was westward transport and overthrusting of partly coeval slope and rise sediment and ophiolite (Stevens, 1970; DeWit, 1972), which together constitute the Humber Arm Allochthon in the south, and Hare Bay Allochthon in the north.

Within the autochthon, a Lower Cambrian sequence, the Labrador Group, composed of shallow-water siliciclastic and carbonate rocks, was deposited on the rifted Grenville basement. This sequence is overlain by a Middle Cambrian

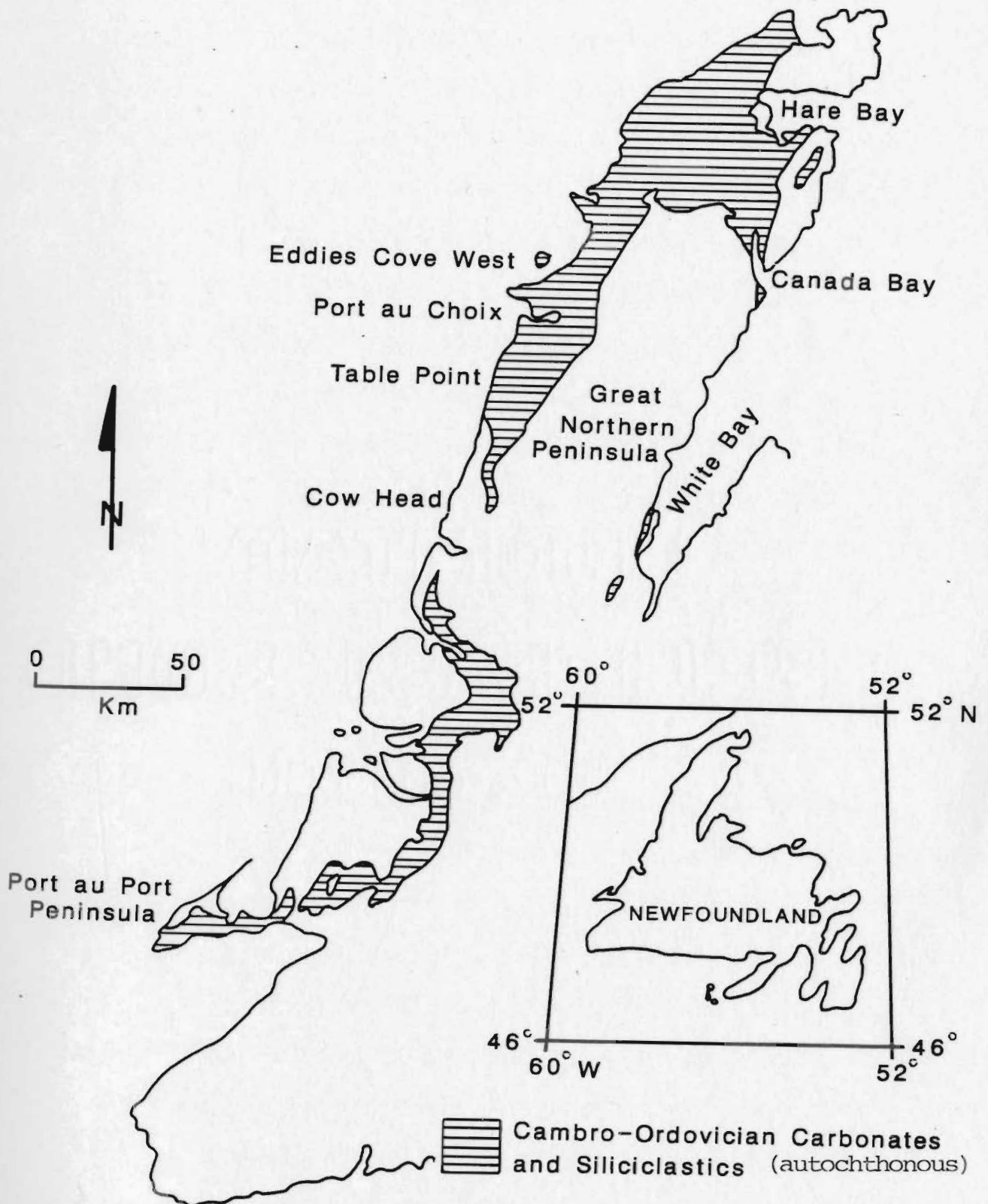


Fig. 2.1. Generalized map of western Newfoundland (Humber Zone), showing the distribution of platformal rocks.

to Lower Ordovician (Port au Port and St. George Groups) shallow-water platformal carbonate sequence. During the Middle Ordovician the platform subsided and received sediments of progressively deeper-water origin. This is recorded in the overlying Middle Ordovician rocks (Table Head Group) which indicate deposition in deepening water.

Within the allochthon the coeval slope and rise sediments are broadly termed the Humber Arm Supergroup, which includes the Cow Head Group and Curling Group (Stevens, 1970). The Humber Arm Allochthon represents a stacked series of rock slices emplaced upon the autochthon. An upper age limit for the emplacement of the Humber Arm Supergroup is indicated by unconformably overlying late Middle Ordovician shallow-water sediments (Long Point Group) on the Port au Port Peninsula (Rodgers, 1965), which in turn is overlain by Silurian-Devonian red beds of the Clam Bank Formation. The root zone of the allochthonous complexes is presumably to the east, perhaps in the White Bay area, which is evident from the presence of metamorphosed rocks that are probable equivalents of the autochthonous sequence in the western White Bay (Lock, 1969, 1972). The allochthon was deformed and partially covered by Carboniferous rocks following the deposition of a cover on it (James and Stevens, 1982).

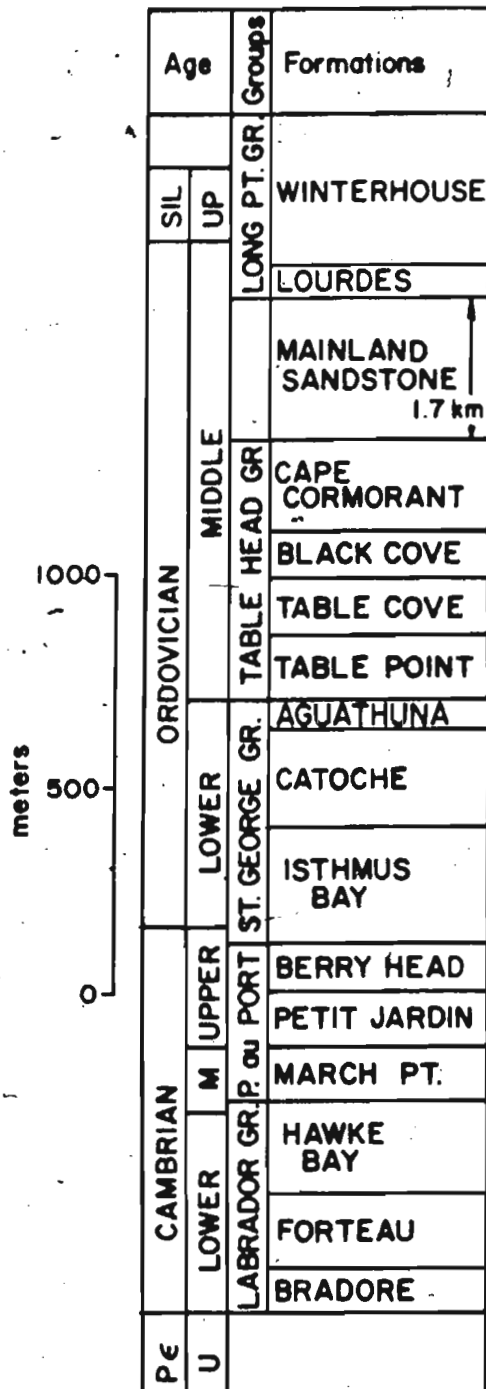
Rocks of the Humber Zone have been affected by three major orogenic events that in general terms can be called the Taconic, Acadian and Alleghenian orogenies. The

Taconic orogeny in the Middle Ordovician led to the destruction of the Proto-Atlantic ocean, and its effects are demonstrated by the presence of the transported Humber Arm Supergroup and by local unconformities in the stratigraphic record of the Humber Zone and along the margins of the Dunnage Zone (Williams, 1980). The Mid-Paleozoic Acadian orogeny (mainly in the Devonian) affected all of the Taconic deformed zone. The Acadian deformation mainly caused the faulting and folding of the Cambrian to Middle Ordovician strata (Schillereff and Williams, 1979; Williams et al., 1985). The effects of the Late Paleozoic Alleghenian orogeny (mainly in the Carboniferous) in the Humber Zone is minimal, compared to its effect elsewhere in the Appalachian orogen (Williams, 1980). However, a possible Alleghenian deformation in some of the Early Paleozoic strata in the Humber Zone cannot be ruled out at this point (R. K. Stevens, personal communication).

The first comprehensive stratigraphic study of the Cambrian-Ordovician succession of rocks in western Newfoundland was undertaken by Schuchert and Dunbar (1934). Some new information was added to the above stratigraphy by the paleontological work of Lochman-Balk (1938). A major breakthrough, however, came with the recognition of two distinct sequences in western Newfoundland by Rodgers and Neale (1963): autochthonous shallow-water carbonates and minor siliciclastics, and

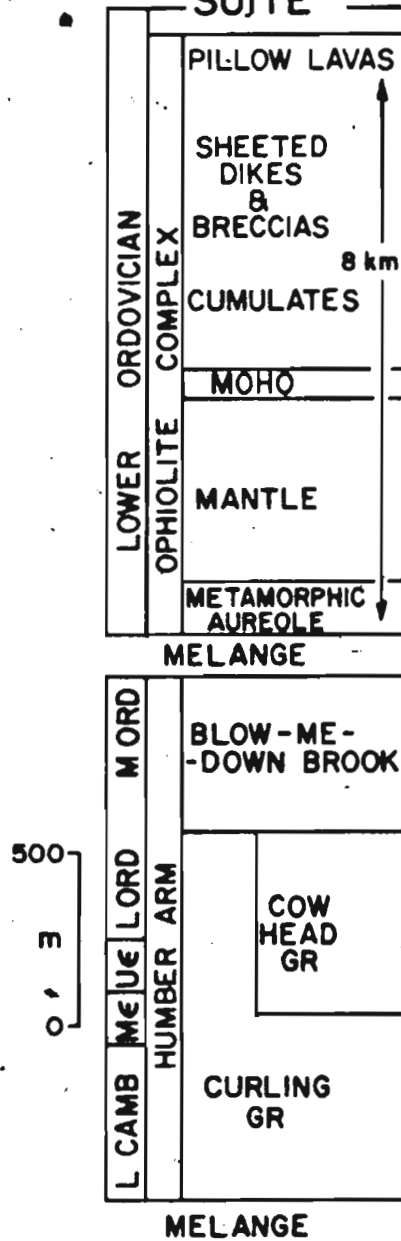
Fig. 2.2. A generalized stratigraphic section of Cambro-Ordovician (a) autochthonous, mainly shallow water strata and (b) allochthonous packages of mainly deep water sediments below and oceanic lithosphere above in western Newfoundland. Different formations within a given Group in (a) are not necessarily to the indicated scale. (Modified after James and Stevens, 1982).

AUTOCHTHONOUS STRATA



(a)

ALLOCHTHONOUS SUITE



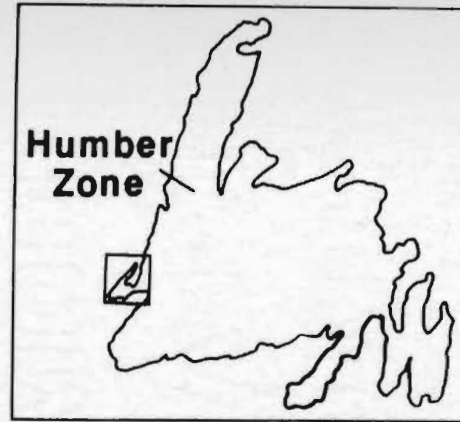
(b)

Fig. 2.2

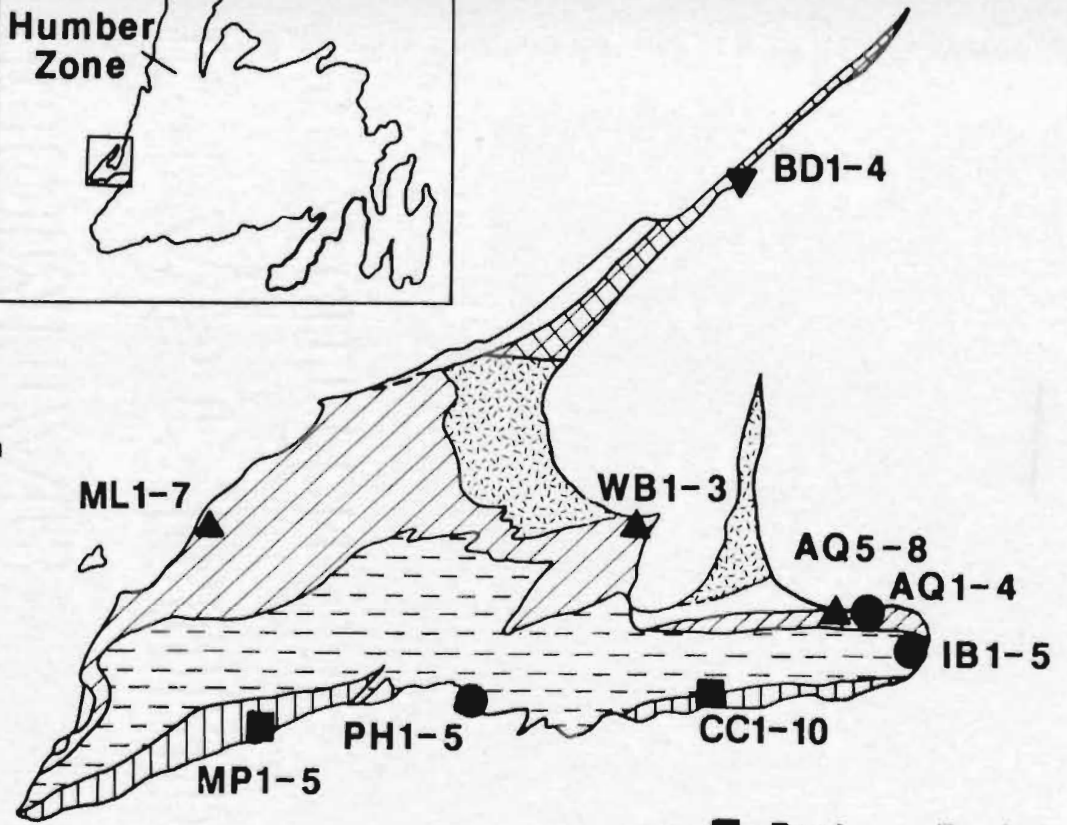
allochthonous deeper-water deposits. Whittington and Kindle (1969) recognized new exposures of Cambrian-Ordovician strata based on new fossil discoveries and discussed the implications of Rodgers and Neale's (1963) theory. Later refinements in the stratigraphy have been carried out mainly by researchers at Memorial University (e.g., Levesque, 1977, Pratt, 1979; Klappa et al., 1980; James et al., 1983) and by the Newfoundland Department of Mines and Energy (e.g., Knight, 1977, 1980; Stouge, 1981). The stratigraphy and various sedimentological and diagenetic aspects of the Cambrian-Ordovician succession are subject to continuing investigation at the above two centers.

The stratigraphy of the autochthonous and allochthonous rocks in western Newfoundland is presented in Figure 2.2. The stratigraphic names are as proposed in Klappa et al. (1980), James and Stevens (1982), and James et al. (1983).

Autochthonous rocks for paleomagnetic studies were collected from the Port au Port Group (March Point and Petit Jardin Formations only), St. George Group (Isthmus Bay, Catoche and Aguathuŕa Formations), Table Head Group (Table Point, Table Cove and Cape Cormorant Formations only) and Long Point Group (Lourdes Limestone only). Allochthonous rocks were collected from the Ordovician strata of the Cow Head Group. Some details of the geological setting of the above rock units are also



- | | | |
|---------------------------|---|-----------------------|
| Silurian to Mississippian | □ | Younger Paleozoic |
| Cambro-Ordovician | ▨ | Humber Arm Allochthon |
| Middle Ordovician | ▧ | Table Head |
| Lower Ordovician | ▩ | Long Point Group |
| | ▨ | St. George Group |
| Cambrian | ▩ | Port au Port Group |



- Port au Port
- ST. George
- ▲ Table Head
- ▼ Long Point

Fig. 2.3. Simplified geologic map of the Port au Port Peninsula showing the sampling localities and sites. (After James and Stevens, 1982).

Fig. 2.4. Simplified geologic map of the Port au Choix area showing the sampling localities and sites. Symbols as in Fig. 2.3. Hatching: Vertical, Port au Port Group; horizontal dashed, St. George Group; oblique, Table Head Group.

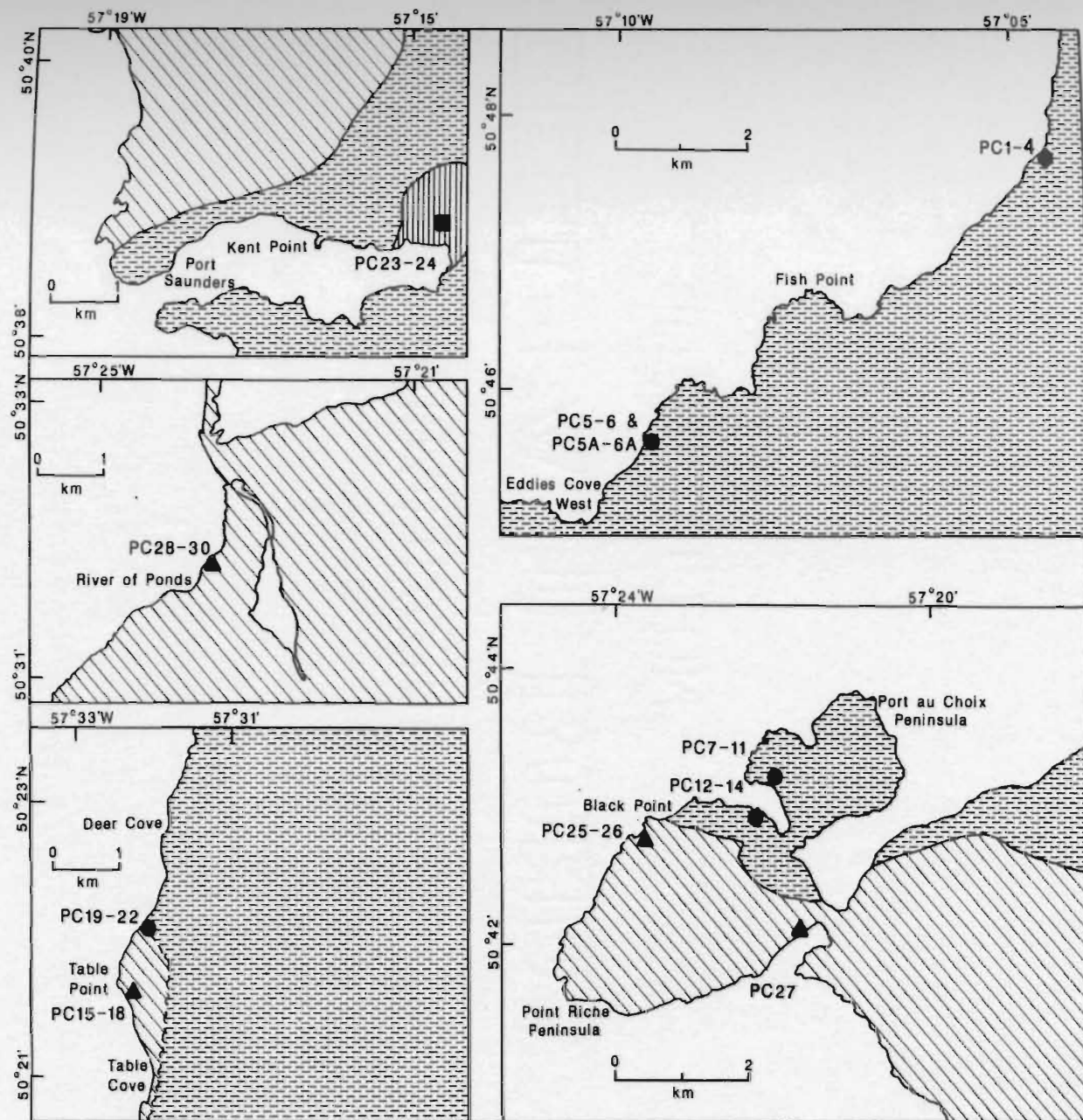


Fig. 2.4

discussed in the chapters to follow.

Sampling was done in three main areas: Port au Port Peninsula, Cow Head Peninsula and Port au Choix area. The "Port au Choix area", as defined here, includes all the sampling localities from Table Point to Eddies Cove West (see Figure 2.1). Figures 2.3-2.4 show the generalized geology and sampling localities in the Port au Port and Port au Choix areas. Figures 2.1-2.4 will be repeatedly referred to in the later chapters as the paleomagnetic results from different localities are being discussed in turn (Chapters 3-7). The generalized geology and sampling localities of the Cow Head Peninsula are shown in Figure 8.1 (Chapter 8). Detailed information on the sampling sites shown in Figures 2.3, 2.4 and 8.1 is given in Appendices B-F. These appendices also include the detailed demagnetization results of samples that yielded meaningful results.

Sample preparation, measurement procedure and basis of statistical analyses are discussed in Appendix A.

CHAPTER THREE
PORT AU PORT GROUP

3.1 Geological Setting

The Port au Port Group in western Newfoundland is Middle to Late Cambrian in age and is preceded by a lower sandstone unit, the Hawke Bay Formation of the Labrador Group (Figure 2.2). The Port au Port Group has been subdivided into three formations: March Point Formation (late Middle Cambrian), Petit Jardin Formation (mostly early Upper Cambrian) and Berry Head Formation (mid - to late Upper Cambrian). The strata of these units mainly comprise a sequence of interbedded carbonates, siltstones and shales and have been interpreted (James et al., 1983) to represent the outer part of a wide carbonate platform which stretched eastward and now lies beneath the Gulf of St. Lawrence. These units display two distinctive and repeated styles of deposition: (a) thin-bedded sequences of silty limestone and dolostone, with shales present as thin beds or partings in the carbonates; and (b) thick-bedded limestones and dolostones composed mainly of oolitic grainstones and laminated dolostones (Levesque, 1977; Levesque et al., 1977).

3.2 Paleomagnetic sampling and results

Eighty-one oriented hand samples were collected from the March Point and Petit Jardin Formations for

paleomagnetic investigation. These samples were collected from a total of 17 sites. The distribution of samples over the two formations is as follows: On the Port au Port Peninsula, 25 samples from 5 sites were sampled from March Point Formation and 45 samples were collected from 10 sites of the Petit Jardin Formation. The remaining 11 samples were collected from 2 sites of the Petit Jardin Formation in the Port au Choix area. The emphasis has been on the Port au Port area, where the rock exposure is excellent and the rocks are relatively undeformed. The sampling localities are shown in Figure 2.3 (MP1-5 and CC1-10) and Figure 2.4 (PC23-24). Additional details about sampling are given in Appendix B.

A minimum of two specimens of a standard size (see Appendix A) were cut from each of the 81 samples. Measurements were conducted on at least one specimen per sample. On detailed investigation, the paleomagnetic results from the Port au Port and the Port au Choix areas were found to be significantly different. Therefore they are discussed separately below.

3.2.1 Port au Port area

The natural remanent magnetization (NRM) vectors were clustered in a steep downward direction, suggesting that a component directed close to the present earth's field (PEF), probably of viscous origin, contributes strongly to the total NRM (Fig. 3.1). However, a directional smear

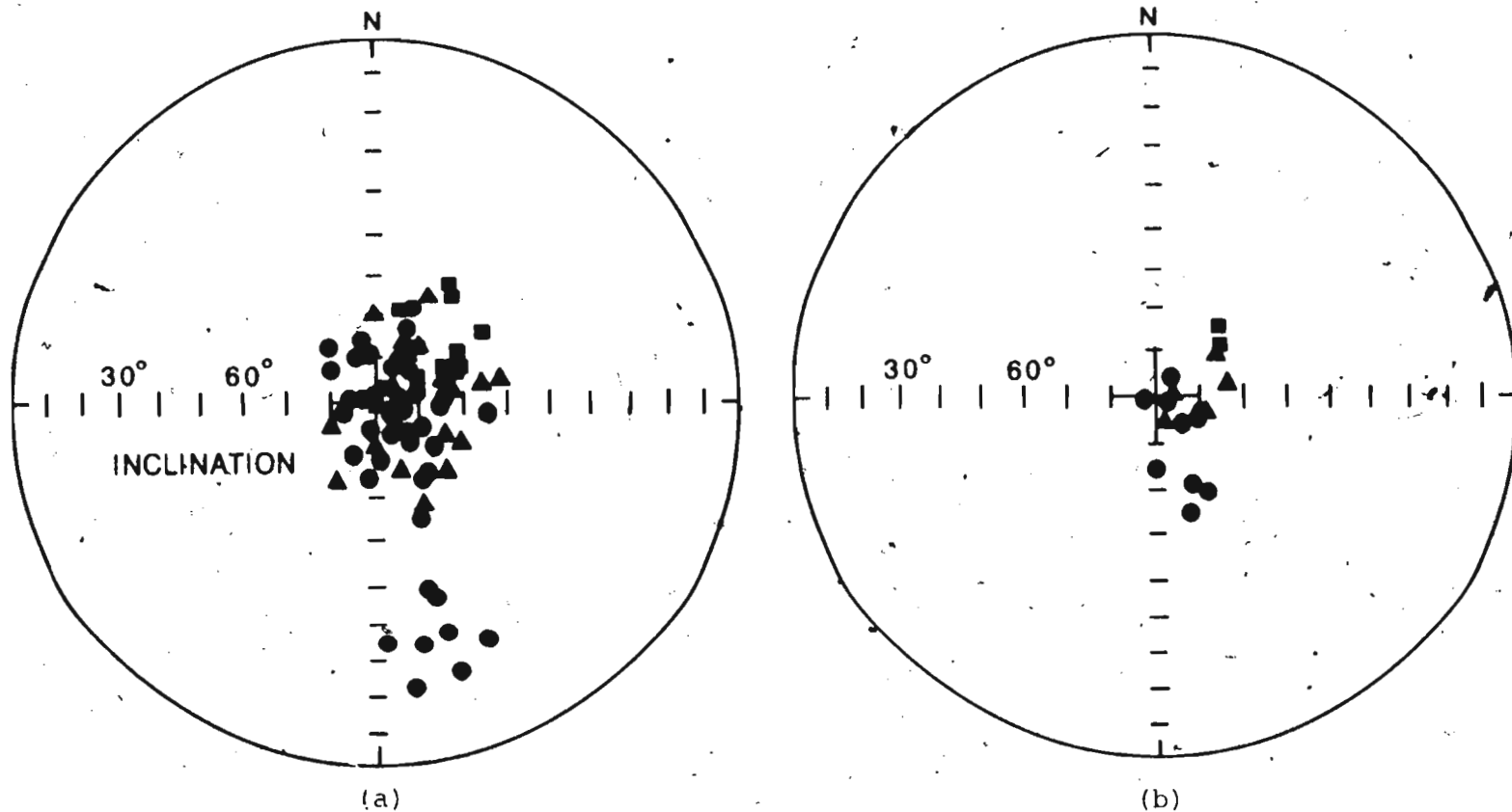


Fig. 3.1. NRM directions of the Port au Port Group: (a) Samples; (b) Site means. The Petit Jardin Formation is represented by circles (Port au Fort area) and squares (Port au Choix area) and the March Point Formation by triangles (Port au Port area only).

extending over the southeast quadrant suggests the presence of a shallower component to the southeast. NRM intensities range between 1×10^{-4} and 2×10^{-3} A/m.

Both alternating field (AF) and thermal demagnetization techniques were used to isolate the stable magnetization(s) in the individual samples. The steps used in these treatments are summarized in Appendix A. Four specimens, each chosen from a different site, were AF demagnetized in detail. Two typical results are shown in Figure 3.2 (top diagrams). As is seen from the figure, the AF treatment failed to isolate any characteristic component from the NRM. In the case of specimen CC1-2 a substantial portion of the remanence intensity still remained after treatment to 100 milli Teslas (mT), whereas in the case of specimen CC6-B, though the intensity decay was complete by 50 mT, the direction did not significantly change from the steeply inclined NRM. The directional change above 50 mT, accompanied by a rise in the intensity in CC6-B, may be due to some spurious magnetization induced in the already weakly magnetized specimen in the low residual field of the AF demagnetizer.

Thermal demagnetization, initially, was conducted in detail on 15 specimens, each chosen from a different site. Two of these specimens were from the same samples for which AF demagnetization results are shown in Figure 3.2. The matching thermal results are shown in the same figure (specimens CC1-1 and CC6-A). They show the unstable

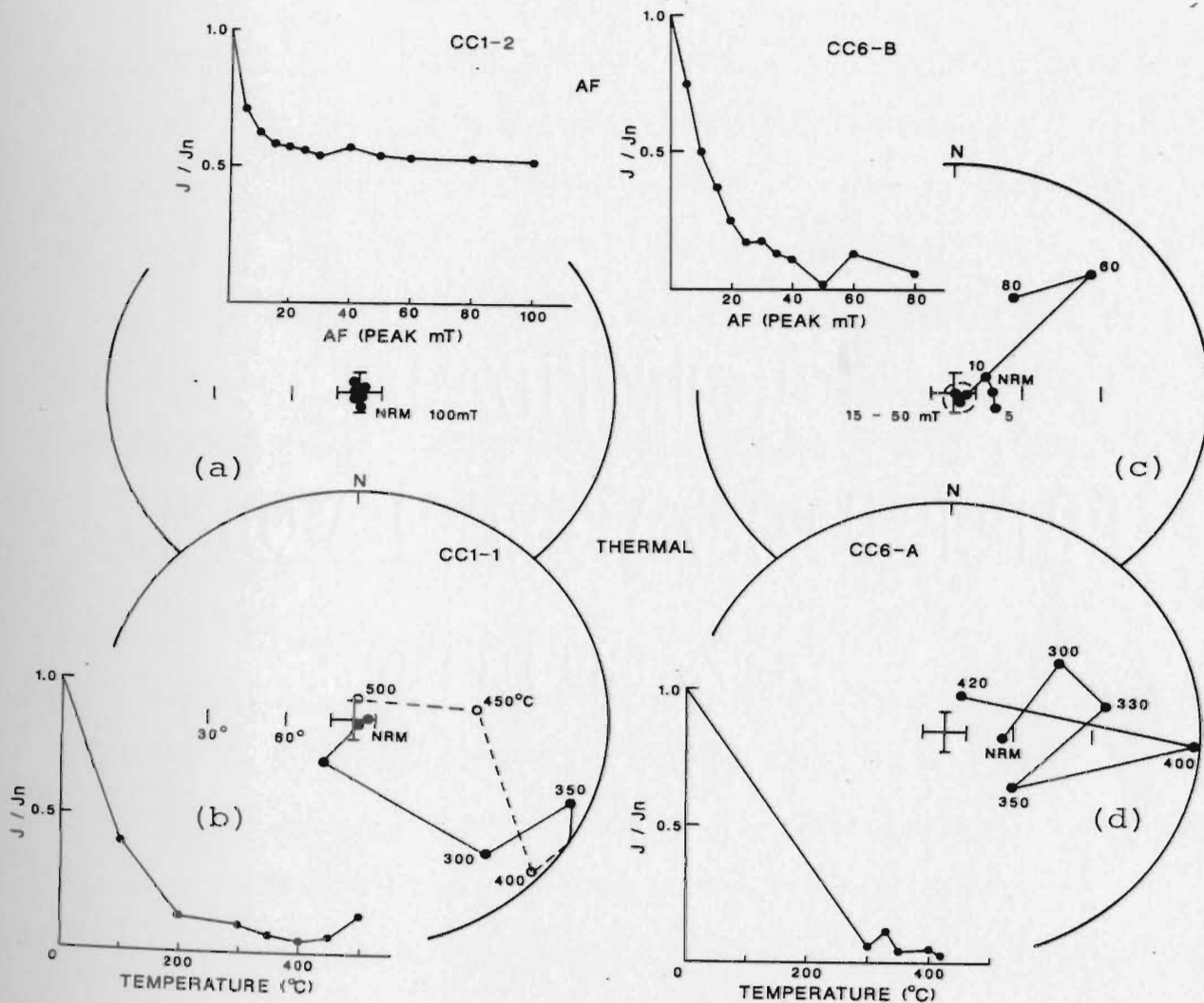


Fig. 3.2. Demagnetization characteristics of specimen pairs (a, b and c, d) from 2 Port au Port Group samples after (a, c) AF demagnetization; (b, d) thermal demagnetization. Solid (open) circles denote lower (upper) hemisphere projections on a stereographic (Wulff) net. Dashed outline in (c) denotes directions in the indicated field range and has no statistical significance. Directions are without tilt correction. J/J_n is the normalized intensity.

character of the NRM. However, a swing away from the steeply inclined NRM direction is clearly seen. At the same time, in both specimens, the magnetic moment at 400°C has fallen to very low values, close to that of the specimen holder; so the erratic intensity changes above 400°C for specimen CC-1 are probably due to spurious magnetization. The unstable behaviour of remanence was noticed in a number of the remaining 13 specimens thermally demagnetized in detail. Between 50 and 95% of the total NRM intensity was lost after heating to 300°C. A stable component appears to be revealed only between 300°C and 500°C in some of these 13 specimens. Generally, the entire magnetization had decayed by the 450°C to 560°C step, when the moment was either reduced to the order of the holder moment or to 1 or 2% of the NRM. As the intensity dropped off sharply in the NRM-300°C range in the 13 pilot specimens, and a stable component was observed only above this temperature, it was decided to insert additional, closely-spaced temperature steps (see Appendix A) between 300°C and 500°C for thermally cleaning specimens from the remainder of the samples. The 100° and 200°C steps were dropped, as these led only to the removal of a steep viscous component. No AF demagnetization was carried out on any further specimens.

In a majority of samples from Port au Port area, the results of thermal demagnetization made it possible to isolate two components, hereafter called the "A" and "B"

components; in addition, the previously mentioned steep viscous component could be erased at lower temperatures. The "A" component is directed along a southeast axis with intermediately steep positive inclination, whereas the "B" component is almost horizontal and directed towards south to southeast. Figures 3.3-3.4 and 3.6-3.7 show representative behaviour upon thermal demagnetization from which the "A" and "B" components have been isolated. —

Samples which yielded the "A" component can be divided into three groups. In the first group, represented by Figure 3.3 (Specimens MP19-A and CC33-A), a dominant steep component carrying about 80% of the total intensity was removed by heating up to 300°C, after which a stable direction was uncovered in the southeast quadrant between 300°C and 450°C. This is evident from almost univectorial decay to the origin on vector diagram (Zijderveld, 1967), corresponding to a stable end point on the stereographic plot. Beyond 400° or 470°C the directions of both the specimens in Figure 3.3 appear to migrate towards the opposite quadrant, but in view of the remaining low intensities (2% of the NRM), it is doubtful that this directional trend is systematic.

In the second group of samples, shown in Figure 3.4, a stable end point represented by three or more closely

Figs. 3.3-3.4. Representative thermal demagnetization results for specimens yielding "A" component from the Port au Port Group. Conventions for stereographic plots are as in Fig. 3.2. In the corresponding orthogonal vector diagrams (r.h.s.), squares are projections of the vector end points on a N-S vertical (V) plane; circles on the horizontal (H) plane. Directions are without tilt correction.

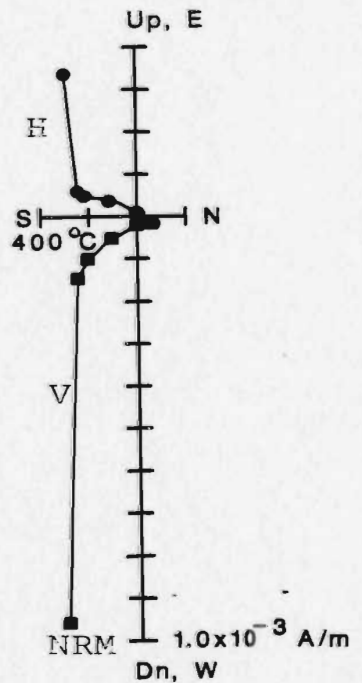
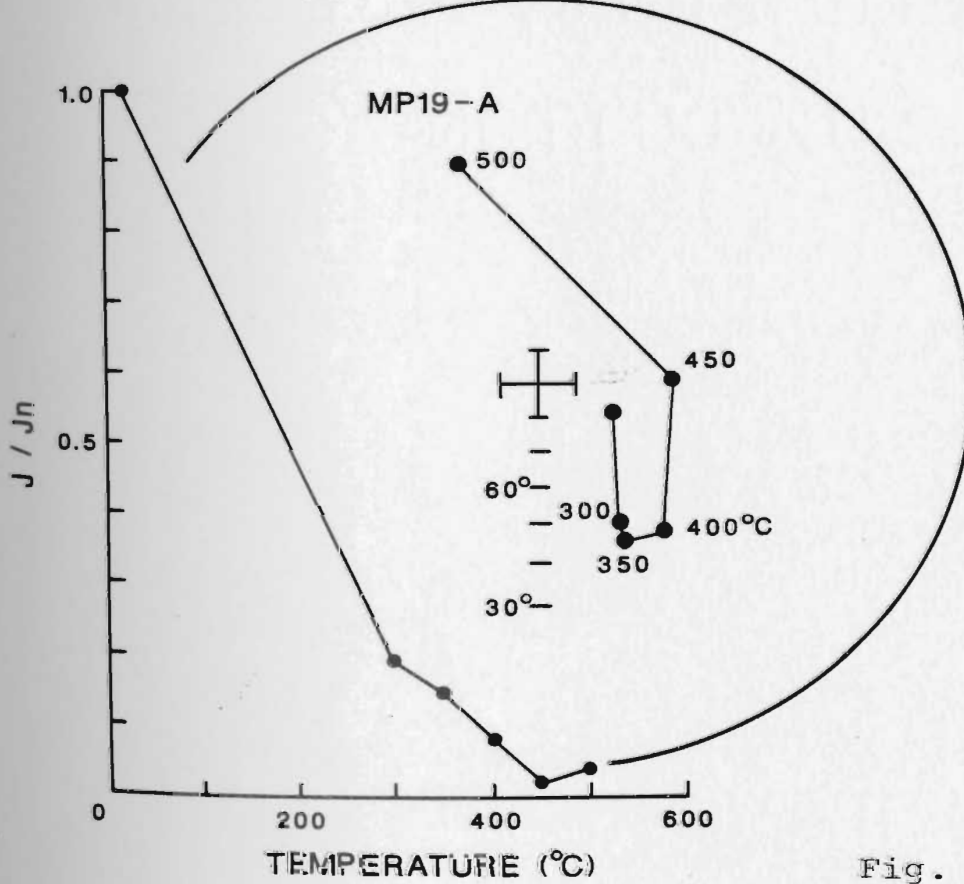
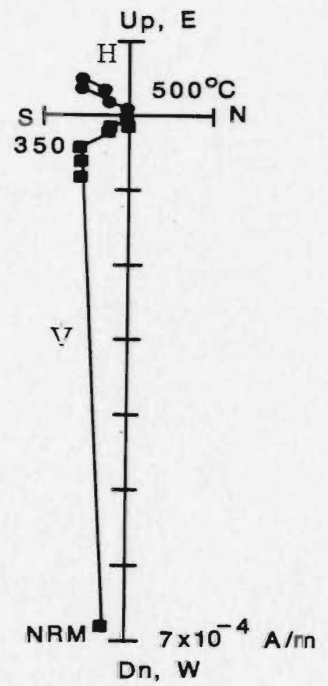
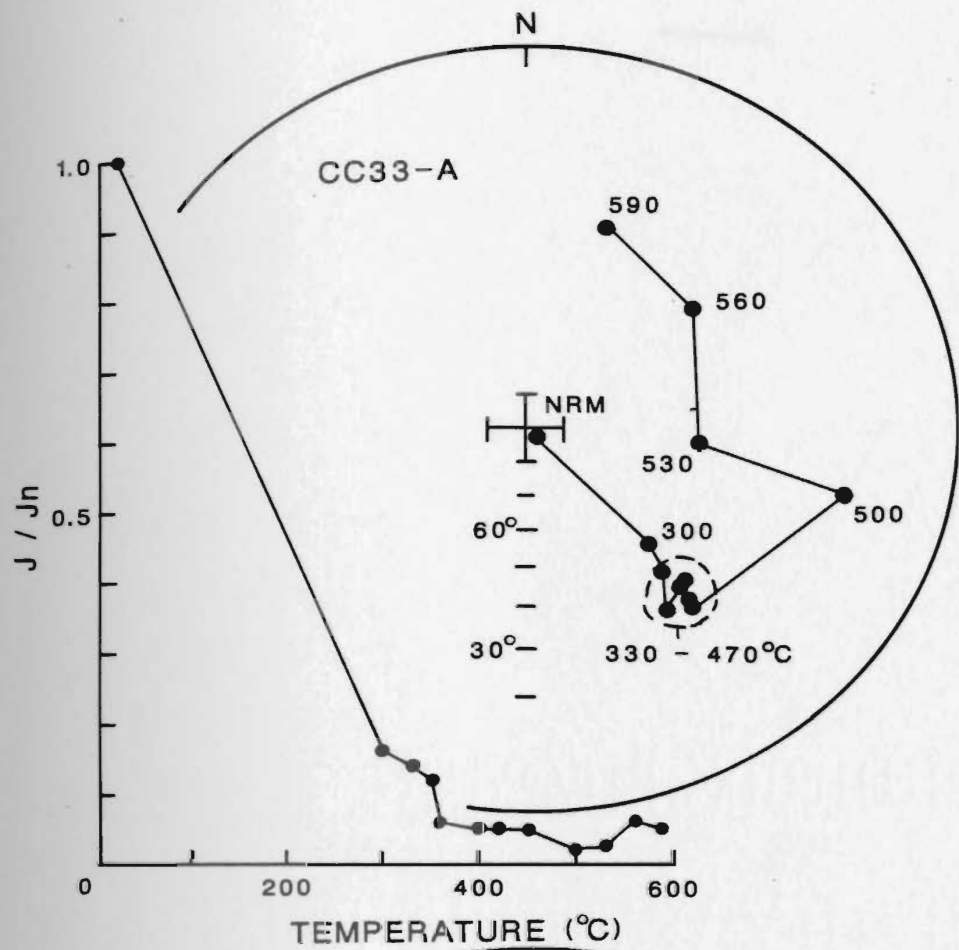


Fig. 3.3

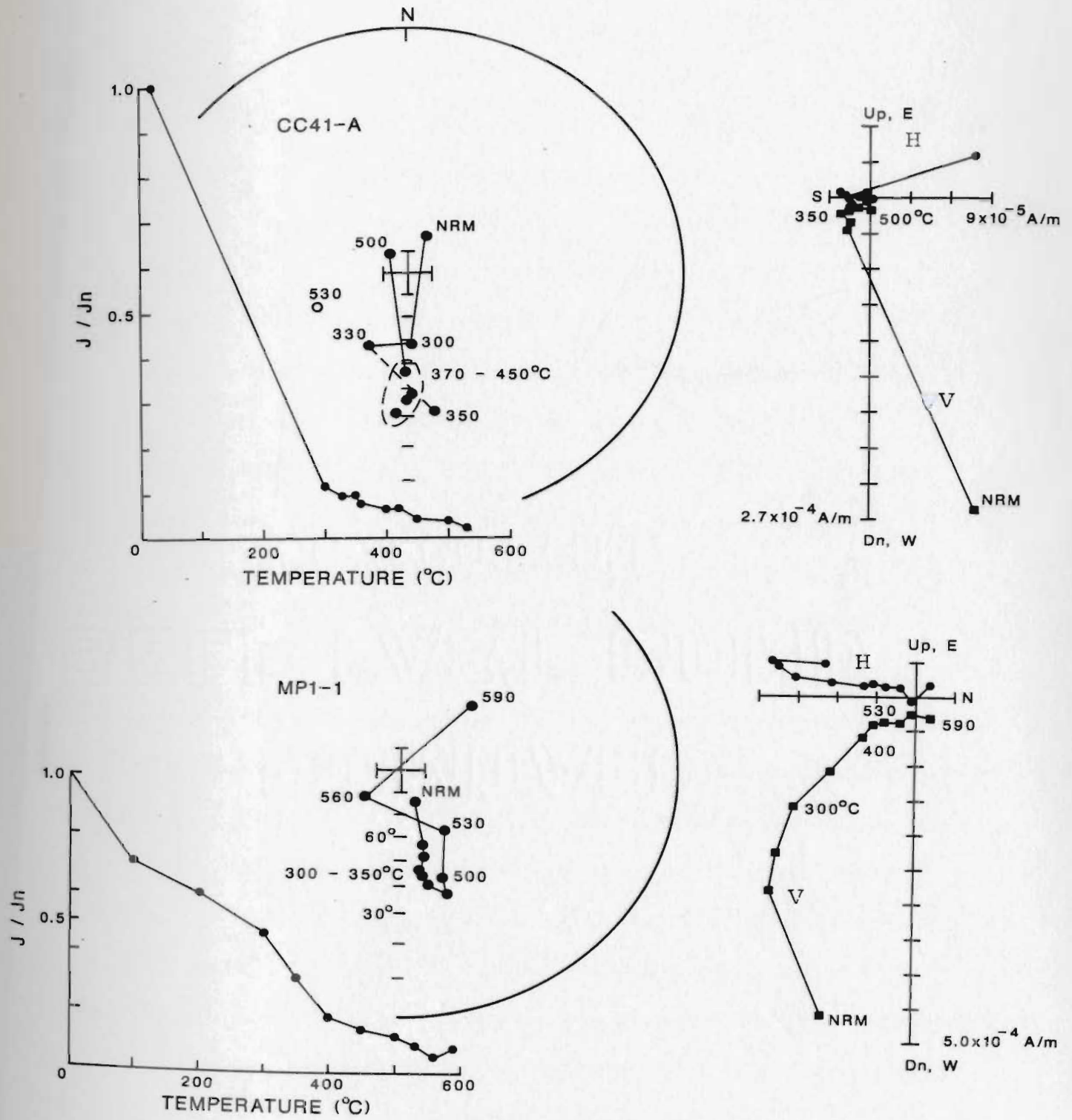


Fig. 3.4. (See caption facing Fig. 3.3.).

spaced vectors associated with progressive intensity reduction over the stable range was observed on the stereographic plot. However, a univectorial decay to the origin at higher temperatures was not clearly discernible on the vector diagrams, as a result of either irregular direction changes occurring within the few remaining percent of the remanence (Specimen CC41-A) or of the suggested multicomponent structure (Specimen MP1-1). In the latter case, the Zijdeveld diagram indicates a steep component between NRM and 300°C, plus a dominant component between 300 and 450°C, then a near-horizontal component (see "B" component below) between 450 and 530°C, and possibly an unresolved final component. The straight-line segments, however, bypass the origin. Therefore, the average of the directions observed in the stable range has been taken as the characteristic direction in the case of this and all other specimens exhibiting this behaviour. The calculation of characteristic directions for the previously mentioned first group of specimens (Figure 3.3) is also based on the average of directions observed over the stable range, rather than on vector subtraction through Zijdeveld diagrams. These directions, however, were confirmed to be almost the same as those obtained from a least squares fit to the straight line marching to the origin on Zijdeveld diagrams.

In the third group of samples (Figure not shown), all the measurable magnetization was lost during the first

three to five steps of thermal demagnetization. By 400°C, their magnetization was either reduced to the order of the holder moment or to less than 2% of the NRM. The computation of characteristic directions in these cases is, therefore, based either on a vector subtraction or on averaging of closely spaced directions confined to the two or three highest temperature steps before the remanence was lost. The characteristic directions obtained in this third group were found to be similar to those from the first and second groups. This finding, coupled with the fact that the remanence is preserved in the last few percent of total magnetization in any specimen, lends credibility to the above analysis based on only a few points. A number of specimens of the third group, however, showed a sharp peak at 350°C in the decay curve, indicating thereby some mineralogical changes or acquisition of some spurious magnetization. Therefore, all specimens showing such erratic behaviour at 350°C have been rejected and a criterion of acceptability in this group has been that the specimens must show stability through 350°C or beyond.

All the characteristic directions corresponding to the "A" component are listed in Table 3.1 and are plotted in Figure 3.5. It must be pointed out here that specimens were heated to a much higher temperature than the highest temperature shown in the stability range of Table 3.1, but no stable component was identified at higher temperatures. Remanence directions at all temperatures are listed in

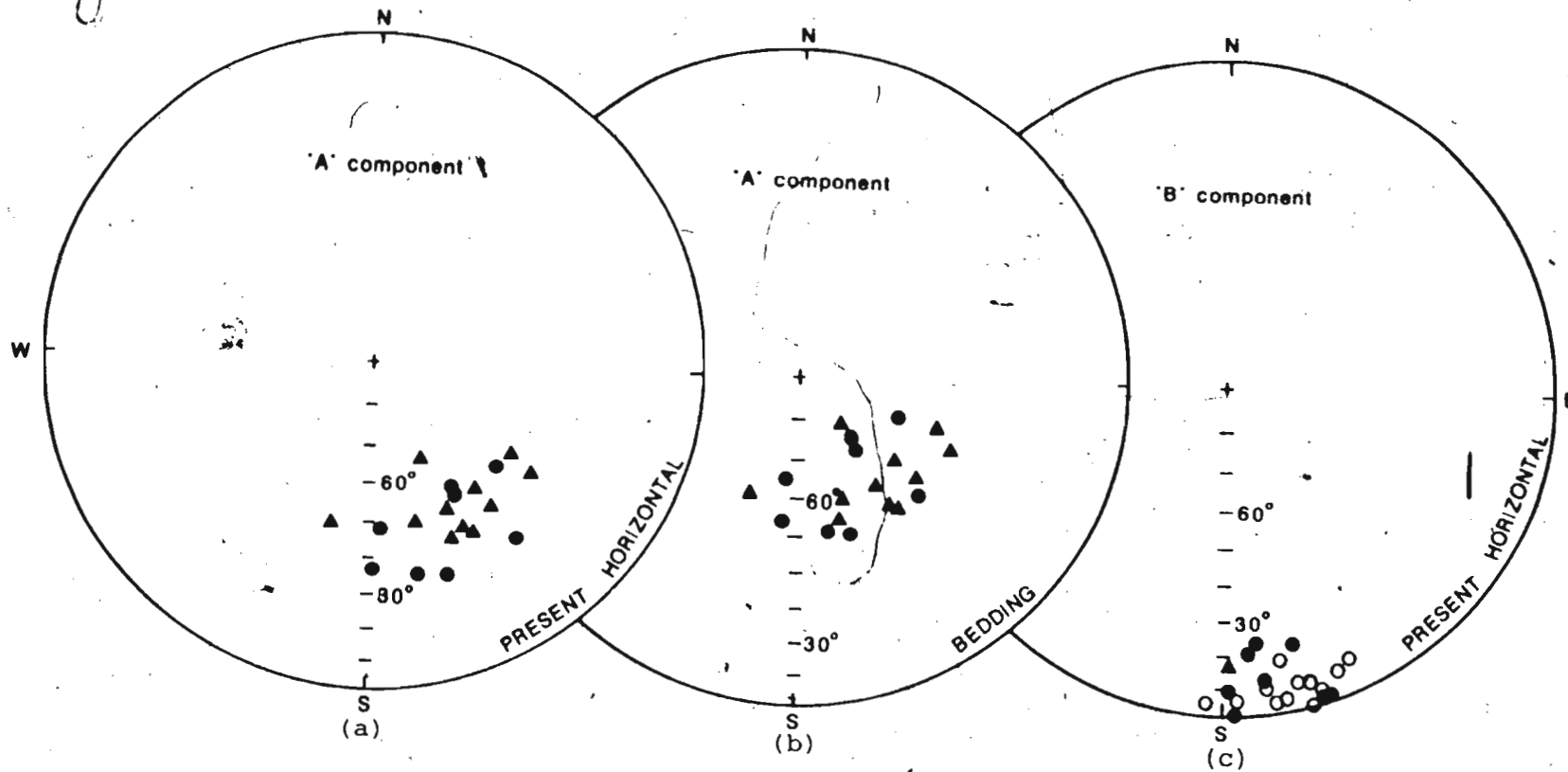


Fig. 3.5. Characteristic sample directions for "A" and "B" components of the Port au Port Group in Port au Port Peninsula. Circles (triangles) represent the Petit Jardin (March Point) Formation. Solid (open) symbols are projections on lower (upper) hemisphere. Equal area projection.

TABLE 3:1

THEMAL DEMAGNETIZATION RESULTS FROM THE PORT AU PORT GROUP
FOR THE "A" COMPONENT, PORT AU PORT AREA.

Site	Specimen	Characteristic direction				Stability range (° C)
		In situ		Tilt-corrected		
		D	I	D	I	
March Point Formation						
MP1	MP1-1	165.3	40.9	163.4	53.3	300-500
MP1	MP2-A	152.3	64.1	136.2	75.2	300-400
MP1	MP3-A	123.7	40.8	113.7	48.2	300-400 (v.s.)
MP2	MP7-B	193.4	48.4	200.6	59.2	350-400
MP2	MP9-B	140.2	49.4	130.4	59.2	300-400 (v.s.)
MP3	MP12-1	148.3	40.2	141.6	48.9	300-400 (v.s.)
MP3	MP13-1	121.9	48.8	109.3	53.1	300-350
MP3	MP14-1	139.0	43.4	130.1	50.7	300-450
MP4	MP19-A	150.0	42.1	143.7	50.8	300-400
MP4	MP20-1	163.9	48.2	159.1	58.1	350-400 (v.s.)
MP5	MP23-1	152.1	49.2	144.0	57.2	300-420 (v.s.)
Petit Jardin Formation						
CC5	CC17-2	175.7	48.4	185.6	64.7	450-500
CC6	CC22-2	147.2	54.2	137.4	71.0	400-560 (v.s.)
CC6	CC24-2	148.4	51.0	141.0	68.0	370-400
CC6	CC25-A	129.1	49.9	112.3	63.8	330-350
CC7	CC29-1	160.2	31.9	160.6	49.4	370-400
CC8	CC33-1	139.5	31.8	133.9	48.0	330-450
CC9	CC37-A	166.8	33.6	169.3	50.9	350-450
CC9	CC41-A	179.0	37.4	186.2	53.5	350-450

NOTES: Each direction, specified by declination (D) and inclination (I) above, represents either the mean direction over the given stability range or the one obtained after vector subtraction (v.s.) in the given range.

D is measured in degrees, clockwise from north.

I is measured in degrees, positive downward (negative upward).

Tilt correction: The procedure and relevant structural data are given in Appendix B.

Appendix B. A total of 19 samples (one specimen each) yielded an in situ mean direction corresponding to the "A" component at $D = 152.6^\circ$, $I = 46.4^\circ$ ($k = 28$, $95 = 6.5^\circ$, $N = 19$ samples). The direction after correction for bedding tilt (15°NW) is $D = 147.0$, $I = 59.4^\circ$ ($k = 27$, $95 = 6.6^\circ$, $N = 19$), the precision being almost unchanged because of the nearly uniform tilt. Making the tilt correction corresponds to the assumption that the "A" component was acquired before the Acadian or later (? See Chapter 2) time of deformation of the beds. This assumption seems to be justified from the arguments given in Section 3.4 below. The tilt-corrected direction corresponds to an antipole position of 3.4°N , 145.6°E ($d_p = 7.4^\circ$, $d_m = 9.9^\circ$). This falls near several reported Cambrian poles of cratonic North America. This result will be discussed later in Chapter 4.

Isolation of the "B" component represented by Figures 3.6 and 3.7 was fairly straightforward. After the removal of a steep component below 300°C , the direction became stabilized with shallow negative inclinations (Specimens CC35-A and CC44-1), shallow positive inclinations (Specimens CC38-1) or near-horizontal directions (Specimen CC30-A) in the southeast quadrant, persisting up to high temperatures. The resulting characteristic "B" directions are listed in Table 3.2 and are plotted in Figure 3.5(c). A total of 21 samples yielded a mean direction of fairly high precision at $D = 168.9^\circ$, $I = +1.0^\circ$ ($k = 35$, 95

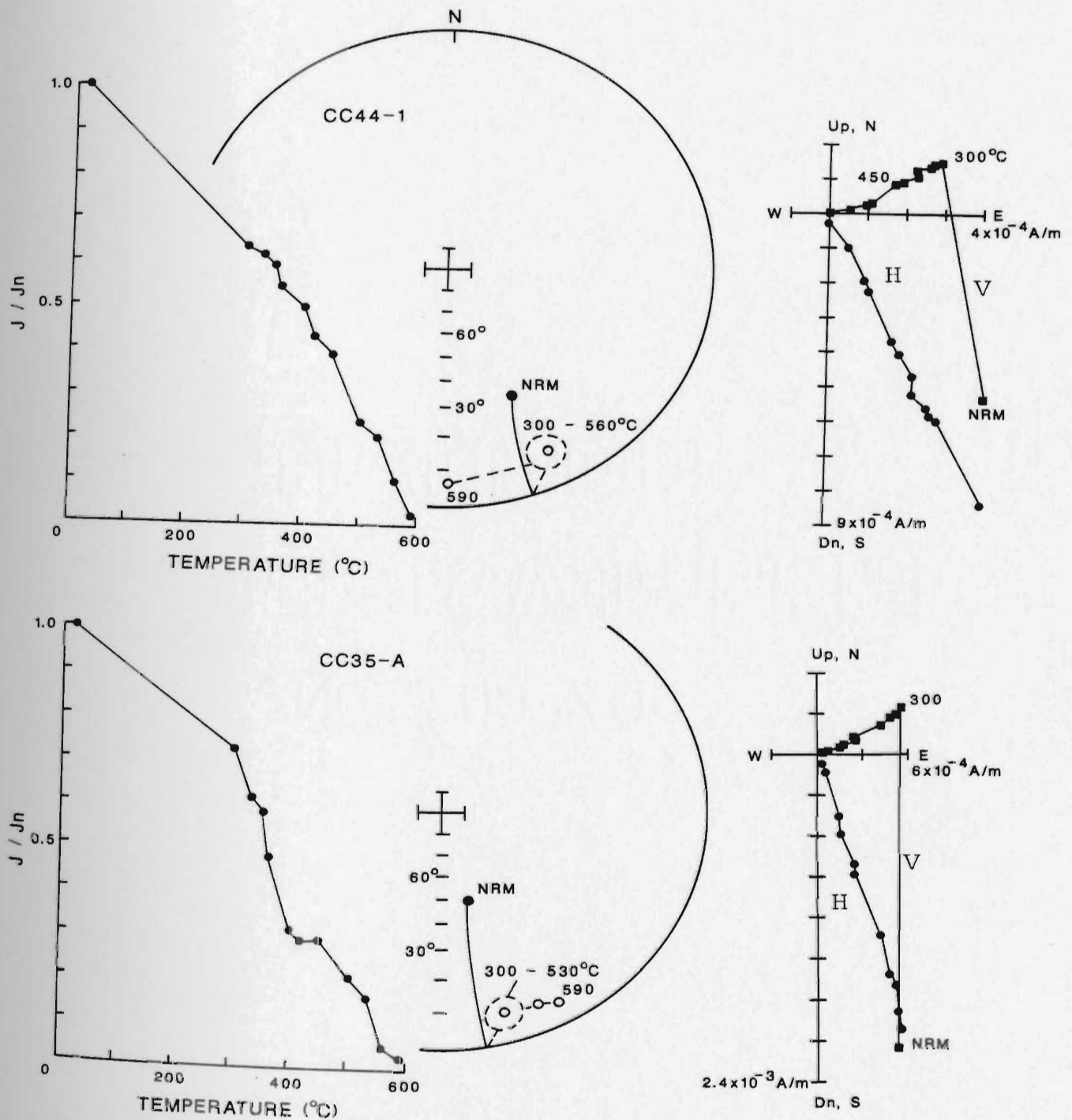


Fig. 3.6. Representative demagnetization results from 2 Port au Port Group specimens yielding "B" component. Conventions as in Figures 3.2-3.4, except on r.h.s., the vertical projection plane is now east-west.

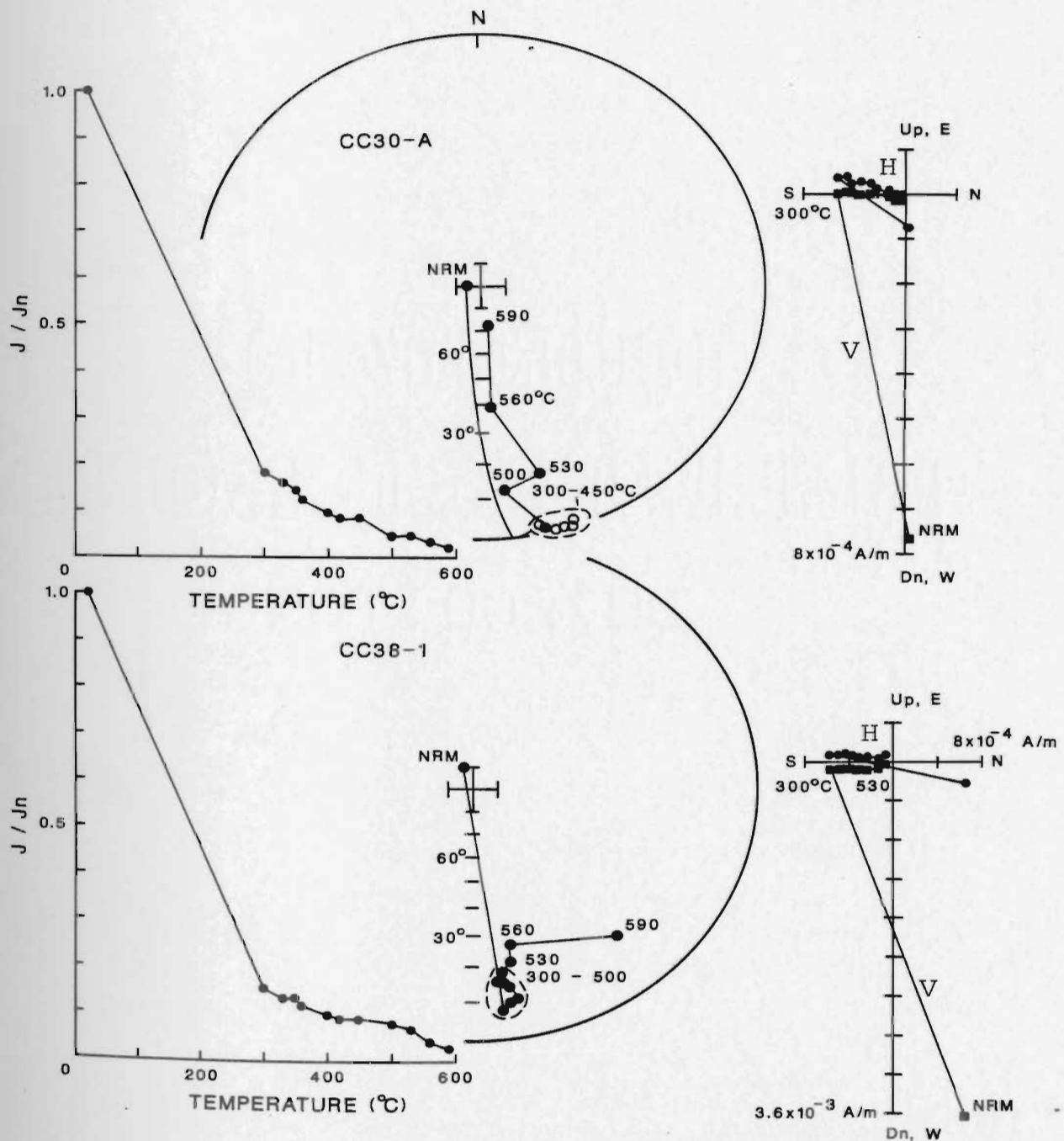


Fig. 3.7. Representative thermal demagnetization results from 2 Port au Port Group specimens yielding "B" component. Conventions as in Figs. 3.2-3.4.

TABLE 3.2

THERMAL DEMAGNETIZATION RESULTS FROM THE PORT AU PORT GROUP
FOR THE "B" COMPONENT, PORT AU PORT AREA.

Site	Specimen	In situ Characteristic		Stability range (° C)
		<u>direction</u>		
		D	I	
March Point Formation				
MP1	MP4-A	178.7	15.5	300-450
Petit Jardin Formation				
CC4	CC16-A	182.8	- 4.8	330-450
CC5	CC19-1	158.3	- 8.8	300-500
CC5	CC20-B	177.9	0.5	300-450
CC5	CC18-A	173.4	22.7	300-450
CC5	CC21-A	175.0	19.6	300-450
CC6	CC23-1	172.0	- 9.1	300-500
CC6	CC26-B	165.7	- 9.1	300-500
CC7	CC30-A	163.8	- 0.5	300-450
CC7	CC31-B	165.1	21.0	300-400
CC8	CC32-B	162.2	- 4.9	400-500
CC8	CC34-A	170.4	- 3.8	300-450
CC8	CC35-A	163.3	- 7.9	300-530
CC9	CC38-1	171.5	12.2	300-500
CC9	CC39-A	162.1	2.0	300-420
CC9	CC40-1	168.4	-16.8	300-450
CC10	CC42-A	178.7	9.4	300-500
CC10	CC43-A	176.5	- 5.7	300-450
CC10	CC44-1	154.8	-10.6	300-560
CC10	CC45-A	159.8	2.0	300-450
CC10	CC46-1	167.7	- 4.5	300-450

NOTES: As in Table 3.1.

TABLE 3.3

MEAN PALEOMAGNETIC DATA FOR THE "A" AND "B" COMPONENTS AFTER THERMAL
DEMAGNETIZATION OF THE PORT AU PORT GROUP, PORT AU PORT AREA.

	D_m	I_m	k	N	α_{95}	λ_p	Antipole
"A" component (in situ)	152.6	46.4	28	19	6.5		
"A" component (tilt-corrected)	147.0	59.4	27	19	6.6	41.2 S	3.4°N, 145.6°E (dp, dm = 7.4°, 9.9°)
"B" component (in situ)	168.9	0.8	35	21	5.5	0.4 S	40.2°N, 135.6°E (dp, dm = 2.7°, 5.5°)
"A" component, March Point Formation only (tilt-corrected)	141.4	58.1	27	11	8.9		
"A" component, Petit Jardin Formation only (tilt-corrected)	155.2	60.9	26	8	11.1		

NOTES: D_m = mean declination, degrees, clockwise from north; I_m = mean inclination, degrees, positive downwards; k = Fisher's precision parameter α_{95} = radius of the 95% circle of confidence, degrees; N = number of samples averaged; λ_p = paleo-latitude, degrees; dp, dm = semi-axes of 95% confidence oval.

= 5.5 , N = 21). This is the in situ direction, no correction for the bedding tilt having been made since it is assumed (Section 3.4) that the "B" magnetization was acquired after deformation of the strata. This direction corresponds to an antipole position of 40.2°N, 135.6°E (dp = 2.7°, dm = 5.5°), which falls near several reported Upper Paleozoic poles and also near some of the high-latitude Cambrian poles for North America.

It is seen from the above discussion that only 40 samples out of a total of 70 (about 57%) in the Port au Port area yielded meaningful characteristic directions along a SSE axis, based on the "A" or "B" component. However, in a number of the remaining samples, a swing in the magnetization direction along the NNW or NNE-SSW axis was observed upon demagnetization. Most of these specimens did not yield any stable end directions. Still, in some cases, anomalous stable directions with steep to intermediate inclinations were observed, the criteria for stability being the same as those discussed previously. Figure 3.8 is an example of two specimens exhibiting a northwesterly (Specimen MP10-1) or northeasterly (Specimen MP16-1) swing of direction with increasing temperatures. The erratic changes in the intensity of specimen MP10-1 in the range 300-400°C and a significant intensity increase above 400°C may be due to spurious magnetization acquired in the thermal demagnetizer, followed by a chemical change (production of magnetite) above 400°C, as observed in many limestones elsewhere (Lowrie and Heller, 1982).

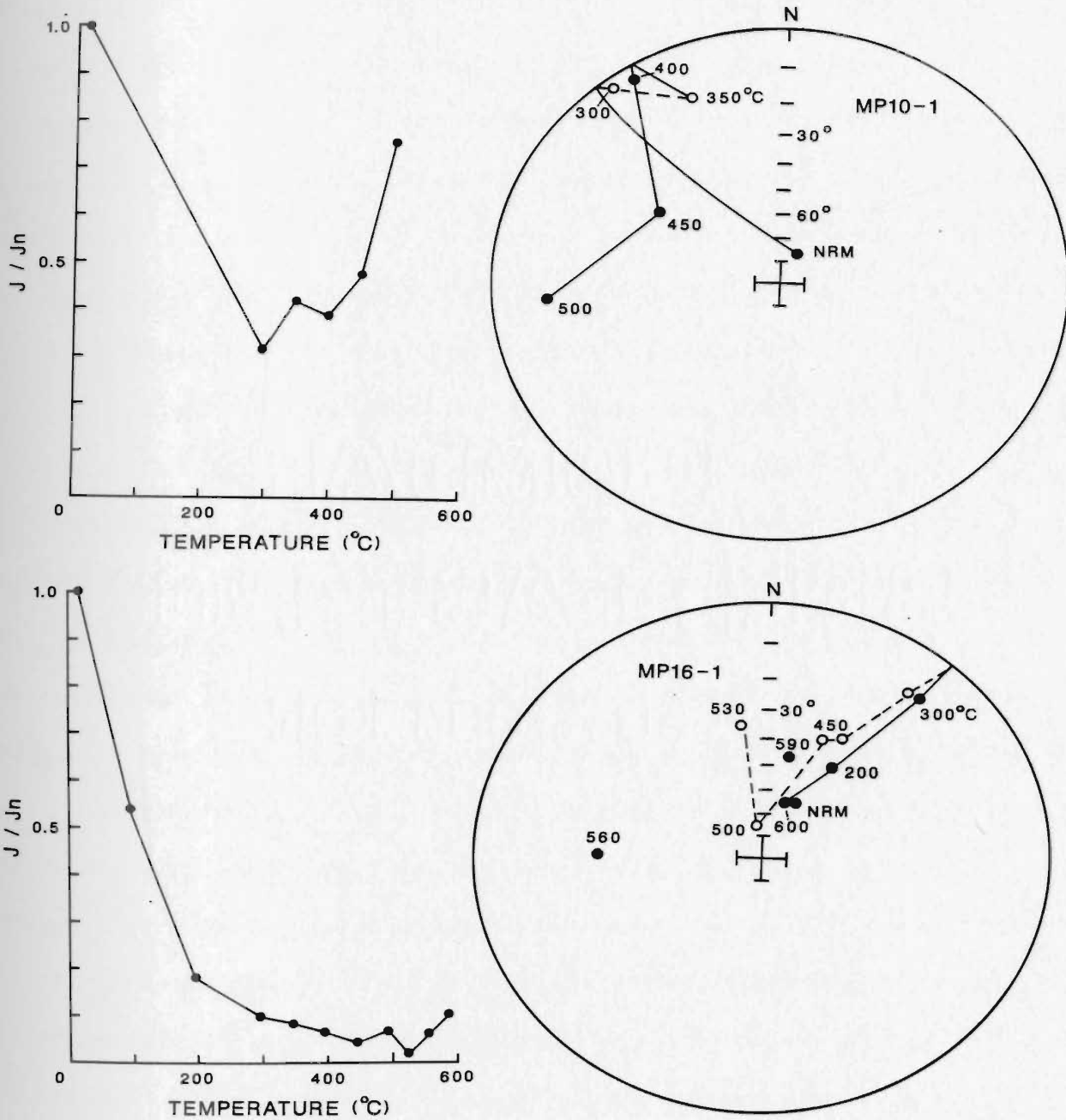


Fig. 3.8. Thermal demagnetization results for 2 Port au Port Group specimens showing normal polarity swing of directions at high temperatures, as opposed to the stable reverse characteristic directions (See previous figures and text). Conventions as in Fig. 3.2.

In specimen MP16-1 the steeply inclined downward-directed NRM swings systematically to the NE with increasing temperatures to 500°C, after which the direction becomes random. There is apparent stability in the range 400-450°C. The anomalous but apparently stable directions have been listed in Table 3.4 and are plotted in Figure 3.11(a). One interpretation of the steep directions of Figure 3.11(a) could be that these directions probably record a complete remagnetization in the present earth's field. However, the entire distribution of all the points in Figure 3.11(a) coupled with the demagnetization behaviour of specimens as exhibited in Figure 3.8, is indicative of a multicomponent system formed by subcomponents of opposite polarity, having closely overlapping stability spectra and directed along one or more paleomagnetic axes. The entire analysis of Port au Port area rocks has indicated the dominating presence of a NNW-SSE axis. While the SSE directions along that axis have been clearly identified from the "A" and "B" components, stable NNW directions were not found in the present investigation. The results do, however, indicate the presence of multicomponents, two of which could be successfully isolated in the present investigation.

3.2.2 Port au Choix area

All the 11 samples (one specimen each) of the Port au

Choix area from the Petit Jardin Formation were thermally demagnetized in detail (12 steps between 100°C and 500°C, see Appendix A). As it turned out, the specimens lost all their measurable magnetization by 450°C. From thermal demagnetization, two groups of stable but different characteristic directions were obtained. Figures 3.9-3.10 are representative of the demagnetization behaviour of each group of directions. In one group, represented by Figure 3.9 (Specimens PC112-A and PC115-1), a steeply inclined, downward-directed NRM systematically moved northwards and a stable direction with a shallow negative inclination was revealed in the range 300-450°C; beyond this the intensity fell to 1% of the NRM which was below the minimum level for reliable measurements. In the second group, represented by Figure 3.10 (Specimens PC116-A and PC120-C), only intermediately steep downward directions, with stability in the range 300-400°C, were observed. However, there is a trend for the remanence vector to migrate towards the shallower directions (e.g., Specimen PC116-A), but it seems that this trend could not be completed because of almost total intensity loss beyond 450°C. Two specimens (figure not shown) yielded apparently stable directions intermediate between these two groups. Stable end directions obtained from all the samples are plotted in Figure 3.11b and are listed in Table 3.5.

It is at once evident from Figure 3.11b that the

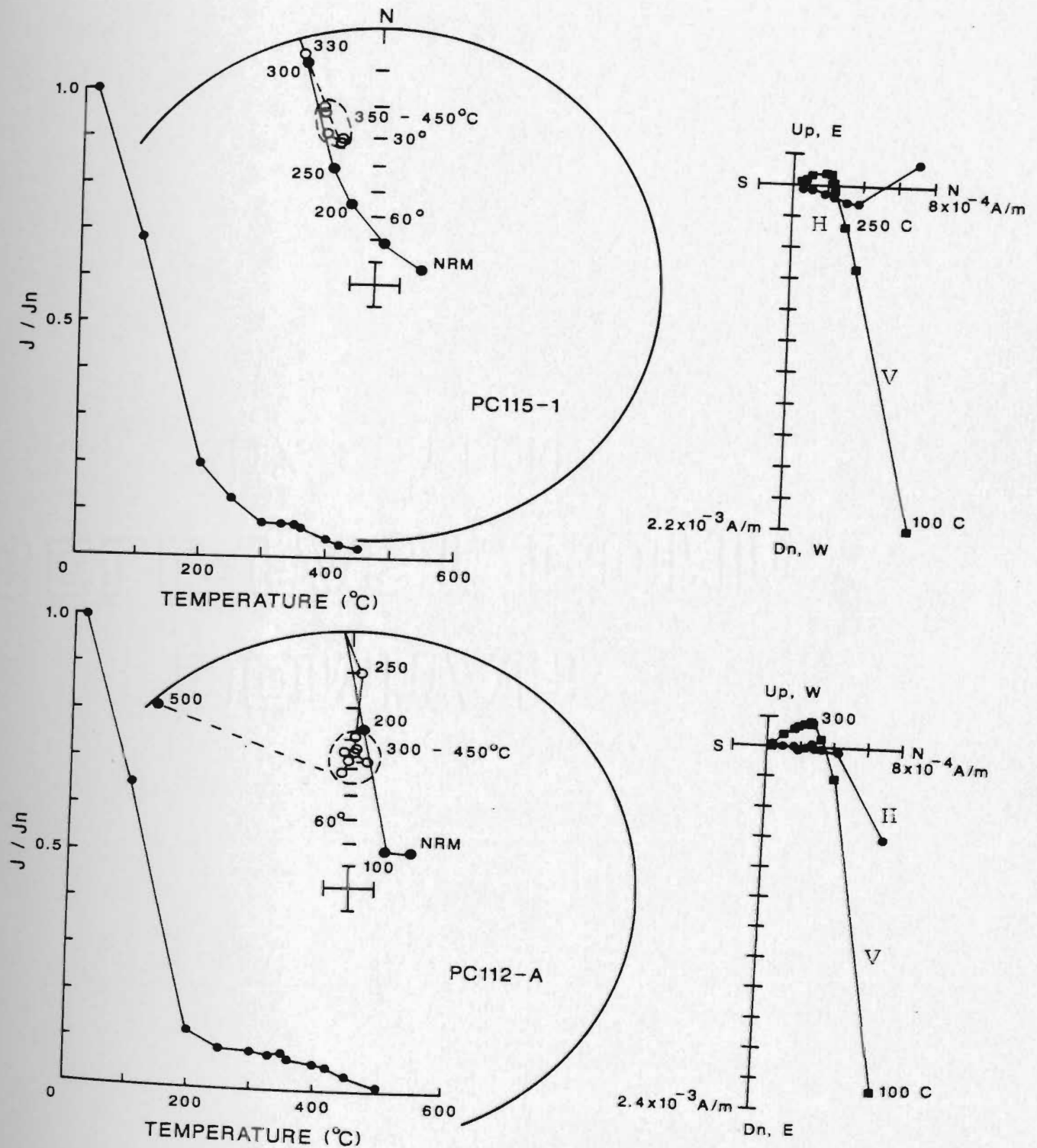


Fig. 3.9. Thermal demagnetization results for 2 Port au Port Group specimens from Port au Choix area yielding a characteristic northerly direction with intermediate negative inclination. NRM directions are not plotted on the vector diagram. Conventions as in Fig. 3.2-3.4.

Fig. 3.10. Thermal demagnetization results for 2 specimens from Port au Port Group, Port au Choix area, yielding intermediately steep down directions. Conventions as in Figs. 3,2-3.4.

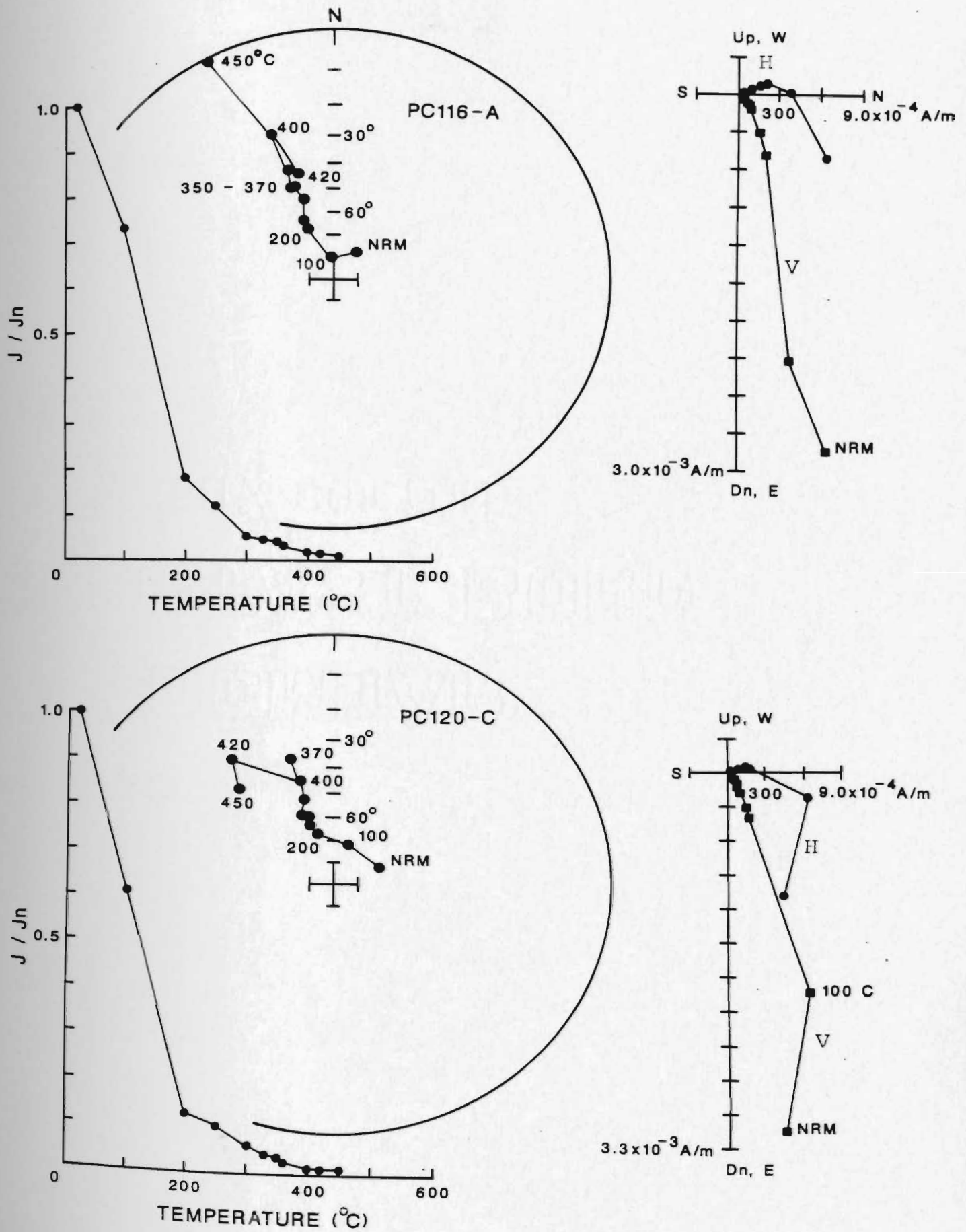


Fig. 3.10.

Fig. 3.11. Uncharacteristic stable directions from Port au Port Group: (a) Port au Port area samples (symbols as in Fig. 3.5); (b) Port au Choix area samples. \oplus and \times are the directions of the axial dipole and present earth's field at the sampling site.

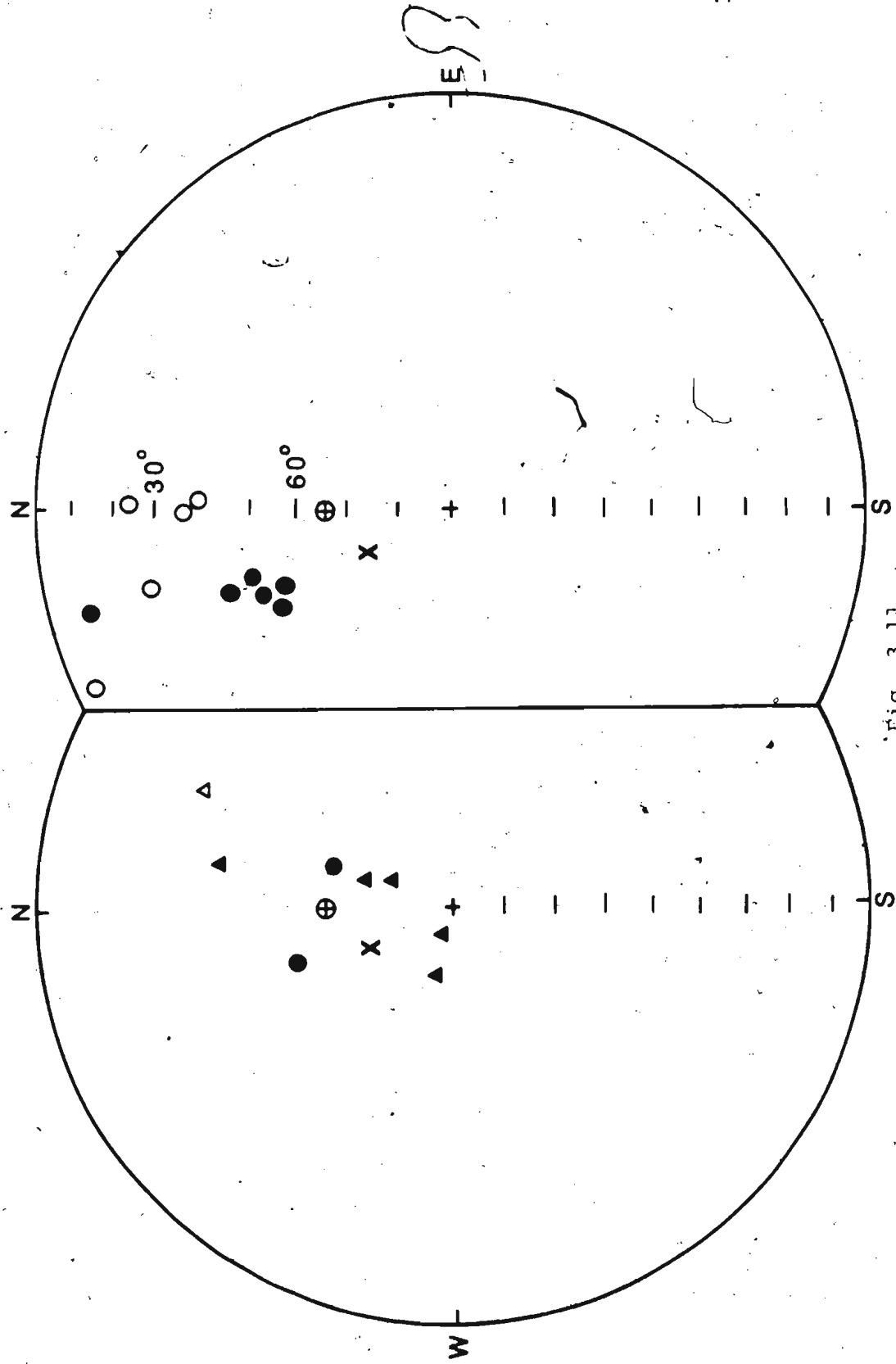


Fig. 3.11 (b)

(a)

TABLE 3.4

ANOMALOUS DIRECTIONS FROM THE PORT AU PORT GROUP AFTER
THERMAL DEMAGNETIZATION, PORT AU PORT AREA.

Site	Specimen	<u>In situ characteristic</u>		Stability range
		<u>direction</u>		
		D	I	(° C)
MP1	MP5-A	284.9	76.9	300-350
MP2	MP6-B	150.6	76.2	300-400
MP3	MP15-2	295.0	84.5	300-350
MP4	MP16-1	25.8	-35.0	400-450
MP5	MP21-B	18.8	72.6	300-400 (v.s.)
MP5	MP22-2	12.3	42.7	300-350
MP5	MP25-2	26.8	78.2	300-350
CC3	CC9-2	341.9	57.8	300-350
CC7	CC27-B	20.7	65.6	NRM-530

TABLE 3.5

THERMAL DEMAGNETIZATION RESULTS FROM THE PORT AU PORT GROUP,
PORT AU CHOIX AREA.

Site	Specimen	<u>In situ characteristic</u>		Stability range
		<u>direction</u>		
		D	I	(° C)
PC23	PC111-A	1.6	-38.8	350-450
PC23	PC112-A	0.2	-35.2	300-450
PC23	PC112-1-A	333.5	-6.4	400-420
PC23	PC113-A	344.5	9.9	330-370
PC23	PC114-A	1.1	-23.4	330-450
PC23	PC115-1	344.7	-25.3	350-450
PC24	PC116-A	339.8	42.6	330-420
PC24	PC117-A	331.4	52.2	330-420
PC24	PC118-A	337.3	49.7	330-400
PC24	PC119-B	336.0	55.0	330-400 (v.s.)
PC24	PC120-C	342.2	49.1	300-400

Symbols as in Table 3.1.

sample directions have a smeared distribution along the NW axis, comprising a range of intermediately steep vectors with positive inclination to moderately shallow vectors with negative inclinations, suggesting the presence of unresolved components in some of them. The end directions exhibited by four specimens of the first group with moderately shallow negative inclinations probably represent a paleomagnetic component with $D = 356.7^\circ$ and $I = -30.9^\circ$ ($N = 4$, $\alpha_{95} = 11.8^\circ$, $k = 62$). The inclination of this vector is intermediate between the inclinations of the "A" and "B" components isolated from the Port au Port area samples and might represent an age of magnetization in between. However, being based on only 4 samples, no significance could be attached to such a conclusion and hence, these results were not used for a paleopole calculation. The main body of results from the Port au Choix area, however, strongly indicates a magnetization significantly different from the Port au Port area rocks.

3.3 Magnetic mineralogy

In order to identify the magnetic phases present in these weakly magnetized carbonates, isothermal remanent magnetization (IRM) studies were done on 10 fresh samples (one specimen each) chosen from different sites. Samples were given an IRM with a D.C. Varian electromagnet in a stepwise manner up to the maximum attainable field of 0.82 Tesla. Three distinct kinds of behaviour typical of many

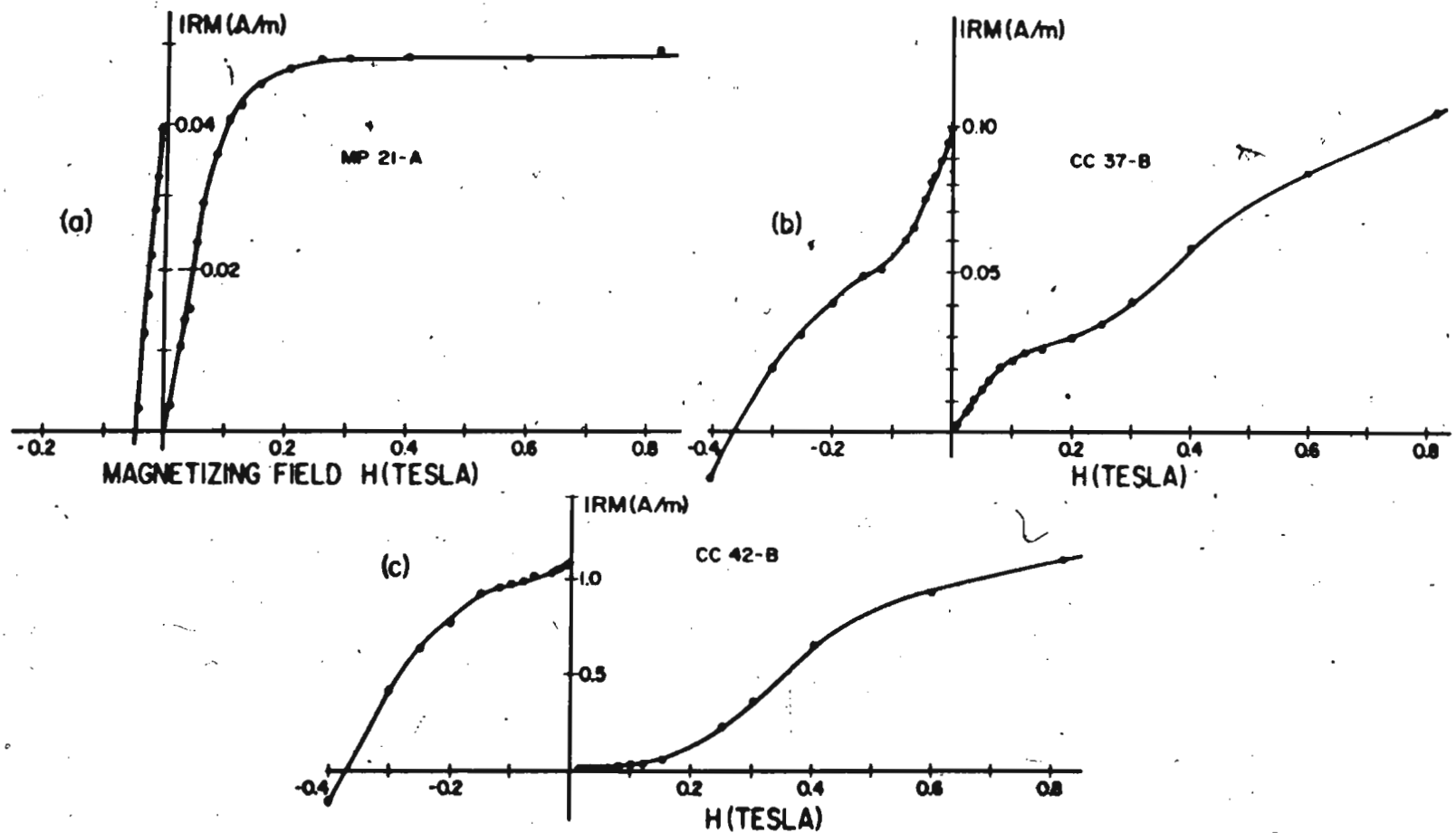


Fig. 3.12. Representative IRM acquisition and back-field characteristics for Port au Port Group specimens.

limestones (Lowrie and Heller 1982) were observed. The first of these ("Type 1"; Figure 3.12a) is characterized by a very steep initial slope which flattens off at 0.25T. When the field was applied stepwise in the opposite direction, the remanence dropped off sharply, showing the presence of a single magnetic phase (coercivity of remanence, $H_{CR} \sim 0.05T$). The low-coercivity phase which dominates the remanence of the samples of this type is most likely magnetite. The fact that Specimen MP 21-A becomes magnetically saturated at about 0.25T rules out a significant content of hematite, although goethite may remain unactivated in fields up to 1T (Lowrie and Heller, 1982) and its presence in these samples cannot be ruled out.

"Type 2" behaviour is represented by specimen CC37-B of Figure 3.11b. The IRM acquisition curve shows a fairly steep slope up to 0.1T, after which it first tends to flatten off but then again rises sharply, showing no saturating trend beyond 0.25T. The back-field characteristics show the presence of more than one magnetic phase in this sample. The low-coercivity phase characterized by a high initial slope in the curve indicates the presence of magnetite coexisting with a phase yielding a high value of H_{CR} , which could be either hematite or goethite, or both.

"Type 3" behaviour is represented by Specimen CC42-B of Figure 3.12c. The acquisition curve is almost flat

initially up to 0.15T, after which the remanence increases sharply up to 0.4T. The curve shows a tendency of flattening off beyond 0.4T. The back-field characteristics do not show any evidence of a low-coercivity phase present in the specimen. This suggests that magnetite is probably absent or unimportant in these samples, which indicates that they contain, exclusively, either hematite or goethite or both. Thus the IRM results indicate the presence of varying amounts of magnetite, hematite and/or goethite in these rocks. IRM characteristic curves of type 2 and 3 were, however, more common, suggesting a dominating influence of hematite and/or goethite.

A comparison of thermal demagnetization behaviour and IRM characteristics of the specimens from the same sample shows that the "A" component was either isolated from type 1 or type 2 samples. The B component was more commonly associated with type 3. Type 2 IRM curves frequently did not yield any stable direction other than a steep one. This suggests that the "A" component probably resides in magnetite, whereas hematite carries the remanence of the "B" component. The steep viscous component might be carried either by magnetite or goethite, the latter resulting from the recent weathering of these rocks. On the basis of blocking temperature alone, however, it is difficult to distinguish magnetite from hematite as the remanence carrier, since the stability range for both the "A" and "B" components is always below the Curie point of

magnetite (Tables 3.1 and 3.2). It is quite possible that fine-grained hematite carries the "B" remanence.

3.4 Discussion

It is probable that magnetites carrying the "A" component occur as detrital grains which have aligned themselves with the ambient geomagnetic field during or shortly after deposition. Alternatively, the original magnetization may have been reset as a result of heating due to burial over geological periods of time. However, the conodont colour alteration index (CAI) for the Port au Port area is 1 (Nowlan and Barnes, 1985), which suggests a maximum burial temperature of 50-60°C (Epstein et al., 1977). Theoretical calculations (Pullaiah et al., 1975) indicate that such a low-level heating of rocks over a period of 100 m.y. would not cause the realignment of magnetites blocked at a temperature of 300°C or above. The blocking temperatures in the Port au Port Group rocks are commonly higher than 400°C (Tables 3.1 and 3.2).

A different, indirect kind of argument against remagnetization can be made, based on a comparison of the present result with published results. This shows that the pole position corresponding to the "A" component falls near the southeastern cluster of the streaked Cambrian poles (Chapter 4) and is significantly displaced from the Upper Paleozoic poles. Thus the "A" component most likely represents a Middle to Late Cambrian field of western

Newfoundland. This interpretation should be regarded as tentative because the result is based on only 19 samples representing a limited stratigraphic thickness. A detailed study of the entire Cambrian section from various other localities is needed to establish a more complete record of the Cambrian field for western Newfoundland.

The "B" component, which is strongly indicated to reside in hematite, may not represent the Cambrian field, although the corresponding pole position falls close to some reported Cambrian poles (Chapter 4, Figure 4.1). The "B" component pole (CCO in Figure 4.1) is also consistent with some Kiaman poles plotted in the above figure along with Cambrian poles. Since hematite is not a likely primary component of carbonates, it is more likely that the "B" component reflects a Kiaman remagnetization. Hematite in carbonates could form diagenetically from goethite or by oxidation of detrital magnetite. More commonly, however, hematization in carbonates results from secondary oxidation of pyrite or ferroan dolomite (Gillett, 1982) which are pervasively present in these rocks (N. Chow, personal communication). Ferroan dolomites are very susceptible to alteration and in some cases can be entirely converted to calcite pseudomorphs ("dedolomite"). Hematite and other iron oxides such as goethite are commonly associated with dedolomite and are generally interpreted as by-products of dedolomitization of ferroan dolomites (Frank, 1981). If indeed hematite in the present study is a result of

dedolomitization or secondary oxidation of pyrite, the magnetization acquired by hematite would be a chemical remanent magnetization (CRM). The time of dedolomitization would be most probably Late Carboniferous to Early Permian, as the "B" component pole is consistent with other Kiaman pole positions. A Kiaman magnetization related to dedolomitization has also been reported (Elmore et al., 1985) from the Lower Ordovician Kindblade Formation in south-central Oklahoma.

CHAPTER 4
CAMBRIAN PALEOPOLES WITH RESPECT TO CRATONIC
NORTH AMERICA

A number of paleomagnetic results have been reported from Cambrian rocks of North America. Despite the increase in the data base, the results from the Cambrian rocks have so far yielded conflicting interpretations. A list of the published Cambrian poles is given in Table 4.1 and they are plotted in Figure 4.1. A few Late Precambrian results are also included. The numbering of the poles referred to in this chapter corresponds to that in Table 4.1 and Figure 4.1. Also plotted in Figure 4.1 are some of the reported reliable poles of "Kiaman" age (listed in Table 4.2), mostly overprints isolated from Cambrian to Lower Carboniferous rocks. As is evident from Figure 4.1, the Cambrian poles are streaked between the equator at about 180° longitude (close to Late Precambrian pole positions) and the cluster of high latitude Late Paleozoic poles (centered at about 45°N , 120°E). The pole position corresponding to the "A" component of the present study (Pole 25) falls near the southeastern cluster of the streaked Cambrian poles, whereas the "B" component pole (CCO) falls close to the northwestern cluster. It was demonstrated in Section 3.4 that the "B" magnetization is a Kiaman overprint, which in Figure 4.1 appears to agree very well with other reported Kiaman overprints isolated from

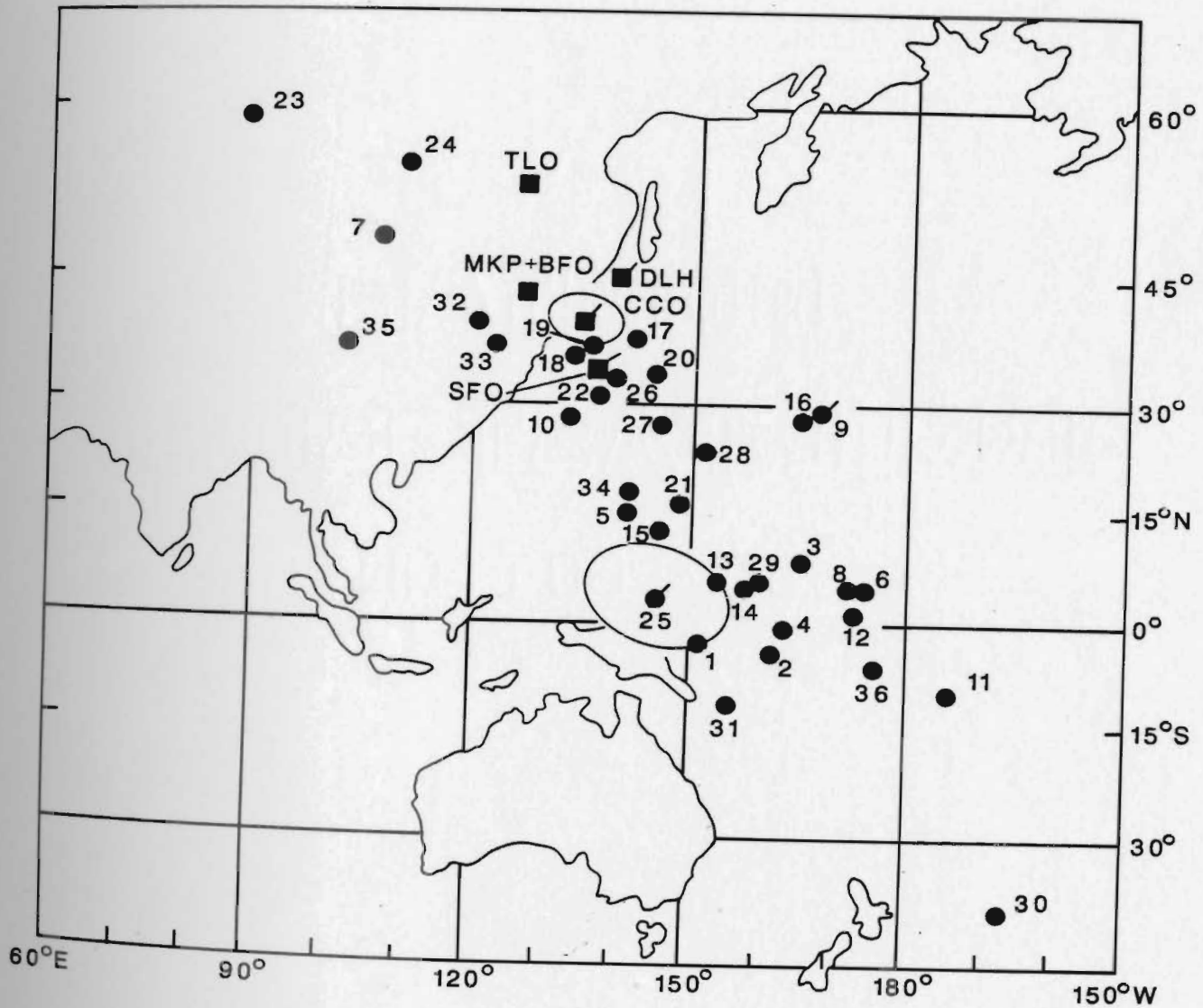


Fig. 4.1. Selected paleopoles from Cambrian rocks of North America plotted with the "A" and "B" component poles of the Port au Port Group and some Late Paleozoic poles (Tables 4.1, 4.2). Circles, poles cited as Cambrian; squares, poles cited as Late Paleozoic (Kiaman). Symbols with bar, Newfoundland poles; without bar, mainland poles.

TABLE 4.1

SELECTED PALEOMAGNETIC POLES FROM LATE PRECAMBRIAN TO CAMBRIAN ROCKS
OF NORTH AMERICA.

Pole No.	Rock unit and location	Age	Pole Position	Reference
1.	Grenville dikes, Québec and Ontario	Late Precambrian to Early Paleozoic	3°S, 151°E	Murthy (1971)
2	Franklin rocks, Canadian Arctic (Group A)	675-625 Ma	4°S, 161°E	Palmer and Hayatsu (1975)
3	Franklin rocks, Canadian Arctic (Group B)	675-625 Ma	8°N, 166°E	Palmer and Hayatsu (1975)
4	Coronation sills, North-western Canadian Shield	647 Ma	1°S, 163°E	Robertson and Baragar (1972)
5	Colorado intrusives I	Late Precambrian- Early Ordovician (704-485 Ma)	15°N, 142°E	French et al. (1977)
6	Colorado intrusives II	Late Precambrian- Early Ordovician (704-485 Ma)	5°N, 174°E	French et al. (1977)
7	Colorado intrusives III	Late Precambrian- Early Ordovician (704-485 Ma)	48°N, 107°E	French et al. (1977)

TABLE 4.1, (CONT'D)

Pole No.	Rock unit and location	Age	Pole Position	Reference
8	Cloud Mountain Basalt, western Newfoundland	Late Precambrian to Early Cambrian (605 Ma)	5°N, 172°E	Deutsch and Rao (1977)
9	Bradore Formation, Western Newfoundland	Early Cambrian	29°N, 167°E	Rao and Deutsch (1976)
10	Wood Canyon Formation, Desert Range, Nevada	Early Cambrian	28°N, 134°E	Gillett and Van Alstine (1979)
11	Buckingham Volcanics, Group I, Quebec	Early Cambrian (573 Ma)	10°S, 186°E	Dankers and Lapointe (1981)
12	Buckingham Volcanics, Group II, Quebec	Early Cambrian (573 Ma)	1°N, 173°E	Dankers and Lapointe (1981)
13	Buckingham Volcanics, Group III, Quebec	Early Cambrian (573 Ma)	6°N, 154°E	Dankers and Lapointe (1981)
14	Tapeats Formation, Arizona	Early to Middle Cambrian	5°N, 158°E	Elston and Bressler (1977)
15	Ophiolite complex, Quebec	550 Ma	13°N, 146°E	Sequin (1976)
16	Waynesboro Formation, eastern Tennessee	Early Middle Cambrian	28°N, 165°E	Watts et al. (1990a)

TABLE 4.1, (CONT'D)

Pole No.	Rock unit and location	Age	Pole Position	Reference
17	Rome Formation, eastern Tennessee	Early Middle Cambrian	38°N, 142°E	Watts et al. (1980a)
18	Carrara Formation, Group I	Middle Cambrian	36°N, 134°E	Gillett and Van Alstine (1979)
19	Carrara Formation, Group II and Bonanza King Formation	Middle Cambrian	37°N, 136°E	Gillett and Van Alstine (1979)
20	Riley Formation, Hickory Member, Texas	Middle Cambrian (Lower Dresbachian)	34°N, 145°E	Watts et al. (1980b)
21	Wichita Granites (AF demagnetization), Oklahoma	Middle Cambrian (525 Ma)	16°N, 149°E	Vincenz et al. (1975)
22	Wichita Granites (thermal demagnetization), Oklahoma	Middle Cambrian (525 Ma)	31°N, 138°E	Vincenz et al. (1975)
23	Abrigo Formation, Arizona	Middle to Late Cambrian	59°N, 89°E	Elston and Bressler (1977)
24	Muav Formation, Arizona	Middle to Late Cambrian	55°N, 110°E	Elston and Bressler (1977)

TABLE 4.1, (CONT'D)

Pole No.	Rock unit and location	Age	Pole Position	Reference
25	March Point and Petit Jardin Formations of Port-au-Port Peninsula, western Newfoundland	Middle to Late Cambrian	3.4°N, 145.6°E	This study
26	Riley Formation, Cap Mountain Member, Texas	Late Cambrian (Early to Middle Dresbachian)	33°N, 140°E	Watts et al. (1980a)
27	Riley Formation, Lion Mountain Member, Texas	Late Cambrian (Late Dresbachian)	27°N, 146°E	Watts et al. (1980b)
28	Wilburns Formation, Morgan Creek-Welge Member, Texas	Late Cambrian (Early to Middle Franconian)	24°N, 151°E	Watts et al. (1980b)
29	Wilburns Formation, Point Peak Member, Texas	Late Cambrian (Upper Franconian)	6°N, 159°E	Van der Voo et al. (1976)
30	Lamotte Formation IIa, south-eastern Missouri	Late Cambrian	38°S, 192°E	Al-Khafaji and Vincenz (1971)
31	Lamotte Formation, IIb, south-eastern Missouri	Late Cambrian	12°S, 155°E	Al-Khafaji and Vincenz (1971)

TABLE 4.1, (CONT'D)

Pole No.	Rock unit and location	Age	Pole Position	Reference
32	Nolichucky Formation, eastern Tennessee	Late Cambrian	40°N, 120°E	Gillett (1982)
33	Colorado intrusives	Cambro-Ordovician	37°N, 122°E	Larson and Mutschler (1971)
34	McClure Mountain alkali complex, Colorado	Cambro-Ordovician	18°N, 142°E	Lynnes and Van der Voo (1984)
35	Black Canyon diabase, southwestern Colorado	Cambro-Ordovician	37°N, 102°E	Larson et al. (1985)
36	Taun Sauk Limestone	Late Cambrian	3.6°S, 175.6°E	Dunn and Elmore (1985)

NOTES: The pole positions shown are as cited by the respective authors and are generally considered to represent geographic north poles. Ages in Ma in brackets are based on radiometric determinations. Pole numbers are very roughly in decreasing order of geological age.

TABLE 4.2

SOME LATE PALEOZOIC POLES OF NORTH AMERICA.

Pole No.	Rock unit and location	Geological Age	Pole Position	Reference
DLH	Deer Lake Group, western Newfoundland	Early Carboniferous	45°N, 140°E	Irving and Strong (1984a)
MKP	See Notes	Late Carboniferous to Early Permian	43°N, 126°E	Irving and Irving (1982)
TLO	Trenton Limestone, Quebec and Ontario	Middle Ordovician	53°N, 127°E	McCabe et al. (1984)
BFO	Bonneterre Formation	Late Cambrian	43°N, 126°E	Wisniowiecki et al. (1983)
CCO	Port au Port Group, western Newfoundland	Middle to Late Cambrian	40.2°N, 135.6°E	This study
SFO	Bay St. George	Early Carboniferous	34.5°N, 137.3°E	Murthy (1985)
MMS	McClure Mountain, alkali complex, Colorado	Cambro-Ordovician	43°N, 114°E	Lynnes and Van der Voo (1984)

NOTES: In each case above the respective authors consider the magnetization as of a Kiaman age (Late Carboniferous to Early Permian).
MKP is the mean Kiaman Pole calculated for the interval 265-295 Ma based on a number of studies compiled in the cited reference and mentioned in Irving and Strong (1984a).

western Newfoundland rocks (poles DLH & SFO) and from other localities of the North American craton (poles MKP, BFO and TLO). The "A" pole is consistent with a number of reported Cambrian poles, but is significantly misaligned with other poles reportedly representing a Cambrian magnetization. As demonstrated by Gillett (1981), the discrepancies are mainly due to one of two causes, tectonic rotation or Late Paleozoic remagnetization or, in some cases, due to both. It is to be noted that many of these poles come from structurally complex rock sequences and it is quite probable that those plotting close to the Late Paleozoic section of the APWP do not record a truly Cambrian field. In the following discussion, possible explanations for the discrepancies, as expressed by the original authors or otherwise, will be advanced as the results of Table 4.1 are discussed in turn.

The only Cambrian strata studied paleomagnetically in western Newfoundland are the Lower Cambrian Bradore sandstone. Two separate studies, one by Black (1964) and the other by Rao and Deutsch (1976), were reported from this. Black's result was based on only AF demagnetization to 30 mT of these hematite bearing rocks, the effectiveness of which was disputed by Rao and Deutsch (1976). They obtained new and different results (Pole 9) after a thorough thermal demagnetization. Their final result is based on the average of sample directions obtained at 665°C, using the best grouping criterion. However, sole

analysis of data in such a manner seems insufficient and a re-analysis of the results would be desirable. Their in situ mean direction of magnetization ($D = 146^\circ$, $I = 18^\circ$) lies between the "A" and "B" magnetizations of this study. It is possible, therefore, that the Bradore Pole reflects a vector sum of unresolved components. The origin of the hematite remanence in the Bradore study merits further investigation. In a recent study (Hodych et al., 1984, 1985) of hematite-bearing rocks it has been demonstrated that the only characteristic magnetization preserved in the hematite was acquired about 130 m.y. after deposition of the rocks. Therefore, hematite remanence has to be interpreted with caution.

Gillett and Van Alstine (1979) originally explained their Cambrian poles (10, 18 and 19) from the Desert Range of Nevada in terms of tectonic rotations. Their argument was based on a comparison with the remanence direction obtained from the Tapeats Sandstone of the Grand Canyon (Pole 14), which is partially coeval with the Wood Canyon-Bonanza King Sequences (Poles 10, 18 & 19). Gillett and Van Alstine (in Gillett, 1981) have since argued that a Late Paleozoic remagnetization rather than tectonic rotation was responsible for the directions giving poles 10, 18 and 19 in Figure 4.1.

A result from the ophiolite complex of Quebec (Pole 15, Seguin, 1976) was derived from a structurally complex area. A re-study of these rocks (Seguin, 1979) yielded a

different result. In the latter study, AF and thermal demagnetizations yielded different results and they are not quoted here. Seguin (1979) noted heterogeneous magnetic behaviour which was not well characterized. There was much scatter in his data, apparently because of the presence of multicomponents. Occasionally two polarities were present within the same specimen.

Watts et al. (1980a) and Gillett (1982) have reported results (Poles 16, 17 and 32) from the structurally complex Valley and Ridge Province of eastern Tennessee. Watts et al. (1980a) presented data (Poles 16, 17) from sites in a number of thrust sheets in the Rome Formation. These strata were shown to have stable, pre-thrusting characteristic magnetizations that reside in hematite. They concluded that no vertical-axis rotation of the thrust sheets as a whole relative to each other took place. Their data, however, show much scatter in declination which requires explanation.

Gillett (1982) reported results from the Late Cambrian Nolichucky Formation (Pole 32). Though the magnetization is shown to reside in detrital magnetite, making it possible that the remanence is primary, a structural test based on different thrust sheets with different bedding attitudes proved negative. Therefore Gillett (1982) did not rule out the possibility of remagnetization. His preferred interpretation was, however, a relative tectonic rotation between the sites, as the structural correction

resulted in a discrepancy mainly in declinations between the sites.

A detailed paleomagnetic study was done on Middle to Late Cambrian strata from the Llano uplift in Texas (Van der Voo et al., 1976; Watts et al., 1980b). Their results show a progression of paleomagnetic pole positions with geologic age (Poles 20, 26-29). Watts et al. (1980b) attempted to interpret the scatter between these poles in terms of apparent polar wandering along a Cambrian loop, situated in the Pacific Ocean, on which the presumed Early and Late Cambrian poles occupy near-equatorial present latitudes, while poles of presumed intermediate Cambrian age occupy high ($\leq 60^{\circ}\text{N}$) latitudes. The magnetizations from the Llano uplift, however, reside in hematite and are from a thin, cratonic section that contains many major unconformities (Gillett, 1982). Therefore, a diagenetic chemical remanent magnetization partially or completely, is a possibility.

The Lamotte Formation of Missouri (Poles 30-31) has been studied by Al-Khafaji and Vincenz (1971). Based on AP demagnetization only, these weakly magnetized white sandstones gave scattered results. They found that the specimens failed to be completely demagnetized even in fields as high as 280 mT. A detailed mineralogical examination showed a complex magnetic mineralogy in these rocks. Furthermore, their thermal demagnetization did not yield reliable results.

The Wichita granites (Poles 21, 22) have been investigated by Vincenz et al. (1975). The pole positions corresponding to thermal and AF results are seen to be significantly different. For both methods of demagnetization, the results were greatly scattered and the remanence changes produced during demagnetization were often erratic and incomplete. Vincenz et al. (1975) attributed the scatter to a complicated remagnetization history. They speculated that most of the magnetization might have been acquired during a Late Paleozoic hydrothermal event.

Results from the Muav and Abrigo Formations of the Colorado Plateau giving high latitude poles (23 and 24) were reported by Elston and Bressler (1977). The magnetization in these Formations resides in hematite.

Samples were obtained near a Cambrian-Devonian disconformity. Therefore, remagnetization due to near-surface processes associated with ground water movement during the Devonian remains a possibility. Also, as the Abrigo is in the southern Basin and Range province, it may have undergone vertical-axis rotations (Gillett, 1982).

Intrusives from Colorado were studied by Larson and Mutschler (1971) and French et al. (1977). The isotopic ages quoted by these authors range in age from 704 to 485 Ma and give a multimodal distribution of paleomagnetic directions (Poles 5-7, 33). The widely scattered pole

positions probably reflect different ages of magnetization, with high latitude poles possibly representing a complete remagnetization in the Late Paleozoic (French et al., 1977).

Two recent results have been reported from Cambro-Ordovician igneous rock sequences (Lynnes and Van der Voo, 1984; Larson et al., 1985) which give pole position entirely different from each other (Poles 34 and 35). Whereas the McClure Mountain alkali complex of Colorado (Pole 34) studied by Lynnes and Van der Voo (1984) falls close to the southeastern, low-latitude cluster of Cambrian paleopoles, the Black Canyon diabase of southwestern Colorado studied by Larson et al., (1985) yields a high-latitude pole position (Pole 35), close to the Late Paleozoic poles (Figure 4.1). Though Larson et al. (1985) have questioned the validity of the published southeastern Cambrian poles, they do not present conclusive evidence against remagnetization in the rocks they studied.

Thus, from the above discussion it is seen that a majority of high-latitude Cambrian poles is associated with problems concerning either geologic structure (tectonic rotation etc.), or possible remagnetization, or uncertainty regarding the age of magnetization. On the other hand, it seems quite probable that the published low-latitude poles with which the present result is in fair agreement represent the reference geomagnetic field for some part of the Cambrian period presumably mid- to Late Cambrian,

relative to cratonic North America. The low-latitude Cambrian poles, few though they are (Figure 4.1, Table 4.1), fall close to some of the reported Late Precambrian poles (1-4). A result (Pole 1) from reportedly Late Precambrian dykes (Murthy, 1971) has been, in fact, interpreted to be largely Early Paleozoic in age (Dankers and Lapointe, 1981), as the dykes span several hundreds of millions of years in age. Elston and Bressler (1977) have reported a low-latitude Cambrian pole (Pole 14) from the Early to Middle Cambrian Tapeats sandstone of Arizona. Though the remanence resides in hematite and no evidence was presented about its possible origin, they found 12 polarity reversals in this rock sequence. The normal and reverse polarity directions were closely antiparallel which, they argued, would favour a penecontemporaneous acquisition of magnetization during deposition of the Tapeats.

Another low-latitude pole (36) was recently reported by Dunn and Elmore (1985) from the Upper Cambrian (Dresbachian stage) Taum Sauk Limestone of southeast Missouri. A Late Paleozoic overprint (close to the lettered poles in Figure 4.1) was also isolated. Both components were shown to be carried by hematite. Though the petrographic examination failed to show a detrital origin of hematite, the low-latitude pole was interpreted to reside in hematite of early diagenetic origin.

There is some scatter in the low-latitude Cambrian

poles, too. The scatter of poles 11-13, obtained from radiometrically dated Lower Cambrian volcanics of Quebec (Lapointe and Dankers, 1981), has been interpreted as a rapid APW motion for the North American craton during the Early Cambrian. The fact that some of the poles in Figure 4.1 cited as mid- to Late Cambrian are close to the above Early Cambrian poles makes Lapointe and Danker's interpretation, which is based on a shorter Cambrian time scale, somewhat speculative. Therefore, the most that can be concluded from the interpretation of the low-latitude poles vis-a-vis their geological ages is that they appear to be representative of some Cambrian reference field for the North American craton. This conclusion is strengthened by the fact that these low-latitude poles are far away from the Late Paleozoic poles; hence the possibility that they were remagnetized in the Late Paleozoic can be discounted. A precise determination of the Cambrian geomagnetic field must, however, await results from more rock exposures from widely distributed localities within the craton.

CHAPTER 5

ST. GEORGE GROUP

5.1 Geological Setting

Rocks of the autochthonous St. George Group of Early Ordovician age are exposed on the Port au Port Peninsula and in several localities along the western coast of the Great Northern Peninsula of Newfoundland. In addition to the classic work of Schuchert and Dunbar (1934), the geology of the St. George Group has been studied by several authors already mentioned in Chapter 2. The following brief geological description is after James and Stevens (1982).

The St. George Group on Port au Port Peninsula comprises 573 meters of thick-bedded dolostone and limestone exposed along the south and east coasts of the peninsula, from the lower contact with the Cambrian Petit Jardin Formation to the upper contact with the Middle Ordovician Table Point Formation. The St. George Group has been subdivided into three Formations. In ascending order, they are: (1) The Isthmus Bay Formation; (2) The Catoche Formation; and (3) The Aguathuna Formation (Figure 2.2). The Isthmus Bay Formation has been provisionally reclassified into the Watts Bight and Boat Harbour Formations (Klappa et al., 1980), but for the present purpose the previous nomenclature, i.e., Isthmus Bay Formation, will be retained. The Isthmus Bay and Aguathuna

Formations are predominantly cyclic carbonates, while the Catoche Formation is mostly subtidal limestone. On the basis of cephalopod distribution, Flower (1978) has confirmed that the strata range in age from Early Canadian to Late Canadian, corresponding to a range from Tremadoc to Early Arenig. The Isthmus Bay Formation is predominantly Gasconadian in age. The Catoche Formation is probably also early Canadian, while the Aguathuna Formation is late Canadian.

Exposures belonging to the Isthmus Bay Formation consist of thin to thick-bedded limestone and dolostone which are repeatedly interbedded. Rocks of the Catoche Formation, comprising the middle, mainly subtidal part of the St. George Group, consist mainly of burrowed, fossiliferous limestone. The fossils are quite often replaced by silica or dolomite. The Aguathuna Formation is thinner than the other two formations, and consists of interbedded dolostone and limestone, with textures identical to that of the Isthmus Bay Formation. Rocks of the Aguathuna Formation and the overlying limestones of the Table Head Group (Table Point Formation) are very well exposed in the Aguathuna quarry (locality AQ in Figure 2.3) along the northeast coast of the Port au Port Peninsula, where the St. George-Table Head contact has been described as an unconformity. At Table Point on the Northern Peninsula, the contact between the St. George and Table Head Groups (Aguathuna and Table Point Formations) is now

considered to be essentially conformable. At both "localities", the limestones in the lower part of the Table Head are lithologically very similar to the limestones developed throughout the St. George Group (Levesque, 1977).

5.2 Paleomagnetic sampling and results

Samples for paleomagnetic investigations were collected in both the Port au Port area and the Port au Choix area from the localities shown in Figures 2.3-2.4 (Chapter 2) and also discussed in Appendix C. Detailed sampling and paleomagnetic results for the two areas are described separately below.

5.2.1 Port au Port Area

Fifty-seven oriented hand samples from 14 sites comprising the three Formations were collected at three localities (Figure 2.3). The distribution of samples over the three Formations is as follows. Isthmus Bay Formation: 5 sites (21 samples); Catoche Formation: 5 sites (20 samples); and Aguathuna Formation: 4 sites (16 samples). Two or more specimens of standard size (see Appendix A) were cut in the laboratory from each sample. Paleomagnetic studies were done on 97 specimens, which include at least one specimen from each of the 57 samples.

The NRMs of one specimen from each of the 57 samples are plotted in Figure 5.1, which shows a streaked distribution mainly in the southeast quadrant with shallow

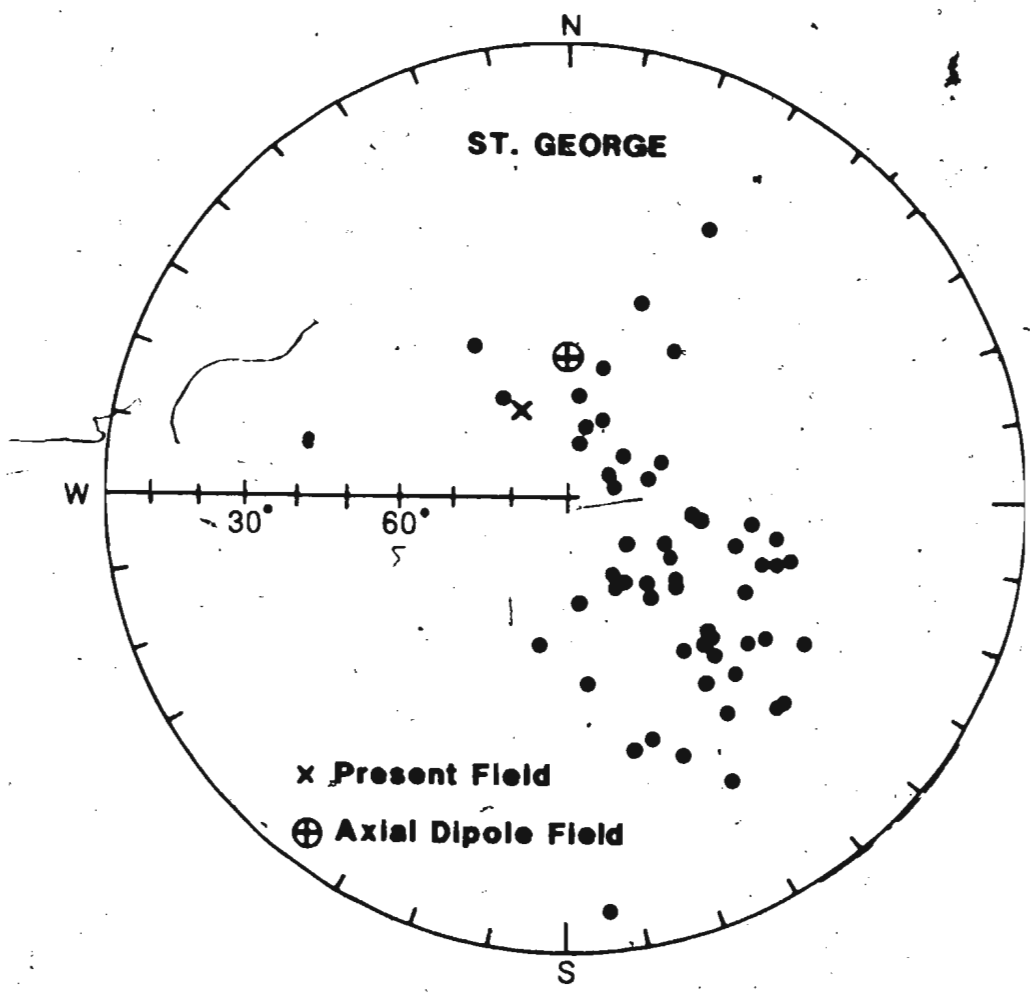


Fig. 5.1. NRM directions of St. George Group samples, Port au Port area. Equal area projection on the lower hemisphere.

to steep downward-directed inclinations. This distribution suggests that the NRM is the resultant of a steep down component and at least one other component inclined less steeply to the southeast. The intensities range between 1×10^{-4} A/m and 3×10^{-3} A/m.

Both AF and thermal demagnetizations were performed on the specimens for the isolation of stable components. At first, 14 samples, each from a different site, were chosen randomly for AF and thermal treatments. At least two specimens from each of these 14 samples were demagnetized in detail - one thermally and the other by AF. Some typical results of the AF and thermal treatments are compared in Figure 5.2., where it is seen that two specimens, AQ11-A and AQ11-C, from the same sample, give comparable results after both treatments. The steep down NRM vector moves to a shallower direction towards southeast at higher temperatures or fields and attains a stable end point in the temperature range of 200-450°C or AF range of 10-40mT. The stable component is uncovered chiefly in the range 300-400°C where there is a sharp drop in intensity as seen on the decay curve. The intensity during AF demagnetization decreases smoothly to a low value by 100 mT, indicating a widely distributed coercivity spectrum.

However, specimens AQ16-B and AQ16-C (Figure 5.2, right) from another sample do not give comparable results after the two treatments. While the thermal behaviour is similar to that shown by the previous sample, the AF

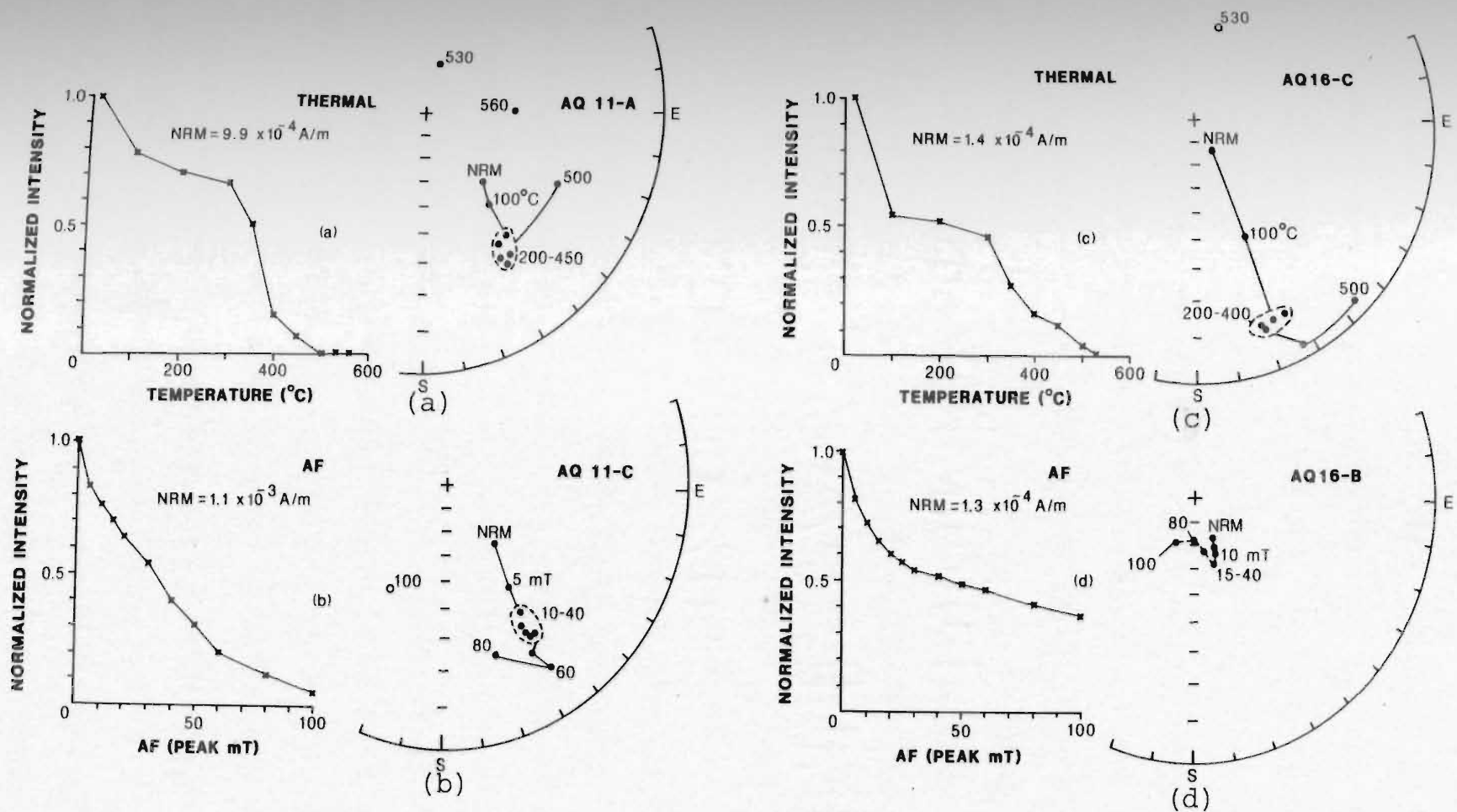


Fig. 5.2. Demagnetization results of specimen pairs (a, b and c, d) from 2 St. George Group samples after (a, c) thermal demagnetization; (b, d) AF demagnetization. Solid (open) circles denote lower (upper) hemisphere projections on a Wulff net. Dashed outlines indicate directions in the temperature or field range shown and have no statistical significance. Directions are without tilt correction.

treatment failed to deflect the steep down NRM significantly. A very stable steep direction is maintained in the range 15-40 mT for specimen AQ16-B, but this direction is very different from the stable shallow direction obtained after thermal demagnetization (Specimen AQ16-C). This discrepancy is probably due to the incomplete decay of the remanence on AF treatment up to 100 mT. It can be seen from the figure that 40% of the intensity remains even after treatment to 100 mT, whereas thermal treatment leads to its almost complete decay by 500°C. It seems quite probable that, in Specimen AQ16-B, a dominating steep component with higher coercivity masks a shallower component of lower coercivity which corresponds to the component isolated by the thermal treatment in Specimen AQ16-C. The fact that this shallow component could be well isolated in the thermal treatment indicates that the steep component has a lower blocking temperature than the shallow component. In other words, the steep and shallow components are well differentiated in regard to their blocking temperatures, but their coercivities are overlapping. A further discussion on this result will be given in Section 5.2.2.

The two treatments, however, do suggest that AF treatment is not always effective in isolating characteristic components from these rocks. Therefore, detailed thermal demagnetizations were carried out on the rest of the specimens for isolating one or more stable

components. For this purpose, one specimen from each of the remaining samples was thermally treated in detail. As in the Cambrian rocks, two distinct, relatively shallow components could be isolated from the results of thermal treatment, in addition to a steep downward-directed component. The steep component could be very easily erased at steps below 300°C and is probably a viscous remanence acquired in a field close to present earth's field (PEF). The two characteristic components are hereafter called the "A" and "B" components, by analogy to the case of the Cambrian rocks (Chapter 3), though the characteristic directions of each component are not necessarily the same for the two periods. The thermal results of Figure 5.2 refer to the "A" component. Two other representative results yielding the "A" component are shown in Figure 5.3, where the results are plotted on a stereogram and as orthogonal vector end points (Zijderveld, 1967). These results are similar to those shown in Figure 5.2, leading to the isolation of a characteristic southeasterly direction with shallow positive inclination, in the range 300-450°C. This is evident from the correspondence between the stable end point on the stereographic plot and the univectorial decay to the origin seen on the vector diagram. Additional vector plots yielding "A" component are shown in Figure 5.4. A total of 37 samples (one specimen each) from 12 sites yielded the characteristic "A" direction. The characteristic directions of individual

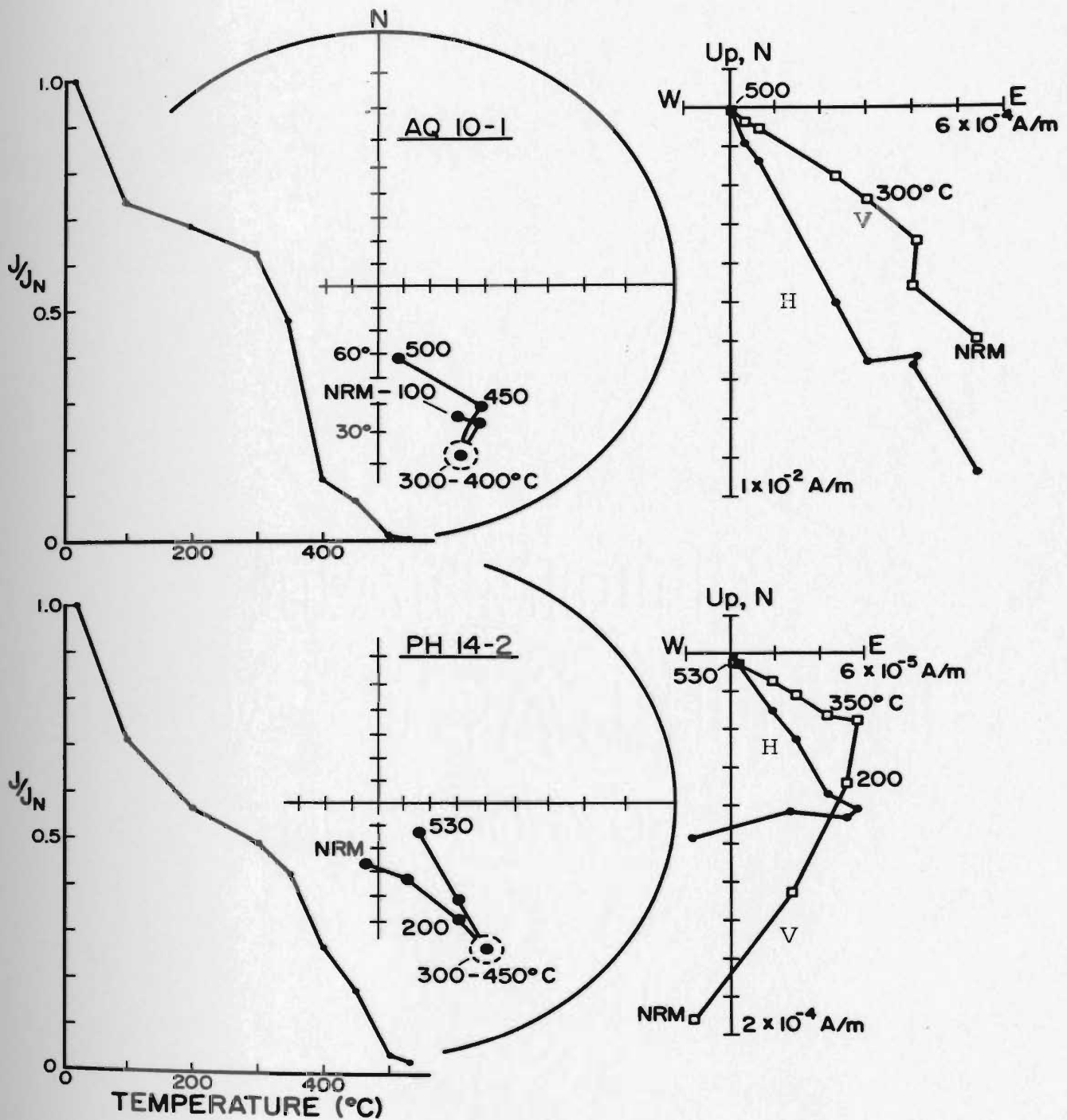


Fig. 5.3. Representative thermal demagnetization results for 2 specimens yielding "A" component from the St. George Group, Port au Port area. Conventions for the stereographic plots are as in Fig. 5.2. J/J_N is the normalized intensity. In the corresponding orthogonal vector diagrams (r.h.s.), open squares are vector end point projections on an E-W vertical (V) plane; solid circles on the horizontal (H) plane.

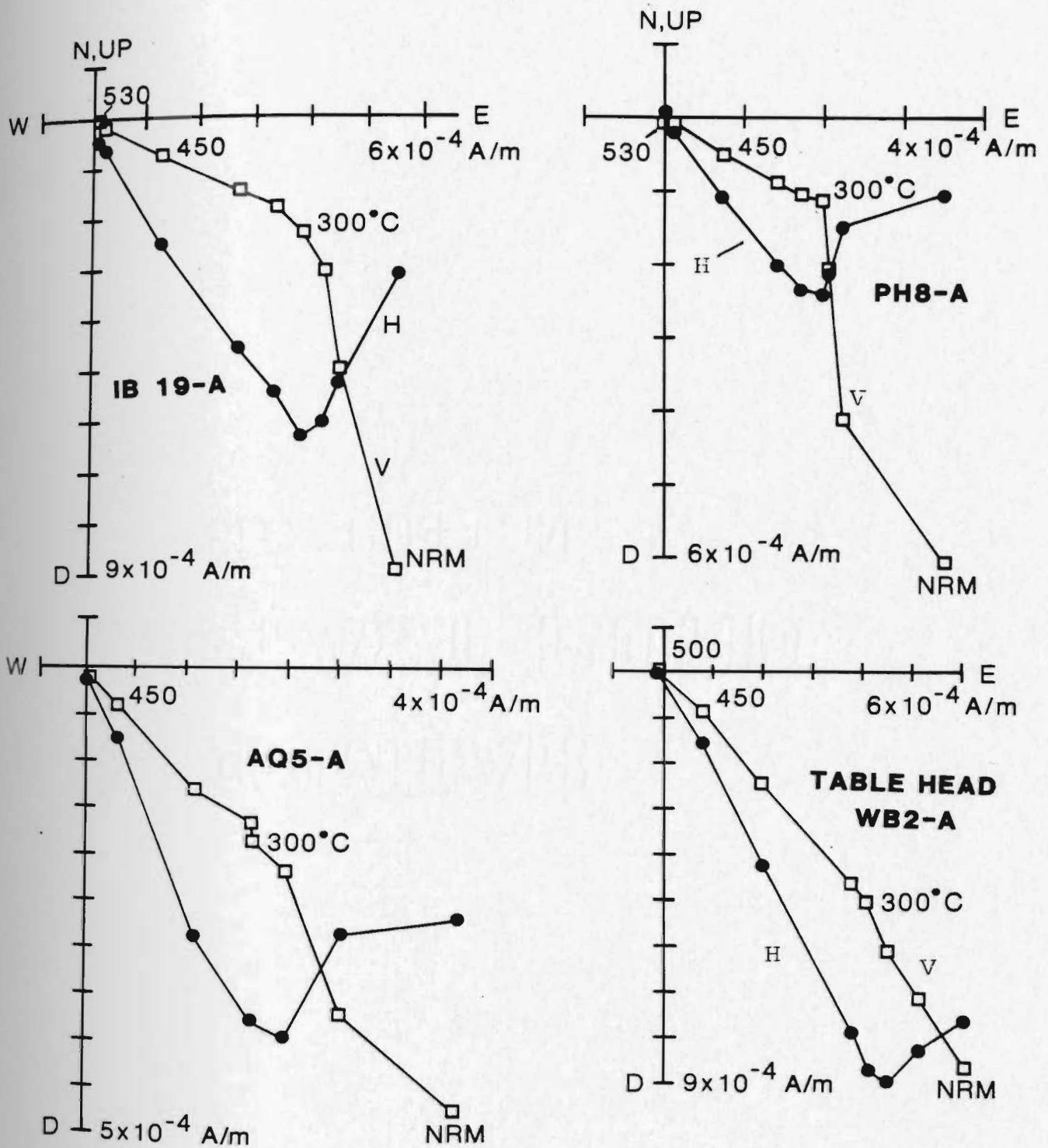


Fig. 5.4. Representative orthogonal vector diagrams of 3 specimens yielding "A" component for the St. George Group, Port au Port area. One specimen from the Table Head Group (bottom right) is included for a comparison which shows a similar direction as the St. George. The Table Head Group is further discussed in Chapter 6. Conventions as in Fig. 5.3.

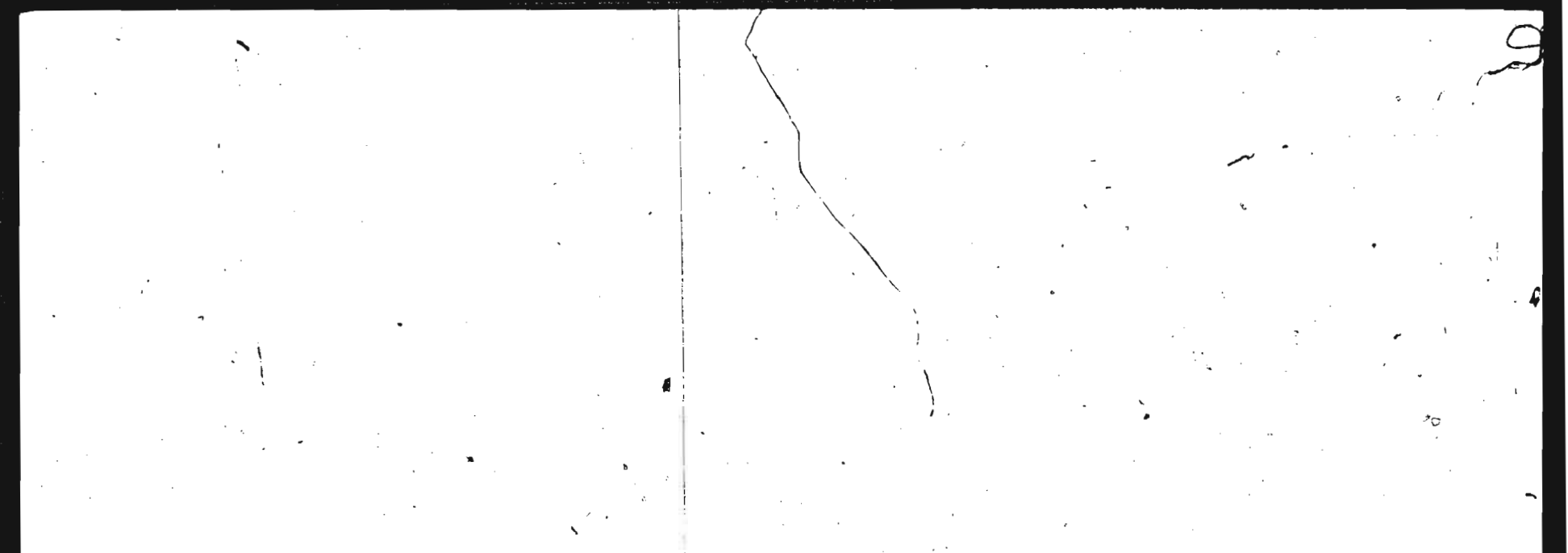


Fig. 5.5. Characteristic sample (left) and site mean (right) directions for the "A" component (after tilt correction) of the St. George Group, Port au Port area. Equal area projection on the lower hemisphere.

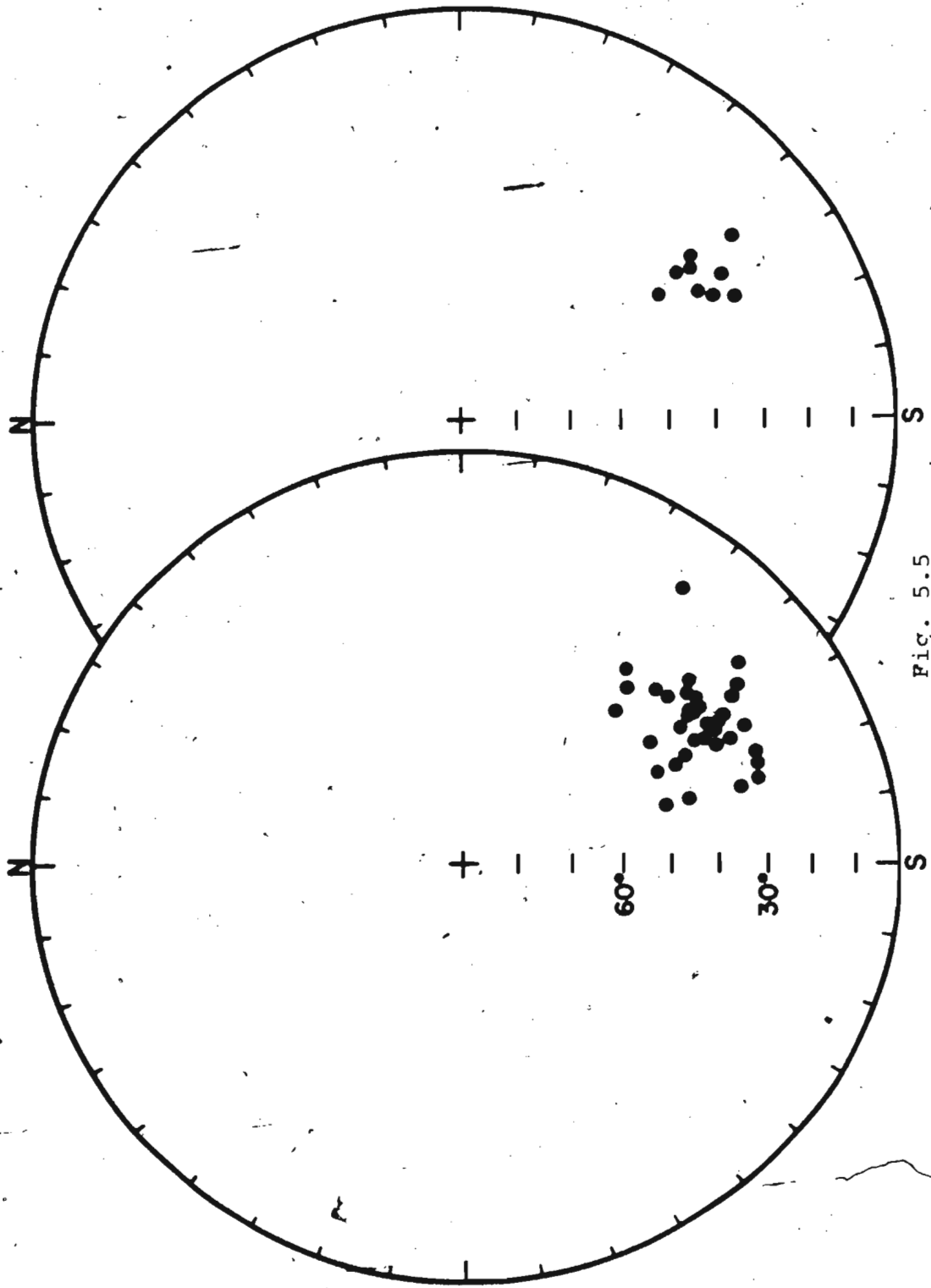


FIG. 5.5

TABLE 5.1

THERMAL DEMAGNETIZATION RESULTS FROM THE ST. GEORGE GROUP FOR THE
"A" COMPONENT, PORT AU PORT AREA.

Site	Specimen	Characteristic direction				Stability range (° C)
		In situ		Tilt-corrected		
		D	I	D	I	
Isthmus Bay Formation						
IB3	IB10-B	161.3	27.2	162.8	44.1	300-350 (ave.)
IB4	IB16-1	138.7	31.0	134.3	47.1	350-400 (ave.)
IB4	IB16A-1	161.1	31.8	162.8	48.7	350-530
IB5	IB17-A	163.1	16.1	164.3	32.9	300-500
IB5	IB18-A	154.0	16.7	153.8	33.7	300-500
IB5	IB19-A	147.5	16.5	146.4	33.3	300-500
IB5	IB20-B	149.3	16.8	148.5	33.7	300-500
Catoche Formation						
PH1	PH4-A	128.5	4.5	127.8	15.9	300-500
PH2	PH5-1	148.8	17.9	149.0	29.8	350-450
PH2	PH7-1	157.4	15.5	158.3	27.2	300-500
PH2	PH8-A	143.8	20.0	143.5	32.0	300-500
PH3	PH9-1	161.4	17.3	162.8	28.8	300-450
PH3	PH10-B	133.8	30.0	131.8	41.6	350-500
PH3	PH11-1	131.3	27.3	129.2	38.9	400-500
PH3	PH12-2	151.7	28.6	152.6	40.5	350-500
PH4	PH13-1	145.1	23.3	144.9	35.3	300-500
PH4	PH14-2	149.8	18.7	150.1	30.6	350-530
PH4	PH15-2	140.8	18.8	140.3	30.8	350-530
PH4	PH16-B	142.7	21.1	142.3	33.0	350-500
PH5	PH17-B	146.9	13.9	146.9	25.9	350-530
PH5	PH18-A	143.0	7.5	142.8	19.5	350-530
PH5	PH19-3	143.2	10.7	143.0	22.7	350-530
PH5	PH20-1	145.6	10.8	145.6	22.8	300-530

TABLE 5.1, (CONT'D)

Site	Specimen	Characteristic direction				Stability range (° C)
		In situ		Tilt-corrected		
		D	I	D	I	
Aguathuna Formation						
AQ1	AQ1-B	160.4	31.7	153.5	47.8	300-530
AQ1	AQ2-A	160.0	28.0	154.0	44.1	300-450
AQ1	AQ3-B	153.5	30.7	145.5	45.6	300-400 (ave.)
AQ1	AQ4-D	144.3	24.4	136.8	37.5	300-500
AQ2	AQ5-A	156.0	22.5	150.5	38.0	300-500
AQ2	AQ6-C	157.5	15.1	153.8	30.9	300-450
AQ2	AQ8-C	153.3	24.1	147.1	39.1	200-450
AQ3	AQ9-A	151.6	21.0	145.9	35.7	300-530
AQ3	AQ10-1	155.3	17.8	150.8	33.2	300-500
AQ3	AQ11-A	147.2	22.9	140.4	36.7	300-500
AQ3	AQ12-B	151.9	20.5	146.4	35.3	350-500
AQ4	AQ13-A	162.9	11.3	160.4	28.0	350-500
AQ4	AQ15-B	156.8	19.9	152.1	35.5	300-530
AQ4	AQ16-C	156.1	11.2	153.0	26.9	300-530

NOTES: All but three (Specimens IB10-B, IB16-1 and AQ3-B) of the above directions have been computed by vector subtraction from the linear segments defined by three or more points on Zijderfeld plots in the temperature range indicated. For the other three specimens, the average (ave.) of directions in the indicated temperature range was taken to be the characteristic direction. Except for Specimen AQ6-C, the linear segments of Zijderfeld plots terminated close to the origin at the highest temperature of the indicated range. Symbols as in Table 3.1.

TABLE 5.2

SITE-LEVEL CHARACTERISTIC DIRECTIONS FROM THE ST. GEORGE GROUP,
"A" COMPONENT, PORT AU PORT AREA.

Site	n/n ₀	In situ		Tilt-corrected			
		D	I	D	I	k	°95
IB5	4/4	153.5	16.6	153.3	33.6	147	7.6
PH2	3/4	150.0	17.9	150.4	29.9	137	10.6
PH3	4/4	144.9	26.3	144.7	38.3	32	16.4
PH4	4/4	144.6	20.5	144.4	32.5	365	4.8
PH5	4/4	144.6	10.7	144.5	22.7	646	3.6
AQ1	4/4	154.4	28.9	147.1	44.0	119	8.4
AQ2	3/4	155.6	20.6	150.6	36.1	242	7.9
AQ3	4/4	151.5	20.6	145.9	35.4	465	4.3
AQ4	3/4	158.6	14.1	155.2	30.2	174	9.4

NOTES: n/n₀ is the number of sample characteristic directions used in computing the site mean/number of samples thermally demagnetized. Other symbols as in Tables 3.1-3.3.

specimens are listed in Table 5.1. All but three of these directions were computed by vector subtraction between three or more collinear points directed to the origin on the orthogonal projections. For the remaining three specimens (Table 5.1) the characteristic directions were taken to be the average of directions in the stable range. In Figure 5.5, individual sample directions and site means are plotted. Site means for any site with fewer than 3 samples have not been plotted, leaving only 9 sites, with a total of 33 samples. The remaining 4 samples are distributed over three other sites. Fisher's statistics (Fisher, 1953) for site-level are listed in Table 5.2. For the reasons to be discussed later in this Chapter, the "A" component is considered to be the depositional or early post-depositional magnetization of these rocks. Therefore, a geological tilt correction has been applied to the characteristic directions in Tables 5.1-5.2.

As discussed earlier, the AF treatment was not found as suitable as the thermal treatment for the isolation of a characteristic magnetization because of the fact that a higher coercivity component seemed to mask the characteristic component in some of the specimens. Nevertheless, a 5-step AF demagnetization in the range 10-60 mT was carried out on one fresh specimen each from 24 samples not previously used in the pilot AF study. Along with the 16 specimens pilot-demagnetized in 10 steps, these 24 specimens used in the 5-step procedure, made a total of

40 specimens (38 samples) which were AF demagnetized. As was found in the detailed (10 to 12-step) study, the 5-step procedure also yielded variable results, most of the specimens showing a directional trend to the southeast, terminating in some cases in a stable direction akin to the typical thermal "A" component direction. However, just over half of the AF-treated specimens failed to end up in a shallow direction. Among all the AF-demagnetized specimens, between 10 and 70% of the intensity still remained after treatment to 60 mT.

The "B" component was isolated from 14 samples (one specimen each) distributed over 6 sites. Figure 5.6 documents the magnetic behaviour leading to the "B" component, as revealed after thermal and AF demagnetization of two specimens. In both of these specimens, a south to southeasterly component with near-horizontal negative inclination is revealed after both thermal and AF treatments. In specimen PH2-1, a dominant steep down component is erased below 200°C, after which a stable component with a shallow negative inclination is uncovered in the range 400-560°C. This is seen on the stereogram and from the orthogonal projection. This stable component resides in the last 15% of the total intensity. The AF treatment of specimen IB2-B reveals the "B" component in the range 20-50 mT after the removal of a steeper component, but a substantial intensity (~ 80% of NRM) still remains after treatment up to 100 mT, again suggesting the

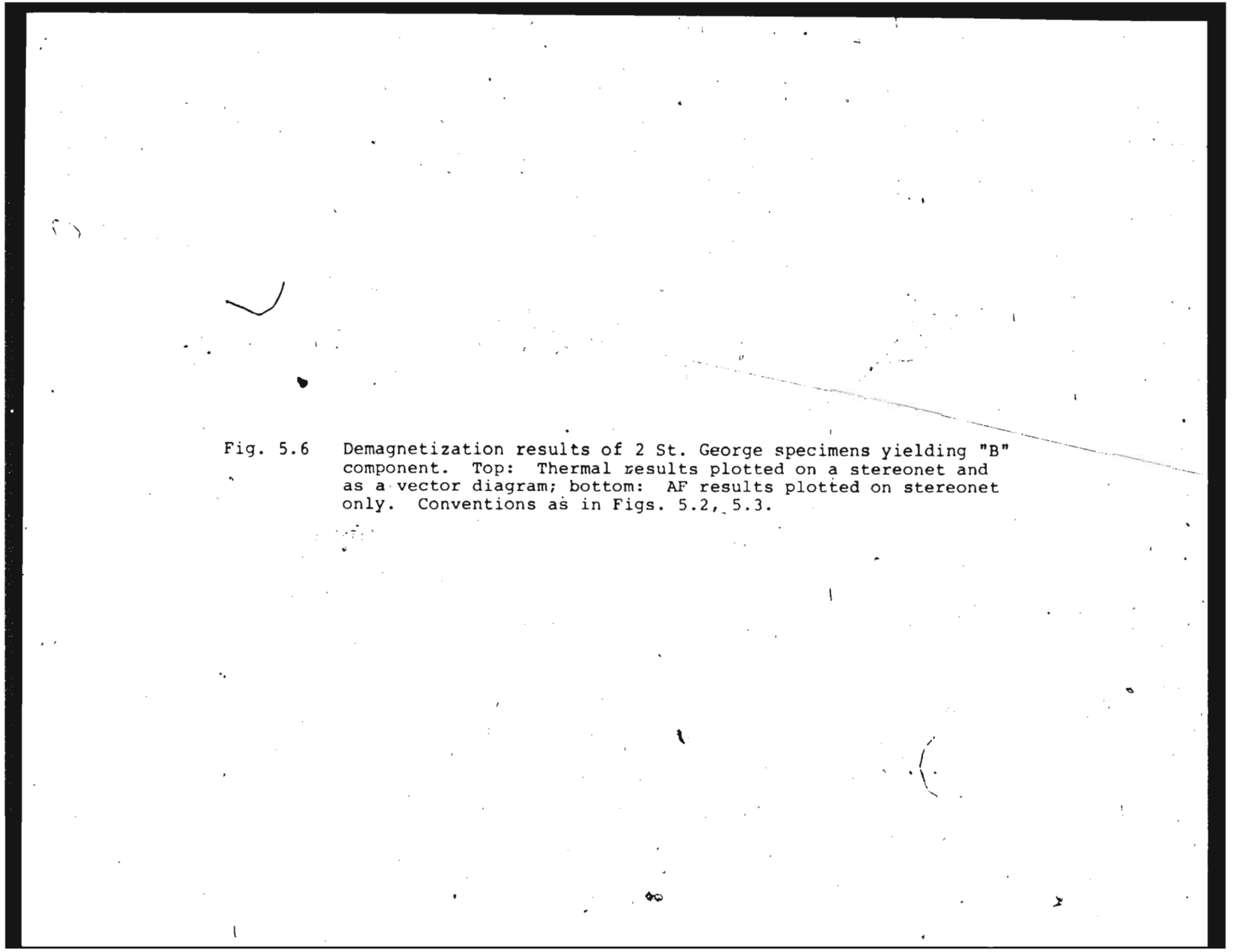


Fig. 5.6 Demagnetization results of 2 St. George specimens yielding "B" component. Top: Thermal results plotted on a stereonet and as a vector diagram; bottom: AF results plotted on stereonet only. Conventions as in Figs. 5.2, 5.3.

presence of relatively high-coercivity grains as the main remanence carrier.

In Figure 5.7 are plotted the thermal demagnetization results of two other specimens yielding the "B" component. Specimen AQ6-C seems to be preserving both the "A" and "B" components which can be separately identified by a close inspection of both the stereographic plot and the orthogonal vector diagram. The "A" component is being erased in the range 300-450°C. This is identified as a linear segment on the vector diagram. Between 450° and 560°C, a stable end point is observed which corresponds to the "B" component. This does not seem to be well defined on the vector diagram, but the evidence using the stable end point criterion is strong. This is the only specimen in the entire collection which clearly revealed the coexistence of both the "A" and "B" components along with the steep viscous component. In the rest of the specimens, either a stable "B" direction or a stable "A" direction was isolated. For example, in Specimen IB1-B in Figure 5.7, the removal of a viscous component below 200°C was followed by the uncovering of a nearly horizontal component which remained stable up to high temperatures well past the Curie point of magnetite. An almost univectorial trend on the Zijdeveld diagram in the range 200-650°C confirms the presence of the above single component at high temperatures. The calculation of the characteristic "B" component in these two specimens and

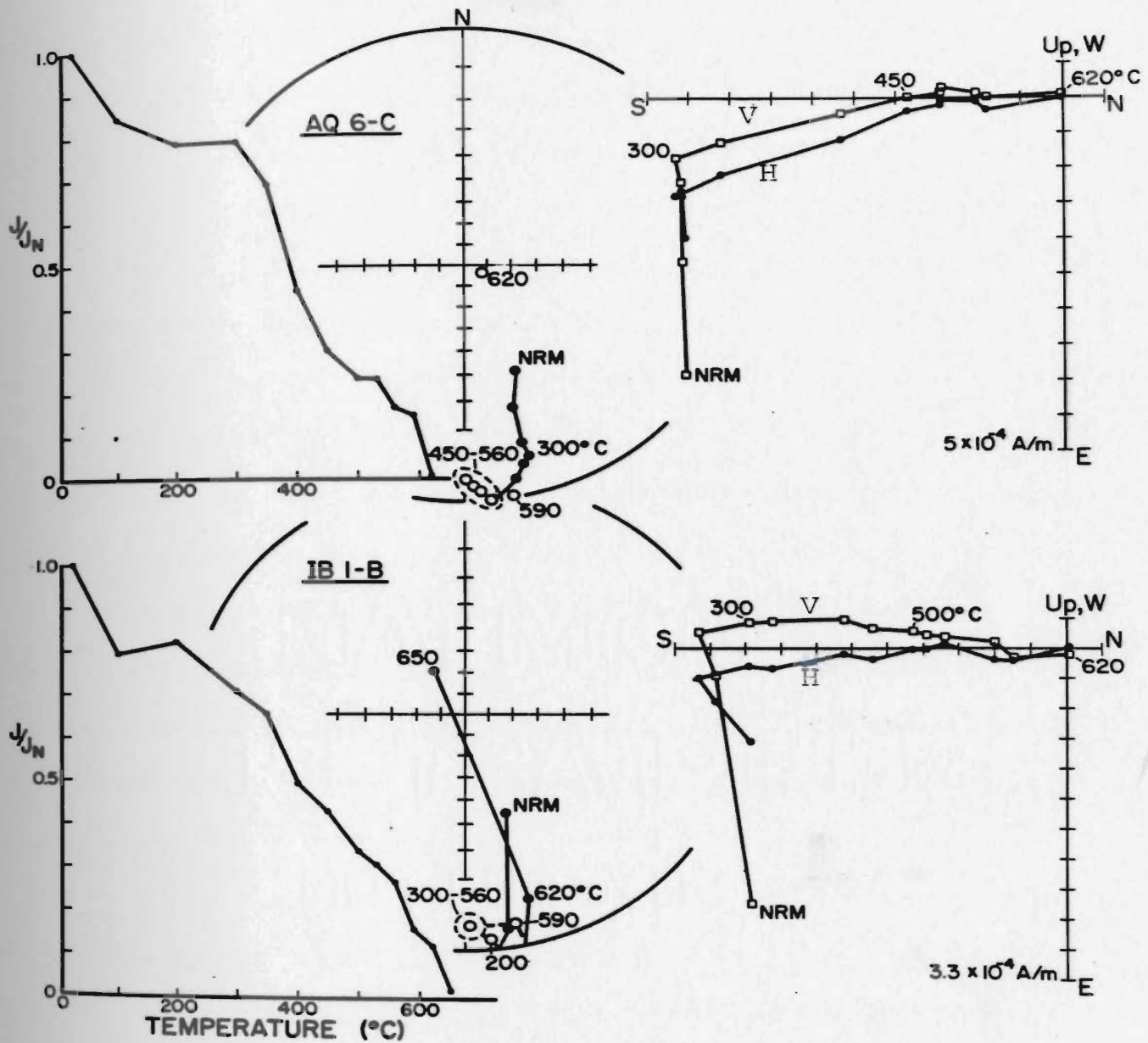


Fig. 5.7. Thermal demagnetization results of 2 St. George specimens yielding (top) both "A" and "B" components and (bottom) only "B" component. The "A" component in AQ6-C is erased in the range 300-450 $^{\circ}\text{C}$ (vector diagram, right); then a stable "B" direction is obtained at high temperatures (stereoplot). Open symbols on vector diagrams are projections on N-S vertical (V) plane. All other conventions as in Figs. 5.2, 5.3.

others like them, however, is based on averaging the directions in the stable range rather than on vector subtraction based on the Zijdeveld diagrams, as the decay to the origin does not seem to be clearly established in these cases. The characteristic directions isolated from 14 samples are listed in Table 5.3, and are plotted in Figure 5.8. No geological tilt correction has been applied to the characteristic directions in Table 5.3, as these are interpreted to be a secondary component (see discussion below) acquired after the tilting of the strata.

In Table 5.4 are listed the results of Fisher's statistics (Fisher, 1953) for the "A" and "B" components of the St. George Group. The overall mean direction of the "A" component, giving unit weight to samples after tilt correction, is $D = 147.9^\circ$, $I = 34.5^\circ$ ($\alpha_{95} = 3.2^\circ$, $k = 57$, $N = 37$ samples), which is almost coincident with the site mean direction, $D = 148.5^\circ$, $I = 33.7^\circ$ ($\alpha_{95} = 4.4^\circ$, $k = 139$, $N = 9$ sites). The site-mean direction is preferred, and the antipole position corresponding to it is 17.5°N , 152.3°E ($dp = 2.8^\circ$, $dm = 4.9^\circ$). This falls near several reported Ordovician poles to be discussed in Chapter 9. The "A" component directions corresponding to the three formations of the St. George Group were separately averaged also (Table 5.4). The three formation means have been plotted with their 95% confidence circles in Figure 5.17 along with the corresponding means from the Port au Choix area and will be further discussed with the

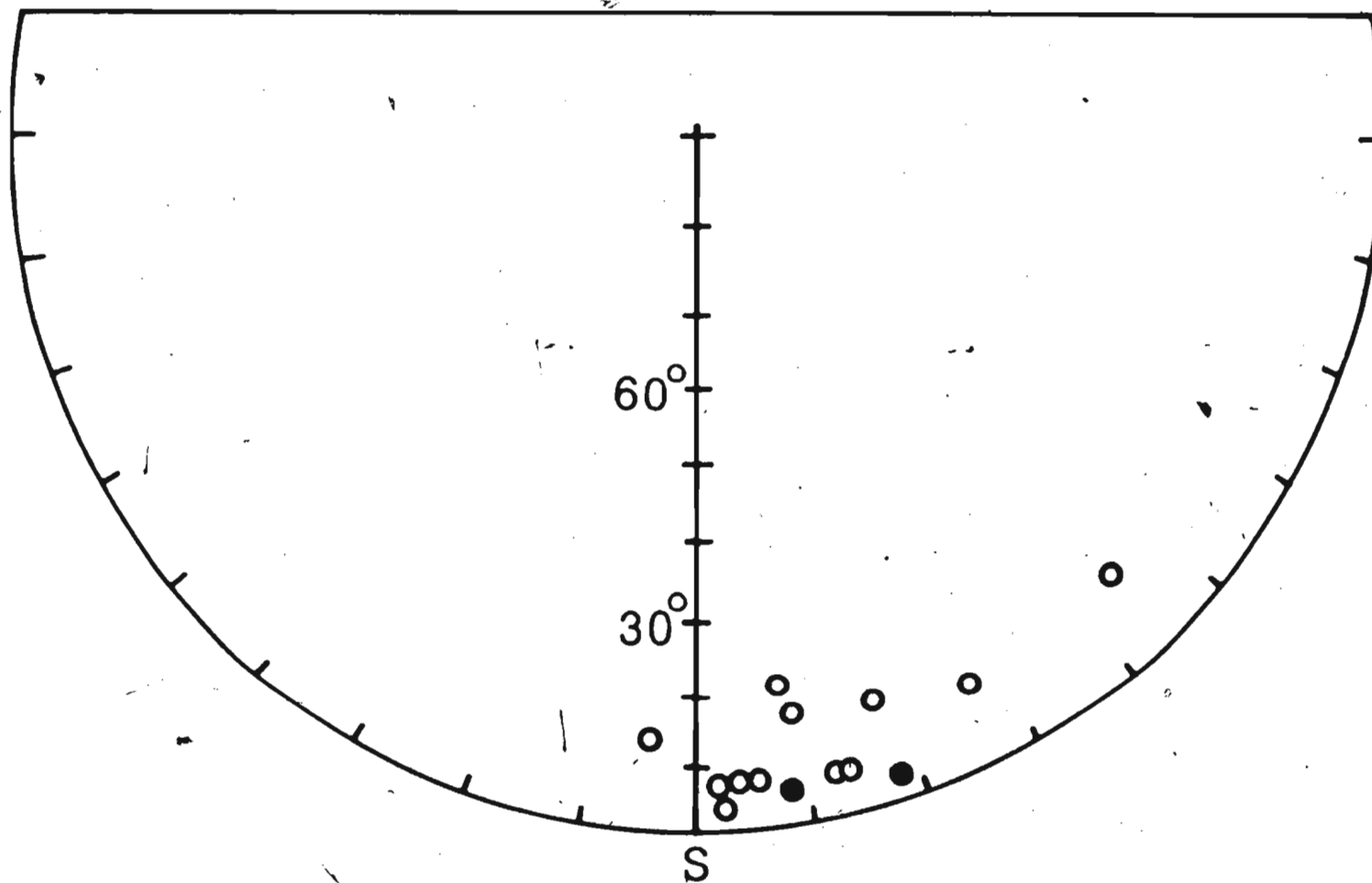


Fig. 5.8. Sample characteristic directions for the "B" component after thermal demagnetization. Solid (open) circles on lower (upper) hemisphere. Equal area projection.

TABLE 5.3

THERMAL DEMAGNETIZATION RESULTS FROM THE ST. GEORGE GROUP
FOR THE "B" COMPONENT, PORT AU PORT AREA.

Formation	Site	Specimen	Characteristic		Stability range (° C)	
			in situ direction			
			D	I		
Isthmus Bay	IB1	IB1-B	178.1	- 6.9	200-590 (ave.)	
"	"	IB2-A	170.8	-21.6	400-530 (ave.)	
"	"	IB3-C	169.7	-17.0	300-650 (ave.)	
"	"	IB4-A	184.4	-14.6	300-560 (ave.)	
"	"	IB2	IB7-2	162.0	4.2	400-560 (v.s.)
"	"	IB2	IB8-1	174.4	- 7.6	350-590 (v.s.)
"	"	IB3	IB9-C	162.3	-16.4	400-560 (v.s.)
"	"	IB3	IB11-A	166.2	- 6.9	350-590 (v.s.)
"	"	IB4	IB13-A	171.2	6.4	350-530 (ave.)
"	"	IB4	IB14-C	175.7	- 8.0	400-560 (ave.)
"	"	IB4	IB15-C	136.4	-13.6	400-500 (v.s.)
Catoche	PH1	PH1-A	167.2	- 7.1	400-530 (v.s.)	
"	PH1	PH2-1	153.2	-13.3	300-560 (v.s.)	
Aguathuna	AQ2	AQ6-C	177.3	- 4.3	450-560 (ave.)	

NOTES: Characteristic directions above are based either on vector subtraction (v.s.) from Zijdeveld plots or average of directions (ave.) in the temperature range indicated.

TABLE 5.4

MEAN PALEOMAGNETIC DATA FOR THE "A" AND "B" COMPONENTS AFTER THERMAL
DEMAGNETIZATION OF THE ST. GEORGE GROUP, PORT AU PORT AREA.

	D_m	I_m	k	N	α_{95}	λ_p	Antipole
St. George Group, 9 sites (33 samples), "A" component, <u>in situ</u>	150.9	19.6	117	9	4.7		
St. George Group, 9 sites (33 samples), "A" component, tilt-corrected	148.5	33.7	139	9	4.4	18.4 S	17.5°N, 152.3°E ($dp = 2.8^\circ$, $dm = 4.9^\circ$)
St. George Group, 37 samples, "A" component, tilt-corrected	147.9	34.5	57	37	3.2		
St. George Group, 14 samples, "B" component, <u>in situ</u>	167.9	-9.2	33	14	6.9	4.6 N	44.9°N, 138.2°E ($dp = 3.6^\circ$, $dm = 7.1^\circ$)
Isthmus Bay Formation, 7 samples, "A" component, tilt-corrected	153.3	39.5	55	7	8.2		
Catoche Formation, 16 samples, "A" component, tilt-corrected	144.5	30.0	55	16	5.0		
Aguathuna Formation, 14 samples, "A" component, tilt-corrected	149.4	36.9	107	14	3.9		

All symbols as in Table 3.3.

Port au Choix results.

The mean direction for the "B" component (Table 5.4) is $D = 167.9^\circ$, $I = -9.2^\circ$ ($\alpha_{95} = 6.9^\circ$, $k = 33$, $N = 14$ samples), corresponding to an antipole at 44.9°N , 138.2°E ($dp = 3.6^\circ$, $dm = 7.1^\circ$) which is consistent with a number of reported Kiaman poles (Figure 9.1, Chapter 9). As in the case of the Cambrian "A" and "B" components (Chapter 3), the south poles are consistent with the presumed APW path for North America, and therefore the polarities of the magnetization are taken to be reverse for these rocks.

About 88% of the St. George collection (50 samples out of a total of 57) was found to be paleomagnetically useable after thermal demagnetization.

5.2.2 Magnetic mineralogy (Port au Port rocks)

Fourteen fresh specimens (all from different samples) were subjected to IRM-acquisition and back-field experiments with a maximum field strength of 0.82 T. Three types of characteristic curves were obtained (Figure 5.9), and are similar to types 1-3 obtained from the Cambrian rocks, which were discussed in detail in Section 3.3. Obviously these curves indicate the presence of either magnetite alone (type 1, Specimen A018-B) or a mixture of magnetite and hematite or goethite (type 2, Specimen PH4-B); it is possible also for hematite or goethite to occur alone or as a mixture (type 3, Specimen IB2-C). It

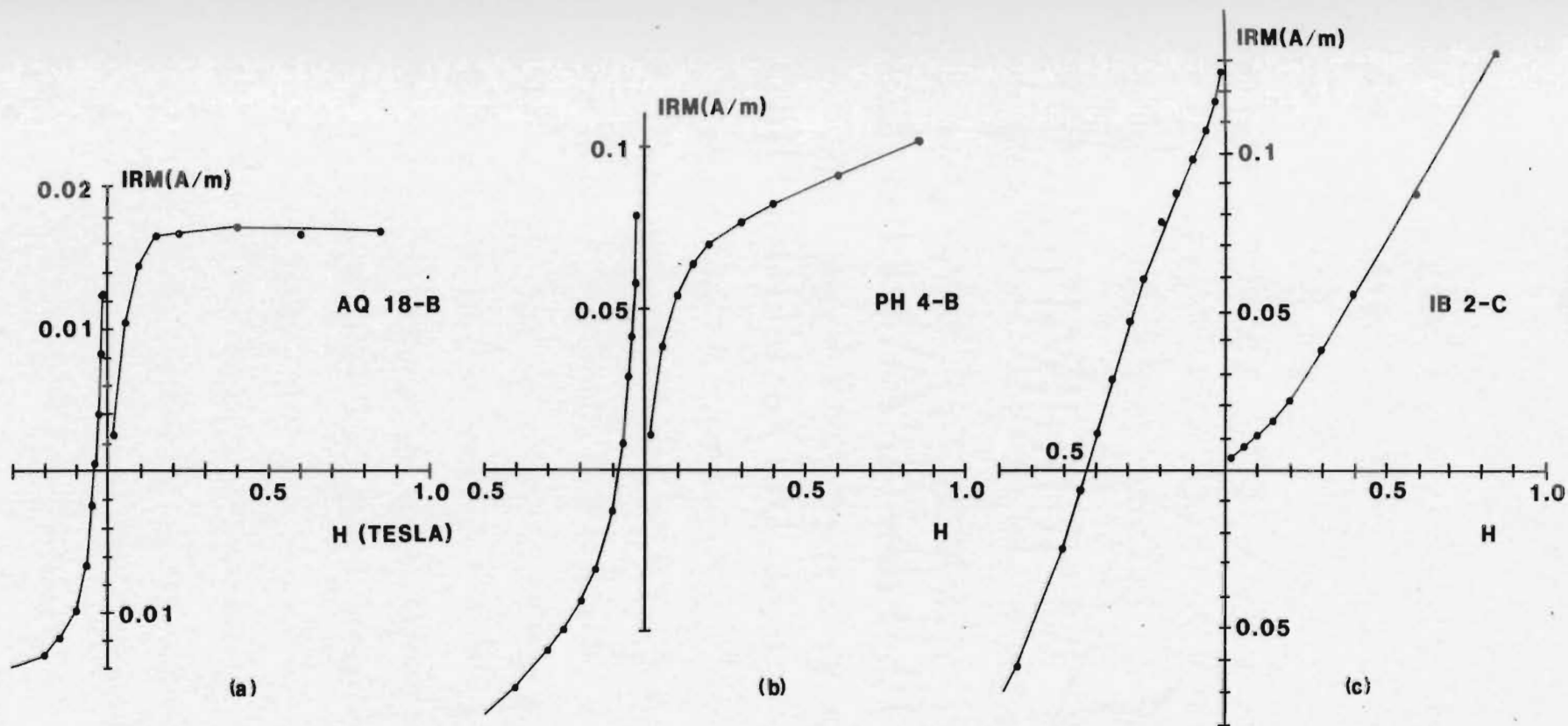


Fig. 5.9. IRM acquisition and back-field characteristics. Curves (a), (b) are characteristic of samples yielding "A" component; curve (c) of samples giving the "B" component, after thermal demagnetization.

is difficult to distinguish between goethite and hematite from type 3 IRM curves (Lowrie and Heller, 1982), but in the absence of magnetite they can be distinguished on the basis of the very much higher blocking temperatures resulting from the presence of hematite. A gradient observable in type 2 (Specimen PH4-B), after a strong initial increase in intensity, could possibly be contributed by the presence of hematite or goethite coexisting with a dominant magnetite phase of type 1, though the presence of goethite in type 1 curves also cannot be ruled out (Lowrie and Heller, 1982).

Combining the evidence from IRM studies with that from the AF and thermal demagnetization results has made it possible to identify the magnetic phases carrying the remanence in these rocks. Those samples giving type 1 IRM curves always yielded the "A" component, which was unblocked in the temperature range 300-500°C (Figures 5.2-5.3). This gives a strong indication of magnetite being the remanence carrier of the "A" component. Type 2 IRM curves are also most often associated with the "A" component. This shows that goethite or hematite are probably not important in most of these samples as a stable remanence carrier. However, the only specimen (AQ6-C; Figure 5.6) where both "A" and "B" components were isolated, is of type 2, as expected. As discussed in Section 5.2.1, the "B" component in specimen AQ6-C retained remanence beyond the Curie Point of magnetite, suggesting

hematite as the remanence carrier. Samples corresponding to type 3 IRM curves either exclusively yielded the "B" component, with unblocking temperatures usually exceeding the Curie Point of magnetite, or they failed to yield a stable remanence at high temperatures. From those "B" component samples which unblocked entirely below the Curie Point of magnetite, no evidence of magnetite was found from the IRM study. Thus the evidence seems to be strongly favouring hematite as the remanence carrier for the "B" component. The origin of hematite in these rocks could be by one of the processes already described in Section 3.3. However, some further comments on the magnetic mineralogy of these rocks are of interest and are given below.

Two samples, one each from the Isthmus Bay and Aguathuna Formations, gave indications of the presence of goethite exclusively as the remanence carrier. The results of AF and thermal demagnetizations on two specimens from the Isthmus Bay sample are shown in Figure 5.10. The AF result (specimen IB6-1) shows very little reduction (15%) in the intensity up to 100 mT, during which the NRM direction remains stable. This steep downward-directed magnetization is close to the present earth's field direction. Thermal demagnetization of the duplicate specimen, IB6-2, shows a 96% reduction in the intensity at 100°C. Such a low blocking temperature is attributed to goethite, a mineral that is fairly common in limestones (Lowrie and Heller, 1982). The remanence direction at

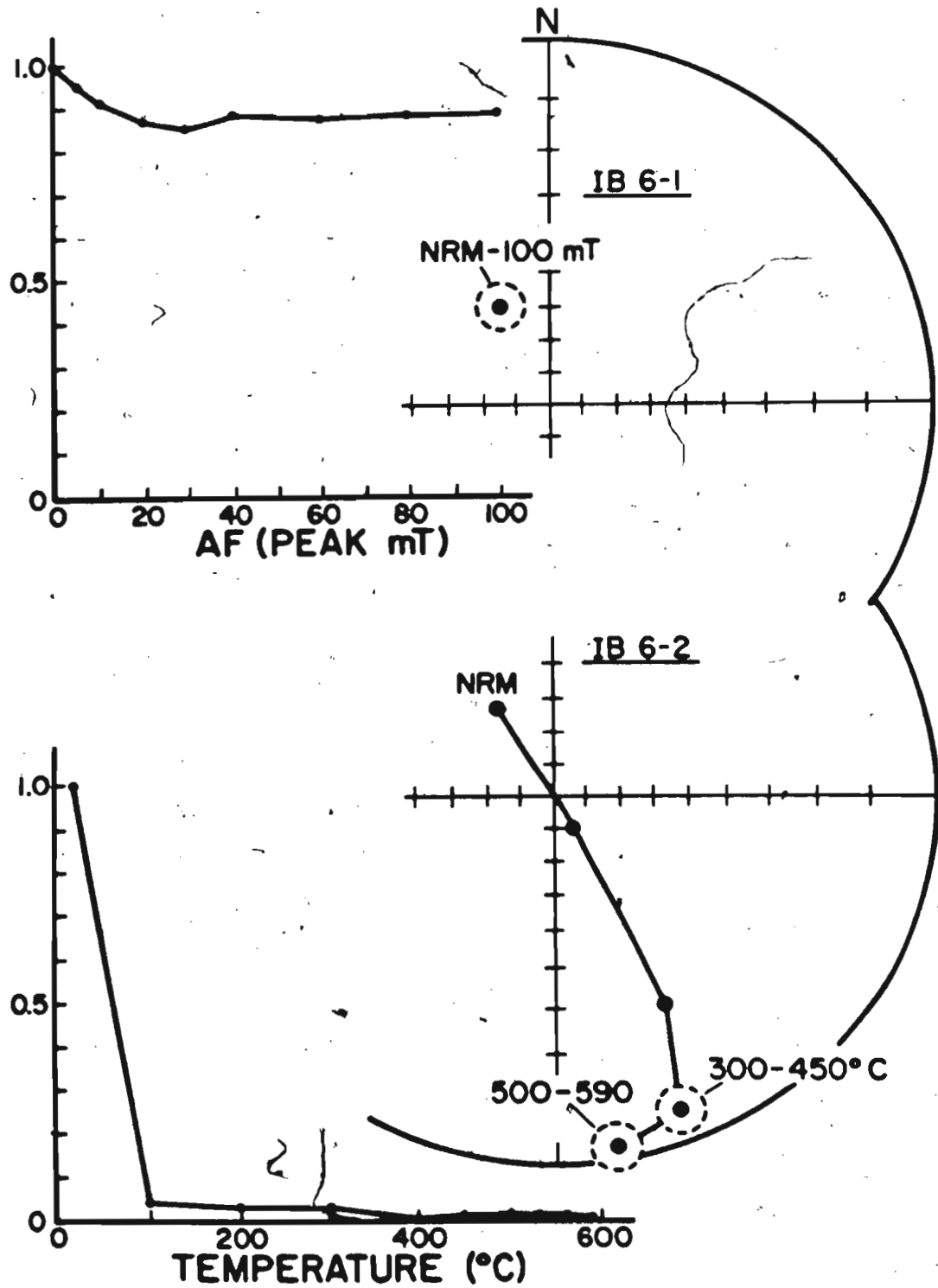


Fig. 5.10. Demagnetization results of specimen pairs from a St. George sample indicating goethite as the main remanence carrier. Conventions as in Fig. 5.2.

higher temperatures, however, is seen to migrate systematically to the southeast (Figure 5.10) and it seems that a near-horizontal ("B" ?) component is preserved in this specimen. However, this specimen has not been included in the final "B" component statistics, because of the chemical changes associated with goethite at high temperatures. It is known that goethite dehydrates to hematite at 300°C, so the thermal demagnetization above this temperature is clouded by uncertainty about the role of a new hematite phase, especially in this case where the remanence seems to be carried almost entirely by goethite.

The possible coexistence of goethite with either magnetite or hematite has been indicated in a number of specimens. It was observed in Figure 5.2 that, on AF demagnetization, a steep-down component with relatively high coercivity has probably shrouded the shallower component that had been revealed on thermal demagnetization. The shallower component, with unblocking temperature well below the Curie point of magnetite, could be easily isolated by the thermal treatment. It is therefore concluded that specimens AQ16-B and AQ16-C (Figure 5.2) probably contain a mixture of magnetite and goethite, in which goethite carries the steep component (which seems to be the same as the very hard component of Specimen IB6-1 in Figure 5.10), whereas magnetite preserves the "A" component. A sharp break in the thermal decay curve of Specimen AQ16-C (Figure 5.2), following 458

intensity reduction at 100°C, seems to reinforce this conclusion. Because the proportion of the remanence attributed here to magnetite is dominant, chemical changes leading to inversion of goethite to hematite probably do not pose a problem in the isolation of the most stable component. However, in 4 to 5 specimens where goethite seems to have carried a larger proportion of remanence, as revealed by 80 to 90% reduction in intensity at 100°C, isolation of the most stable component was a problem. Most of these specimens failed to yield a consistent component at higher temperatures and the measurements were often noisy. The specimens which posed this problem are exclusively from the Isthmus Bay Formation, from those sites where a "B" component was isolated. Thus the problem seems to be related to those specimens where probably hematite and goethite exist together, with goethite carrying the larger proportion of remanence.

5.2.3 Port au Choix area

Ninety-nine oriented hand samples were collected from 20 sites spanning all three Formations of the St. George Group (Figures 2.2, 2.4). The distribution of samples is as follows. Isthmus Bay Formation: 39 samples (8 sites); Catoche Formation: 40 samples (8 sites); Aguathuna Formation: 20 samples (4 sites). At least two standard specimens were cut from each of these samples. Remanence measurements were done on at least one specimen per sample.

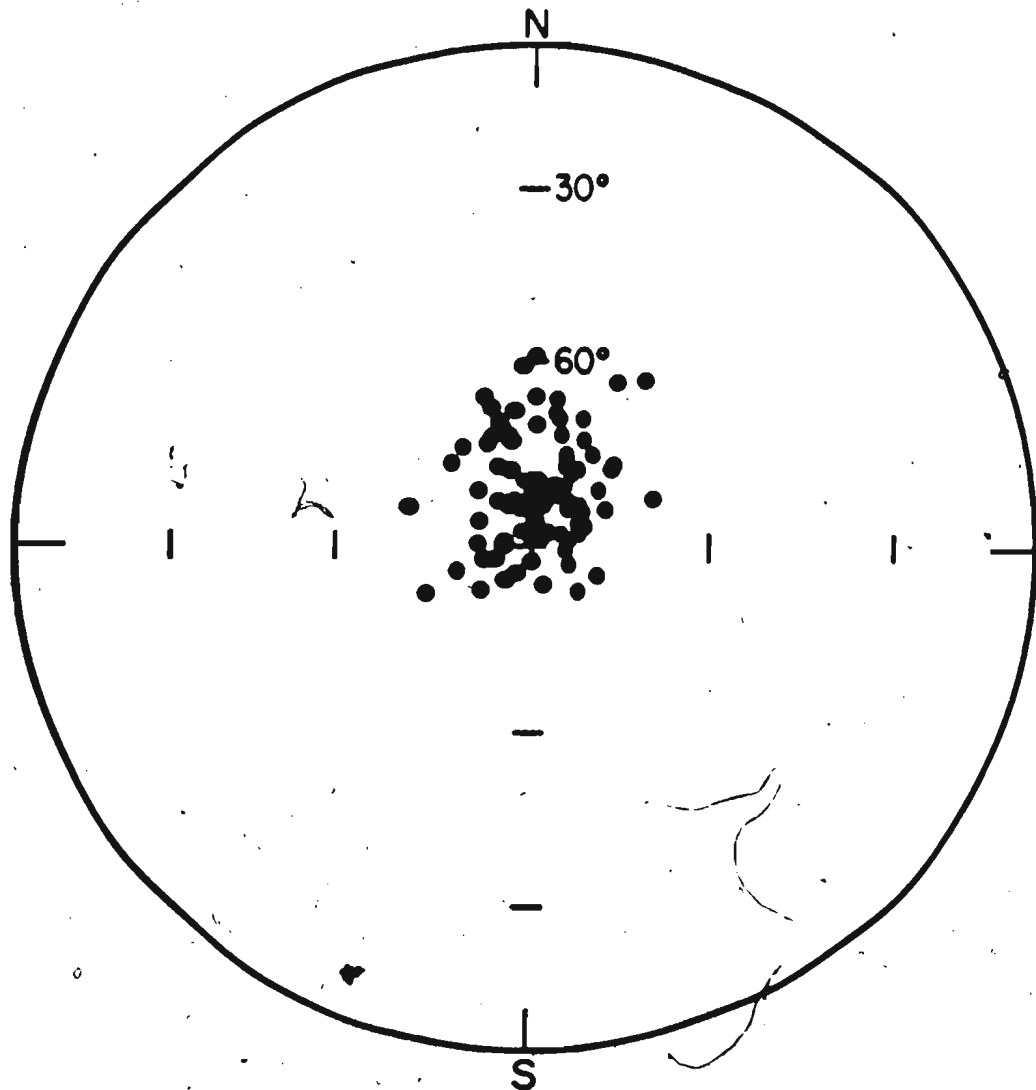


Fig. 5.11. NRM directions of St. George Group samples, Port au Choix area. Equal area projection on the lower hemisphere.

The NRM directions of all the samples (one specimen each) are plotted in Figure 5.11. They are tightly grouped in a steep downward direction. The NRM intensities range from 3×10^{-4} A/m to 7×10^{-3} A/m, with a large majority of samples having intensities in the range 1 to 3×10^{-3} A/m. AF demagnetization was carried out on 20 specimens, each chosen from a different site. Figure 5.12 represents the demagnetization characteristics of these specimens. It shows that the steep downward-directed NRM either remains steep (Specimen PC91-A), or moves to a shallower, but still downward stable direction (Specimen PC21-C), or else changes sign to end up in a shallow upward direction (Specimen PC6-2). The intensity decay in all the three specimens was smooth and almost complete ($J/J_n < 5\%$) well below 100 mT, which suggests the absence of high-coercivity grains as remanence carriers. These three apparently stable, but widely divergent directions probably indicate the presence of components with partly to almost completely (PC91-A) overlapping coercivity spectra which cannot be resolved by AF treatment. For two specimens (PC6-2 and PC21-C) the trend of directional change at higher fields, however, seems to favour a north to northeasterly characteristic component which is represented by Specimen PC6-2, showing a shallow, upward-directed end point.

Thermal demagnetization was found to be more effective in isolating characteristic magnetizations from a majority

Fig. 5.12: AF demagnetization results for 3 St. George specimens from Port au Choix area, yielding three distinct stable directions. Conventions for stereoplots as in Fig. 5.2 and for vector diagrams as in Fig. 5.7.

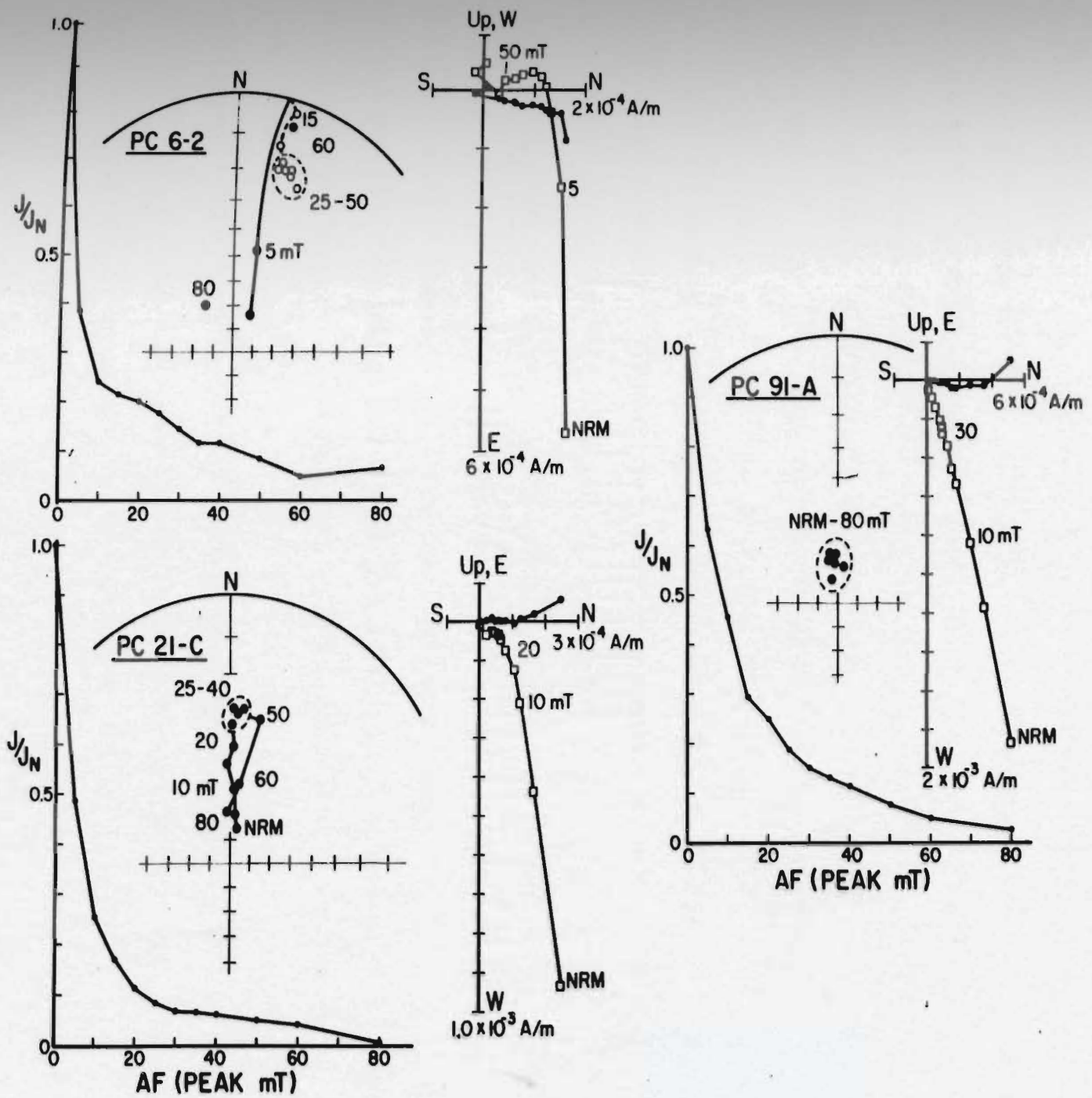


Fig. 5.12

of the samples. One specimen from each of 99 samples was thus thermally demagnetized according to the step-schedule outlined in Appendix A. Based on the result of some detailed pilot demagnetizations, it was found that treatment at temperatures of 100°C and 200°C only indicated the removal of a large, steeply inclined component close to present earth's field, probably of viscous origin. Therefore it was decided, in the majority of specimens, to proceed directly from NRM to the 300°C step. For these specimens, the results are based usually on a 4-step demagnetization between 300°C and 450°C, after which the intensity was often reduced to 1 to 2% of the NRM. Wherever a substantial moment (> 5% of NRM) remained, the specimens were then treated to higher temperatures. Results of thermal demagnetization (Figures 5.13 to 5.15) show that a characteristic component is uncovered in the range 300-450°C. This is indicated in Figure 5.13 by a well-defined, stable end point and a straight-line decay to the origin on the orthogonal vector diagrams. In Figure 5.14, stable end points are not as well defined, but the vector subtractions yield linear high-temperature segments. In Specimen PC19-2, this segment misses the origin though it terminates close to the measurable limit of intensity. Therefore the subtracted vector between 300 and 450°C has been considered acceptable as the most stable component in this case also.

The characteristic magnetization in Figures 5.13-5.14

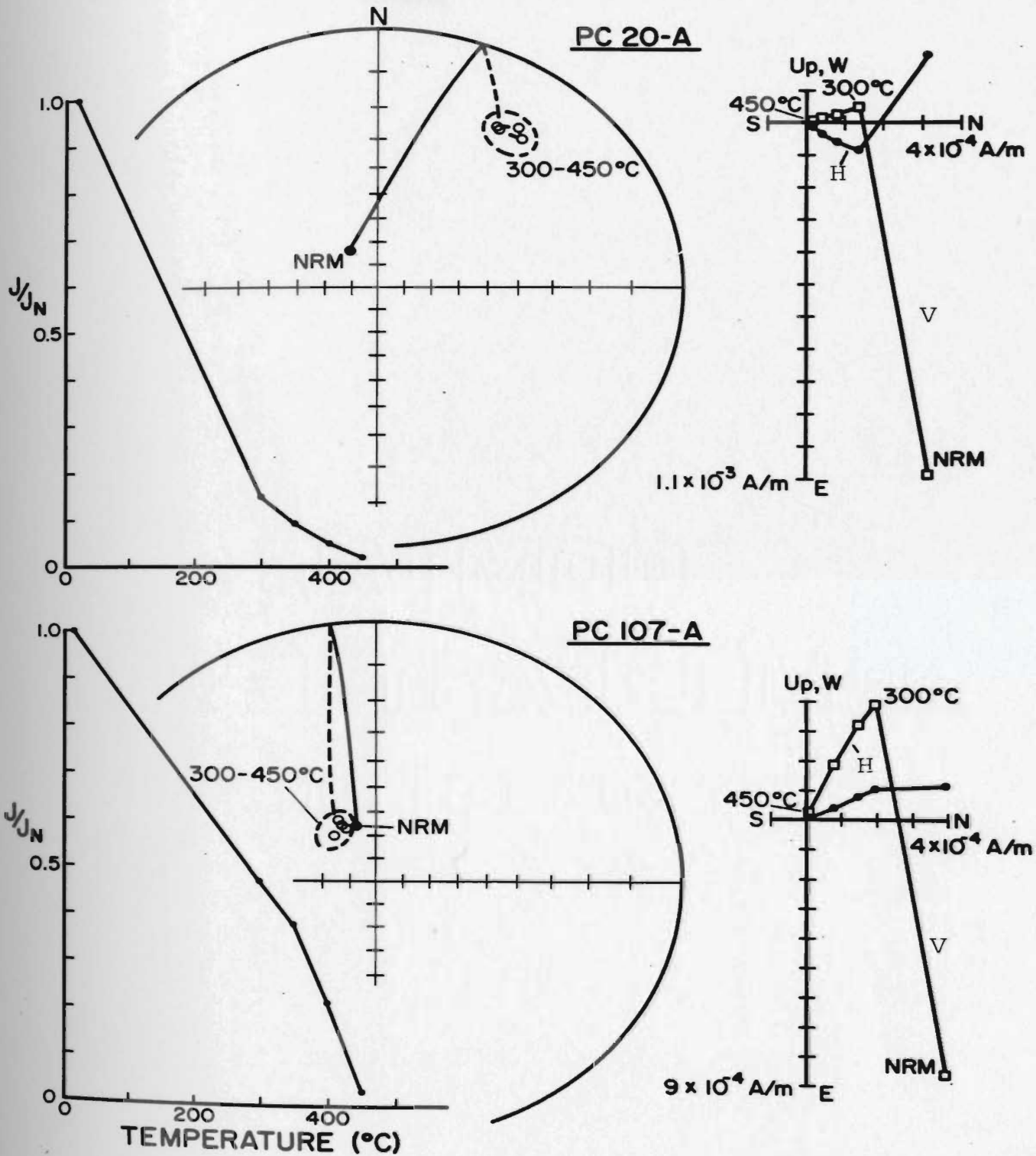


Fig. 5.13. Representative thermal demagnetization results for 2 St. George specimens from Port au Choix area that define stable end point magnetization. Closed (open) circles on the stereoplot are downward (upward) pointing directions. Open squares on the vector diagram are vector end point projections on a N-S vertical (V) plane and solid dots on the horizontal (H) plane.

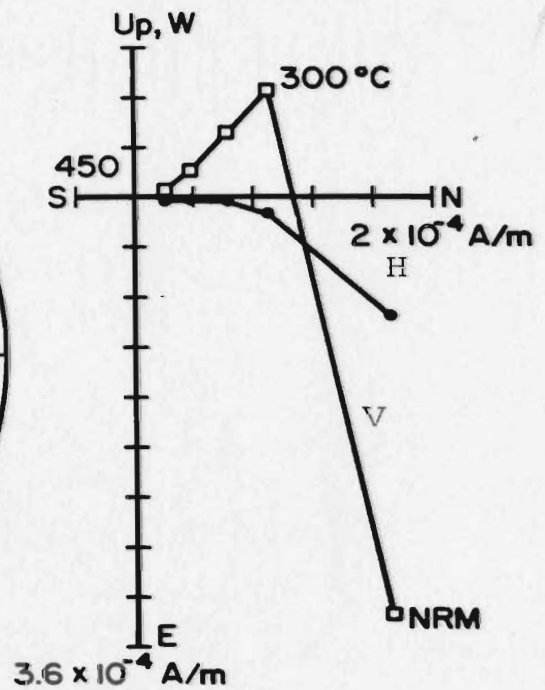
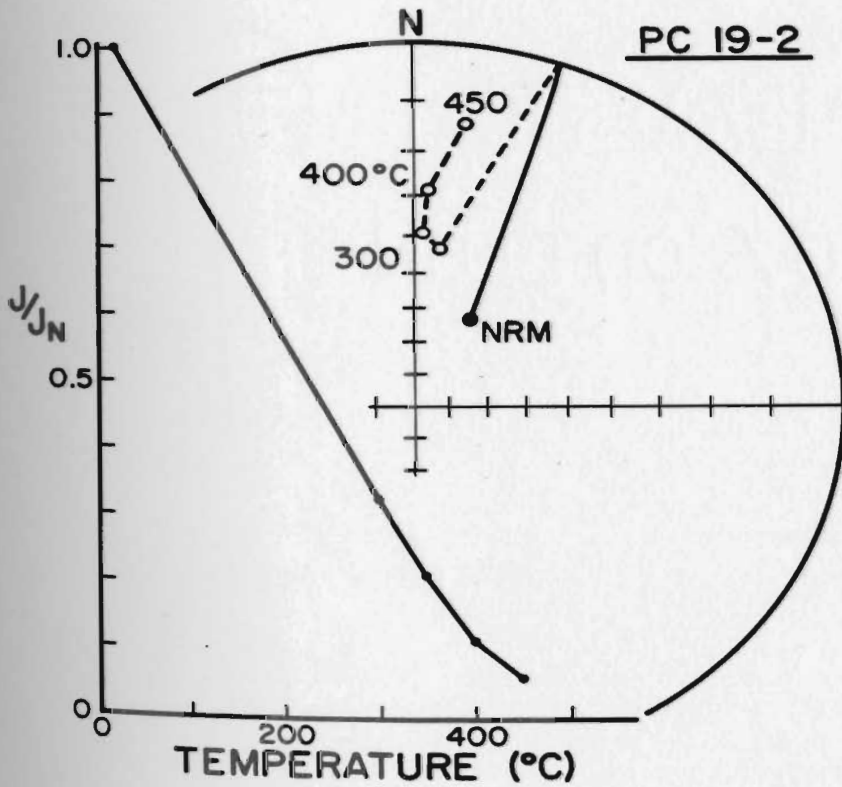
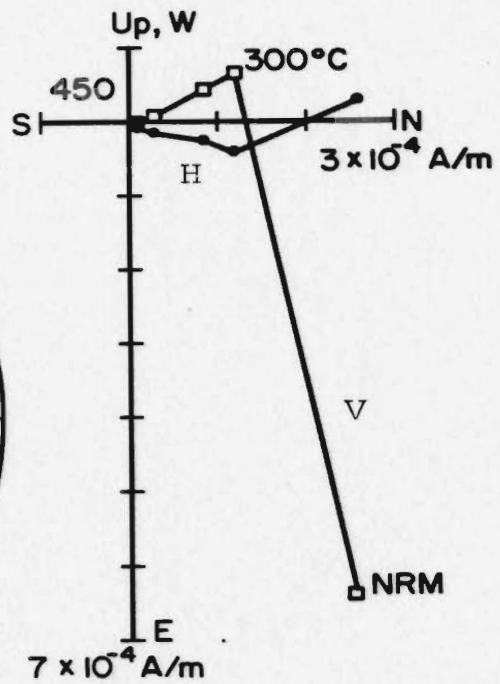
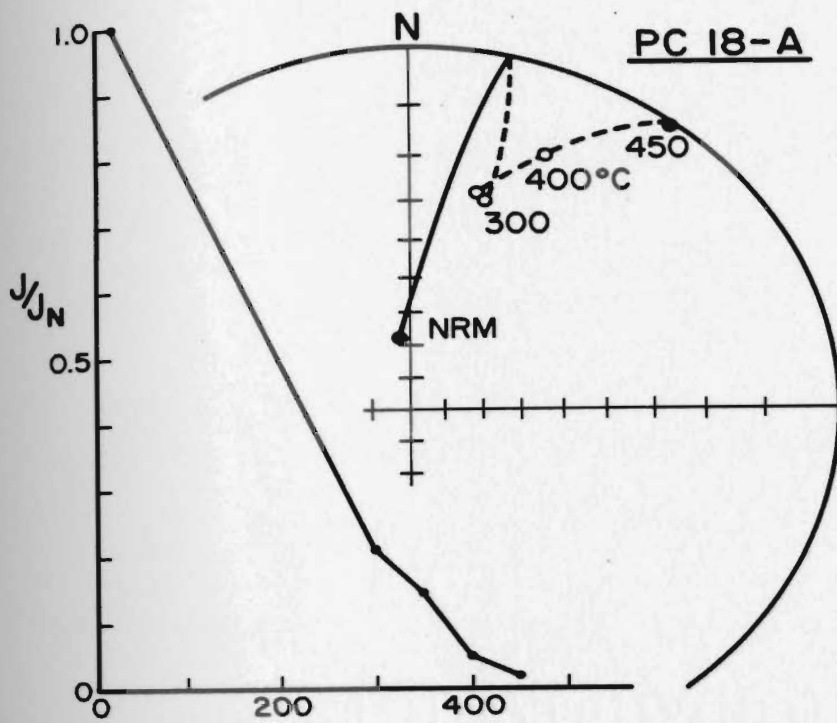


Fig. 5.14. Representative thermal demagnetization results for 2 St. George specimens from the Port au Choix area, yielding the characteristic direction after vector subtraction from the vector diagrams. Conventions as in Fig. 5.13.

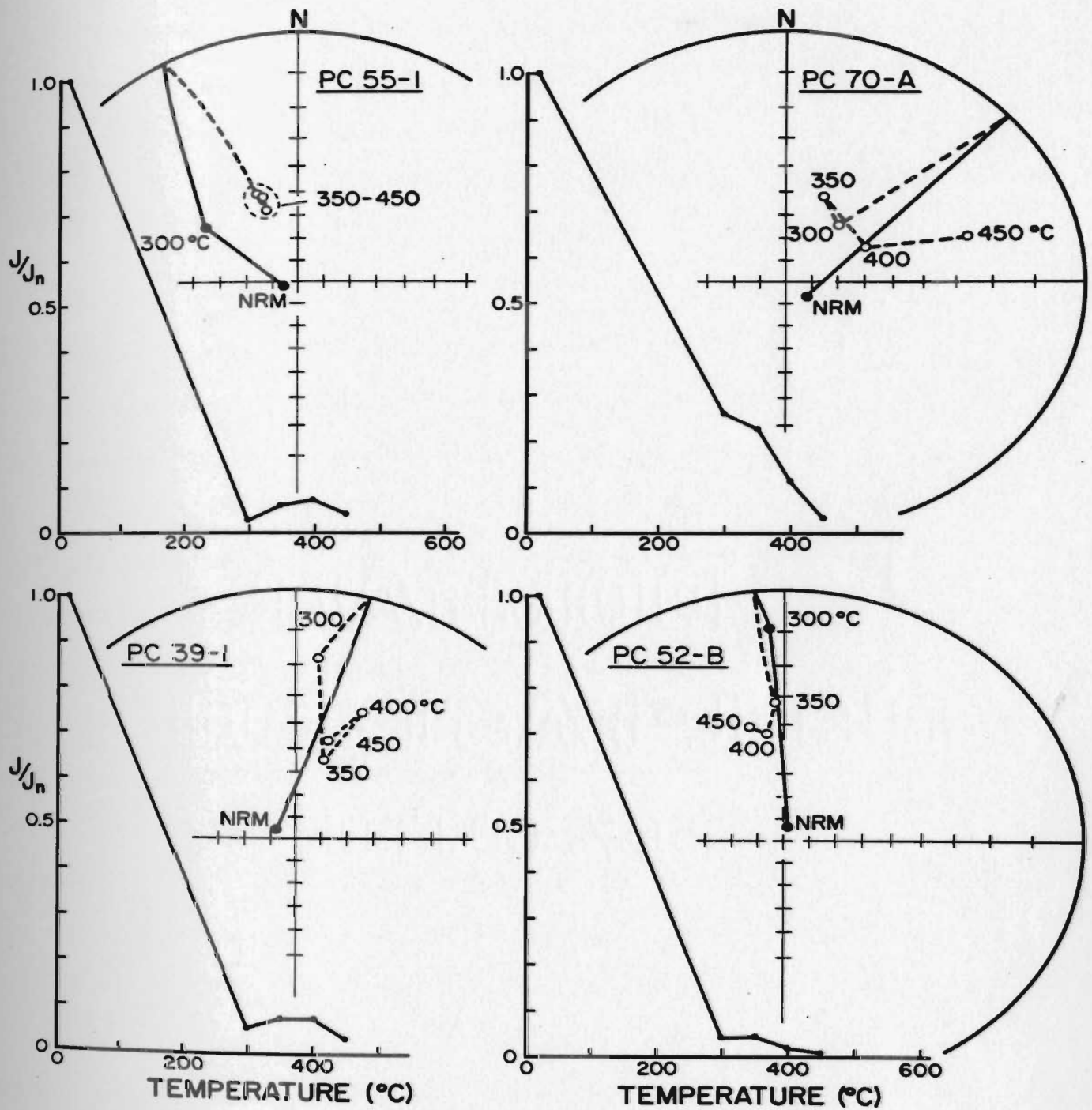


Fig. 5.15. Representative thermal demagnetization results for 4 St. George specimens from Port au Choix area where the characteristic remanence resides in the last few percent of the total remanence. Conventions as in Fig. 5.13.

is contained in a range between 15 and 45% of the total remanence. More frequent, however, was the isolation of a characteristic component below 15% of the total NRM. Figure 5.15 gives four typical examples of specimens where a characteristic component resided in as little as 4 to 8%, and in one case 25%, of the NRM. These specimens yielded a reasonably well-defined, stable end point at high temperatures. Because of the fact that the most stable component was carried by a very low proportion of the NRM, the vector plots become very erratic in the highest temperature range, and are not shown for these specimens. The calculation of a characteristic component is here based on the stable end point criterion.

The magnetizations thus isolated from all the thermally demagnetized specimens that gave characteristic final directions are listed in Table 5.5 and are plotted in Figure 5.16. These directions were successfully isolated in 48 out of a total of 99 samples. The directional scatter as seen in Figure 5.16 is large; the inclinations range from shallow to intermediately steep. The formation means with their radii of 95% confidence, both before and after tilt correction, are plotted in Figure 5.17 along with the corresponding mean directions for the Port au Port rocks for a comparison. The tilt-correction does not appear to improve the grouping of Formation means, which is not unexpected because of the small between-site variations in dip and strike. However, the Formation means of the

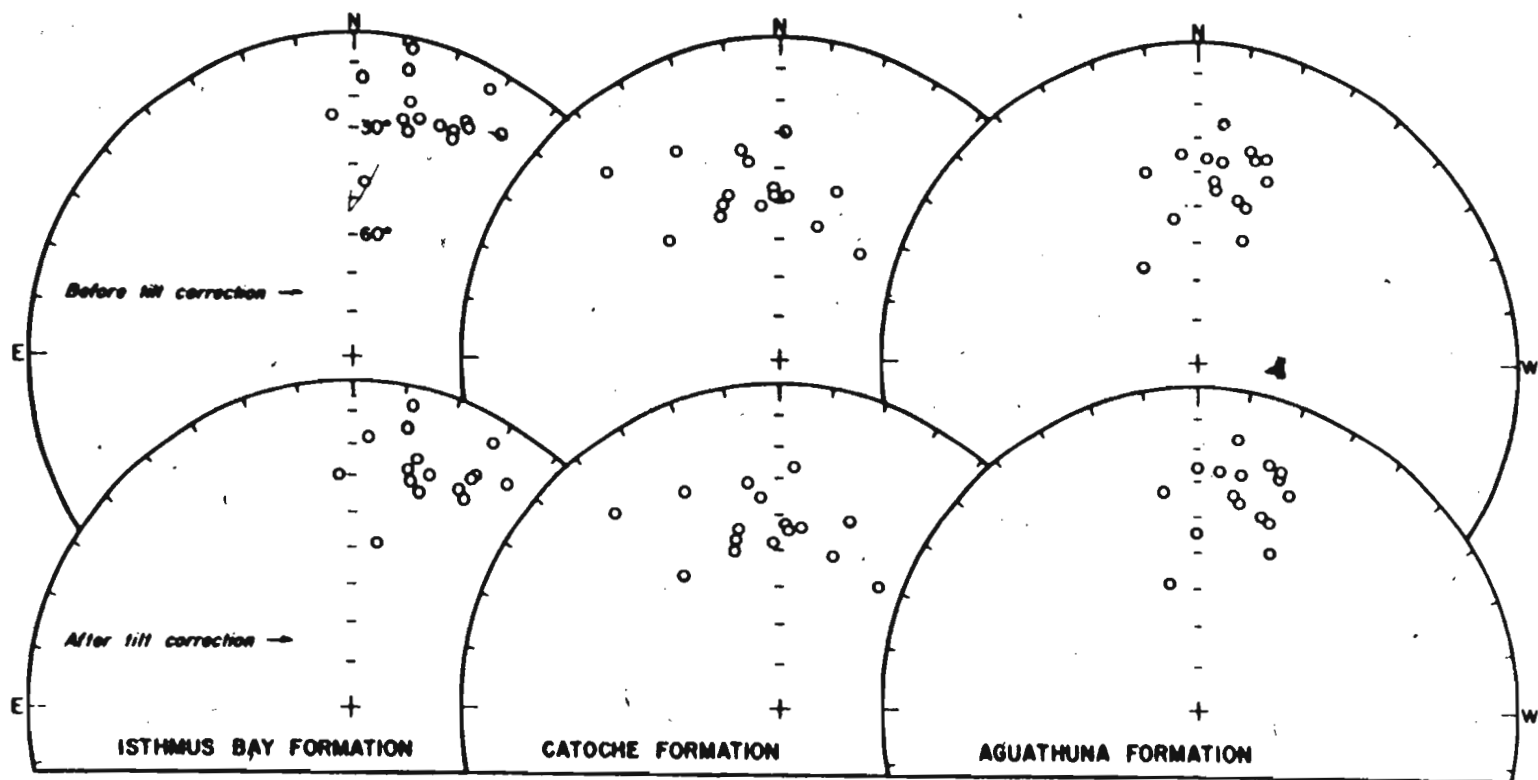


Fig. 5/16. Sample characteristic directions from the St. George Group, Port au Choix area. Equal area projection on the upper hemisphere.

Fig. 5.17. Formation means with their 95% confidence circles for the St. George Group in the two main sampling areas: (a) before tilt correction; (b) after tilt correction. Conventions as in Fig. 5.13. Equal area projection.

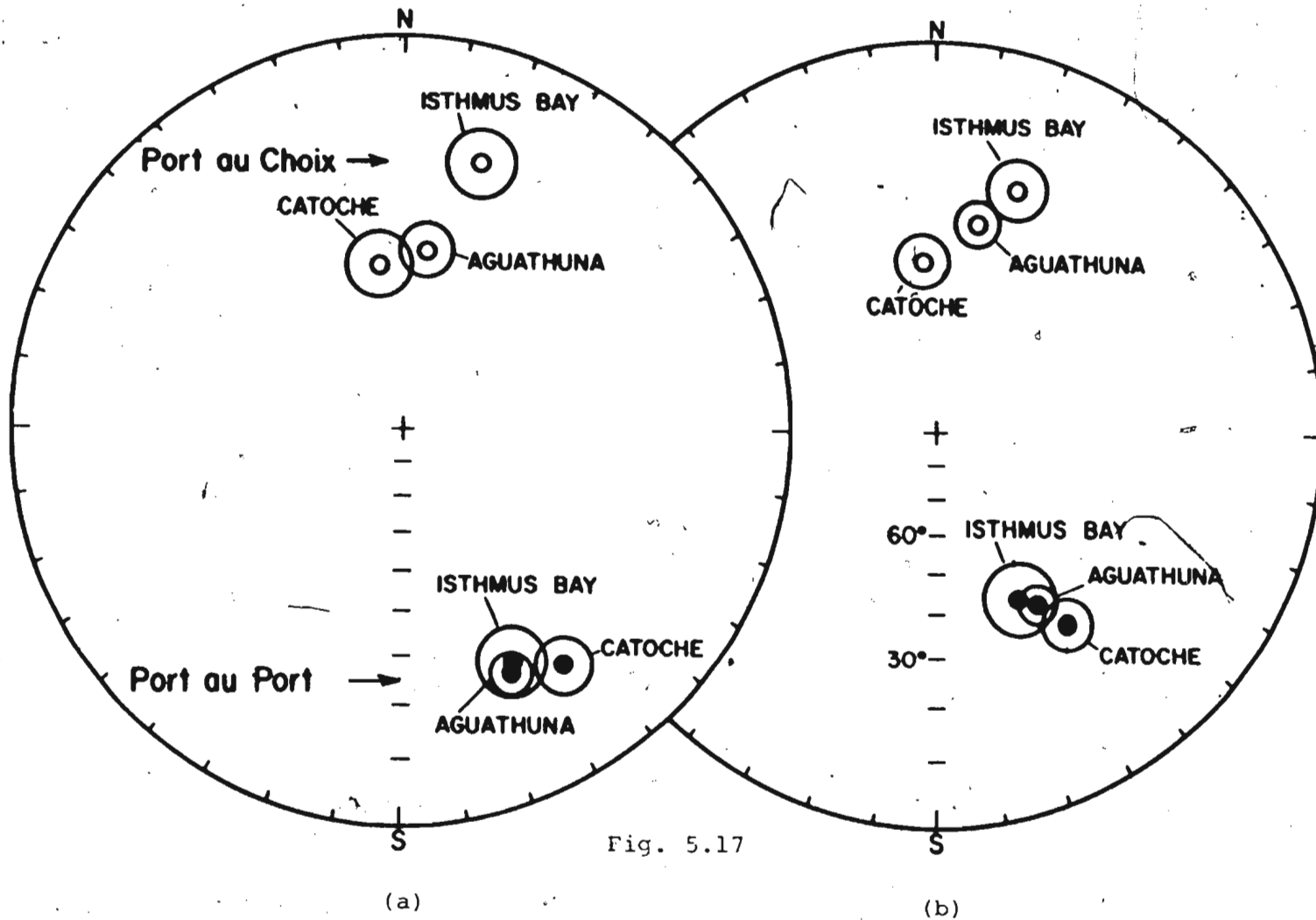


Fig. 5.17

TABLE 5.5

THERMAL DEMAGNETIZATION RESULTS FROM THE ST. GEORGE GROUP,
PORT AU CHOIX AREA.

Site	Specimen	Characteristic direction				Stability range (° C)
		<u>In situ</u>		Tilt-corrected		
		D	I	D	I	
Isthmus Bay Formation						
PC1	PC1-1	12.0	- 3.3	12.3	- 6.8	300-500 (v.s.)
PC1	PC3-A	28.0	- 5.5	28.5	- 7.9	300-450 (v.s.)
PC1	PC4-A	27.6	-21.0	29.4	-23.4	300-450 (v.s.)
PC2	PC6-1	12.0	-24.0	13.7	-27.5	300-450 (v.s.)
PC2	PC8-A	356.0	-26.1	357.3	-30.4	300-400 (v.s.)
PC2	PC9-A	3.0	-14.3	3.9	-18.4	300-350 (ave.)
PC2	PC10-A	13.9	-19.7	15.3	-23.1	300-400 (v.s.)
PC3	PC11-B	27.3	-20.0	29.0	-22.4	300-450 (v.s.)
PC3	PC13-B	13.1	-26.3	15.0	-29.7	300-450 (ave.)
PC3	PC14-A	26.3	-26.2	28.6	-28.7	300-400 (ave.)
PC3	PC15-2	24.6	-24.2	26.6	-26.8	300-450 (v.s.)
PC4	PC18-A	15.4	-29.0	17.7	-32.2	300-450 (v.s.)
PC4	PC19-2	5.2	-45.2	8.7	-49.0	300-450 (v.s.)
PC4	PC20-A	34.8	-16.5	36.3	-18.3	300-450 (ave.)
PC5	PC21-A	17.3	-23.7	19.1	-26.8	350-450 (ave.)
PC5	PC25-B	11.6	-10.1	12.3	-13.6	400-450 (ave.)
Catoche Formation						
PC7	PC31-2	359.3	-48.0	3.0	-44.5	350-450 (v.s.)
PC7	PC33-A	333.9	-29.4	336.5	-27.8	350-450 (ave.)
PC7	PC35-A	349.7	-33.6	352.3	-30.8	350-400 (ave.)
PC8	PC36-B	343.1	-45.7	347.4	-43.3	350-500 (v.s.)
PC8	PC37-A	353.7	-51.0	358.1	-47.9	350-400 (ave.)
PC8	PC39-1	19.5	-43.7	21.1	-39.2	350-450 (ave.)
PC11	PC51-A	340.4	-47.8	345.1	-45.6	350-450 (v.s.)
PC11	PC52-B	351.9	-37.9	354.9	-34.9	350-450 (ave.)
PC11	PC53-A	3.9	-47.5	7.3	-43.7	350-450 (v.s.)
PC11	PC54-B	316.9	-49.2	322.7	-49.0	350-400 (ave.)
PC11	PC55-1	338.3	-51.0	343.7	-49.0	350-450 (ave.)
PC12	PC56-A	317.0	-21.8	319.0	-21.7	400-500 (v.s.)
PC13	PC62-B	358.8	-46.0	2.3	-42.6	350-400 (v.s.)
PC13	PC63-B	16.6	-54.7	19.7	-50.3	350-450 (v.s.)
PC14	PC68-B	1.8	-30.2	3.7	-26.6	300-450 (v.s.)
PC14	PC70-A	39.0	-56.1	39.9	-51.1	300-400 (ave.)

TABLE 5.5 (CONT'D)

Site	Specimen	Characteristic direction				Stability range (° C)
		<u>In situ</u>		Tilt-corrected		
		D	I	D	I	
Aguathuna Formation						
PC19	PC92-A	356.0	-34.5	0.0 ^d	-26.3	350-450 (ave.)
PC19	PC93-1	351.3	-52.7	0.0	-44.8	350-400 (ave.)
PC19	PC94-A	345.0	-38.9	351.2	-32.1	400-450 (v.s.)
PC19	PC95-1	22.1	-39.0	24.2	-28.5	350-450 (ave.)
PC20	PC98-A	7.4	-44.9	12.1	-35.4	300-400 (ave.)
PC20	PC99-A	7.6	-36.9	11.1	-27.4	350-400 (ave.)
PC20	PC100-A	18.0	-33.5	20.1	-23.2	350-450 (v.s.)
PC21	PC101-A	18.9	-48.1	22.3	-37.7	400-450 (v.s.)
PC21	PC102-A	5.8	-42.6	10.3	-33.2	400-450 (v.s.)
PC21	PC103-A	2.5	-36.2	6.5	-27.2	300-400 (ave.)
PC21	PC104-A	15.0	-32.1	17.3	-22.0	350-400 (ave.)
PC22	PC106-2	17.5	-34.2	19.7	-24.0	400-450 (ave.)
PC22	PC107-A	330.3	-63.1	347.4	-57.7	300-450 (ave.)
PC22	PC108-A	15.0	-46.7	18.8	-36.6	300-400 (ave.)
PC22	PC109-A	22.3	-56.7	26.1	-46.1	300-450 (v.s.)
PC22	PC110-1	7.2	-25.7	9.4	-16.3	300-450 (ave.)

All symbols and explanations as in Tables 3.1. and 5.3

TABLE 5.6

MEAN PALEOMAGNETIC DATA AFTER THERMAL DEMAGNETIZATION OF THE ST. GEORGE GROUP,
PORT AU CHOIX AREA.

	D_m	I_m	k	N	α_{95}	λ_p	Pole Position
Isthmus Bay Formation, 16 samples, <u>in situ</u>	17.0	-21.2	34	16	6.4	10.9 S	
Isthmus Bay Formation, 16 samples, tilt- corrected	18.6	-24.4	34	16	6.4	12.7 S	24.5°N, 102.8°E (d_p , d_m = 3.7°, 6.9°)
Catoche Formation, 16 samples, <u>in situ</u>	351.2	-45.2	20	16	8.4	26.7 S	
Catoche Formation, 16 samples, tilt- corrected	355.1	-42.3	20	16	8.4	24.4 S	14.7°N, 127.3°E (d_p , d_m = 6.3°, 10.3°)
Aguathuna Formation, 16 samples, <u>in situ</u>	7.3	-42.3	34	16	6.4	24.5 S	
Aguathuna Formation, 16 samples, tilt- corrected	11.6	-32.8	34	16	6.4	17.9 S	20.7°N, 110.6°E (d_p , d_m = 4.1°, 7.3°)
St. George Group (above three Formations combined), 48 samples, tilt-corrected	9.3	-33.5	19	48	4.8	18.3 S	20.5°N, 113.3°E (d_p , d_m = 3.1°, 5.5°)

All symbols as in Table 3.3

Port au Choix rocks are more widely spaced than in the case of Port au Port, where the confidence circles are overlapping. An F-ratio test (Watson, 1956; Larochelle, 1967) was applied to examine the statistical significance of the differences in formation means. The test indicated that the formation means are significantly different at 99% level of confidence, both before and after tilt correction, for the Port au Port as well as the Port au Choix areas.

The pole positions corresponding to the three Formation means are listed in Table 5.6 along with their statistical parameters. The north pole positions are consistent with the presumed APWP for cratonic North America, and therefore these poles are taken to be of normal polarity.

Finally, certain aspects of the magnetization behaviour of some of the specimens not yielding a meaningful, stable direction are discussed. Figure 5.18 shows plots of demagnetization behaviour with temperature of six representative specimens. Four of these (Specimens BH2A, PC3-A, PC41-1 and PC24-1) show systematic directional changes respectively to the west, northeast followed by southwest, southeast and northeast. A complete decay of intensity in these specimens probably precludes the completion of the observed directional trend. Three of these 4 specimens (excluding PC41-1) come from the Isthmus Bay Formation, where a characteristic component with a shallow negative inclination towards N to NE had been

Fig. 5.18 Thermal demagnetization results for 6 St. George specimens from Port au Choix area, not always yielding a characteristic direction. These results show the presence of unresolved superposed components (See text). Conventions as in Fig. 5.13.

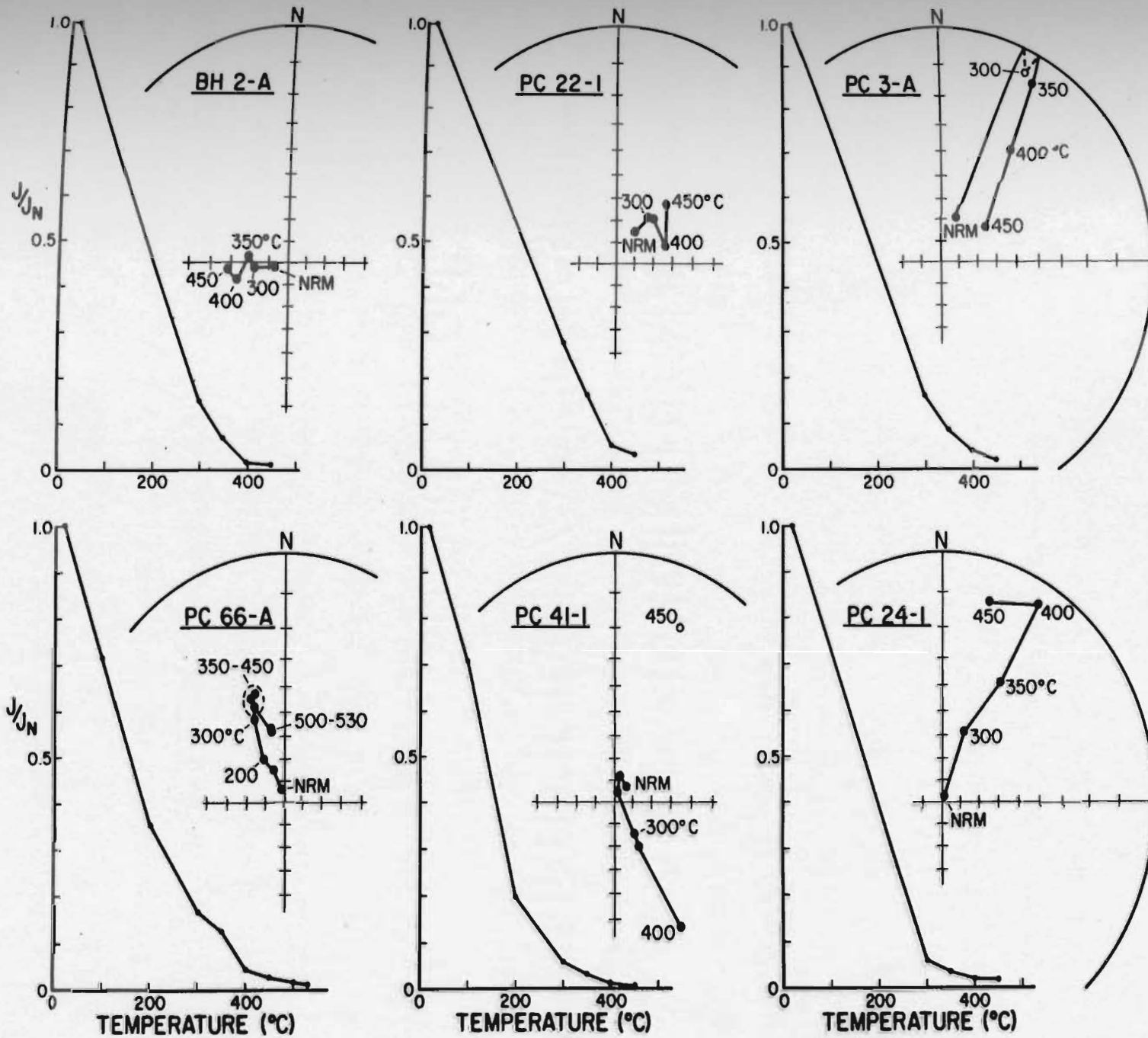


Fig. 5.18

isolated from the specimen directions (Figure 5.16). The direction of Specimen PC24-1 shows a trend towards that goal, while in Specimen PC3-A a shallow northeasterly end point direction also is obtained by vector subtraction between 300 and 450°C. The vector subtracted direction of Specimen PC3-A has been included for averaging in Figure 5.16.

The two other specimens, PC22-1 and PC66-A, in Figure 5.18 show some stability in the range 300-450°C, the stable direction in the former case being steep downward towards NE, and that in the latter case being preceded by a swing towards N to NW. The apparently stable directions exhibited by these two specimens are anomalous in the sense that they are very steep. One interpretation could be that these specimens have been completely remagnetized close to the recent geomagnetic field at the site. However, a closer examination of the demagnetization behaviour of other specimens in Figure 5.18 suggest that the steep, but apparently stable directions in these two specimens could have resulted from a multicomponent system with overlapping stability spectra, which sometimes may comprise normal and reverse components. This would partly explain why a large proportion (50%) of specimens, of the 99 St. George Group samples from Port au Choix failed to yield consistent directions.

5.2.4 Magnetic mineralogy (Port au Choix rocks)

An IRM study was done on six samples (one specimen each) representing all the sampling localities. All the specimens showed a strong initial increase of the remanence intensity in fields up to 0.1 Tesla. Above 0.1 T, the increase became very small and all but one specimen reached saturation magnetization in fields of about 0.2 T. The corresponding IRM curves are very similar to the "magnetite" curves of Figure 5.9 (type 1) and are not shown here. The only exception was a specimen in which, after a rapid initial increase in the remanence intensity up to 0.1 T, a slight gradient was still maintained up to 0.82 T. However, the back-field characteristics always yielded a single coercivity of remanence (H_{Cr}) value of about 0.05 T. All this suggests that while some of these rocks might contain a very small amount of hematite or goethite, magnetite is the only carrier of magnetization in a large majority of the samples. This conclusion is further reinforced by the limited AF demagnetization experiments (Figure 5.12) where no high-coercivity components have been recognized. The thermal demagnetization results (Figures 5.13-5.15) also reveal low blocking temperature components, strongly indicating the presence of magnetite only.

5.3 Discussion

The "A" component isolated in the rocks of Port au Port area, which has been demonstrated to reside in

magnetite, is interpreted to be the signature of an Early Ordovician geomagnetic field in western Newfoundland for the following reasons:

(1) The conodont colour alteration index (CAI) in the Port au Port area is 1 (Nowlan and Barnes, 1985). For any reasonable length of burial time (10^8 yr.), maximum burial temperatures of 50-60°C are indicated (Epstein et al. 1977). On the assumption of a burial temperature of 60°C, even a burial time as long as 300 million years would not suffice to reset the magnetization, blocked in the range 450-500°C (Pullaiah et al., 1975). This suggests that the remanence is not a thermal remagnetization.

(2) The pole position corresponding to the "A" component is nowhere near the reported Middle to Upper Paleozoic poles of cratonic North America, which makes any long-time chemical remagnetization of the magnetite remanence (Scotese et al., 1982; Wisniowiecki et al., 1983; McCabe et al., 1983, 1984) highly unlikely.

(3) The "A" pole is consistent with some published Cambro-Ordovician poles of cratonic North America (Chapter 9).

The Port au Choix rocks, on the other hand, give quite a different result. A comparison with the Port au Port rocks (Tables 5.4 - 5.6; Figure 5.17) indicates that the normal polarity directions of the Port au Choix rocks differ from the former mainly in declination, by -140° .

One interpretation could be that there has been a relative tectonic rotation of about 40° between the Port au Port and Port au Choix areas since the rocks in both areas acquired their magnetizations. This interpretation would be valid only if it can be demonstrated that the magnetization of the Port au Choix rocks is primary. The thermal history of the Port au Choix rocks, however, favours a possible thermal remagnetization. The conodont CAI values in the sampling area (between Table Point and Eddies Cove, Figure 2.1) are in the range 2 to 3.5 (Nowlan and Barnes, 1985), indicating a maximum burial temperature of $100-150^\circ\text{C}$ (Epsstein et al., 1977). Theoretical calculations of Pullaiah et al., (1975) suggest that, while a blocking temperature of 380°C or less would be reset if the rocks were heated to 150°C for 10^8 yr., a blocking temperature of 400°C or above should survive. On this premise it would seem that the Port au Choix rocks probably survived the thermal resetting of magnetization, as the blocking temperatures are in the range $400-450^\circ\text{C}$ (Table 5.5). A recent study (Kent, 1985), however, indicates that the thermoviscous remagnetization at moderately elevated burial temperatures could reset the magnetic grains blocked at much higher temperature than predicted by Pullaiah et al. (1975). If this is the case, it is quite probable that the stable remanences carried by magnetite in the Port au Choix rocks reflect a complete thermal overprint. Significant differences in the formation means are probably

indicative of a long time interval in the remagnetization of the formations, or alternatively, of rapid polar wandering during the short times the rocks were being magnetized.

It is worthwhile to speculate on an age of magnetization for the presumably secondary magnetization of Port au Choix rocks. In this respect it is noted that pole positions of the Port au Choix rocks are significantly displaced from the Kiaman poles (see Chapter 9 for comparison) and are of normal polarity. Therefore (a Kiaman) remagnetization is ruled out. A post-Paleozoic age also is very unlikely, since one would expect characteristic Mesozoic and Cenozoic field directions relative to western Newfoundland to be much steeper than the observed directions. This leaves one to speculate on an age of magnetization anywhere between Middle Ordovician and Early Carboniferous. Middle Ordovician north poles obtained from this study (Chapter 6) are nowhere near the three Port au Choix poles. A comparison with published poles shows these three poles to be close to Late Ordovician to Early Carboniferous poles from other parts of the North American craton. Of special relevance here are the recent results from Early Carboniferous rocks of western Newfoundland (Irving and Strong, 1984a; Murthy, 1985) and a result from Late Devonian rocks (Irving and Strong, 1985) in eastern Newfoundland. The pole positions reported in the above studies fall near the same general

area as the three Port au Choix St. George poles. It is probable therefore that the poles from the Early Ordovician rocks of the Port au Choix area represent the earth's magnetic field direction during or after the Acadian orogeny (Middle to Late Devonian). If so, then the tilt correction done in the paleomagnetic data may be questionable, if the deformation of beds is Acadian. Since the magnitude of tilt is very low ($0-10^\circ$), the final result would not change significantly if the tilt correction were not done. Moreover, since there is uncertainty in the age of deformation (Chapter 2), which could be later than the Acadian, the tilt-corrected directions have been preferred.

A pre-Devonian magnetization for the St. George Group of Port au Choix area is also a possibility, as some published Silurian poles from the North American craton (e.g., French and Van der Voo, 1979; McCabe et al., 1985) are close to the three Port au Choix poles (Table 5.6) of the present study.

The "B" component isolated from the rocks of Port au Port Peninsula is interpreted to be a chemical remanent magnetization (CRM) residing in diagenetic hematite that was acquired probably during late Carboniferous to Early Permian (Kiaman) times. The pole position corresponding to the "B" component agrees very well with the Kiaman pole isolated from the Cambrian rocks (Chapter 3) and from Paleozoic rocks in other parts of the craton (e.g., Irving

and Irving, 1982; Irving and Strong, 1984a, 1985; McCabe et al., 1984). Furthermore, it is to be noted that the "B" component was isolated mostly from the lowermost part of the St. George Group (Isthmus Bay Formation). Rocks on the higher stratigraphic level are not pervasively overprinted.

The present results are further compared and discussed in relation to some other Ordovician and Kiaman poles in Chapter 9.

CHAPTER 6

TABLE HEAD GROUP

6.1 Geological Setting

Rocks of the Middle Ordovician Table Head Group are exposed at various localities in western Newfoundland, from the Port au Port Peninsula in the south to Hare Bay in the north (Figure 2.1), as part of the autochthonous Cambrian-Ordovician platform of the northern Appalachians. This platform is thought to have been subsiding at the time of sedimentation of the Table Head Group, when it received deeper water sediments (James and Stevens, 1982). The Table Head Group is therefore a critical sedimentary unit which probably documents completely the collapse of a continental margin (Klappa et al., 1980).

Based on lithologic and faunal differences, the Table Head Group has been subdivided into four Formations by Klappa et al. (1980). From oldest to youngest, these are: Table Point, Table Cove, Black Cove, and Cape Cormorant Formations (Figure 2.2). The following brief observation about the four Formations is due to Klappa et al. (1980).

The Table Point Formation comprises bioturbated massive grey limestones and interbedded limestone-dolostone units. This Formation is characterized by a heterogeneous package of shelf carbonates.

The Table Cove Formation is characterized by bioturbated, thin- to medium-bedded limestone of possible

pelagic origin, and interbedded shales. Deposition of sediments comprising the Table Cove Formation is thought to have occurred on the slopes of platform margin basins.

The Black Cove Formation comprises black shale/mudstones at the type locality on Port au Port Peninsula. Its deposition took place in basins of restricted circulation by suspension settling of fine clastic material.

The Cape Cormorant Formation consists of dark calcareous shales, green siltstones and interbedded calcareous rocks. It contains one or more well developed lime breccia-conglomerate beds, made up essentially of reworked shelf (Table Point) and upper slope (Table Cove) limestone clasts. The Cape Cormorant Formation represents the last record of deposition on the shelf before the onset of flysch deposits derived from the east (Stevens, 1970).

6.2 Paleomagnetic sampling and results

For paleomagnetic investigations, Table Head rocks were hand sampled as follows: In the Port au Port area, 16 samples from the Table Point Formation, 12 from the Table Cove Formation and 27 from the Cape Cormorant Formation were taken, giving a total of 55 samples distributed at 14 sites. In the Port au Choix area, 48 samples were collected from 10 sites, all from the Table Point Formation. The sampling localities are shown in Figures 2.3-2.4 and details are given in Appendix D. However, one

important distinction between the bedding attitudes of the different Formations must be noted. Whereas the Table Point and Table Cove Formations are moderately dipping ($11-16^{\circ}\text{NW}$), the Cape Cormorant Formation dips much more steeply ($\sim 50^{\circ}\text{NW}$). This variation in tilt at the different sites therefore provides an opportunity to test whether the stable magnetization is pre- or post-tilting. Paleomagnetic results from the Port au Port and Port au Choix areas are described separately in the following Sections.

6.2.1 Port au Port area

Paleomagnetic measurements were carried out on 54 samples (89 specimens). All specimen NRM directions are plotted in Figure 6.1. The NRM intensities ranged from 4×10^{-5} to 3×10^{-3} A/m; however, intensities of the order of 1 to 3×10^{-4} A/m were found to be the most common. Figure 6.1 shows that the NRM vectors for Table Cove are better grouped than those of the other two Formations. All Table Cove NRM directions and most of the Table Point and Cape Cormorant directions are significantly misaligned with the present earth's field, indicating the presence of some ancient component(s) in them. The Table Cove specimens had the highest intensities (1 to 3×10^{-3} A/m).

To isolate the stable components from the NRMs, one specimen from each of the 14 sites was first stepwise demagnetized by AF to a peak field of 100 mT. Results for

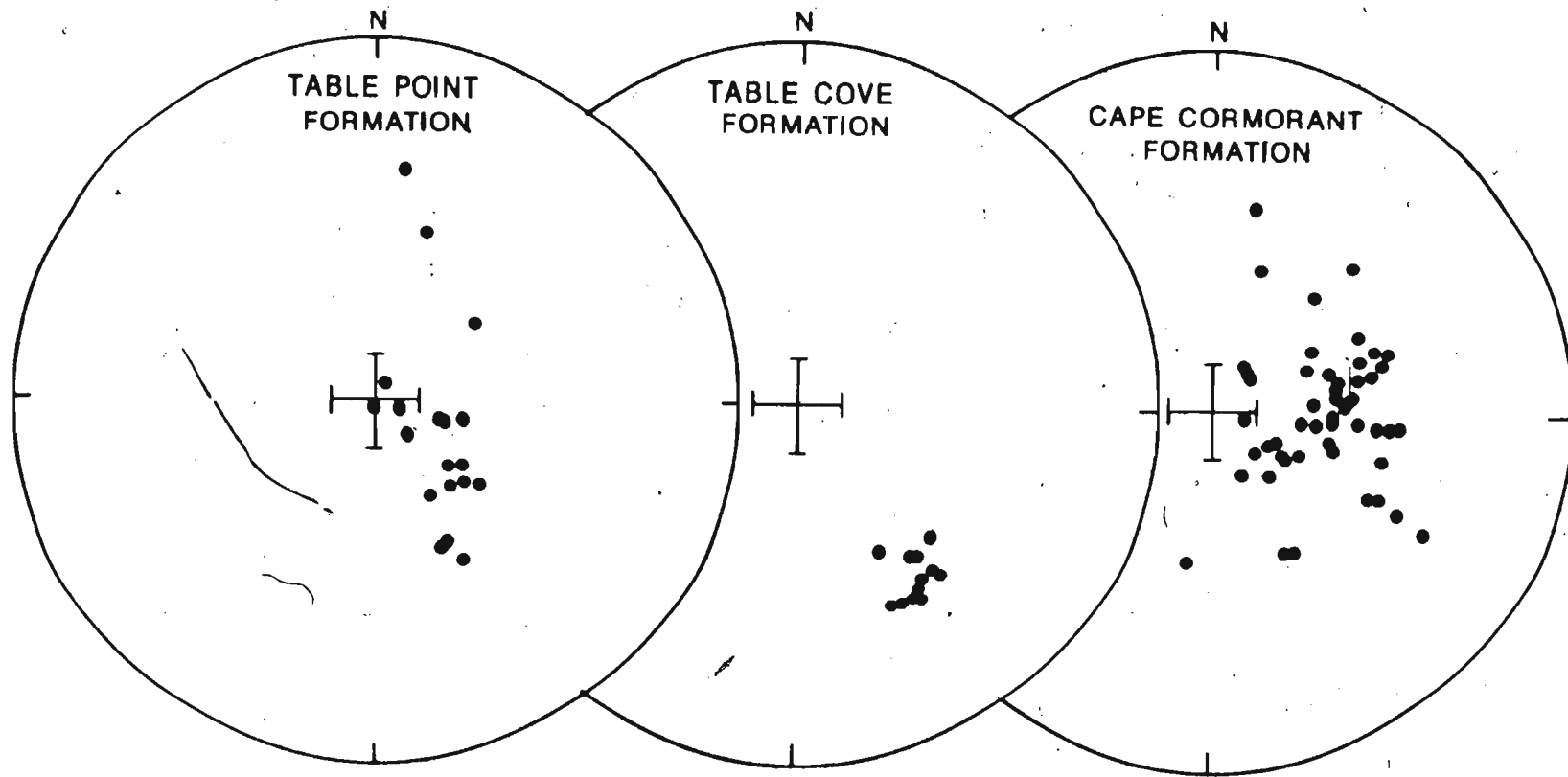


Fig. 6.1. NRM directions of Table Head Group specimens, Fort au Port area. Equal area projection on the lower hemisphere.

one representative specimen each from the three Formations are depicted in Figure 6.2, which shows that in all cases the steep down NRM moves to a shallower southeasterly direction. Whereas in the case of specimen WB8-B the remanence direction stabilizes between 15 to 60 mT, the other two specimens do not appear to exhibit any directional stability. The situation is worst in the case of specimen ML12-B, which shows an erratic change in the direction and intensity as it is progressively demagnetized. AF demagnetization was therefore not pursued further. The detailed analysis is based on results from thermal demagnetization only, described below. It should be noted, however, that the intensity decay is almost complete in 60 to 100 mT fields, which suggests the absence of high-coercivity grains carrying a remanence.

One specimen from each of 28 samples of the Table Point and Table Cove Formations was thermally demagnetized according to the schedule outlined in Appendix A. In the case of the Cape Cormorant Formation, the results of thermal demagnetization were found to be scattered and quite frequently unstable. Hence 2 specimens, wherever possible, from each of the Cape Cormorant samples were thermally treated for a total of 47 specimens (26 samples). Because of significantly different characteristic magnetizations before tilt correction between the Cape Cormorant Formation on the one hand and the combined Table Point and Table Cove Formations on the

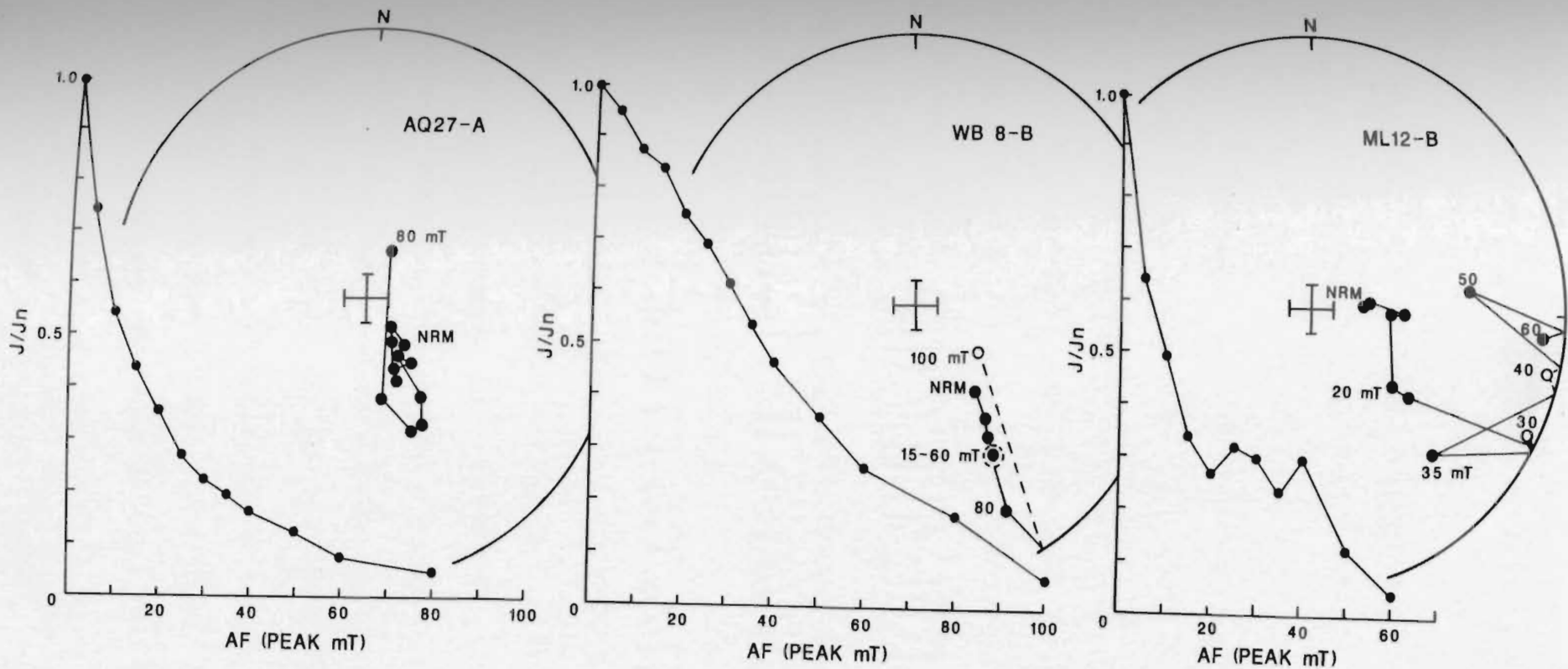


Fig. 6.2. Alternating field (AF) demagnetization results for 3 representative specimens of the Table Head Group, Port au Port area. Solid (open) circles denote downward (upward) directions on a Wulff net. Dashed outline indicates directions in the field range shown and has no statistical significance. Directions are without tilt correction.

other, their results after thermal demagnetization are discussed in turn.

Figures 6.3 - 6.4 represent typical thermal demagnetization results for Table Point and Table Cove specimens. It can be seen that a characteristic component with shallow positive inclination along the southeast is isolated between the 300-450 or 500°C steps, beyond which no consistent magnetization is observed. The erratic directional as well as intensity changes in Specimen AQ29-A may be caused by a spurious moment acquired by the specimen after the stable component is unblocked at 450°C. A similar explanation could be given for Specimens WB3-1 and WB11-A whose intensities tend to increase, along with erratic directional changes beyond 450°C. The computation of characteristic directions in all but two of the Table Point and Table Cove specimens is based on a vector subtraction (Table 6.1) between 3 or more end points defining a final linear segment directed to the origin on the Zijdeveld diagram. However, in cases where a linear trend to the origin was not seen, the average of directions in the stable range was taken as the characteristic direction. An example is Specimen AQ23-A (Figure 6.3) where a stable end point is observed in the range 300-500°C, but the Zijdeveld plot in the same range gives an arcuate pattern on the vertical projection plane. Of the 28 Table Point and Table Cove samples, 21 yielded tightly grouped remanence vectors with a mean in situ

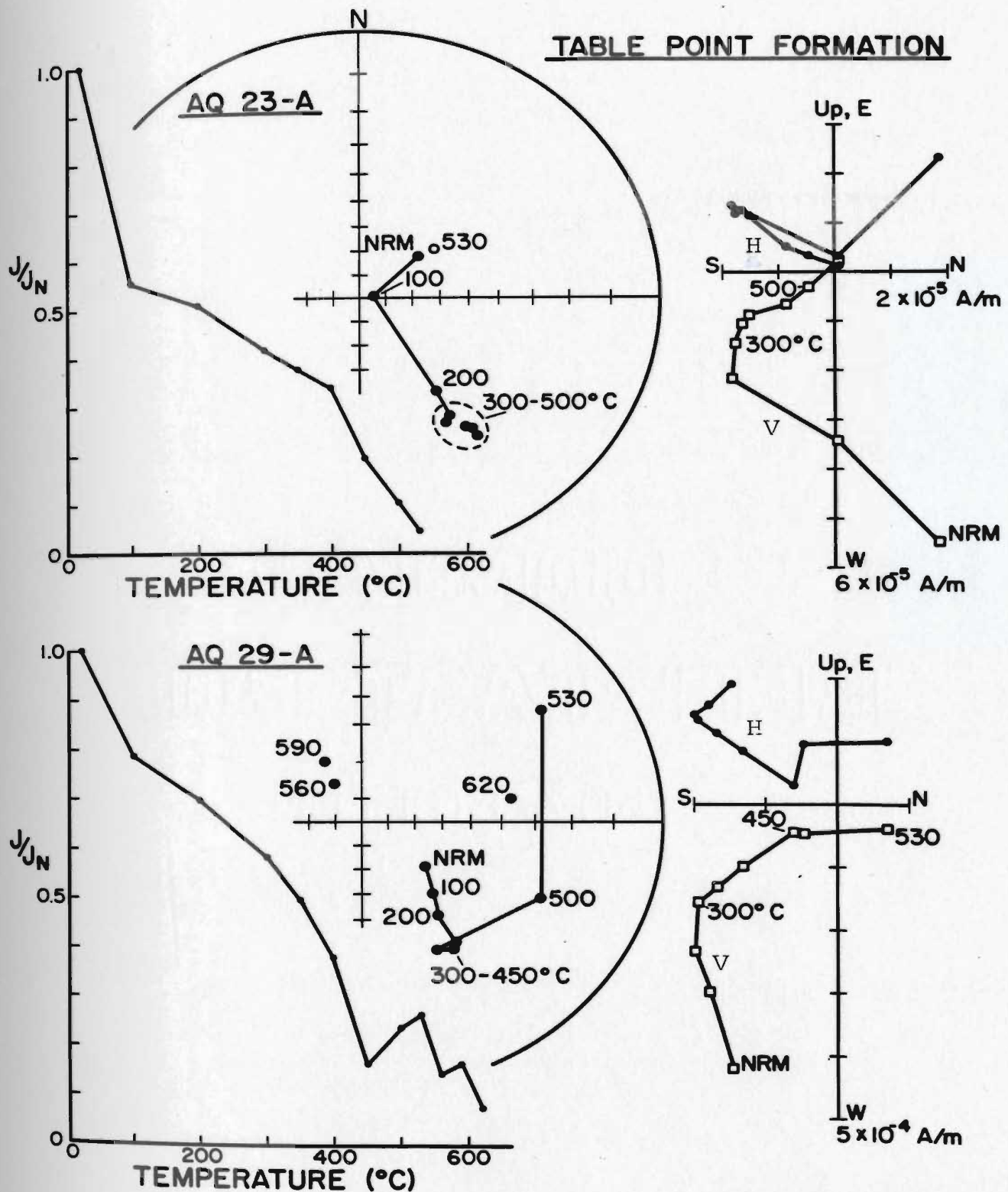


Fig. 6.3. Representative thermal demagnetization results from 2 Table Head Group specimens, Port au Port area. Conventions for the stereoplot are as in Fig. 6.2. On the orthogonal vector diagrams, open squares, vector end point projections on a N-S vertical (V) plane and solid dots, on the horizontal (H) plane.

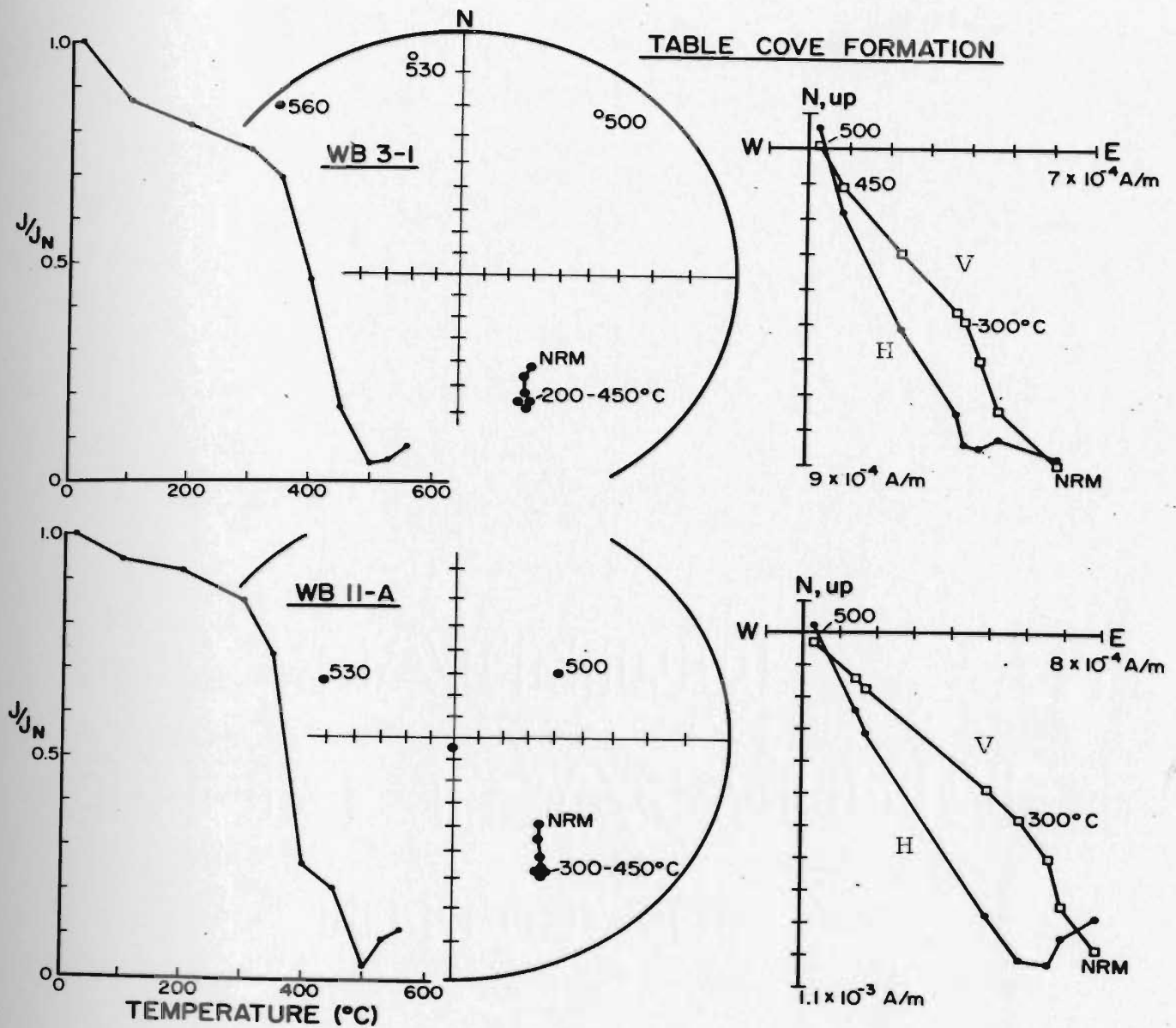


Fig. 6.4. Representative thermal demagnetization results for 2 Table Head Group specimens, Port au Port area. Open squares on the vector diagrams are projections on an east-west vertical (V) plane. Other conventions as in Fig. 6.3.

direction of $D = 153.6^\circ$, $I = 28.6^\circ$ ($\alpha_{95} = 2.2$, $k = 202$, $N = 21$ samples). Assuming that the magnetization preceded the Acadian (?) tilting, the tilt-corrected mean direction is $D = 150.4^\circ$, $I = 40.5^\circ$ corresponding to a reverse pole at 13.6°N , 148.9°E (Table 6.2). The characteristic directions of individual specimens are listed in Table 6.1 and are plotted in Figure 6.6 along with the Cape Cormorant characteristic directions.

The demagnetization behaviour of two representative specimens from Cape Cormorant Formation, yielding a stable characteristic magnetization, is shown in Figure 6.5. In specimen ML11-B, after the removal of a dominant steep down component below 300°C , a stable component directed to the southeast with a shallow negative inclination is uncovered between 350° and 400°C . There is a sharp drop in intensity in the $350\text{--}400^\circ\text{C}$ range, after which it starts increasing, and the directional change becomes large. The residual intensity at 400°C is $\sim 2 \times 10^{-5}$ A/m, which is low enough for the induction of spurious magnetizations to become significant. The corresponding Zijderveld diagram, though not good, does indicate a decay trend to the origin between 350°C and 400°C . The characteristic direction in this specimen (Table 6.1) is, however, based on the average of directions at the two temperatures.

In Specimen ML24-2 (Figure 6.5) there is a sharp drop in intensity between NRM and 300°C , corresponding to the removal of a steep down component. The intensity then

CAPE CORMORANT FORMATION

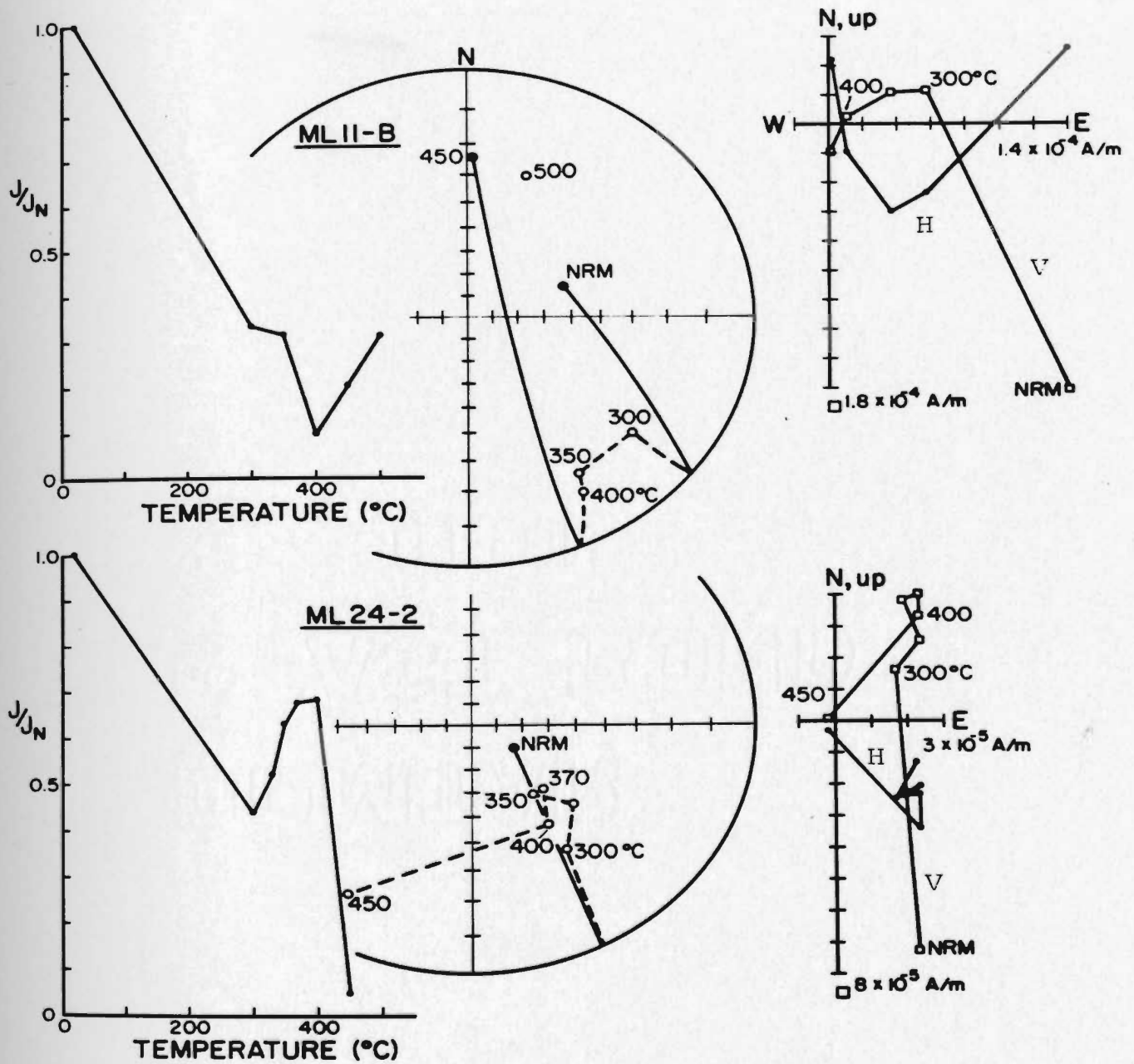


Fig. 6.5. Representative thermal demagnetization results for 2 Table Head Group specimens, Port au Port area. Conventions are as in Fig. 6.4.

Fig. 6.6. Characteristic specimen directions after thermal demagnetization, from the Table Head Group, Port au Port area. Circles denote Table Point and Table Cove Formations, and triangles the Cape Cormorant Formation. Solid (open) symbols represent downward (upward) directions. Equal area projection.

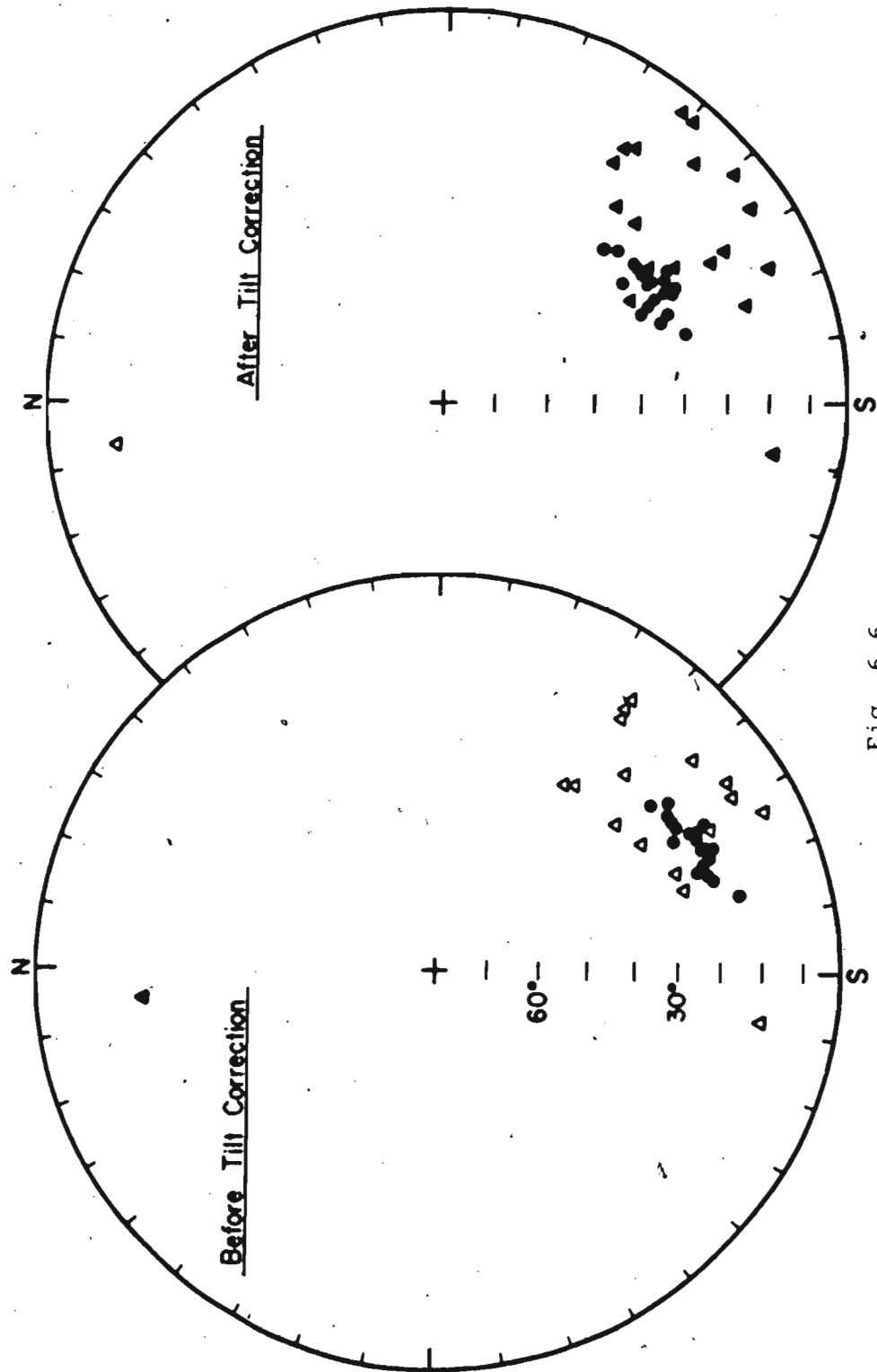


Fig. 6.6

TABLE 6.1

THERMAL DEMAGNETIZATION RESULTS FROM THE TABLE HEAD GROUP,
PORT AU PORT AREA.

Site	Specimen	Characteristic direction				Stability range (° C)
		In situ		Tilt-corrected		
		D	I	D	I	
Table Point Formation						
AQ5	AQ17-C	156.5	26.9	152.6	40.7	200-450 (v.s.)
AQ5	AQ18-A	157.6	29.2	153.6	43.2	300-500 (v.s.)
AQ5	AQ19-A	162.1	27.8	159.1	42.2	400-530 (v.s.)
AQ5	AQ20-A	153.4	27.9	148.9	41.4	300-530 (v.s.)
AQ6	AQ21-B	165.6	22.8	163.8	37.5	300-500 (v.s.)
AQ6	AQ23-A	144.3	29.4	138.0	41.6	300-500 (ave.)
AQ8	AQ29-A	142.1	32.6	134.6	44.3	300-500 (v.s.)
AQ8	AQ30-A	151.2	32.6	145.3	45.8	400-530 (v.s.)
AQ8	AQ32-1	159.2	31.1	155.2	45.2	200-500 (v.s.)
Table Cove Formation						
WB1	WB1-1	159.7	28.8	158.4	39.6	300-450 (v.s.)
WB1	WB2-A	154.6	27.9	152.7	38.5	300-500 (v.s.)
WB1	WB3-1	154.5	28.3	152.5	38.9	300-450 (v.s.)
WB1	WB4-2	151.1	29.2	148.6	39.6	300-450 (v.s.)
WB2	WB5-1	146.0	31.2	142.6	41.2	300-450 (v.s.)
WB2	WB6-1	147.0	30.7	143.8	40.8	300-450 (v.s.)
WB2	WB7-1	155.2	26.6	153.5	37.2	350-450 (v.s.)
WB2	WB8-A	152.3	26.5	150.2	37.0	300-450 (v.s.)
WB3	WB9-A	155.1	27.7	153.2	38.3	200-450 (v.s.)
WB3	WB10-B	155.5	25.3	153.8	36.0	300-500 (v.s.)
WB3	WB11-A	151.1	25.1	149.0	35.5	300-500 (v.s.)
WB3	WB12-B	148.9	30.9	145.9	41.1	300-450 (v.s.)
Cape Cormorant Formation						
ML1	ML2-A	153.9	-10.3	150.5	46.0	300-400 (v.s.)
ML1	ML3-A	161.9	-35.4	161.9	21.6	350-450 (ave.)
ML1	ML4-C	139.7	-17.8	135.9	34.9	350-400 (ave.)
ML2	ML6-B	125.8	-23.1	126.2	21.3	330-400 (ave.)
ML2	ML6-C	151.6	-24.8	151.6	25.1	300-450 (ave.)
	Combined ML 6-B & 6-C	138.6	-24.5	138.7	23.7	

TABLE 6.1 (CONT'D)

Site	Specimen	<u>Characteristic direction</u>				Stability range (° C)
		<u>In situ</u>		Tilt-corrected		
		D	I	D	I	
Cape Gannorant Formation						
ML3	ML10-A*	354.6	28.0	352.9	-17.9	300-450 (ave.)
ML3	ML10-C	133.1	-33.0	135.7	14.0	300-400 (ave.)
ML3	ML11-B	149.4	-14.5	148.9	34.4	350-400 (v.s.)
ML3	ML11-C	158.2	-35.7	157.2	13.1	300-400 (ave.)
	Combined ML 11-B & 11-C	153.4	-25.2	153.4	23.8	
ML4	ML14-B	125.1	-16.6	123.8	23.0	300-350 (ave.)
ML4	ML14-C*	189.4	-19.5	189.0	17.9	300-400 (ave.)
ML5	ML17-1	132.8	-15.5	130.1	34.6	370-400 (v.s.)
ML5	ML17-4	146.6	-13.5	146.3	38.5	400-450 (v.s.)
	Combined ML 17-1 & 17-4	139.7	-14.6	137.9	36.8	
ML7	ML24-1	126.0	-42.4	130.7	6.0	300-400 (ave.)
	ML24-2	140.4	-42.0	141.3	7.9	300-400 (ave.)
	Combined ML 24-1 & 24-2	133.2	-42.4	136.0	7.0	
ML7	ML25-1	147.8	-39.9	147.0	10.0	300-400 (ave.)
	ML25-2	151.3	-28.5	150.9	21.2	400-450 (v.s.)
	Combined ML 25-1 & 25-2	149.7	-34.2	148.9	15.6	
ML7	ML27-1	125.2	-20.2	124.1	27.3	300-400 (ave.)
ML7	ML27-2	123.5	-42.5	129.0	5.4	300-400 (ave.)
	Combined ML 27-1 & 27-2	124.5	-31.4	126.7	16.4	

Specimens with * were excluded from the final statistics. All symbols and explanations as in Tables 3.1, 5.1, 5.3.

TABLE 6.2

MEAN PALEOMAGNETIC DATA FROM THE TABLE HEAD GROUP, PORT AU PORT AREA.

	D_m	I_m	k	N	α_{95}	λ_p	Antipole
Table Point Formation, 9 samples, <u>in situ</u>	154.8	29.1	118	9	4.8		
Table Point Formation, 9 samples, tilt- corrected	150.3	42.8	117	9	4.8		
Table Cove Formation, 12 samples, <u>in situ</u>	152.6	28.2	401	12	2.2		
Table Cove Formation, 12 samples, tilt- corrected	150.4	38.7	402	12	2.2		
Cape Cormorant Formation, 11 samples, <u>in situ</u>	141.2	-26.4	30	11	8.5		
Cape Cormorant Formation, 11 samples, tilt-corrected	140.6	24.3	27	11	8.9	12.7 S	19.5°N, 162.1°E ($d_p, d_m = 5.1^\circ, 9.5^\circ$)
Table Point and Table Cove Formation combined, 21 samples tilt-corrected	150.4	40.5	184	21	2.3	23.1 S	13.6°N, 148.9°E ($d_p, d_m = 1.7^\circ, 2.8^\circ$)

TABLE 6.2 (CONT'D)

	D_m	L_m	k	N	α_{95}	λ_p	Antipole
As above, 5 sites, tilt-corrected	150.0	40.7	394	5	3.9	23.3 S	13.4 ^o N, 149.2 ^o E ($d_p, d_m = 2.9^{\circ}, 4.7^{\circ}$)
Table Head Group, 32 samples, <u>in situ</u>	149.3	10.7	8	32	9.4		
Table Head Group, 32 samples, tilt- corrected	146.7	35.1	38	32	4.1	19.4 S	15.9 ^o N, 153.6 ^o E ($d_p, d_m = 2.8^{\circ}, 4.7^{\circ}$)

All symbols as in Table 3.3

increases gradually on further heating to 400°C, during which the direction remains stable along the southeast with intermediate upward inclination. This suggests the removal of a component antiparallel to the observed direction. On the Zijdeveld diagram, the component being removed is not clearly indicated because of scatter and erratic changes in the observed direction. The average of the 300-400°C directions has been accepted as the characteristic direction for this specimen. A sharp drop in the intensity between 400 to 450°C corresponds to the removal of a vector whose direction is close to the characteristic direction. Only 19 specimens (11 samples) out of a total of 47 specimens (26 samples) from the Cape Cormorant Formation yielded stable, characteristic directions (Table 6.1, Figure 6.6).

A large majority of Cape Cormorant specimens displayed unstable behaviour and no consistent component could be identified in them. A detailed perusal of the demagnetization results suggests the presence of multicomponent remanences with overlapping stability spectra, making them difficult to resolve. Figures 6.7-6.8 depict the complex types of demagnetization behaviour exhibited by some representative specimens. Four specimens of Figure 6.7 yield different high-temperature directions which seem reasonably stable. It is to be noted that two specimens, ML10-A and ML10-C (Figure 6.7) from a single sample, seem to give fairly stable directions which are

d

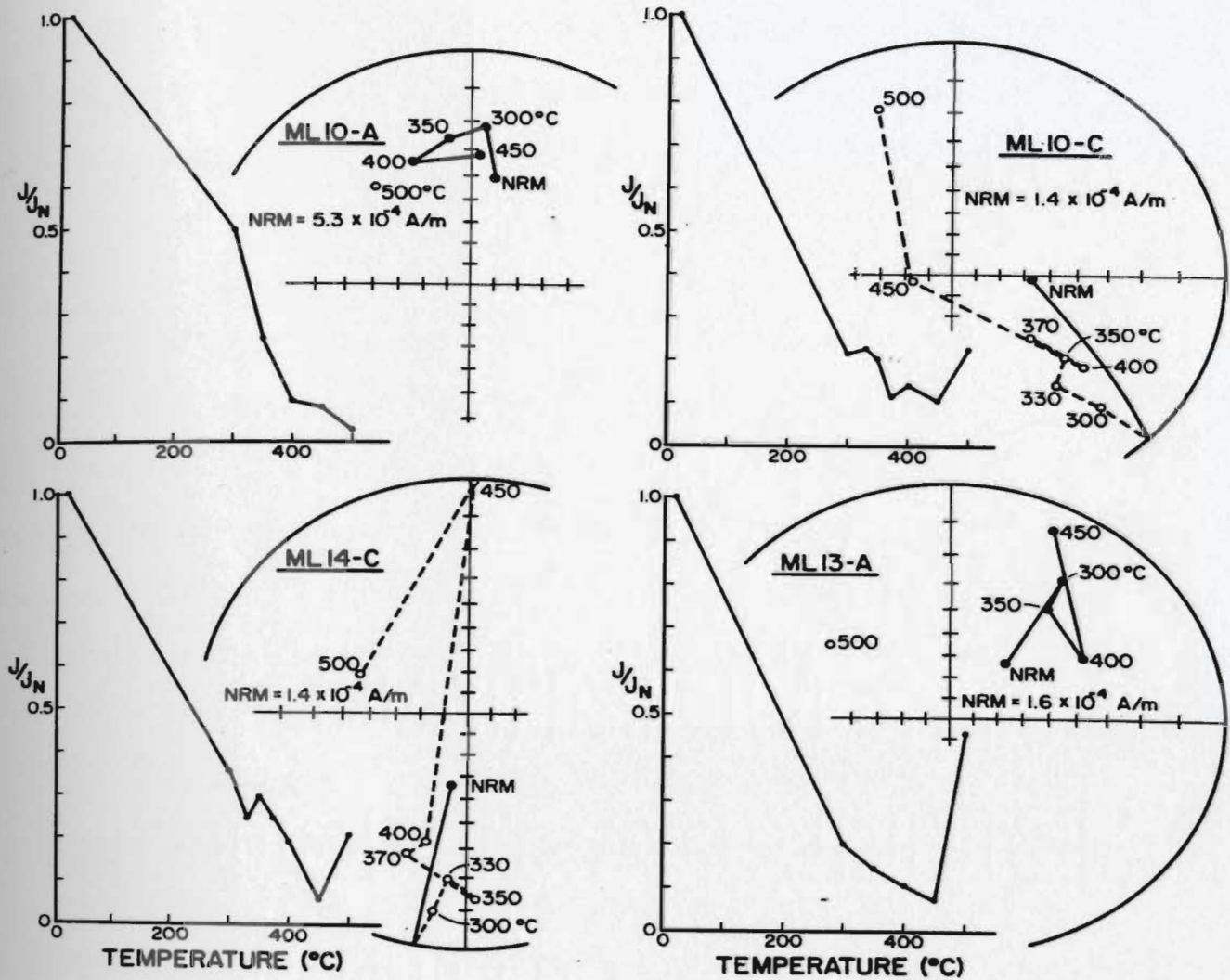


Fig. 6.7. Thermal demagnetization results for 4 Cape Cormorant specimens showing the presence of distinctly different stable directions. Widely divergent directions of specimen pairs (ML10-A and ML10-C) from a single sample show that the magnetization is not homogeneous throughout the sample volume. Presence of both normal and reverse polarities may be inferred from different specimens. Conventions as in Fig. 6.2.

120-130 apart. The southeasterly stable direction in Specimen ML10-C has a northwesterly trend at higher temperatures, possibly approaching the direction of the stable downward component observed in the second specimen, ML10-A.

A similar kind of behaviour is observed in Specimens ML13-A and ML14-C which in this case come from two different samples, but collected at the same site. The stable directions of Specimens ML10-A and ML14-C are nearly antiparallel. A second specimen, ML14-B, from the latter sample yielded a stable direction along the southeast (Table 6.1), comparable to Specimen ML10-C. Specimens ML10-A and ML14-C have been excluded from the final statistics because of their obvious large misalignment with the directions of the characteristic SE cluster. A sharp rise in intensity beyond 450°C in three of the specimens of Figure 6.7 might be due to mineralogical changes (production of secondary magnetite?) quite often observed when heating limestones (Lowrie and Heller, 1982).

One inference one may draw from Figure 6.7 is that the magnetization of these rocks was acquired over a prolonged time span during which the earth's field might have reversed its polarity and perhaps also changed its direction relative to the sampling area. The occurrence of widely different stable directions in the specimens of a single block sample and in two different specimens from the same site suggests that the rocks are not homogeneously

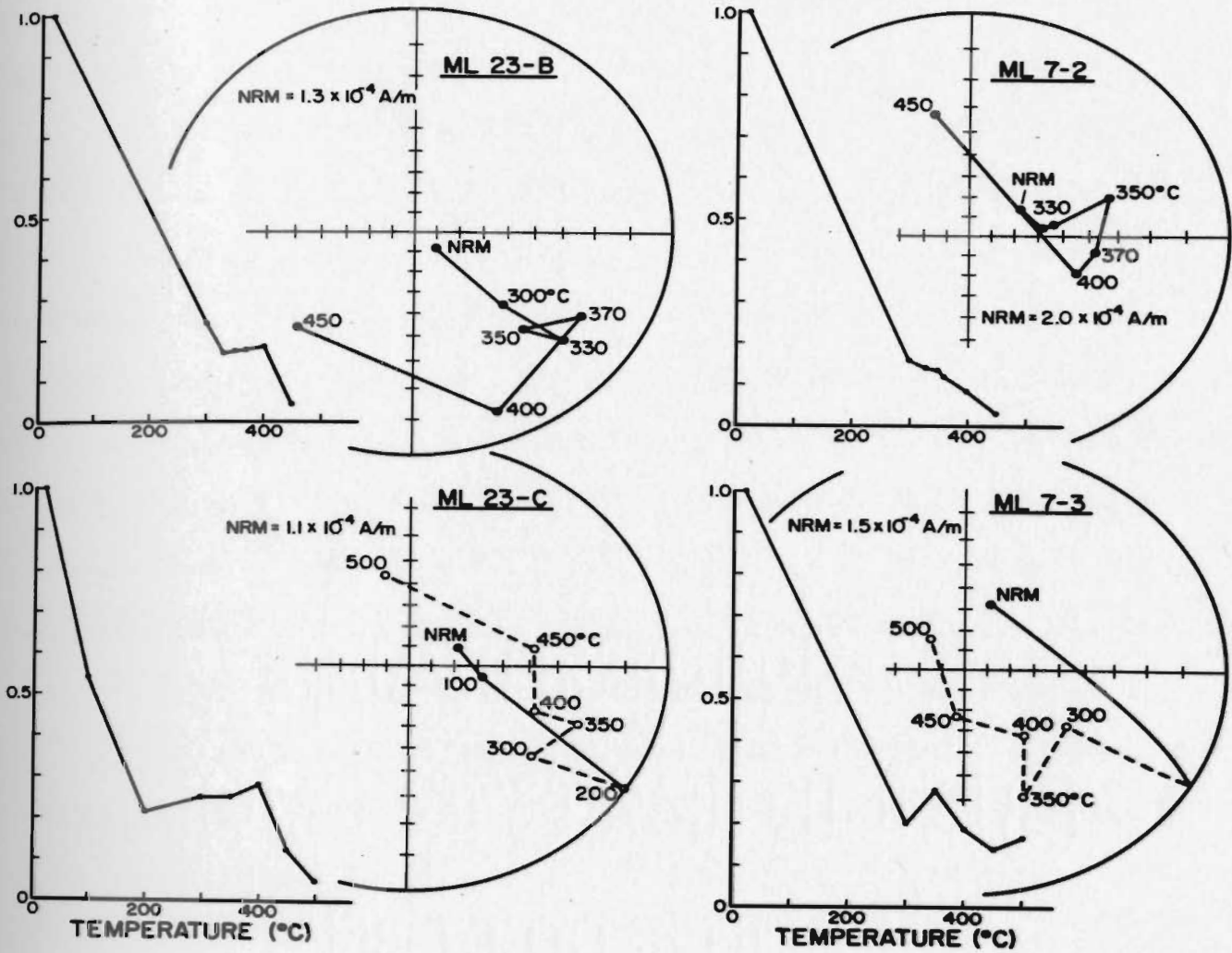


Fig. 6.8. Thermal demagnetization results of specimen pairs (l.h.s. and r.h.s.) from 2 Cape Cormorant samples, showing the presence of superposed components of opposite polarity in individual specimens. Conventions as in Fig. 6.2.

magnetized and might carry superimposed components that have remained unresolved. This observation is further supported by the demagnetization results of another four specimens from two samples (Fig. 6.8). The steep down NRM vectors in both Specimens ML23-B and ML23-C move to shallower directions by 300°C in the SE quadrant. In the case of ML23-B, a stable direction with shallow positive inclination along the southeast appears to be isolated in the temperature range 330-370°C. However, the intensity remains almost constant in this range. In the companion specimen (ML23-C), a large steep down component is erased below 200°C. The direction then switches to a negative inclination in the southeast quadrant, showing a trend roughly to the northwest, but stability is not attained. The abrupt intensity decrease to 200°C is followed by a gentle increase in the range 200-400°C, during which the vector moves to a steeper direction with negative inclination. It seems quite probable, therefore, that Specimens ML23-B & C each might carry superimposed but unresolved normal and reverse components that are being removed simultaneously. In the case of Specimen ML23-C, the southeasterly (reverse?) component seems to be erased at a higher rate than the hidden (normal?) component, whereas in Specimen ML23-B, the removal of the two components may be nearly at the same rate. A similar behaviour is exhibited by the specimen pair ML7-2 and ML7-3 in Figure 6.8.

The strong indication of superimposed components in the specimens of the Cape Cormorant Formation, as discussed above, probably explains why a majority of the specimens failed to yield stable magnetizations, unlike those of the Table Point and Table Cove Formations. The larger scatter of the Cape Cormorant directions (Figure 6.6) may be due, in part, to the imperfect resolution of superimposed components. However, the Cape Cormorant characteristic directions suggest a significant southeasterly component with shallow up inclination, despite a relatively large scatter. The in situ mean based on 11 samples (17 specimens, Tables 6.1-6.2) yielding a characteristic component is $D = 141.2^\circ$, $I = -27.6^\circ$ ($\alpha_{95} = 8.5^\circ$, $k = 30$). This mean direction is far removed from the in situ mean of the Table Point and Table Cove Formations. However, after correction for geological tilt, the mean direction for Cape Cormorant becomes $D = 140.6^\circ$, $I = 24.3^\circ$, ($\alpha_{95} = 8.9^\circ$, $k = 27$). The small changes in α_{95} and k are due to small differences in tilt at various sites and are not significant. The tilt correction brings the Cape Cormorant directions much closer to those of the Table Point and Table Cove Formations (Figure 6.6). The mean direction of the Table Head Group (all three Formations) before tilt correction is $D = 149.3^\circ$, $I = 10.7^\circ$ ($\alpha_{95} = 9.4^\circ$, $k = 8$, $N = 32$ samples). After tilt correction, the mean direction is $D = 146.7^\circ$, $I = 35.1^\circ$ ($\alpha_{95} = 4.1^\circ$, $k = 38$, $N = 32$ samples). A substantial

improvement in the statistical parameters after tilt-correction indicates that the magnetization of the Table Head Group was acquired prior to the tilting of the strata, probably during the Acadian orogeny (Chapter 2). However, the significance of this structural correction could not be adequately tested (e.g., F-test) because of the large differences in sample variance between the three Formations. These results are further discussed in Section 6.4.

6.2.2 Port au Choix area

Paleomagnetic measurements were done on 53 specimens, choosing at least one from each of the 48 samples collected from the Port au Choix area. The NRM directions are plotted in Figure 6.9 and are seen to be steep and tightly grouped. The NRM intensities are of the order of 10^{-3} to 10^{-4} A/m. Five specimens, each from a different site, were AF demagnetized. This treatment (results not shown) failed to deflect the steep down NRM significantly, although the intensity decayed smoothly to about 1-2% by the 80 mT step. This indicates the inability of the AF treatment to isolate any characteristic component(s), but at the same time gives valuable information showing the absence of higher coercivity grains carrying a remanence.

Thermal demagnetization was carried out on 48 specimens, one from each of the 48 samples. Results of thermal demagnetization for two specimens are represented -

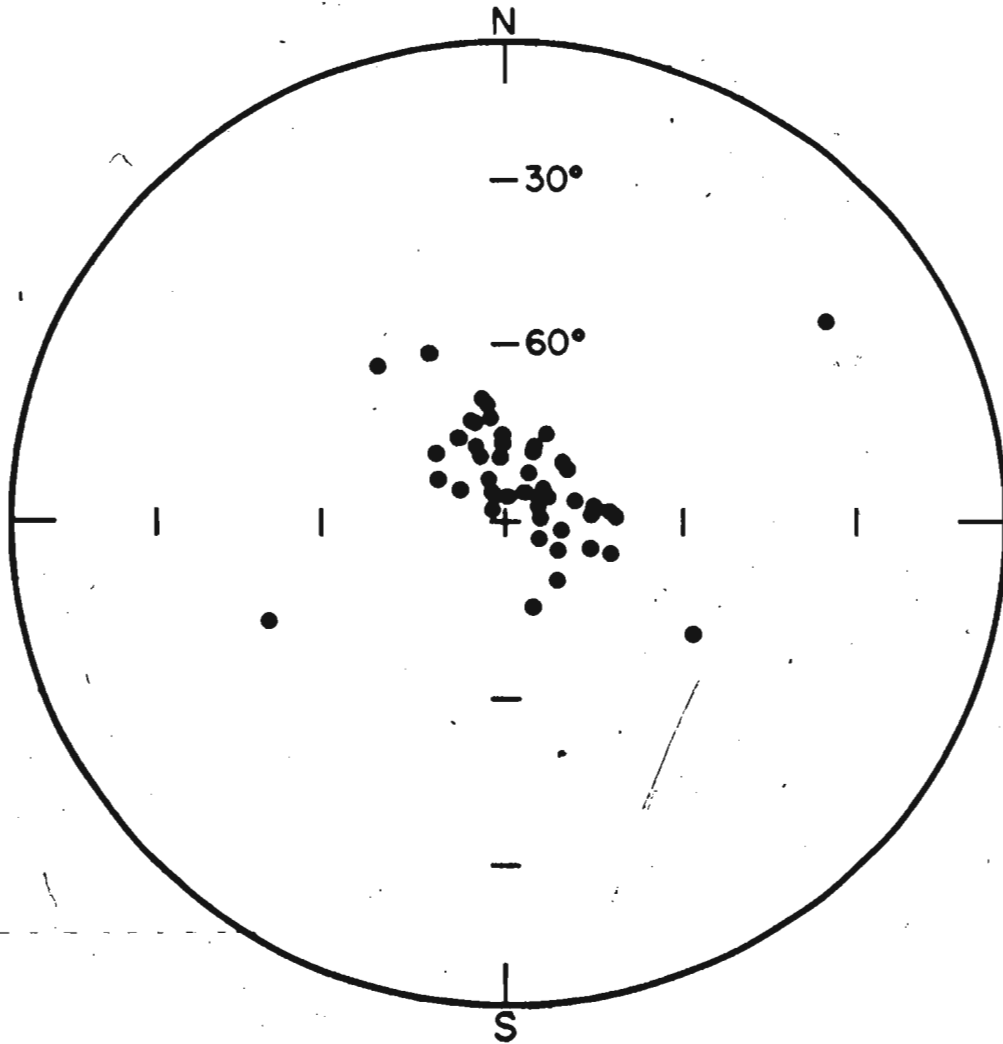


Fig. 6.9. NRM sample directions for Table Head Group, Port au Choix area. Equal area projection on the lower hemisphere.

in Figure 6.10. In Specimen PC122-A the steep down NRM moves to a very shallow, almost horizontal southeast direction with a linear decay to the origin at high temperatures on the Zijderveld diagram. Specimen PC127-1 shows the same trend, except that the stable direction is intermediately steep. Stable southeast end-point directions were obtained from a number of specimens (Table 6.3), but these directions are smeared in inclinations which range from $+10^{\circ}$ to $+80^{\circ}$. In all these cases the intensity decay was complete and the stable component was contained in the last 10-20% of the total NRM.

Figure 6.11 shows other examples of demagnetization behaviour exhibited by quite a few specimens. The four specimens of this figure display quite different trends compared to those in Figure 6.10. Specimens PC74-2 and PC82-1 each lose 95% of their total intensity by the 300°C step, changing from the steep down NRM direction to a northerly direction with a negative inclination. The final directions are intermediately steep. Because the intensities of these specimens are completely lost by 450°C , with directions becoming random in some cases at the highest temperature treated (e.g. PC74-2 at 450°C), it is assumed that the terminal direction in a specimen exhibiting a systematic directional change represent a kind of stable end point. However, unless the directions at the two highest temperatures (generally 400° and 450°C) were closely spaced, they were not accepted as stable

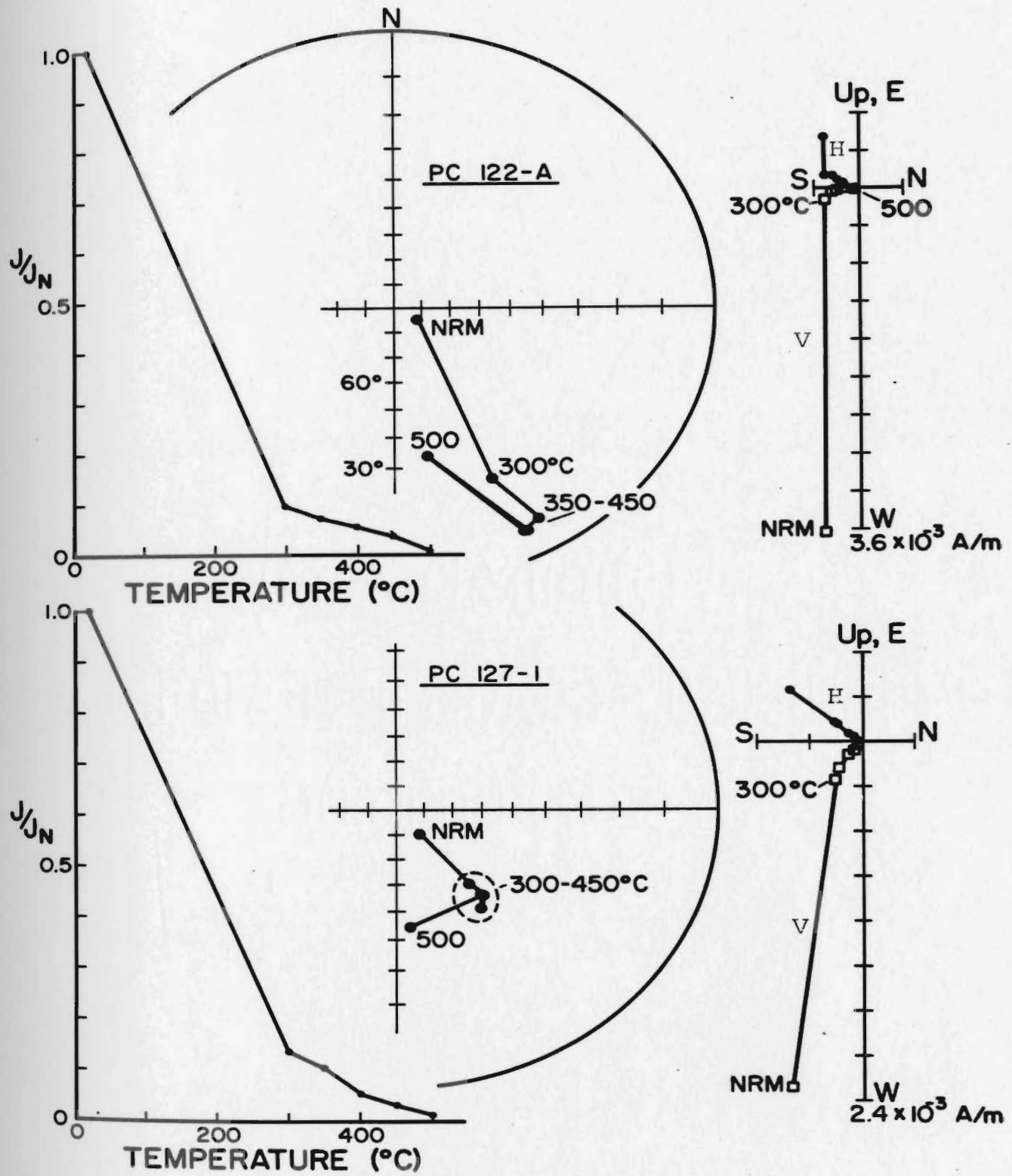


Fig. 6.10. Representative thermal demagnetization results for 2 Table Head specimens from Port au Choix area, yielding a shallow to steep southeast component. Conventions for stereoplots are as in Fig. 6.2 and for orthogonal vector diagrams as in Fig. 6.3.

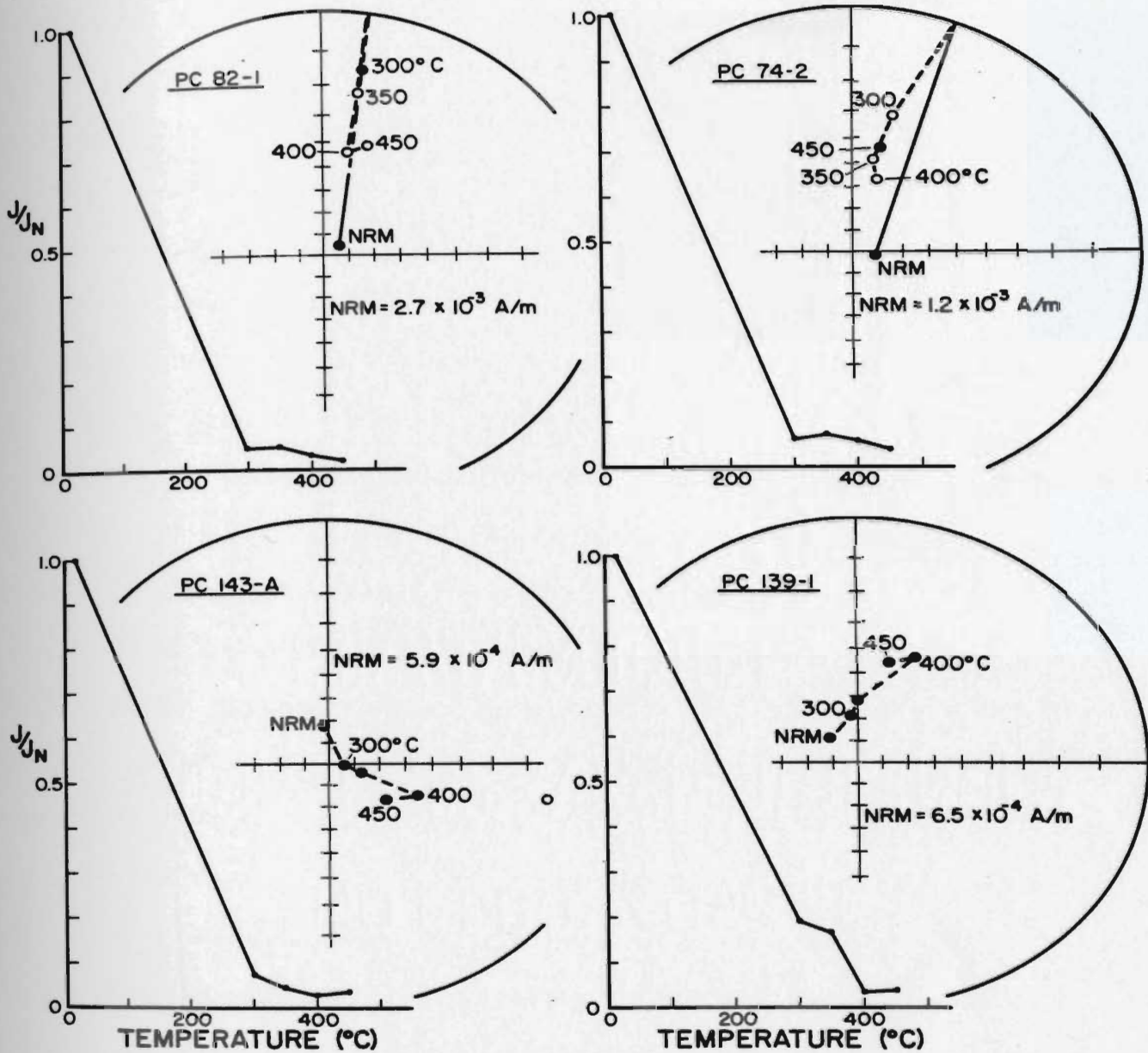


Fig. 6.11. Representative thermal demagnetization results for 4 Table Head specimens from Port au Choix area, yielding a northerly upward directions (top) and intermediate to steeply inclined down directions (bottom). Conventions as in Fig. 6.2.

directions. Thus in the case of Specimen PC82-1, the average of the 400° and 450°C directions and in PC74-2, the average of the 350° and 400°C directions, was taken as the stable component. A similar acceptability criterion and similar averaging was applied to specimens PC139-1 and PC143-A, though the remanence vectors of these specimens are seen to move in different directions, that is towards northeast and southeast, respectively.

Stable directions were thus isolated from 35 samples (Table 6.3 and Figure 6.12). A very large smear in these directions along a roughly N-S axis makes any statistical analysis difficult. Nine samples yielding N to NE directions with negative inclinations form a distinctive cluster and might represent a characteristic component for the Table Point Formation of the Port au Choix area. These samples had all been collected from the limestone strata of the Table Point area (Figure 2.4). The underlying dolostone strata of the Aguathuna Formation (St. George Group) in the same locality yielded similar directions (Chapter 5). This suggests either that the ages of magnetization of the two Formations are similar, or that no significant polar wander occurred during the time they became magnetized. Apart from this, no other characteristic component seems to be identified from the directions in Figure 6.12, though the presence of a S to SE component is strongly indicated. Most of these directions came from samples of the Black Point area (Figure 2.4).

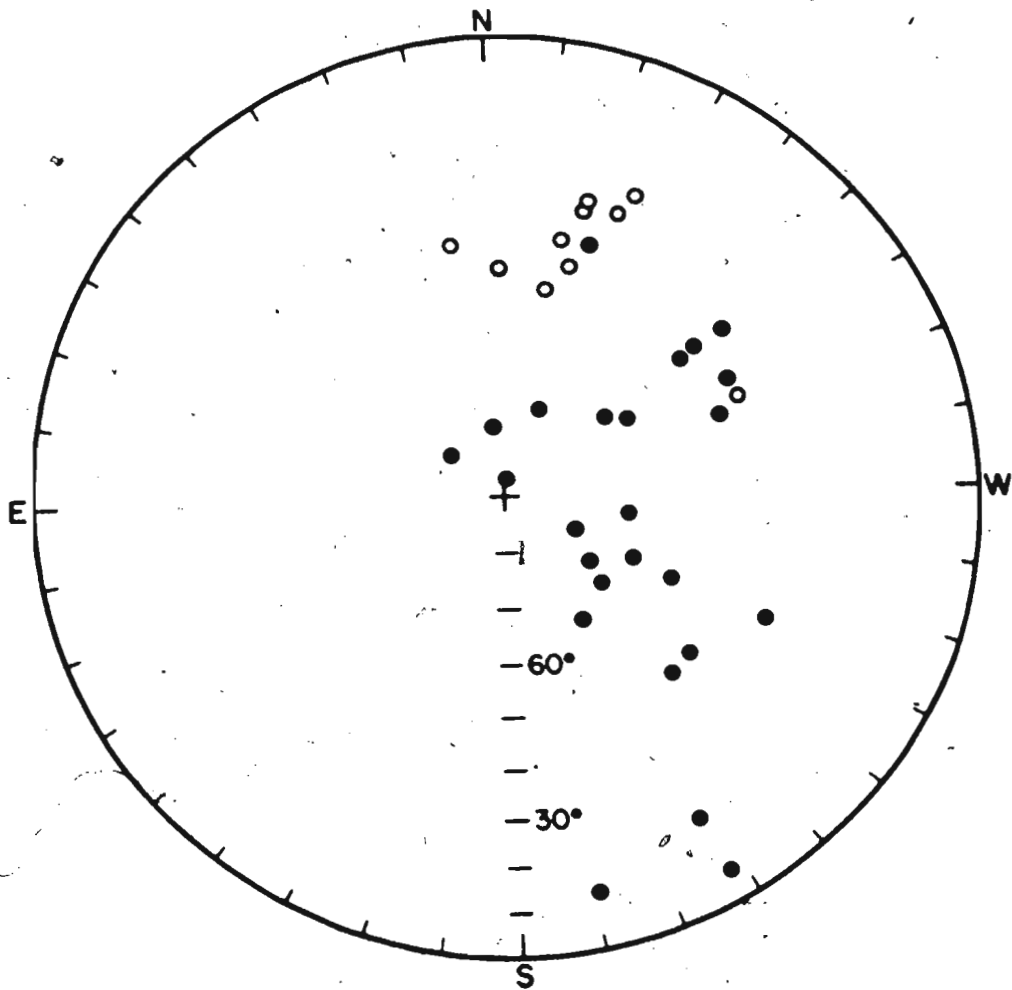


Fig. 6.12. Characteristic sample directions from the Table Head Group, Port au Choix area. Solid (open) circles are equal area projections on lower (upper) hemisphere.

TABLE 6.3

THERMAL DEMAGNETIZATION RESULTS FROM THE TABLE HEAD GROUP,
PORT AU CHOIX AREA.

Site	Specimen	In situ stable direction		Stability range (° C)
		D	I	
PC15	PC72-1	18.4	-35.5	350-400
PC15	PC73-1	24.0	-33.9	350-400
PC15	PC74-2	13.7	-52.1	350-400
PC15	PC75-2	25.6	-28.5	350-400
PC16	PC76-B	68.3	-44.9	300-400 (v.s.)
PC16	PC78-1	63.0	45.0	350-400
PC17	PC81-2	351.0	-44.2	400-450
PC17	PC82-1	15.4	-41.6	400-450
PC17	PC83-2	1.7	-49.2	400-450
PC17	PC84-2	18.3	-46.5	400-450
PC17	PC85-2	18.4	-33.5	300-450
PC18	PC90-1	53.6	40.5	400-450
PC25	PC121-B	168.9	12.0	400-450
PC25	PC122-A	151.7	6.2	350-450
PC25	PC123-2	135.7	67.1	300-450
PC25	PC124-2	117.6	76.3	300-450
PC25	PC125-A	151.5	19.6	400-450
PC26	PC126-1	133.8	48.3	300-400
PC26	PC127-1	139.8	46.3	300-450
PC26	PC128-A	152.3	63.9	300-450
PC26	PC129-B	119.4	65.9	300-450
PC26	PC130-A	131.2	71.6	300-400
PC27	PC131-B	358.3	77.6	300-450
PC27	PC133-A	100.6	69.0	300-400 (v.s.)
PC27	PC135-A	54.4	50.7	300-400 (v.s.)
PC28	PC137-1	311.6	79.4	NRM-350
PC28	PC138-1	23.9	73.5	NRM-350
PC28	PC139-1	20.4	41.8	400-450
PC28	PC140-B	117.5	38.5	300-450 (v.s.)
PC29	PC142-1	58.6	65.1	300-400
PC29	PC143-A	119.4	57.6	400-450
PC29	PC145-B	53.1	46.5	350-400
PC30	PC146-A	70.2	50.0	400-450
PC30	PC147-1	53.4	68.0	350-400
PC30	PC149-2	12.4	87.0	NRM-350

NOTES: The computation of stable direction is based on the average of directions in the range indicated except for a few specimens for which vector subtraction (v.s.) was used.

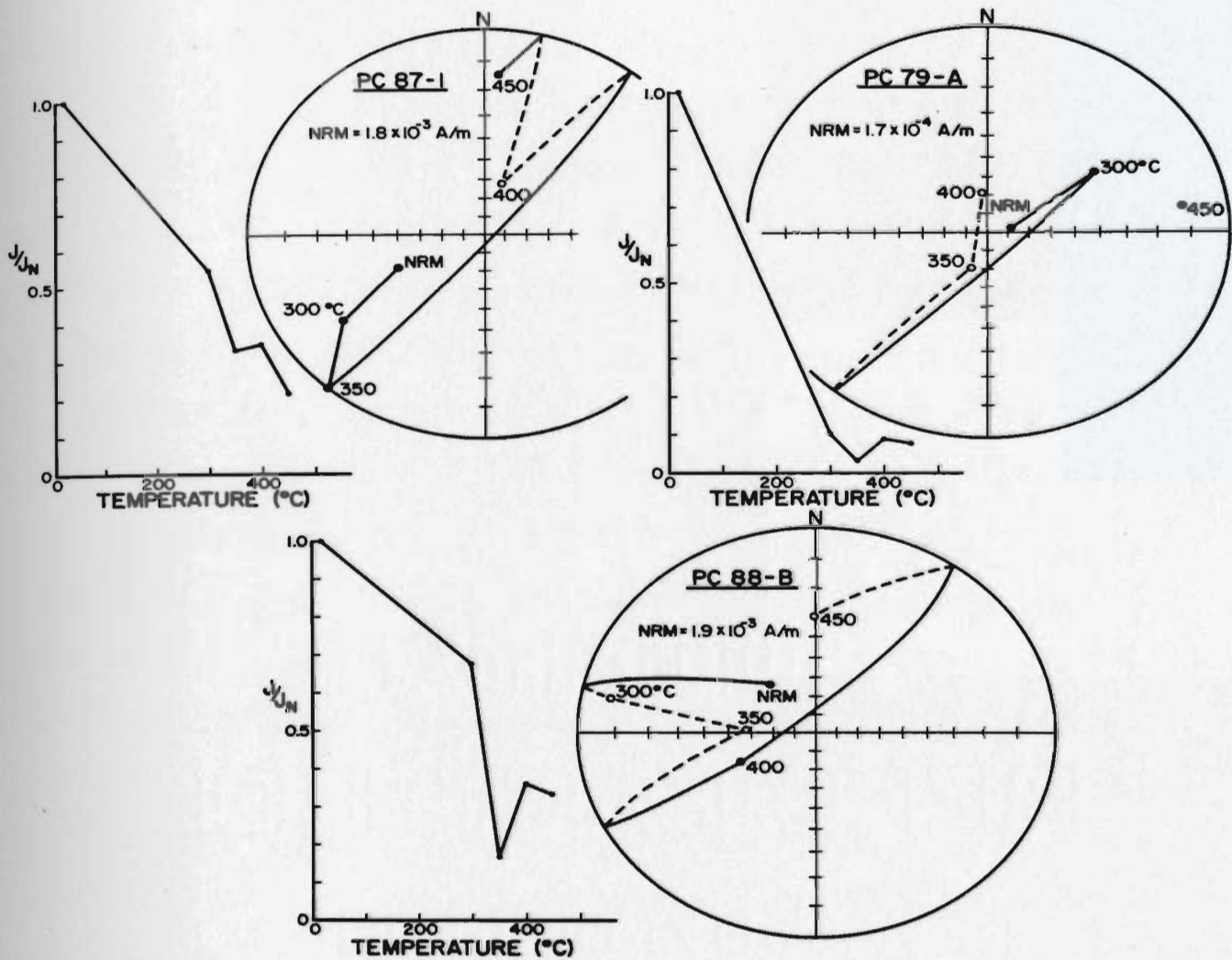


Fig. 6.13. Unstable thermal demagnetization behaviour of 3 Table Head specimens from Port au Choix area, showing a NE-SW axis of magnetization. Conventions as in Fig. 6.2.

Though the presence of a paleomagnetic axis directed roughly N-S is clearly highlighted in Figure 6.12, a number of specimens revealed a NE-SW axis of magnetization without showing any stability. Figure 6.13 shows three examples of such unstable behaviour. An increase in intensity beyond 350°C in all 3 specimens is probably caused by the acquisition of some spurious moment after the intensity is reduced to a very low value, or alternatively, by a chemical change in the limestones beyond that temperature.

On the basis of the results discussed above, it seems most likely that the large dispersion of stable directions evident in Figure 6.12 is caused by the presence of two or more superimposed components which could not be perfectly resolved. Most of the steep directions shown in Figure 6.12 could possibly have resulted from the simultaneous removal of a two-component (normal and reverse) magnetization in the specimen concerned.

6.3 Magnetic mineralogy

IRM studies on 8 representative samples from both the Port au Port and Port au Choix areas reveal the presence of exclusively magnetites in the rocks of the Table Head Group. All the IRM curves are similar to type 1 of the Port au Port and St. George Groups already discussed in Chapters 3 and 5. Therefore the IRM results are not shown here. The thermal and limited AF demagnetization results, as discussed in Sections 6.2.1 and

6.2.2, further confirm that magnetite is the remanence carrier in the carbonates of the Table Head Group.

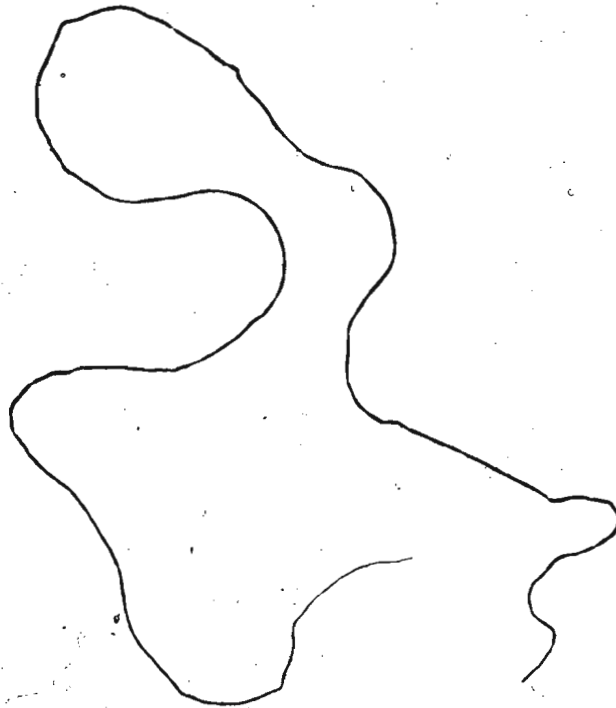
6.4 Discussion

A pre-tilting magnetization has been isolated from the Table Head Group in the Port au Port area. The magnetite-bearing remanence cannot be a thermal overprint because of a low conodont CAI (≈ 1) in the area (Chapters 3 and 5). It is likely that the magnetite grains were aligned parallel to the ambient geomagnetic field during or shortly after deposition and early diagenesis of these rocks. The pole position corresponding to this magnetization therefore most probably represents a mid-Ordovician paleofield. This pole is plotted along with the other Ordovician poles in Figure 9.1. It is seen from this plot that the Table Head pole is very close to the Lower Ordovician St. George pole for Port au Port. This indicates that there was probably no significant apparent polar wandering during Lower to mid-Ordovician times. It is also important to note that no Kiaman overprints were found in the Table Head samples.

It seems that the oxidizing conditions related to the formation of diagenetic hematite (which carries Kiaman overprints in the Port au Port and St. George Groups) did not prevail in the case of the Table Head Group. It is noteworthy that hematization is pervasive in the Late Cambrian rocks (Petit Jardin Formation), but higher up in

the stratigraphic sequence it progressively becomes less pervasive until the Table Head Group where no evidence of hematite is found, leaving them unaffected by Late Paleozoic overprinting.

The Table Head rocks in the Port au Choix area mostly show multicomponents which could not be resolved by demagnetization techniques. Therefore no meaningful result could be obtained from them.



CHAPTER 7

THE LONG POINT GROUP

7.1 Geological Setting

The late Middle Ordovician Long Point Group is exposed along the southeast shore of the Long Point, forming the northeast extension of Port au Port Peninsula (Figure 2.3). It has been divided into two Formations (Bergstrom et al., 1974): the Lourdes Limestone and the Winterhouse Formation (Figure 2.2). The Long Point Group overlies the Humber Arm Supergroup unconformably at West Bay (Rodgers, 1965), but it lies on the autochthon conformably (Stevens, 1970) near Mainland (Localities WB and ML respectively in Figure 2.3). Rocks of this Group are comprised of shallow-water siliciclastic and carbonate sediments interbedded with shales and red beds near the top. Fossil evidence suggests an early Caradocian age for the Lourdes Limestone (Fahraeus, 1973; Bergstrom et al., 1974). These authors point out that the age of Lourdes Limestone is critical, as it defines the upper time limit of emplacement of the Humber Arm allochthon.

7.2 Paleomagnetic sampling and results

To investigate these rocks paleomagnetically, 17 samples were collected at 4 sites from the Lourdes Limestone (Figures 2.2, 2.3). The strata in the sampling area are dipping $\sim 40^\circ$ to the NW. Thirty-five specimens

from the 17 samples were investigated. The NRMs of all these specimens were found to be steeply downward-directed, suggesting the presence of a recent component. Four specimens, one from each site, were AF demagnetized in detail according to the schedule described in Appendix A. The AF results showed unstable magnetic behaviour upon demagnetization. Both the direction and the intensity of magnetization changed erratically at each successive demagnetization step. No definite trend in the directional migration was noticeable and therefore the results are not shown here. The intensity, however, was reduced to 15-20% of the NRM in all 4 specimens.

Thermal demagnetization was carried out on 31 specimens representing all 17 samples. As in the AF treatment the magnetization was observed to be of unstable character in a large majority of specimens. However, there was a definite directional trend with increasing temperature in the case of most specimens. Unlike the ~~older Formations~~ (Chapters 3, 5-6) of the Port au Port Peninsula, where the directions moved to the southeast at high temperatures, the directional change in most of the Long Point specimens showed a N to NW trend upon thermal demagnetization. In none of these specimens did a stability of direction seem to be well established. More often, the directional change was associated with erratic changes in the intensity, and almost all the specimens showed evidence of chemical changes after heating to

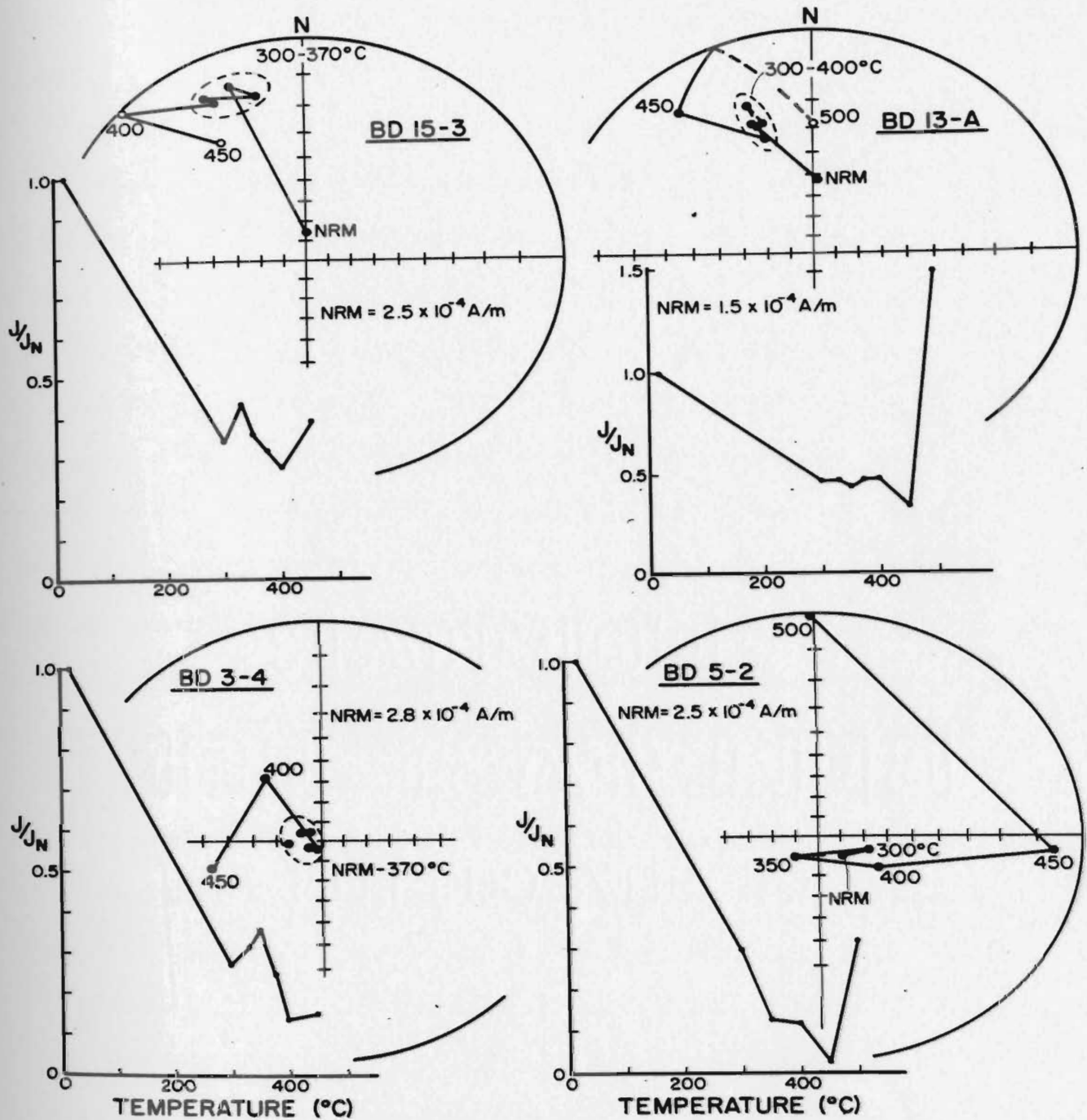


Fig. 7.1. Representative thermal demagnetization results for 4 Long Point specimens yielding a north-westerly direction (top) and a steep down direction (bottom). Solid (open) circles denote down (up) directions without tilt correction. Wulff net.

400°C or beyond, indicated by a sharp rise in the remanent intensity.

Figure 7.1 represents the thermal demagnetization results of some specimens which seem to show stability of magnetization. The steep down NRM's of Specimens BD13-A and BD15-3 in this figure move to a shallower direction along the northwest which is stable for 4 consecutive demagnetization steps. The intensity, however, either changes erratically (Specimen BD15-3) or shows no significant reduction (Specimen BD13-A) over the stable range of directions. In both of these specimens, a large proportion of intensity remains before the onset of chemical changes when the directions become random. The bottom diagrams of Figure 7.1 (Specimens BD3-4 and BD5-2) shows a stable direction, almost vertically downward. Again, there is evidence of erratic changes in the intensity and of chemical change beyond 450°C. Such steep and stable directions were obtained in other formations also and have been discussed at length in the preceding chapters. The northwesterly and shallow directions whose stability seems questionable, were obtained from only 10 specimens (6 samples) and are listed in Table 7.1 and are plotted in Figure 7.2. The scattered nature of these directions indicates that the characteristic components have not been well resolved in these specimens. A persistent tendency of these directions, however, to cluster in a northwesterly shallow

LONG POINT GROUP

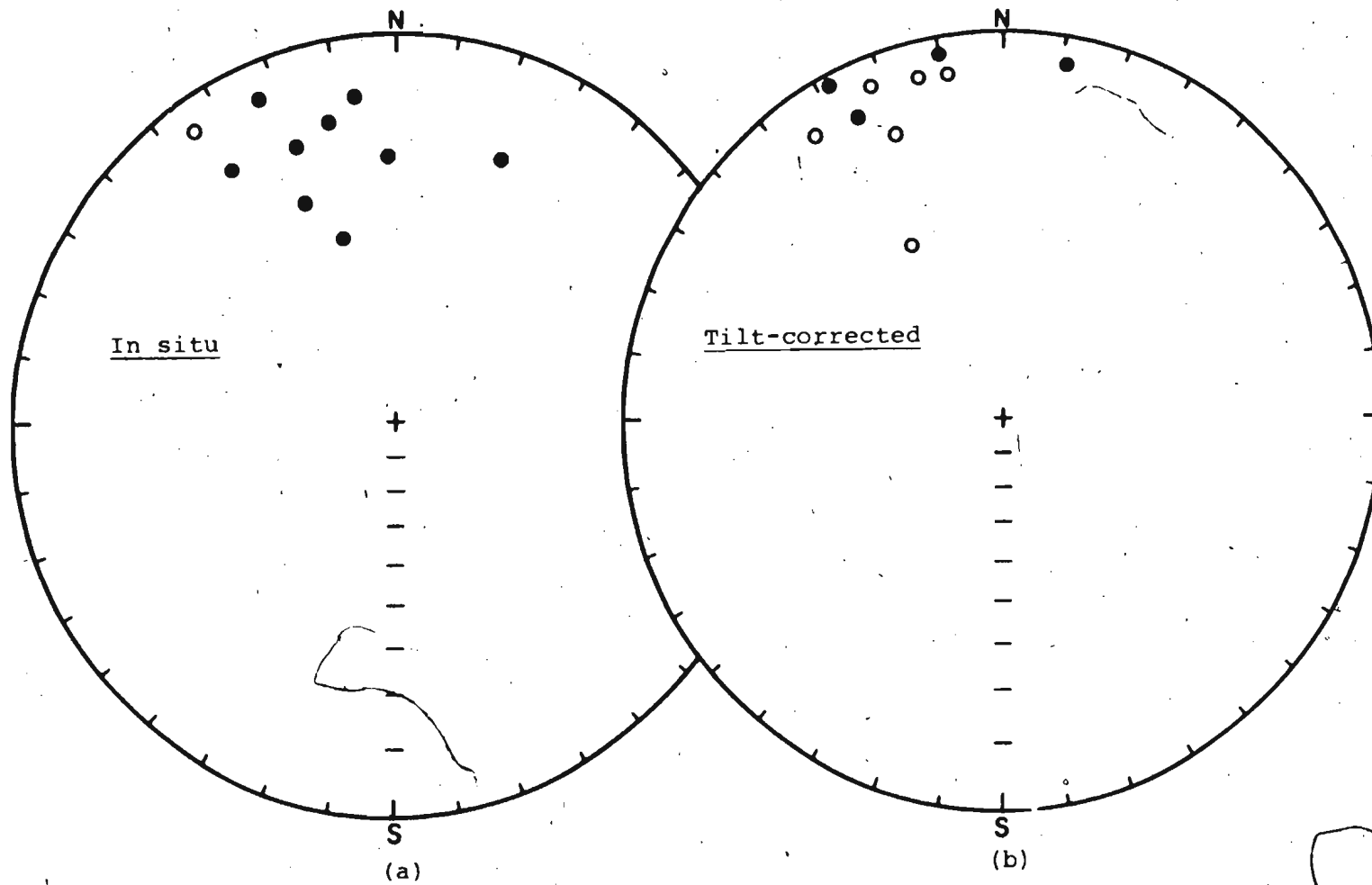


Fig. 7.2. Characteristic specimen directions, after thermal demagnetization. Solid (open) circles are down (up) magnetizations. Equal area projection.

TABLE 7.1

THERMAL DEMAGNETIZATION RESULTS FROM THE LONG POINT GROUP,
PORT AU PORT AREA.

Site	Specimen	Characteristic direction				Stability range (° C)
		<u>In situ</u>		Tilt-corrected		
		D	I	D	I	
BD1	BD1-B	348.1	21.9	345.6	-10.6	300-350 (v.s.)
BD1	BD1-D	325.0	-9.7	332.3	-47.8	300-370 (v.s.)
	Combined BD1-B & 1-D	336.2	6.2	340.2	-29.4	
BD2	BD6-D	22.6	27.9	10.9	9.3	300-370 (ave.)
BD4	BD13-A	339.8	25.5	337.5	-9.3	300-400 (ave.)
BD4	BD13-D	344.7	49.9	333.9	15.2	300-400 (ave.)
	Combined BD13-A & 13-D	342.2	37.7	336.0	3.0	
BD4	BD14-A	337.7	40.0	332.0	4.3	300-400 (ave.)
BD4	BD15-1	327.1	24.1	326.3	-13.0	300-400 (ave.)
BD4	BD15-3	337.3	11.9	338.9	-23.0	300-400 (ave.)
	Combined BD15-1 & 15-3	332.1	18.1	332.4	-18.1	
BD4	BD17-B	352.6	18.3	351.3	-12.1	350-400 (ave.)
BD4	BD17-C	358.6	33.2	350.1	3.7	300-370 (ave.)
	Combined BD17-B & 17-C	355.4	25.8	350.7	-4.2	

	<u>In situ</u>	<u>Tilt-corrected</u>
Overall mean:	$D_m = 347.3, I_m = 27.0$	$D_m = 343.7, I_m = -5.9$
	$\alpha_{95} = 17.8, k = 15,$	$\alpha_{95} = 17.9, k = 15.0,$
	$N = 6$ samples	$N = 6$ samples

NOTES: All symbols and explanations as in Tables 3.1-3.3.

direction is clearly evident. The in situ mean of 6 samples is $D_m = 347.3^\circ$, $I_m = 27.0^\circ$ ($\alpha_{95} = 17.8^\circ$, $k = 15$) which after a geological tilt correction becomes $D_m = 343.7^\circ$, $I_m = -5.9^\circ$, ($\alpha_{95} = 17.9^\circ$, $k = 15$). This tilt corrected mean direction compares well with the mean direction ($D = 331.1^\circ$, $I = -13.7^\circ$, $\alpha_{95} = 8.4^\circ$, $k = 30$, $N = 11$ sites) from the uppermost member of the Long Point Group (Murthy, 1983). However, since the present result is based on only six samples with doubtful stability, no pole position is quoted for the Long Point Group. The importance of the present investigation is emphasized in the discussion below.

IRM studies were done on two specimens, each from a different site; the results (figure not shown), indicated the presence of magnetite exclusively in these rocks. The thermal and AF demagnetization results also do not show any evidence of the presence of high coercivity or high blocking temperature components. Thus it can be concluded that the remanence carriers in the Long Point Group are magnetite only.

7.3 Discussion

It would not be statistically meaningful to assign a paleofield in which the Long Point Group of rocks acquired magnetization. However, based on the results from a limited number of samples it seems to be well established that the Lourdes Limestone of the Long Point Group acquired

its magnetization in a field which was of opposite polarity to that of the field in which the older rocks of the Port au Port Peninsula became magnetized. It was shown in the preceding chapters that a characteristic southeasterly direction is present in each of the Middle Cambrian to Middle Ordovician Formations on the Port au Port Peninsula that were measured. It was also noted that a number of specimens in those earlier Formations showed a northerly trend of directional migration at higher temperatures. This northerly trend was exhibited by a number of specimens which either did not show any stable direction (e.g., Port au Port Group), or more often, yielded a stable southeasterly component (St. George and Table Head Groups) before showing a northerly trend. This normal polarity trend was more pronounced in the Cape Cormorant Formation (uppermost Table Head Group). It was noted that in the Cape Cormorant samples (Chapter 6), overlapping normal and reverse components were probably responsible for the unstable magnetic behaviour of most of the specimens. One Cape Cormorant specimen was found to give a stable northerly direction (See Figure 6.7) widely divergent from others. All these observations point to the existence of a polarity reversal during the time span represented by the Cape Cormorant Formation of the Table Head Group and the Lourdes Limestone of the Long Point Group.

It should also be noted here that, as in the case of the Table Head Group, Kiaman overprinting was absent in the

Long Point Group. Thus Kiaman overprinting seems to have affected the Port au Port strata selectively, being confined to Upper ~~Cambrian to Lower Ordovician~~ rocks, whereas the Middle Ordovician rocks escaped its effects.



CHAPTER 8
COW HEAD GROUP

8.1 Geological setting

The Cow Head Group is a sequence of interbedded strata comprising thinly bedded limestones (~5-30 cm), thinly bedded shales, carbonate conglomerates and breccias, and carbonate megabreccias (James, 1981). These rocks represent essentially continuous deposition in deep water over a period of some 70 million years ranging in age from Middle Cambrian to Middle Ordovician (Kindle and Whittington, 1958; Hubert et al., 1977; Fahraeus and Nowlan, 1978).

The Cow Head Group was deposited near the base of the Lower Paleozoic continental slope of North America as a series of submarine gravity flows that moved from the outer shelf and upper continental slope into an area of active deposition (Stevens, 1970; Williams and Stevens, 1974). This rock sequence is presently regarded as allochthonous, having been transported from some area east of its present location. The westward thrust from the original site took place during the Taconic orogeny in the Middle Ordovician, and the strata now structurally overlie the autochthonous sediments of the St. George and Table Head Groups. However, there remains the possibility that the Cow Head sequence is more or less in place, because the basal contact is not seen anywhere and no melange zone has

been noted in close proximity (Nowlan, 1974).

The following general observation about these rocks is mainly based on the classic study of Kindle and Whittington (1958) and by other investigators mentioned above. The breccia beds are composed of both deep-water slope limestone clasts and shallow water boulders and range in thickness from 0.3 m to more than 60 m. Flat angular pebbles and slabs are similar in composition to the surrounding thin-bedded slope limestones and comprise the majority of clasts in the breccias. Moderately rounded limestone boulders are of shallow water origin, probably derived from the shelf-edge (R. K. Stevens, personal communication). Fossil studies in the interbedded shales and limestones have shown that with some exceptions, "the boulders of any conglomerate are approximately of the same age as the immediately underlying strata" (Kindle and Whittington, 1958). The Cow Head strata were deformed, either during the Taconic or the Acadian orogeny. An Acadian deformation, however, seems to be more likely (R.K. Stevens, personal communication).

The Ordovician strata of the Cow Head Group in Cow Head Peninsula (Figure 8.1) were chosen for paleomagnetic investigations in preference to the Cambrian strata as the former offered the opportunity for making a fold test. The objective was to isolate a characteristic magnetization and see if the upper age-limit of magnetization can be constrained.

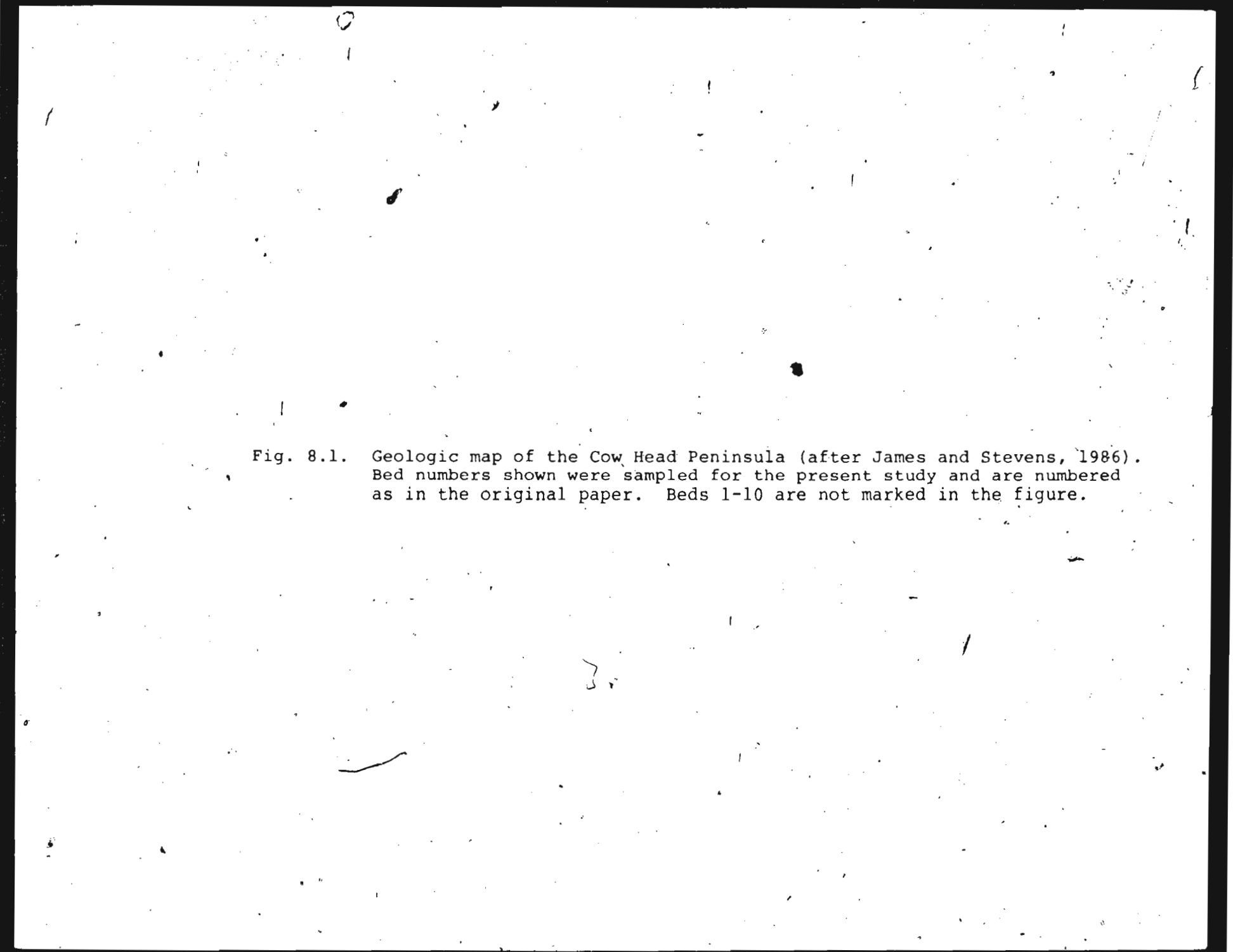
The image shows a geologic map of the Cow Head Peninsula, which is mostly blank with some faint, illegible markings and scattered dark spots. The map is intended to show geological features and sampling locations for various beds.

Fig. 8.1. Geologic map of the Cow Head Peninsula (after James and Stevens, 1986).
Bed numbers shown were sampled for the present study and are numbered
as in the original paper. Beds 1-10 are not marked in the figure.

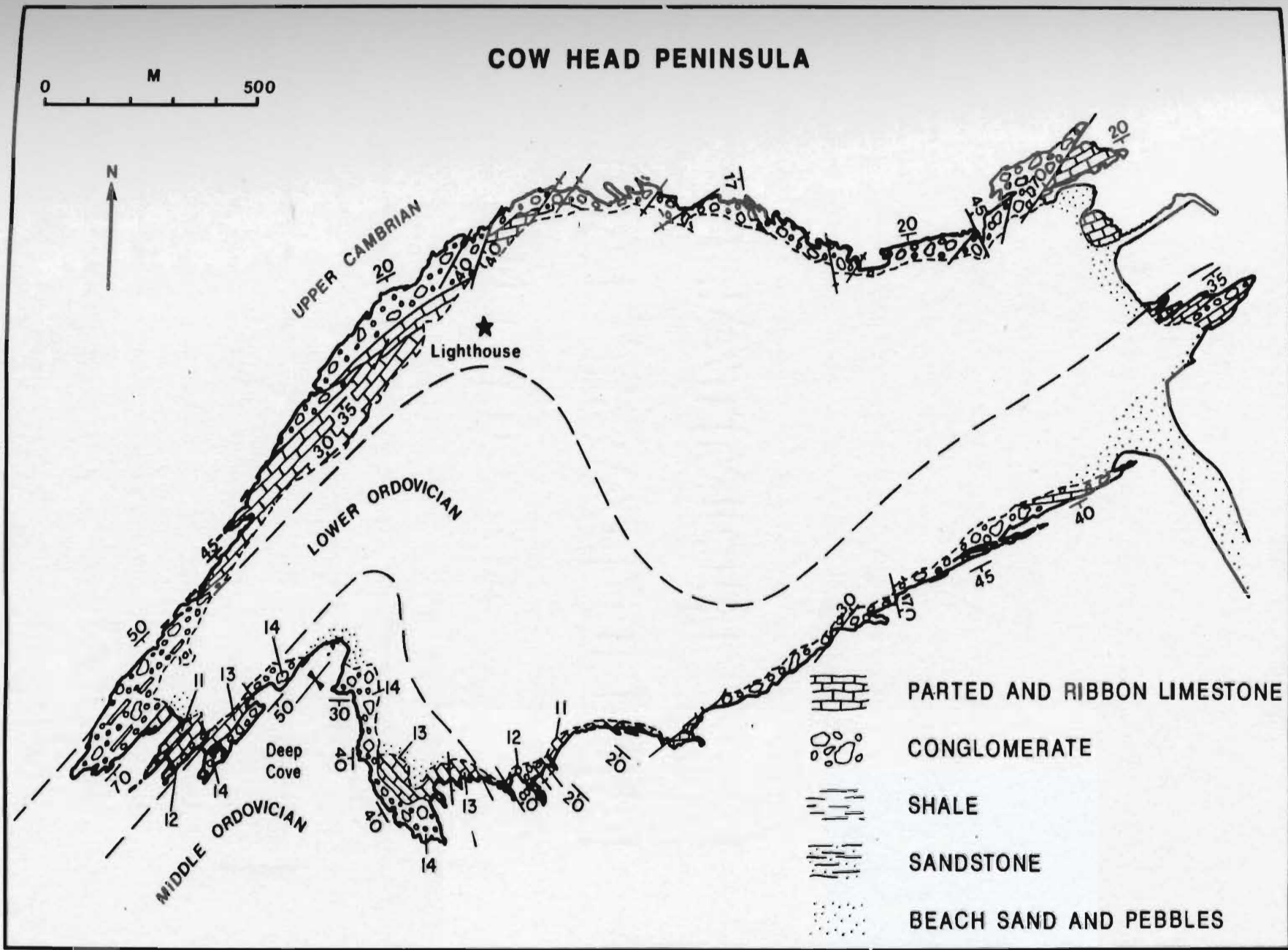


Fig. 8.1

The rocks in the study area are folded into a broad syncline, the axis of which strikes 208° and is plunging southwest. A calculation based on the strike and dip measurements on the bedded rocks adjacent to the syncline (Middle Ordovician Bed No. 13, Figure 8.1) yielded a magnitude of 30.5° for the plunge (Figure 8.2 and Appendix F). However, another calculation of plunge, based on measurements on the Lower Ordovician Bed No. 11, indicates a more southerly strike and a lower magnitude ($\sim 20^{\circ}$) for the plunge. This discrepancy arises because of the change in the nature of the fold, which changes from syncline to anticline as one moves farther east from the syncline axis. As the fold becomes increasingly non-cylindrical to the east it is not possible to unequivocally restore the strata to their original horizontal position (T. Calon, personal communication). However, despite this complexity of the overall structure, Beds 13 and 14 (Figure 8.1), which are next to the syncline axis, can be restored to the paleohorizontal. Therefore, the folded rocks of Bed 13 are suitable for carrying out a fold test (Graham, 1949). In addition, the breccia bed (No. 14) lends itself to a conglomerate test (Graham, 1949). With these objectives, oriented hand samples were collected from both limbs of the syncline. The two limbs lie on either side of Deep Cove (Figure 8.1). Only the samples from Beds 13 and 14 were studied, because of the above-mentioned structural complexities affecting the older

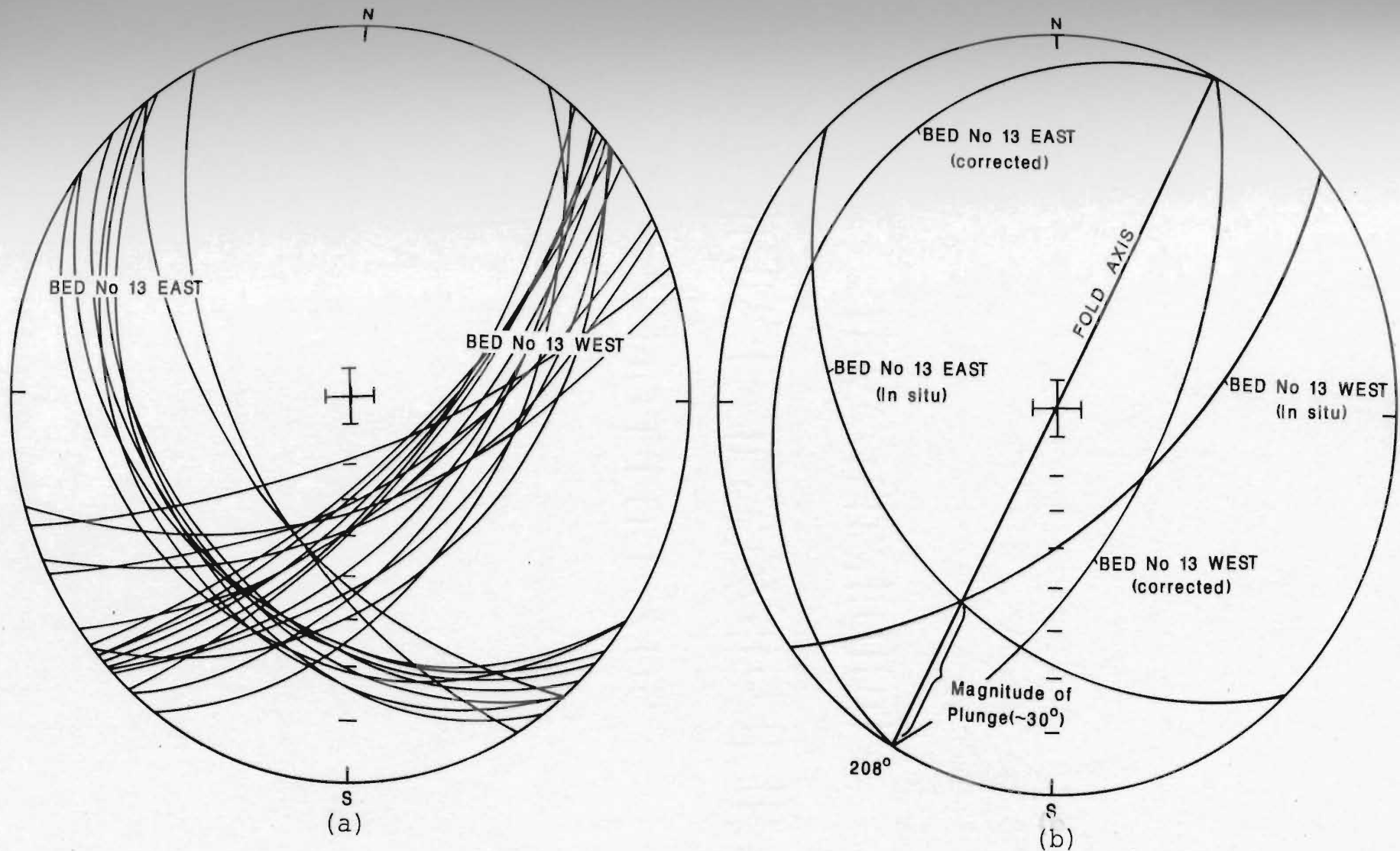


Fig. 8.2. Bedding correction for the plunging fold: (a) In situ orientation of bedding planes shown by great circles in stereographic projection; (b) Mean in situ and plunge-corrected bedding orientation for the two limbs of the syncline. See Appendix F for details of the reconstruction.

strata. These beds are believed to have formed during the major hiatus that separates Lower and Middle Ordovician strata on the North American craton (Sloss, 1963).

8.2 Paleomagnetic sampling and results

Ten samples from 2 sites on the eastern limb and 15 samples from 3 sites on the western limb of the syncline were collected from Bed 13. The total stratigraphic thickness covered by these samples is 1.8 m in the eastern limb and 2 m in the western limb. Forty samples, comprising 20 from each of the eastern and western limbs were collected from Breccia Bed 14, which is the youngest in the Cow Head Peninsula. Thus a total of 65 samples - 25 from non-conglomeratic bedded rocks and 40 from blocks in the conglomerates - were collected for paleomagnetic studies.

The NRM directions of the samples were found to be steep with positive inclination. The intensity was in the range 1×10^{-4} to 2×10^{-3} A/m. AF demagnetization of two samples, one from each limb of the syncline (results not shown), showed the presence of only one component, directed steep down. This component was found to be very stable. The intensity fell smoothly to a low value at increasing fields, while the directions did not change significantly from the NRM. The remanent intensity at 100 mT was 2-4% of NRM. This suggests that the remanence is carried dominantly by low-coercivity grains, probably

Fig. 8.3. Representative thermal demagnetization results for 2 Cow Head Group specimens. Solid (open) circles denote down (up) magnetizations on a Wulff net. On orthogonal vector diagrams, squares are the projections on an east-west vertical (V) plane and circles, on the horizontal (H) plane.

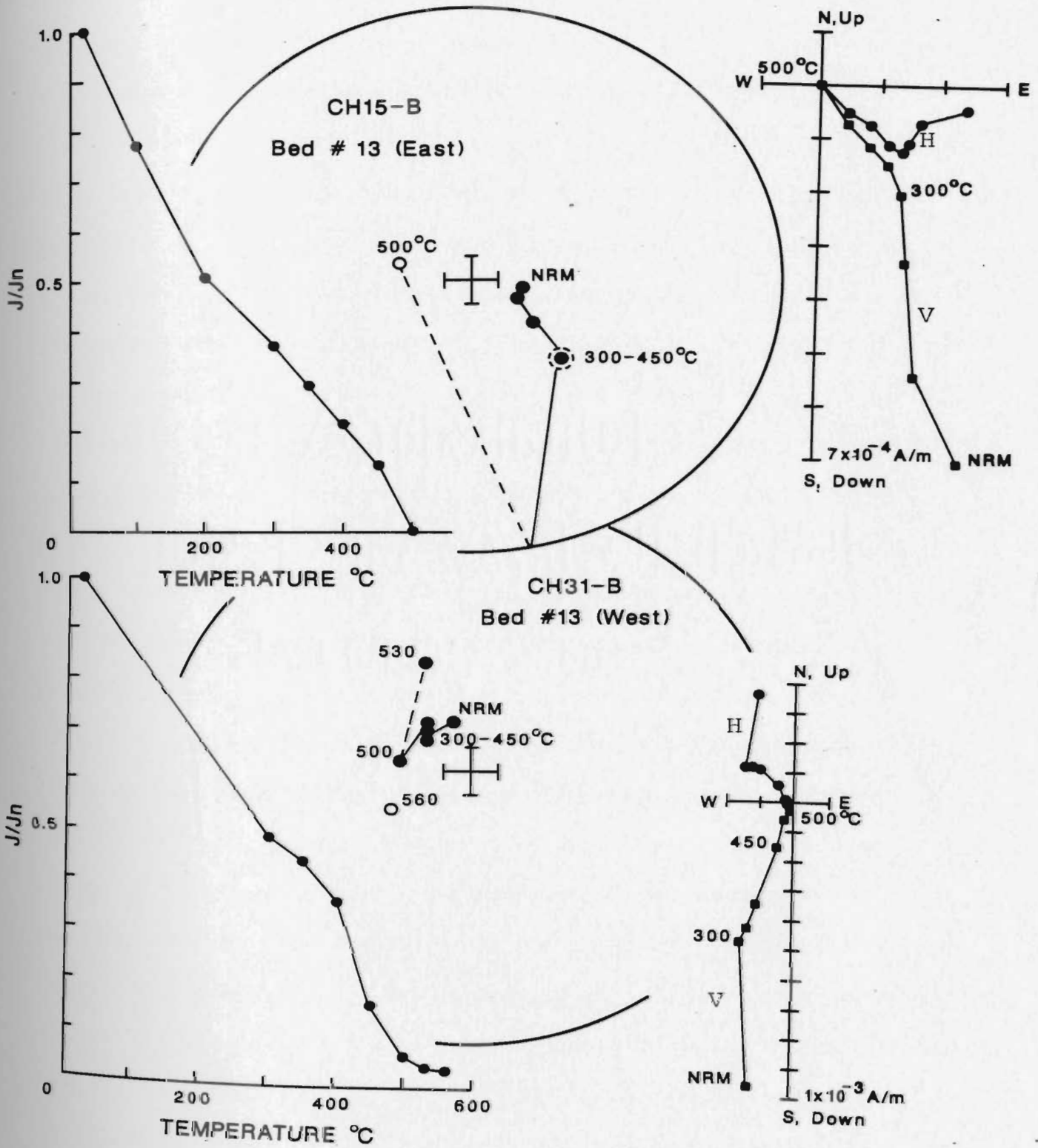


Fig. 8.3

magnetite.

Since the AF results yielded only steep magnetizations, thermal demagnetization was carried out on the rest of the specimens to isolate any other component(s). Figure 8.3 shows demagnetization results on two representative specimens. Specimens CH15-B and CH31-B are from the respective eastern and western limbs of the fold. An intermediately steep component in the southeast quadrant was isolated from Specimen CH15-B beyond 300°C, as indicated on both the stereographic plot and the vector diagram. Specimen CH31-B yields a steep down characteristic component, similar in direction to the stable component isolated by the AF treatment. Stable directions were obtained from a large majority (23 out of 25) of the samples (one specimen each). These characteristic directions are listed in Table 8.1 and are plotted in Figure 8.4, both before and after a two-step structural correction (plunge and fold; see Appendix F). The site mean directions are listed in Table 8.2 and are plotted in Figure 8.4. The overall paleomagnetic parameters are summarized in Table 8.3. Figure 8.4 and Table 8.3 show that the grouping of directions considerably improves after the structural correction, suggesting that the magnetization is pre-folding. The mean direction, based on 22 samples, before structural correction, is $D = 116.9^\circ$, $I = 76.6^\circ$, ($\alpha_{95} = 11^\circ$, $k = 9.4$). After structural correction it becomes $D = 155.3^\circ$, $I = 40.9^\circ$,

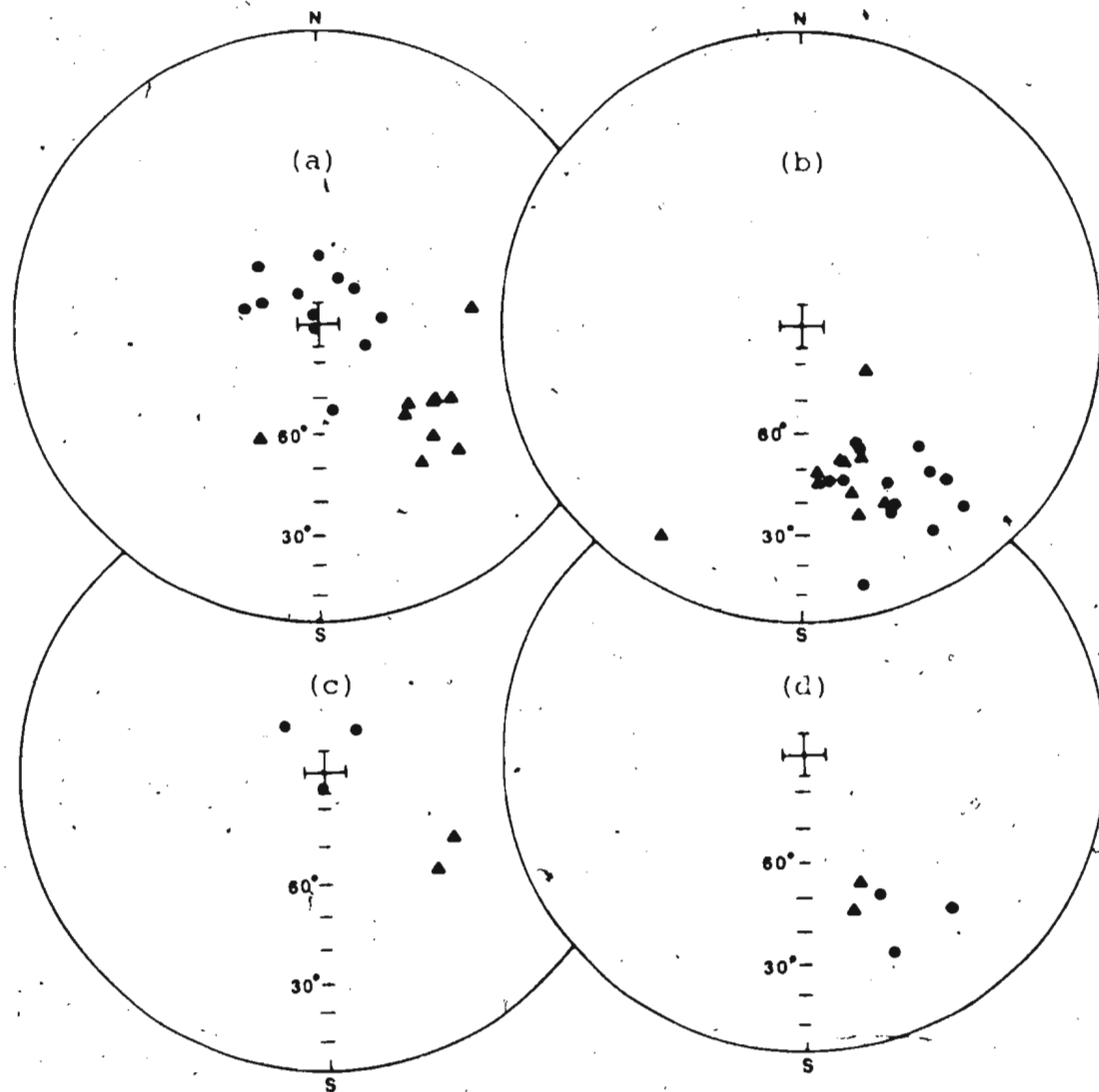


Fig. 8.4. Characteristic sample (a, b) and site mean (c, d) directions from Bed 13, Cow Head Peninsula: (a) and (c) are before structural corrections; and (b) and (d), after two-step (plunge and fold) correction. Circles are from the western limb and triangles from the eastern limb of the syncline. Equal area projection on the lower hemisphere.

TABLE 8.1

THERMAL DEMAGNETIZATION RESULTS FROM THE MIDDLE ORDOVICIAN BEDDED
LIMESTONES OF THE COW HEAD GROUP, COW HEAD PENINSULA

Site	Specimen	Characteristic direction				Stability range (° C)
		Before structural correction		After structural correction		
		D	I	D	I	
<u>Bed No. 13 East</u>						
CH4	CH14-C	141.6	41.6	163.8	33.9	300-400
CH4	CH15-B	134.7	46.4	163.4	40.8	300-450
CH4	CH16-B	136.5	55.8	174.1	46.3	300-400
CH4	CH17-A	124.6	53.0	164.4	50.1	300-400
CH4	CH18-B	119.2	48.7	155.9	50.2	300-400
CH5	CH19-A	131.7	57.4	173.6	49.4	300-450
CH5	CH20-1*	208.1	54.7	213.7	23.6	300-450
CH5	CH21-A	182.7	48.1	125.3	69.3	300-450
CH5	CH22-A	123.5	52.7	163.4	50.4	300-450
CH5	CH23-B	133.4	38.1	155.3	35.4	300-400
<u>Bed No. 13 West</u>						
CH6	CH24-B	112.4	77.3	148.2	18.9	300-450
CH6	CH25-B	337.0	87.4	153.1	32.9	NRM-400
CH6	CH26-B	242.0	89.5	154.6	30.5	NRM-450
CH6	CH27-B	172.2	66.8	167.0	10.6	300-400
CH6	CH28-1	291.7	73.1	164.7	45.1	NRM-500
CH7	CH29-1	23.3	76.4	138.9	35.3	NRM-500
CH7	CH30-1	315.5	66.9	155.9	53.5	300-450
CH7	CH31-B	315.4	66.7	156.0	53.7	300-450
CH7	CH32-1	328.5	80.4	151.8	39.9	NRM-500
CH7	CH33-A	284.1	69.7	170.4	46.3	NRM-500
CH12	CH54-A	84.0	73.0	139.5	19.7	NRM-450
CH12	CH55-A	44.1	75.7	137.5	30.4	300-400
CH12	CH58-B	0.6	70.8	136.3	43.5	NRM-400

NOTES: Specimen with * was excluded from the final statistics. The characteristic directions are based on the average of directions in the range indicated for all specimens except CH55-A, for which vector subtraction was used. Sites CH1-3 and CH8-11 were in the Lower Ordovician bed for which the results are not presented (See text).

TABLE 8.2

SITE-LEVEL CHARACTERISTIC DIRECTIONS OF THE COW HEAD GROUP,
COW HEAD PENINSULA

Site	n/n ₀	In situ		After structural correction			
		D	I	D	I	k	95
CH4	5/5	131.6	49.4	164.4	44.4	97	7.8
CH5	4/5	118.2	51.0	158.1	52.1	21	20
CH6	5/5	186.7	86.1	157.4	27.8	29	14
CH7	5/5	318.7	74.2	153.9	46.2	50	11
CH12	3/5	41.0	76.1	137.9	31.2	46	18

All symbols as in Tables 3.1, 3.3 and 5.2

TABLE 8.3

MEAN PALEOMAGNETIC DATA FROM THE COW HEAD GROUP,
COW HEAD PENINSULA.

	D_m	I_m	k	N	α_{95}	λ_p	Antipole
Mean of all samples, in situ	116.9	76.6	9.4	22	11		
Mean of all samples, tilt-corrected	155.3	40.9	25	22	6.3	29.4 S	13.3°N, 145.8°E ($\alpha_p, \alpha_m = 4.6^\circ, 7.6^\circ$)
Mean of sites, in situ	112.1	76.3	10	5	25		
Mean of sites, tilt-corrected	153.8	40.7	39	5	12		
Mean of all samples, from Bed 13 East, in situ	125.9	50.3	39	9	8.8		
As above, after structural correction	161.9	47.8	39	9	8.8		
Mean of all samples, from Bed 13 West, in situ	339.4	84.1	25	13	8.4		
As above, after structural correction	151.4	35.9	25	13	8.4		

All symbols as in Table 3.3

($\alpha_{95} = 6.3^\circ$, $k = 25$). A fold test (McFadden and Jones, 1981) was performed to test the statistical significance of improved precision after unfolding. The results of this test are discussed below.

8.3 Fold test

If the precisions of population from different limbs of a fold are the same, the fold test may be performed by testing whether the overall mean directions from the different limbs may be distinguished statistically. For the case of two limbs, the hypothesis of a common true mean direction may be rejected if (McFadden and Jones, 1981),

$$\frac{[R_a + R_b - R^2 / (R_a + R_b)]}{2(N - R_a - R_b)} > \left(\frac{1}{p}\right)^{\frac{1}{\sqrt{2}}} - 1$$

where R = length of the resultant vector of all the site mean directions (i.e., of the vectors \vec{R}_a and \vec{R}_b)

p = level of significance

N = total no. of sites

In the present case, let R_a and R_b be the lengths of the site mean vectors in the eastern and western limb of the syncline respectively. A separate statistical test, comparing the precisions of the populations of the two limbs, showed that the two precisions are not different at 95% level; hence the above mentioned fold-test is applicable. From observation,

$R_a = 1.9942$; 2 sites

$R_b = 2.9481$; 3 sites

$$R = R_1 \text{ (in situ)} = 4.5984$$

$$R = R_2 \text{ (after unfolding)} = 4.8979$$

$$R_a + R_b = 4.9423$$

$$2(N - R_a - R_b) = 0.1154, \text{ where } N=5 \text{ sites}$$

Hence, the hypothesis of a common true mean direction would be rejected at the 95% level of confidence (ie. $p = 0.05$) if

$$\frac{4.9423 - R^2/4.9423}{0.1154} > 1.714$$

With $R = R_2 = 4.8979$, the left side of the above equation is 0.7660 and the hypothesis of common true mean direction cannot be rejected. Using $R = R_1 = 4.5984$, the left side of the equation is 5.753 and the hypothesis of a common true mean direction in situ may be rejected.

Hence the fold test is in fact significant, and it may be concluded that the Cow Head rocks acquired their observed magnetization before the Acadian (?) folding.

8.4 Conglomerate test

One specimen from each of the 40 oriented pebbles collected from the two limbs of the syncline in Bed 14 was subjected to stepwise thermal treatment. Some stable directions obtained by this treatment are shown in Figures 8.5-8.6. A high temperature ($> 450^\circ\text{C}$) stable component is preserved in all the 4 specimens shown. However, the stable directions from either pair of boulders from the same bed (Specimens B1-1 and B12-A or C1-A and C18-B) are

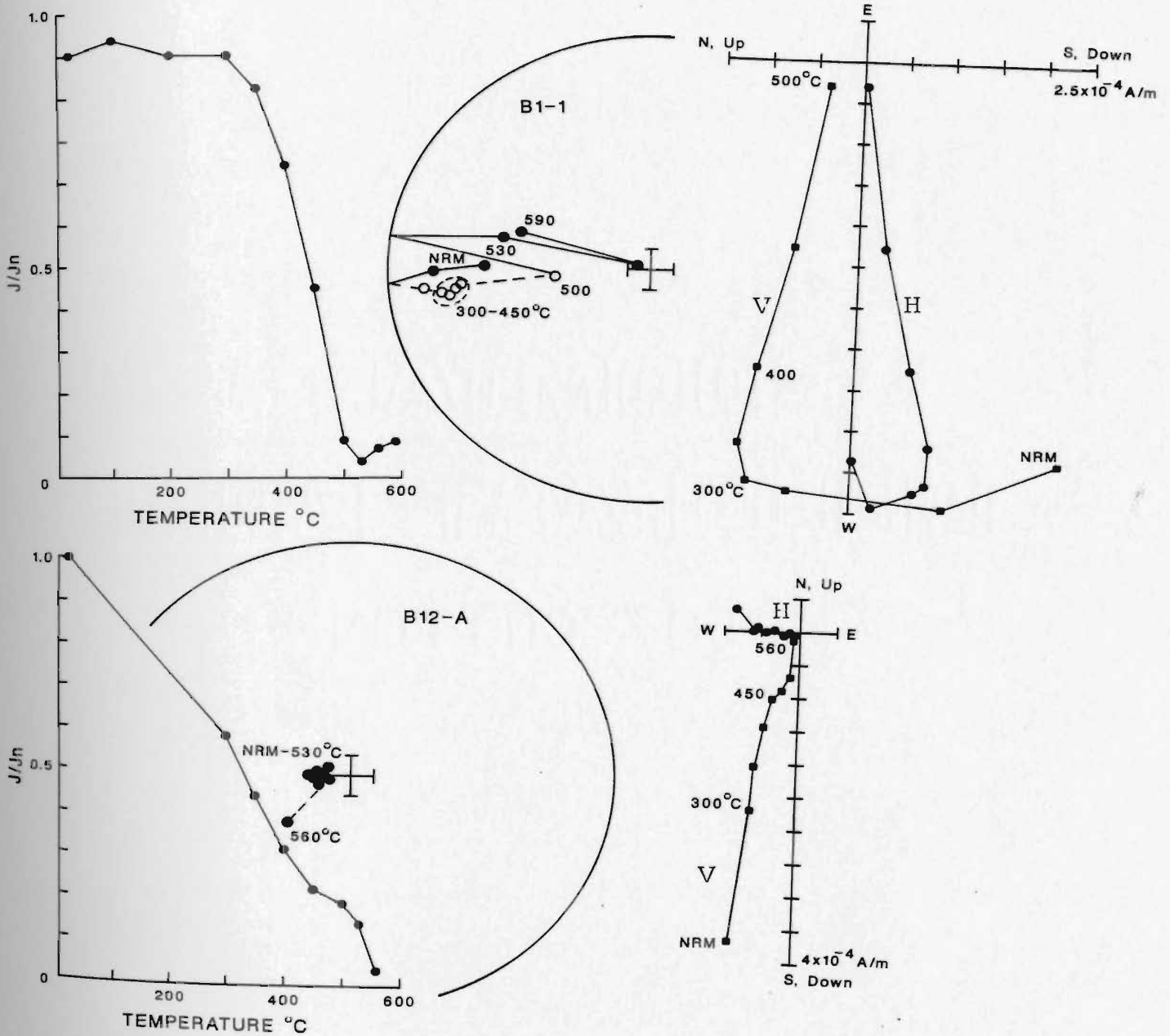


Fig. 8.5. Thermal demagnetization results for one specimen each from 2 pebbles in breccia Bed 14 (western limb), showing widely divergent stable directions. Conventions as in Fig. 8.3.

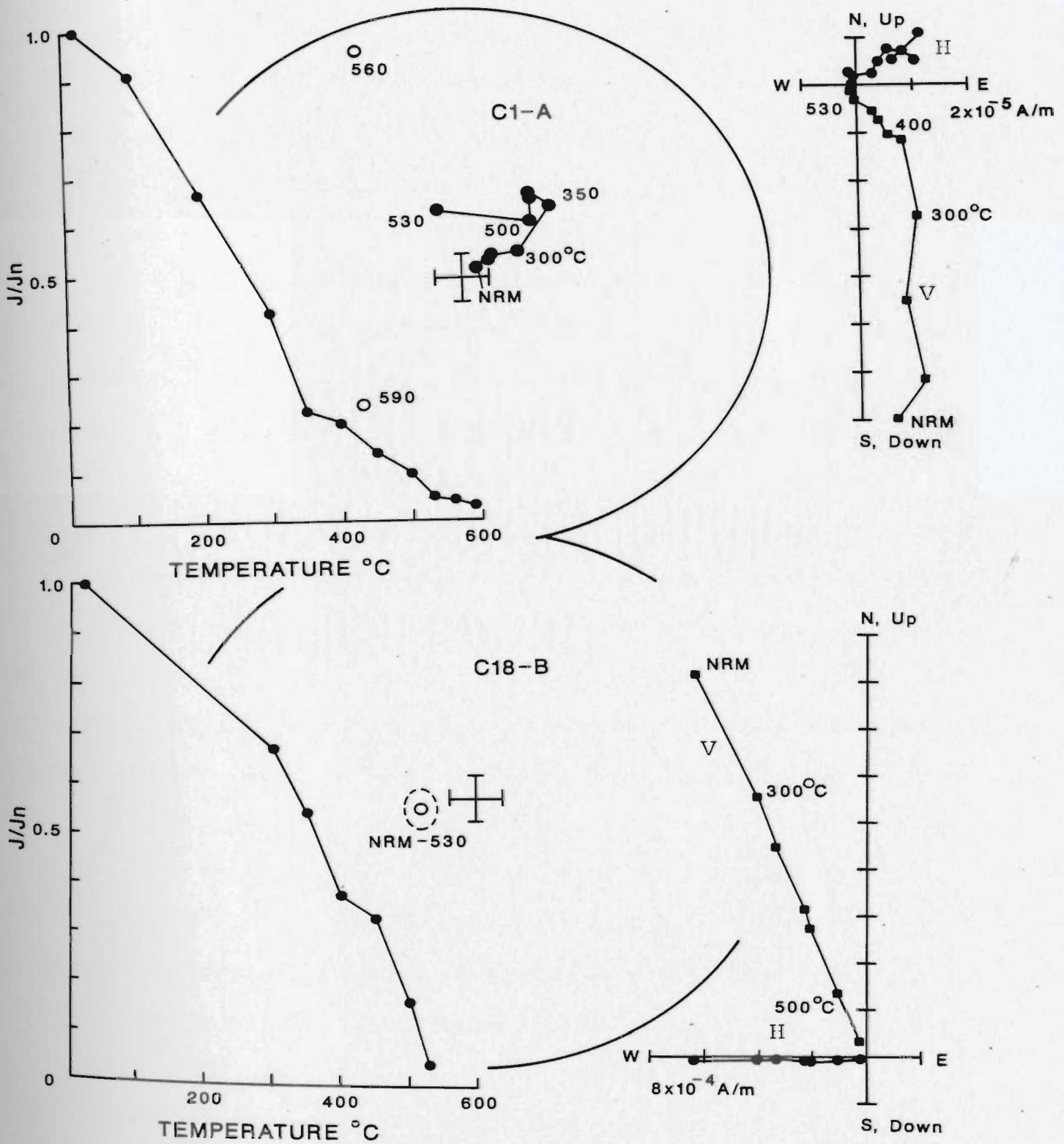


Fig. 8.6. Thermal demagnetization results for one specimen each from 2 pebbles in breccia Bed 14 (eastern limb), giving widely divergent directions. Conventions as in Fig. 8.3.

grossly misaligned with each other. This probably is the result of scattering of the vector directions between different boulders as a result of brecciation. However, such large scattering was not observed in most of the remaining boulders after demagnetization.

Twenty-six samples (one specimen each) out of the 40 yielded stable magnetizations after thermal treatment, with blocking temperatures always less than the Curie point of magnetite. The directions are listed in Table 8.4 and are plotted separately for the two limbs of the syncline in Figure 8.7. Also plotted in Figure 8.7 are the respective mean directions of magnetization from the underlying Bed 13.

Some interesting features can be observed in Figure 8.7. While some of the pebbles from the eastern limb of the syncline yielded scattered directions, and all are far removed from the in situ mean direction of the underlying bedded rocks, this is not the case for the majority of pebbles from the western limb. However, four samples from the western limb do yield stable components grossly misaligned with the majority of directions. Fisher's statistics were performed on the conglomerates from the eastern and western limbs separately. The results (Table 8.4) show very large cones of confidence associated with the means for both the limbs. Whereas the mean direction ($D = 350^\circ$, $I = 86^\circ$, $\alpha_{95} \approx 36^\circ$, $k = 2.2$, $N = 14$ samples) of the scattered pebble directions in the western

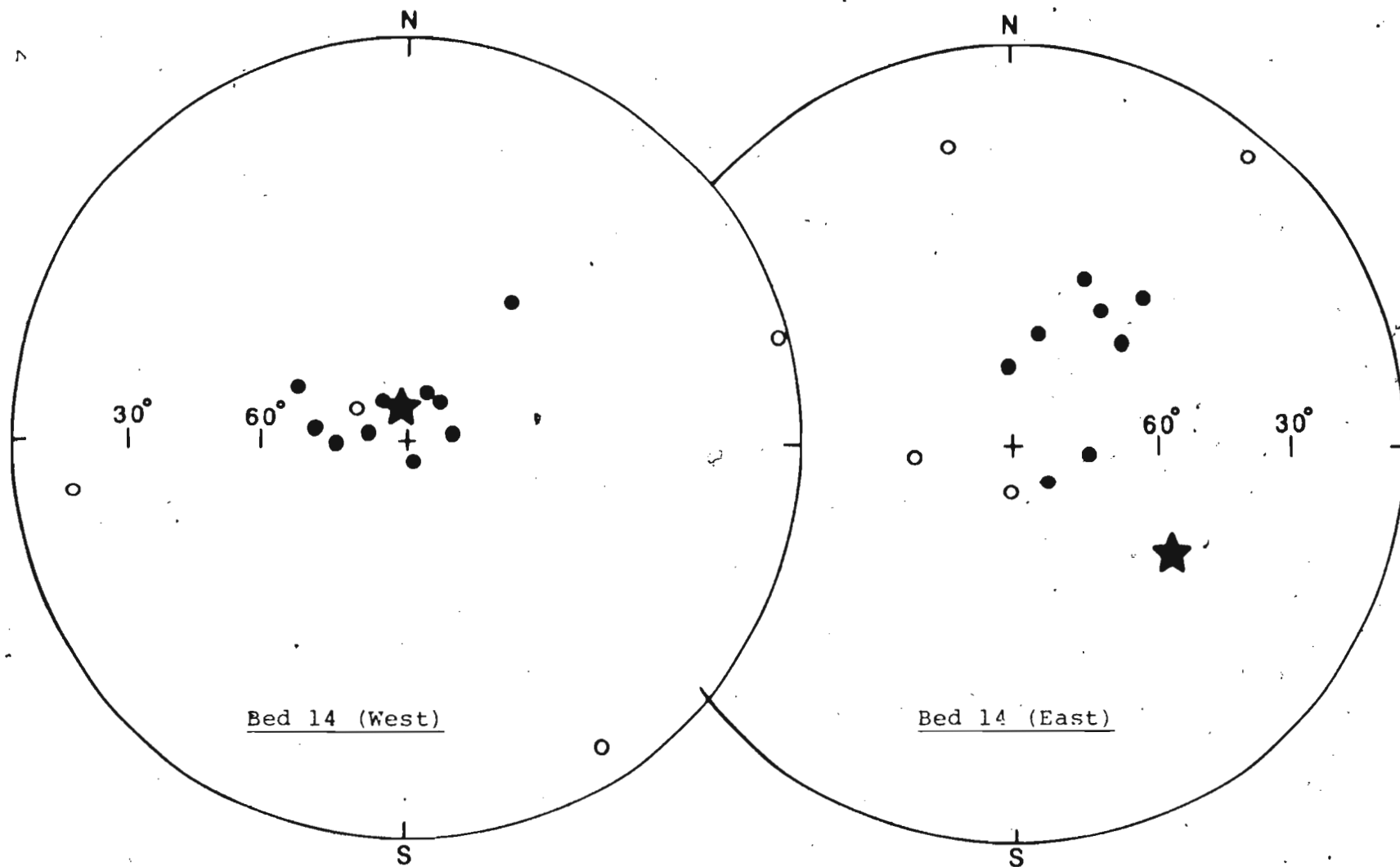


Fig. 8.7. Characteristic pebble directions from breccia Bed 14: Stars denote the mean directions from the underlying non-conglomeratic bedded rocks (Bed 13). Conventions as in Fig. 8.3. No tilt correction has been applied.

TABLE 8.4

THERMAL DEMAGNETIZATION RESULTS FOR PEBBLES FROM A BRECCIA BED
OF THE COW HEAD GROUP, COW HEAD PENINSULA.

Specimen	Stability			Specimen	Stability		
	Stable direction		range		Stable direction		range
	D	I	(° C)		D	I	(° C)
<u>Bed No. 14 East</u>				<u>Bed No. 14 West</u>			
C1-A	42.6	50.1	350-500	B1-1	261.0	-14.7	300-450
C3-B	356.5	74.9	NRM-400	B6-2	40.3	80.3	NRM-400
C4-A	48.7	59.8	NRM-450	B7-A	155.5	85.8	NRM-500
C10-B	139.2	80.1	NRM-500	B8-2	80.2	81.1	NRM-500
C11-A	39.5	7.1	400-530	B9-2	329.2	80.8	NRM-400
C14-A	35.8	57.8	NRM-450	B10-2	74.5	- 3.4	400-450
C15	13.5	67.8	NRM-400	B12-A	269.8	76.2	NRM-530
C16-1	98.4	74.8	NRM-450	B13-A	295.7	64.6	NRM-500
C17-A	24.8	53.5	NRM-450	B14-2	147.4	- 9.9	300-400
C18-B	264.2	-69.7	NRM-530	B15-A	277.9	71.2	NRM-560
C19-A	180.5	-80.1	NRM-450	B16-1	301.8	-77.9	NRM-560
C20-1	347.7	-25.3	NRM-400	B17-A	22.0	79.7	NRM-530
				B18-A	284.5	82.0	NRM-560
				B20-1	37.9	54.7	NRM-530

Overall mean:

$D_m = 27.4$, $I_m = 49.8$,
 $N = 12$, $\alpha_{95} = 43$, $k = 2.0$
 $R = 6.414$

Overall mean:

$D_m = 350.2$, $I_m = 86.4$,
 $N = 14$, $\alpha_{95} = 36$, $k = 2.2$
 $R = 8.123$

NOTES: R is the length of the resultant mean vector. All other symbols and explanations as in Tables 3.1-3.3.

limb falls close to the in situ mean direction of the underlying bedded rocks ($D = 339^\circ$, $I = 84^\circ$, $\alpha_{95} = 8^\circ$ in Table 8.3), the mean of pebble directions in the eastern limb ($D = 27^\circ$, $I = 50^\circ$, $\alpha_{95} = 36^\circ$, $k = 2.0$, $N = 12$ samples) is far removed from that of the in situ mean of the underlying bedded rocks ($D = 126^\circ$, $I = 50^\circ$, $\alpha_{95} = 8.8^\circ$, in Table 8.3). For neither limb of the syncline do the pebble directions pass a statistical test of randomness (Irving, 1964, p. 63). However, in the case of the eastern limb, the directions are close to random, in which case they would meet a minimum condition for a positive conglomerate test. In order to obtain a conclusive test it is also necessary to demonstrate that the directions of the stable component in multiple specimens from the same pebble are coherent. In view of an apparently negative result of the conglomerate test, this internal consistency test was not attempted. The conglomerate test in the present study is therefore inconclusive. The most that can be concluded from this partial conglomerate test is that the widely scattered stable directions of some of the pebbles may antedate brecciation.

8.5 Magnetic mineralogy

An IRM study was done on 4 samples chosen from both limbs of the syncline. Results for two samples are shown in Figure 8.8. A sharp increase in intensity at lower

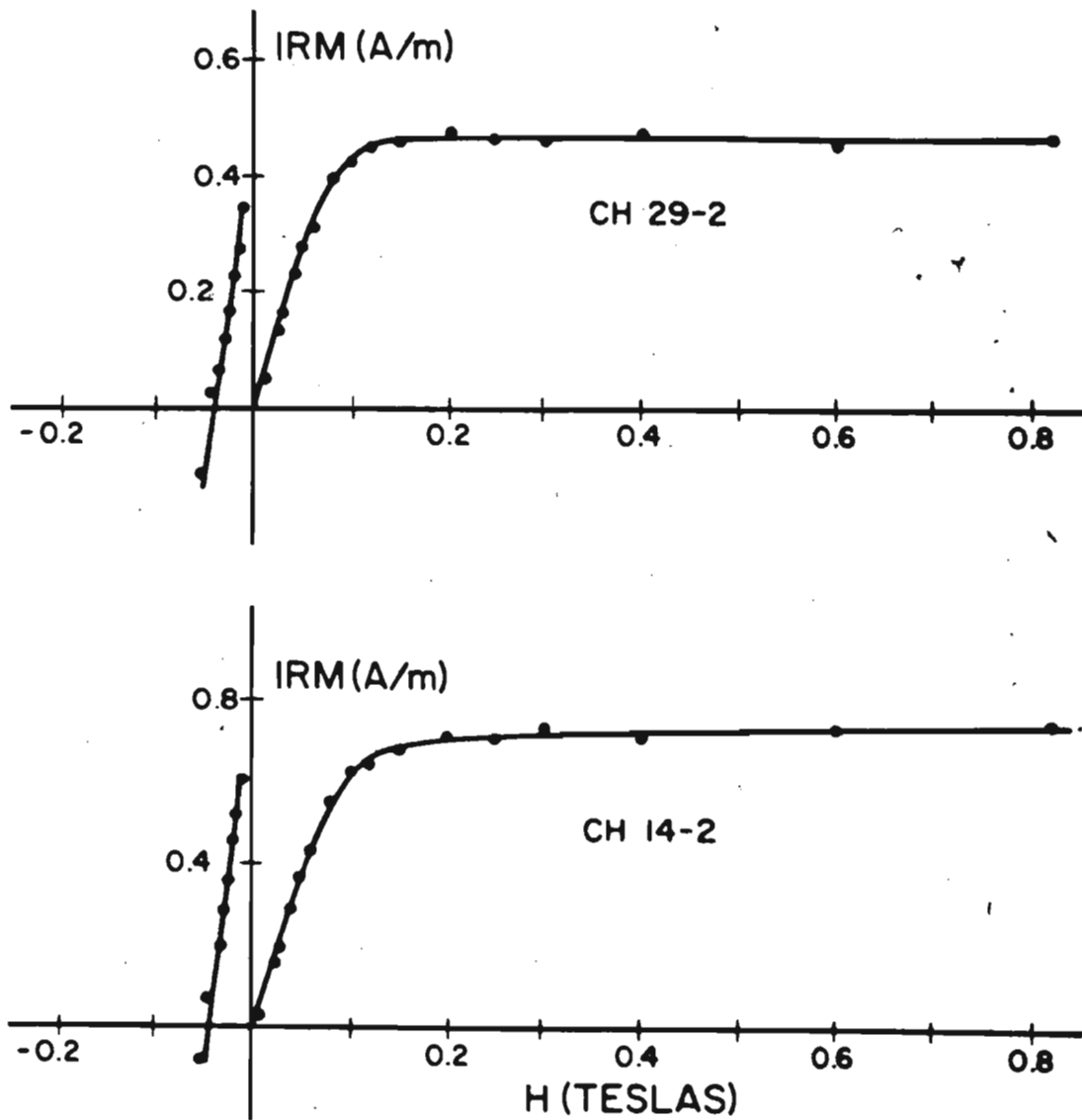


Fig. 8.8. IRM acquisition and back-field characteristics of 2 representative specimens from the Cow Head Group. The curves strongly indicate the presence of only magnetite.

magnetizing fields, with attainment of saturation at 0.10-0.15 T, indicates the presence of magnetite. This is further seen from the back-field IRM curves which show the presence of a single phase of magnetic grains with low values of coercivity of remanence ($H_{Cr} \sim 0.040-0.045$ T), characteristic of magnetite. The results of the IRM study, coupled with the low blocking temperatures (450-500°C) observed during thermal demagnetization, and the limited AF results, confirm that magnetite is the remanence carrier.

8.6 Discussion

A stable, possibly primary, characteristic direction was isolated from the Middle Ordovician non-conglomeratic bed of the Cow Head Group. This magnetization resides in magnetite which unblocks in the range 400-500°C. The conodont CAI for these rocks is 1.5 (Nowlan and Barnes, 1985), which suggests a maximum temperature of less than 60-80°C. From the theoretical data of Pullaiah et al. (1975), a magnetization with blocking temperature of 300°C or less would be reset by heating to 60-70°C for 100 m.y. Since the blocking temperature far exceeds 300°C, it is improbable that the rocks were thermally remagnetized after deposition. Besides, the results of a structural (fold and plunge) test strengthen the case for a pre-folding, or perhaps even primary origin of the magnetization. There is some mild support for this conclusion from the partial conglomerate test, though that

test as a whole proved inconclusive.

The antipole position corresponding to the structurally corrected mean direction ($D = 155.3^\circ$, $I = 40.9^\circ$) for Bed 13 is 13.3°N , 145.8°E ($dp = 4.6^\circ$, $dm = 7.6^\circ$, $\lambda_p = 23.4^\circ\text{S}$). This pole (Figure 9,1) is very close to the poles obtained from the autochthonous Table Head and St. George Groups of the Port au Port area. The close proximity of these poles can be interpreted in terms of one of the following possibilities:

(1) The Cow Head Group is either in place or was not transported far. A transport of a few kilometers might not change the previous in situ paleomagnetic direction appreciably if the process of transport did not involve complex motions including tectonic rotations. In any case, this interpretation requires that the magnetization was acquired before the deformation of both the platformal rocks and the transported Cow Head rocks. Also, the interpretation again implies that there was little, if any, apparent polar wandering during the time interval involved.

(2) The Cow Head Group is truly allochthonous and was magnetized after being emplaced on the autochthon, though before the deformation of both the autochthonous and allochthonous strata. This interpretation would introduce an element of uncertainty in the age of magnetization of the autochthonous rock sequence. This uncertainty, however, would be confined to a time interval between Lower and Middle Ordovician, as no published cratonic pole

younger than Middle Ordovician lies close to the Port au Port Ordovician poles.

Out of the above two interpretations the first is favoured, since it was argued in earlier chapters that the St. George and Table Head magnetizations of Port au Port area were acquired close to the time of deposition. However, the conclusions from this limited study of the Cow Head rocks must be treated as tentative and should be tested by a more detailed investigation of the allochthonous rocks from other localities on the Western Platform of Newfoundland with different structural attitudes.

CHAPTER 9

ORDOVICIAN PALEOPOLES OF NORTH AMERICA AND ROTATION OF NEWFOUNDLAND

9.1 Ordovician paleopoles

Some reported Ordovician poles from cratonic North America have been listed in Table 9.1 along with the results from the present study. These poles are plotted in Figure 9.1 and are numbered as in Table 9.1. Also plotted in Figure 9.1 are some Kiaman poles (Table 4.2), as well as the "B" component pole (SGO) isolated from the St. George Group (Chapter 5). All paleopoles of the present study are shown with their error ovals. The Ordovician poles of Figure 9.1, like the Cambrian poles, are scattered. Though their overall scatter is less than that of the Cambrian poles, some of the Ordovician poles also lie close to Late Paleozoic poles, as in the Cambrian case. Following is a brief review of the poles plotted in Figure 9.1

There have been two earlier paleomagnetic investigations from the St. George Group. Beales et al. (1974) studied paleomagnetically the relationship between host limestone and sulphide ore at Daniel's Harbour in the northern Peninsula (close to Table Point of Figure 2.2). Only AF demagnetization was performed on the samples, which was effective in removing a steep viscous component. Beales, et al. reported difficulty in measuring remanence because of the low intensity of their samples. Their

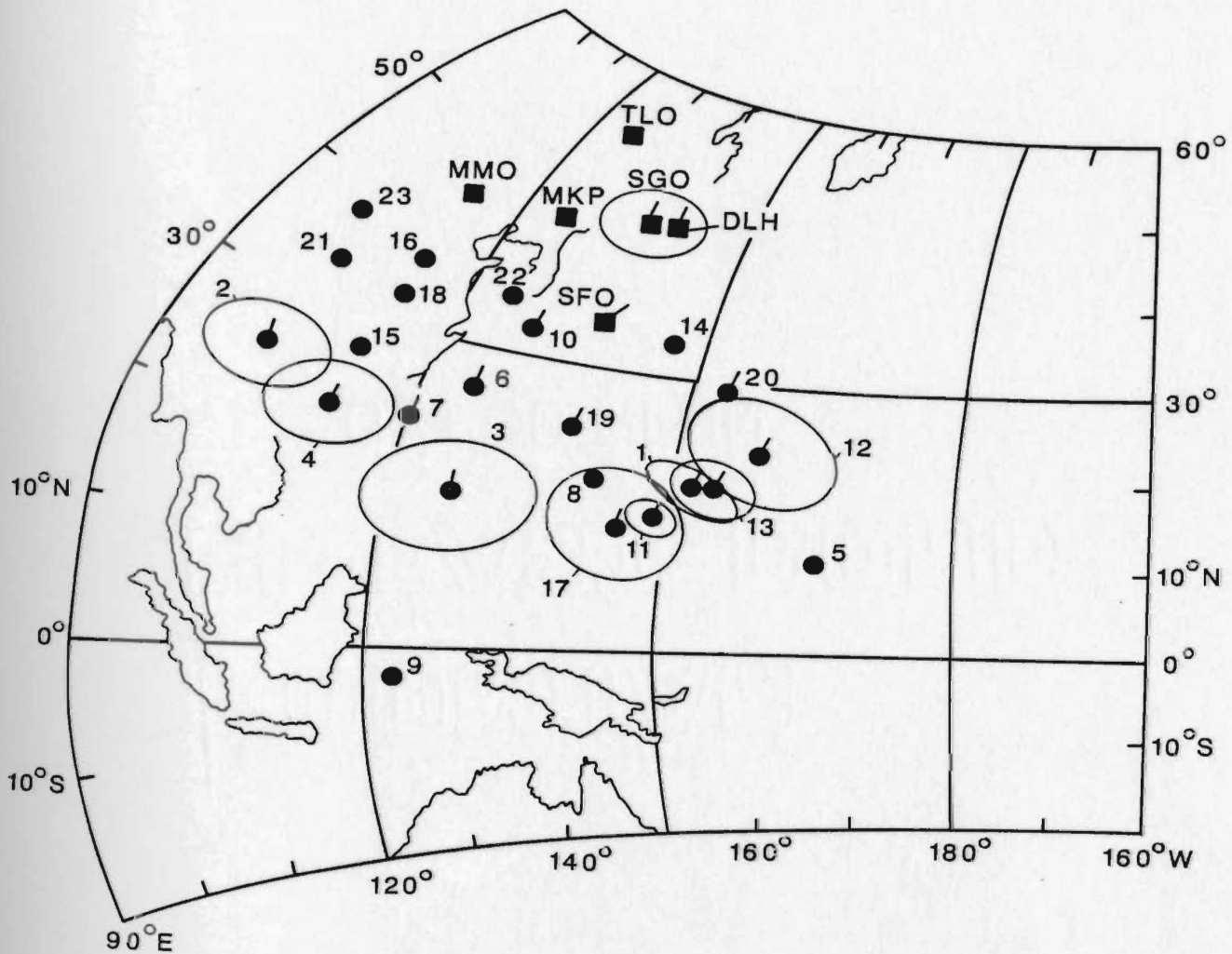


Fig. 9.1. Paleopoles from the Ordovician rocks of this study plotted with selected Ordovician and Late Paleozoic poles for cratonic North America (Tables 9.1, 4.2). Circles, poles cited as Ordovician; squares, poles cited as Kiaman (Late Carboniferous to Early Permian). Poles of this study are plotted with 95% confidence ovals. Symbols with bar, Newfoundland poles; without bar, mainland poles.

TABLE 9.1

SELECTED PALEOMAGNETIC POLE POSITIONS FROM ORDOVICIAN ROCKS OF NORTH AMERICA.

Pole No.	Rock unit and location'	Age	Pole Position	Reference
1	St. George Group, "A" component, Port au Port Peninsula, western Newfoundland	Lower Ordovician	17.5°N, 152.3°E	This study
2	Isthmus Bay Formation St. George Group, Port au Choix area, western Newfoundland	Lower Ordovician	24.5°N, 102.7°E	This study
3	Catoche Formation, St. George Group, Port au Choix area	Lower Ordovician	14.7°N, 127.3°E	This study
4	Aguathuna Formation, St. George Group, Port au Choix area	Lower Ordovician	20.7°N, 110.6°E	This study
5	Oneota Dolomite, upper Mississippi River Valley	Lower Ordovician	10.4°N, 166.4°E	Jackson and Van der Voo (1985)
6	St. George Group, western Newfoundland	Lower Ordovician	26°N, 126°E	Beales et al. (1974)

TABLE 9.1 (CONT'D)

Pole No.	Rock unit & location	Age	Pole Position	Reference
7	St. George Group, western Newfoundland	Lower Ordovician	22°N, 120°E	Deutsch & Rao (1977)
8	McClure Mountain alkali complex, Colorado	Cambro-Ordovician	18°N, 142°E	Lynnes and Van der Voo (1984)
9	Buckingham Volcanics	(497 Ma)	3°S, 123°E	Dankers and Lapointe (1981)
10	Moreton's Harbour basalt, central Newfoundland	Lower Ordovician	32°N, 130°E	Deutsch & Rao (1977)
11	Table Head Gp. (Table Point & Table Cove Formations), Port au Port Peninsula	Middle Ordovician	13.6°N, 148.9°E	This study
12	Table Head Group (Cape Cormorant Formation)	Middle Ordovician	19.5°N, 162.1°E	This study
13	Table Head Group (Table Point, Table Cove and Cape Cormorant Formations combined)	Middle Ordovician	15.9°N, 153.6°E	This study
14	Moccasin-Bays Formation, eastern Tennessee	Middle Ordovician	33°N, 146°E	Watts and Van der Voo (1979)

TABLE 9.1, (CONT'D)

Pole No.	Rock unit & Location	Age	Pole Position	Reference
15	Chapman Ridge Formation, eastern Tennessee	Middle Ordovician	27°N, 112°E	Watts and Van der Voo (1979)
16	Trenton Limestone, New York	Middle Ordovician	36°N, 114°E	McElhinny and Opdyke (1973)
17	Cow Head Group, western Newfoundland	Middle Ordovician	13.3°N, 145.8°E	This study
18	Juniata Formation, central Appalachians	Late Ordovician	32°N, 114°E	Van der Voo and French (1977)
19	Steel Mountain pluton, western Newfoundland	(450 Ma)	23°N, 139°E	Murthy and Rao (1976)
20	Long Point Formation, western Newfoundland	Late Ordovician	29°N, 154°E	Murthy (1983)
21	Richmond Group, Quebec	Late Ordovician	33°N, 105°E	Seguin and Michaud (1985)
22	Beemerville complex, New Jersey	Late Ordovician- Silurian	35°N, 126°E	Proko and Hargraves (1973)
23	Black Canyon diabases, southwestern Colorado	Cambro-Ordovician	37°N, 102°E	Larson et al. (1985)

NOTES: As in Table 4.1.

final result (Pole 6) is based on a remanence direction obtained at the 10 mT step. On the average, 64 to 87% of the intensity remained after treatment to 10 mT. Therefore, it is quite likely that unresolved magnetizations may be present in their data. Deutsch and Rao (1977) reported some paleomagnetic data from the Port au Port Peninsula (Pole 7) in connection with a test for possible tectonic rotation of Newfoundland. Based on AF demagnetization at 30 mT, they presented results very similar to that of Beales et al., (1974), so that the possibility of unresolved magnetizations also remains in Deutsch and Rao's data. Therefore the results from the St. George Group in the present study should be taken to supersede the earlier two results. Deutsch and Rao (1977), in addition, presented data (Pole 10) from the Moreton's Harbour basalts of Lower to mid-Ordovician age in central Newfoundland. This area is in the Dunnage Zone of the Newfoundland Appalachians and, though this is not a part of the craton, the rocks in question were interpreted to have originated as part of the North American margin. Deutsch and Rao mentioned that the rocks had undergone low-grade greenschist facies metamorphism. The conodont CAI values from the Lower Ordovician strata in the Dunnage Zone of Newfoundland are greater than 5 (Nowlan and Barnes, 1985), which indicates a burial temperature of 300°C or more (Epstein et al., 1977). Such a high temperature would theoretically reset any magnetization blocked at about

500°C over a time period of 100 m.y. (Pullaiah et al., 1975). According to Nowlan and Barnes (1985), thermal alteration of Lower Ordovician rocks in the Dunnage Zone was initiated during the Taconic orogeny and completed by the end of the Acadian orogeny. Therefore, a mid-Paleozoic thermal remagnetization of Moreton's Harbour basalts cannot be ruled out.

Murthy (1983) reported paleomagnetic data from the Late Ordovician strata of the Long Point Formation. There is some controversy whether these strata belong to the Late Ordovician Long Point Formation or the Early Silurian Clam Bank Formation. However, based on O'Brien's (1975) arguments for a late Mid-Ordovician age for that section of the Long Point, the paleomagnetic result (Pole 20) was taken as Late Ordovician. The remanence, which resides in hematite, was inferred to have a dual polarity after unfolding the strata, and the data passed a positive fold test on overturned beds. This pole is not very far from the Lower and Middle Ordovician poles from the Port au Port area of the present study (Poles 1, 11-13).

Lynnes and Van der Voo (1984) presented paleomagnetic data from the radiometrically dated Cambro-Ordovician McClure Mountain alkali complex, Colorado. Two widely different magnetizations were found. The trachyte dykes dated 495 Ma. yielded a pole position (Pole MMO, Figure 9.1) which was interpreted to be a Late Paleozoic overprint carried by hematite. The syenites and nepheline syenites

dated at 535 Ma. yielded a pole (Pole 8) which is close to some of the Cambrian poles of North America, as well as the Ordovician Port au Port poles of this study. Thus the age of magnetization is uncertain to some extent. However, because of the close proximity of Pole 8 to the Ordovician Poles 1 and 11-13, it is quite likely that the magnetization of the McClure Mountain syenites was acquired in Ordovician times.

A Lower Ordovician pole (Pole 5) was recently reported by Jackson and Van der Voo (1985) from the Oneota Dolomite of the Upper Mississippi River Valley, based on a presumed two-polarity pair of characteristic directions. However, the "normal" and "reversed" directions are not antiparallel. There is a downward bias in both, which was attributed to the presence of a drilling-induced component in the (resultant) magnetization. The "normal" and "reversed" directions were averaged, with the aim of annulling the effect of the downward bias. However, the mean direction quoted by Jackson and Van der Voo is based on the average of unequal numbers of samples in the two polarity sets. Therefore, there is some uncertainty associated with this pole position, which is significantly displaced from most of the presumably Ordovician poles, but is close to some reported Upper Cambrian poles.

Paleomagnetic data were reported from a diabase dyke (Pole 9) in southern Quebec by Dankers and Lapointe (1981). This pole is widely discrepant from other

Ordovician results. The authors have acknowledged structural uncertainties in the sampled area; also, discordant K-Ar ages obtained from the dyke at one place reported by them suggests that the age of magnetization might not be well constrained.

Watts and Van der Voo (1979) presented paleomagnetic data from the Middle Ordovician of the Valley and Ridge Province in Tennessee (Poles 14 and 15). A two-polarity magnetization residing in hematite was found in both the Moccasin and the Bays Formations and was shown to have been acquired before the Alleghenian folding. Pole 14 is the combined result for both these Formations. The characteristic magnetization of the Chapman Ridge Formation (Pole 15) also resides in hematite, but occurs as a single (normal) polarity which also antedates the Alleghenian folding. In these studies (Poles 14 and 15), the existence of positive fold tests and (in the case of Pole 14) of two polarities, lends some confidence to the inference that the magnetizations are original. However, these poles have also been criticized, e.g., by Gillett (1981), who suggested that burial remagnetization is possible in the case of both these units because of high (3-4) conodont CAI values. A related problem could be the timing of hematite acquisition (See discussion, Section 3.4). In fact, Watts and Van der Voo (1979) have proposed that the misalignment between the Chapman Ridge and Moccasin-Bays direction could be the result of hematite formation in the Late Ordovician to

Silurian, as the Chapman Ridge pole is close to reported Silurian poles.

Van der Voo and French (1977) presented paleomagnetic data from the Late Ordovician Juniata Formation (Pole 18) of the Appalachians. A two-polarity, high blocking-temperature characteristic magnetization residing in hematite was isolated which was shown to have been acquired before Alleghenian folding. They also isolated a pervasive overprint which was attributed to Kiaman age. The conodont CAI values in this area are 4-4.5 (Gillett, 1981), indicating maximum temperatures in the range 190-240°C (Epstein et al., 1977). This, together with the fact that the remanence is carried by hematite, warrants further study of the timing of remanence acquisition.

Paleomagnetic data from the Late Ordovician to Silurian Beemerville alkaline igneous complex (Pole 22) were reported by Proko and Hargraves (1973). The results are based on only AF demagnetization to 30 mT. The carriers of the highly scattered characteristic directions were attributed to both coarse-grained magnetite and fine-grained hematite. Rocks in this area are reported to have been deeply buried (CAI 5, Gillett 1982), making a partial to complete thermal remagnetization possible. The authors themselves point out that the large directional scatter and uncertainties in the magnetization age of these rocks detract from the value of their results.

Murthy and Rao (1976) studied the Precambrian Steel Mountain anorthosite of western Newfoundland (Pole 19), citing a K-Ar age of 450 Ma. (mid-Ordovician). This age was interpreted to be the result of overprinting during Taconic metamorphism. Murthy and Rao isolated a characteristic magnetization residing in hematite that is discordant with data from similar anorthosites elsewhere in North America having presumed Grenville magnetization ages. Therefore they suggested that the magnetization of the Steel Mountain rocks reflects their K-Ar age. Further study of these hematite-bearing rocks is needed to test this suggestion.

Paleomagnetic data from the Middle Ordovician Trenton limestones in New York (Pole 16) were reported by McElhinny and Opdyke (1973). A re-examination of these limestones by McCabe et al. (1984) yielded a different characteristic direction (Pole TLO, Table 4.2) which was interpreted to be a Kiaman magnetization. McCabe et al. concluded that the Trenton series was completely remagnetized in the Late Paleozoic. They showed that the earlier result of McElhinny and Opdyke (1973) can be explained as resulting from insufficient demagnetization. The quoted mean remanence direction of McElhinny and Opdyke was shown to be the resultant of the characteristic mean direction of McCabe et al. and the present earth's field direction. Ironically, a number of published Ordovician poles plot close to McElhinny and Opdyke's Trenton pole. This raises

the question of reliability of all those poles.

Recently, Seguin and Michaud (1985) reported paleomagnetic results (Pole 22) from the Late Ordovician Richmond Group sediments in Quebec. The characteristic magnetization, which resides in hematite, yields a pole position which is close to McElhinny and Opdyke's Trenton pole.

Another recent result was reported by Larson et al., (1985) from the Cambro-Ordovician diabases (Pole 23) in southwestern Colorado. This has already been discussed in Section 4.3.

From the above discussion it is very difficult to pinpoint reliable Ordovician poles. Like the Cambrian poles, the Ordovician poles have two clusters - one close to the Late Paleozoic poles ($\sim 120^{\circ}\text{E}$, at intermediate latitudes) and the other at $\sim 150^{\circ}\text{E}$ and low latitudes. The low-latitude cluster, unlike in the case of Cambrian poles, contains fewer poles than the high-latitude cluster. The series of poles (1 and 11-13) from Lower to Middle Ordovician rocks from Port au Port area in the present study fall in the low-latitude cluster and may be true representatives of the Lower to mid-Ordovician geomagnetic field of cratonic North America. A final verdict on the Ordovician field relative to the craton must, however, await results from more rock formations from widely distributed localities of the craton.

9.2 Rotation of Newfoundland

It is appropriate at this point to discuss the old problem of rotation of western Newfoundland in the light of new paleomagnetic data from this study. Different possible interpretations and inconsistencies associated with them are discussed below.

(1) A relative block rotation between Port au Port and Port au Choix areas may be inferred from the Lower Ordovician results, and this was briefly discussed in Chapter 5. The possibility of a relative rotation between the two sampling areas could not be adequately tested because of a possible secondary origin of magnetization of the Port au Choix rocks. If the Port au Choix magnetizations are primary, the following possibilities exist:

(a) Port au Choix rotated clockwise relative to Port au Port by 30° - 40° after being magnetized in a SE field as are the Port au Port rocks. However, such a rotation would have to be confined to a portion of the Northern Peninsula north of the Cow Head Peninsula, because of the SE magnetizations found also in the Cow Head rocks.

(b) Port au Port rotated anticlockwise relative to Port au Choix by 30° - 40° after acquiring magnetizations in a NS field, as did the Port au Choix rocks. Both interpretations (a) and (b), however, would be difficult to reconcile with the prominent occurrence of both NW-SE and

N-S magnetizations reported from mainland Ordovician rocks (Figure 9.1). A similar incongruity applies if the comparison is extended to Cambrian rocks (Figure 4.1).

(2) Western Newfoundland rotated 30-40° anticlockwise (see Chapter 1) after the Port au Port rocks acquired a magnetization in an original N-S field, but before the Port au Choix rocks acquired their (secondary) magnetization in a N-S field. This interpretation again would leave one to explain the occurrence of SE magnetizations in the mainland rocks.

The following interpretation seems more plausible. Western Newfoundland did not rotate significantly with respect to the mainland. The Port au Port rocks became magnetized in an original SE magnetic field and the Port au Choix rocks acquired their magnetization much later when apparent polar wandering had occurred. This interpretation would be consistent with the fact that both the N-S and NW-SE were observed also in the different studies of mainland. Then the implication is that, in the case of both the mainland and Newfoundland, the N-S magnetizations were most probably acquired later than the NW-SE magnetizations. A possible alternative is that the N-S remanence observed in some Ordovician and Cambrian mainland rocks was caused by a local clockwise rotation of the sampling area reorienting the original NW-SE declination to N-S. This would correspond to Interpretation 1(a) in the case of Newfoundland rocks.

Therefore, the hypothesis of rotation of Newfoundland relative to mainland North America does not seem to be supported by the paleomagnetic data.

CHAPTER 10

SUMMARY AND CONCLUSIONS

Nine formations ranging in age from Middle Cambrian to Middle Ordovician belonging to autochthonous strata and a section of the allochthonous strata of early Middle Ordovician age were sampled from the Humber Zone in western Newfoundland for paleomagnetic investigations. The objective was to extract stable magnetizations and identify various components of magnetization for comparison with published paleomagnetic data.

All the units sampled are carbonates which are very weakly magnetized. These weak magnetizations (mainly in the 1×10^{-4} to 3×10^{-3} A/m range) were nevertheless measurable by the cryogenic magnetometer. In most of the specimens, the remanence after demagnetization could be measured to the order of 1-2% of the NRM without any difficulty.

In this entire rock sequence a steep downward-directed viscous component was found to coexist with stable components. The viscous component in most cases could be erased by thermal demagnetization at low temperatures.

Middle to Late Cambrian rocks belonging to the Port au Port Group yielded two characteristic components, "A" and "B". The "A" component, which resides in magnetite gives a reverse pole at 3.4°N , 145.6°E in very good agreement with some reported Cambrian poles and is also close to some

Late Precambrian pole positions for cratonic North America. The "B" component, which most likely is carried by diagenetic hematite, is an overprint consistent with a number of reported Kiaman magnetization for North America. The pole position corresponding to the "B" component is of reverse polarity at 40.2°N , 135.6°E .

The magnetization history of the Lower Ordovician St. George Group is more complex. The Port au Choix area rocks give entirely different directions compared to the Port au Port rocks, as follows.

From the Port au Port area, two characteristic components of magnetization were isolated from the St. George Group, analogous to, but somewhat different in direction from, the Cambrian rocks. The magnetite-bearing "A" component has a reverse pole position at 17.5°N , 152.3°E and probably represents the Lower Ordovician geomagnetic field relative to western Newfoundland. The "B" component is interpreted to be a Kiaman overprint residing in hematite, with corresponding reverse pole position at 44.9°N , 138.2°E . This pole is very close to the "B" component pole isolated from the Cambrian rocks. The respective Lower Ordovician and Cambrian "A" poles differ by 15° , which suggests that there was moderate but significant apparent polar wandering between mid-Cambrian and Early Ordovician time relative to western Newfoundland.

No evidence of Kiaman overprinting was found in the

St. George Group of the Port au Choix area. Rocks in this area yielded stable magnetizations of normal polarity. The three Formation means within the Group were more dispersed than the corresponding means in the Port au Port rocks. The overall mean directions of the St. George Group for the two areas differ mainly in declination. Therefore a relative tectonic rotation between the two areas would be indicated from the paleomagnetic data, if the magnetizations at Port au Port and Port au Choix had been contemporaneous. However, the thermal history of the Port au Choix rocks indicates a probable thermoviscous remagnetization that may be related to the Acadian orogeny. The Port au Choix pole positions are close to some reported Late Ordovician to Early Carboniferous poles from Newfoundland and other parts of the craton. The difference between the remanence directions for Port au Port and Port au Choix could be attributed to apparent polar wandering occurring between the times the respective magnetizations were acquired.

The Middle Ordovician Table Head Group in the Port au Port area also showed the absence of any Kiaman overprint. A shallow southeasterly component of magnetization was isolated; corresponding to a pole position at 15.9°N , 153.6°E , which is not significantly different from the St. George "A" component pole. This suggests little apparent polar wandering, if any, between Lower and Middle Ordovician times.

The Cape Cormorant Formation within the Table Head Group gives relatively scattered directions compared to two other Formations, Table Point and Table Cove, which yield tightly grouped characteristic directions. The scatter in the Cape Cormorant rocks is apparently due to the presence of unresolved multicomponents and to the samples being inhomogeneously magnetized. From a minority of samples of these steeply inclined beds, a characteristic southeast component was isolated which, after structural correction, is coherent with other Formations of the Group. This suggests that the magnetization preceded the presumably Acadian folding. The pole position for the Table Head Group quoted above includes the Cape Cormorant characteristic directions.

The Table Head rocks of the Port au Choix area give a smeared distribution of stable directions, mainly along north-south. Due to overlapping stability spectra the superimposed components could not be separated. However, a distinct northerly component in a minority of samples is noticeable amidst the smeared directions, and might have paleomagnetic significance. A similarity in direction between this component and stable components isolated in the Port au Choix area from the St. George Group and a few samples of the Port au Port Group, strongly suggests that in all three above cases the magnetization is secondary and was acquired at about the same (post mid-Ordovician) time.

The late Middle Ordovician Long Point Group from the

Port au Port area mostly yielded unstable magnetizations. A minority of samples that did yield a stable component is of normal polarity. This is in contrast to all other (Cambrian-Ordovician) Formations in the Port au Port area which yielded magnetizations of reverse polarity. This indicates that a polarity change occurred at some time between the deposition of uppermost Table Head and lowermost Long Point rocks.

Middle Ordovician bedded rocks of the allochthonous Cow Head Group yield a magnetization preceding the Acadian (?) folding, residing in magnetite. The corresponding pole, of reverse polarity, is at 13.3°N , 145.8°E , which is close to the Lower and Middle Ordovician poles from the Port au Port Peninsula. This suggests that these rocks are either more or less in place or, if they were transported, their displacement did not involve complex motions including tectonic rotation.

The total absence of Late Paleozoic overprinting in the Middle Ordovician rocks, both in the autochthonous and allochthonous sequence, is noteworthy. The remagnetization, which resides in diagenetic hematite, seems to have selectively affected the Port au Port Group and preferentially the lower parts of the St. George Group on the Port au Port Peninsula.

The entire rock sequence in the Port au Choix area, unlike the rocks of the Port au Port area, shows the presence of magnetite only and the absence of any Kiaman

overprints in them. In this connection, it is noted that there are no Carboniferous cover rocks in the Port au Choix area. The Port au Port area, on the other hand, has Carboniferous strata unconformably overlying the Lower Paleozoic strata. There is evidence of oxidizing conditions related to subaerial exposure and groundwater movement during the Carboniferous in the Port au Port rocks (R. K. Stevens, personal communication). This may well be the reason for the pervasive hematization in some of the rock sequence in the Port au Port area and a lack of it in the Port au Choix area.

While a better picture of the Lower Paleozoic paleofield relative to western Newfoundland has emerged from this study, the results did not support the hypothesis of rotation of western Newfoundland relative to mainland North America. However, a local rotation of the Port au Choix area relative to Port au Port area cannot be ruled out from the Ordovician paleomagnetic data. Such a rotation could have taken place with respect to one of the several faults seen in the region.

Paleolatitudes inferred in this study show a large latitudinal displacement of western Newfoundland between Cambrian and Ordovician - from a latitude of about 40°S in the Middle to Late Cambrian to about 20°S in Lower to Middle Ordovician times. The paleolatitudes during Late Carboniferous to Early Permian times, as calculated from Kiaman overprints, are near-equatorial.

In conclusion, it is to be noted that the Lower Paleozoic rocks of western Newfoundland, by virtue of their almost continuous stratigraphic exposure and presence of stable magnetization in them, as revealed by this study, are well suited for unravelling the magnetic history of cratonic North America. There is ample scope for further paleomagnetic study in this region, based on rock exposures not included in this study.

REFERENCES

- Al-Khafaji, S.A., and Vincenz, S.A., 1971. Magnetization of the Cambrian Lamotte Formation in Missouri. *Geophys. J. R. Astron. Soc.*, 24, pp. 175-202.
- Beales, F.W., Carracedo, J.C. and Strangway, D.W., 1974. Paleomagnetism and the origin of Mississippi Valley-type ore deposits. *Can. J. Earth Sci.*, 11, pp. 211-223.
- Bergstrom, S.M., Riva, J., and Kay, M., 1974. Significance of conodonts, graptolites, and shelly faunas from the Ordovician of western and north-central Newfoundland. *Can. J. Earth Sci.*, 11, pp. 1625-1660.
- Black, R.F., 1964. Paleomagnetic support of the theory of rotation of the western part of the island of Newfoundland. *Nature*, 202, pp. 945-948.
- Collinson, D.W., 1983. *Methods in Rock Magnetism and Paleomagnetism*. Chapman and Hall, London, 503p.
- Creer, K.M., 1968. Paleozoic paleomagnetism. *Nature*, 219, pp. 246-250.
- Dankers, P., and Lapointe, P. 1981. Paleomagnetism of Lower Cambrian volcanics and a cross-cutting Cambro-Ordovician diabase dyke from Buckingham (Quebec). *Can. J. Earth Sci.*, 18, pp. 1174-1186.
- Deutsch, E.R., 1980. Magnetism of the mid-Ordovician Tramore volcanics, SE Ireland, and the question of a wide Proto-Atlantic Ocean. *J. Geomag. Geoelect.*, 32, pp. SIII 77-98.

- Deutsch, E.R., 1984. Mid-Ordovician paleomagnetism and the Proto Atlantic ocean in Ireland. In "Plate Reconstruction From Paleozoic Paleomagnetism" (Edited by R. Van der Voo, C.R. Scotese and N. Bonhommet). Geodynamics Series, 12, pp. 116-119.
- Deutsch, E.R. and Rao, K.V., 1977. New paleomagnetic evidence fails to support rotation of western Newfoundland. Nature, 266, pp. 314-318.
- Dewey, J.F., 1969. Evolution of the Appalachian/Caledonian orogen. Nature, 222, pp. 314-318.
- DeWit, M.J., 1972. The geology around Bear Cove, eastern White Bay, Newfoundland. Unpublished Ph.D. thesis, Cambridge University, Cambridge, England, 232p.
- Dunn, W.J. and Elmore, R.D., 1985. Paleomagnetic and petrographic investigation of the Taum Sauk Limestone, southeast Missouri. J. Geophys. Res., 90, pp. 11,469-11,483.
- Elmore, R.D., Dunn, W. and Peck, C., 1985. Absolute dating of dedolomitization by means of paleomagnetic techniques. Geology, 13, pp. 558-561.
- Elston, D.P. and Bressler, S.L., 1977. Paleomagnetic poles and polarity zonation from Cambrian and Devonian strata of Arizona. Earth Planet. Sci. Lett. 36, pp. 423-433.
- Epstein, A.G., Epstein, J.B. and Harris, L.D., 1977. Conodont color alteration - an index to organic metamorphism. U.S. Geol. Surv. Professional Paper 995, 27p.

- Fahraeus, L.E., 1973. Depositional environment of the Long Point Formation (Middle Ordovician), western Newfoundland. *Can. J. Earth Sci.*, 10, pp. 1822-1833.
- Fahraeus, L.E. and Nowlan, G.S., 1978. Franconian (Late Cambrian) to early Champlainian (Middle Ordovician) conodonts from the Cow Head Group, western Newfoundland. *J. Paleontol.*, 52, pp. 444-471.
- Fisher, R.A., (1953). Dispersion on a sphere. *Proc. Roy. Soc. London*, A217, pp. 295-305.
- Flower, R.H., 1978. St. George and Table Head cephalopod zonation in western Newfoundland. *Geol. Surv. Canada Paper 78-1A*: pp. 217-224.
- Frank, J.R., 1981. Dedolomitization in the Taum Sauk Limestone (Upper Cambrian), southeast Missouri: *J. Sediment. Petrology*, 51, pp. 7-18.
- French, R.B., Alexander, D.H. and Van der Voo, R., 1977. Paleomagnetism of Upper Precambrian to Lower Paleozoic intrusive rocks from Colorado. *Geol. Soc. Amer. Bull.*, 83, pp. 1785-1792.
- French, A.N. and Van der Voo, R., 1979. The magnetization of the Rose Hill Formation at the classical site of Graham's fold test. *J. Geophys. Res.*, 84, pp. 7688-7696.
- Gillett, S.L., 1981. Magnetization and remagnetization processes in some Early Paleozoic limestones from the Great Basin. Unpublished Ph.D. thesis, State University of New York at Stony Brook, N.Y., 500p.

Gillett, S.L., 1982. Paleomagnetism of the Late Cambrian Crepicephalus - Aphelaspis trilobite zone boundary in North America - divergent poles from isochronous strata. Earth Planet. Sci. Let., 58, pp. 383-394.

Gillett, S.L. and Van Alstine, D.R., 1979. Paleomagnetism of Lower and Middle Cambrian sedimentary rocks from the Desert Range, Nevada. J. Geophys. Res., 84, pp. 4475-4489.

Goree, W.S. and Fuller, M.D., 1976. Magnetometers using RF driven squids and their application in rock magnetism and paleomagnetism.

Rev. Geophys. Space Phys., 14, pp. 591-608.

Graham, J.W., 1949. The stability and significance of magnetism in sedimentary rocks. J. Geophys. Res., 54, pp. 131-168.

Harland, W.B., 1967. Early history of the North Atlantic ocean and its margins. Nature, 216, p. 464.

Hodych, J.P., Patzold, R.R. and Buchan, K.L., 1984.

Paleomagnetic dating of the transformation of oolitic goethite to hematite in iron ore. Can. J. Earth Sci., 21, no. 1, pp. 127-130.

Hodych, J.P., Patzold, R.R. and Buchan, K.L., 1985.

Chemical remanent magnetization due to deep-burial diagenesis in oolitic hematite-bearing ironstones of Alabama. Phys. Earth Planet. Interiors, 37, pp. 261-284.

Hubert, J.F., Suckecki, R.K. and Callahan, R.K.M., 1977.

The Cow Head breccia: sedimentology of the
Cambro-Ordovician continental margin, Newfoundland.
Society of Economic Paleontologists and Mineralogists,
Special Publication No. 25, pp. 125-154.

Irving, E., 1964. Paleomagnetism and its Application to
Geological and Geophysical Problems. Wiley, N.Y.,
399p.

Irving, E. and Irving, G.A., 1982. Apparent polar wander
paths, Carboniferous through Cenozoic and the assembly
of Gondwana. Geophys. Surv. 5, pp. 141-188.

Irving, E. and Strong, D.F., 1984a. Paleomagnetism of the
Early Carboniferous Deer Lake Group, western
Newfoundland: no evidence for mid-Carboniferous
displacement of "Acadia". Earth Planet. Sci. Lett.,
69, pp. 379-390.

Irving, E. and Strong, D.F., 1984b. Evidence against
large-scale Carboniferous strike-slip faulting in the
Appalachian-Caledonian orogen. Nature, 310, pp.
762-764.

Irving, E. and Strong, D.F., 1985. Paleomagnetism of rocks
from Burin Peninsula, Newfoundland: Hypothesis of
Late Paleozoic displacement of Acadia criticized. J.
Geophys. Res., 90, pp. 1949-1962.

Jackson, M. and Van der Voo, R., 1985. A Lower Ordovician
paleomagnetic pole from the Oneota Dolomite, Upper
Mississippi River Valley. J. Geophys. Res., 90, pp.
10,449-10,461.

- James, N.P., 1981. Megablocks of calcified algae in the Cow Head Group, western Newfoundland: vestiges of a Cambro-Ordovician platform margin. *Geol. Soc. Amer. Bull.*, 92, pp. 799-811.
- James, N.P. and Stevens, R.K., 1982. Anatomy and evolution of a Lower Paleozoic continental margin, western Newfoundland. *Field Excursion Guide Book of International Association of Sedimentologists, Eleventh International Congress on Sedimentology*, McMaster University, Hamilton, Ontario, 75p.
- James, N.P., Knight, I. and Chow, N., 1983. Middle and Upper Cambrian platform carbonates, western Newfoundland: Anatomy of a high-energy shelf. *Geol. Assoc. Canada, Newfoundland Section, 1983 Annual Spring Meeting (Abstract)*, St. John's.
- James, N.P. and Stevens, R.K., 1986. Stratigraphy and correlation of the Cow Head Group, (Cambro-Ordovician), western Newfoundland. *Geol. Surv. Canada Bull.*, 366 (In press).
- Kent, D.V., 1985. Thermoviscous remagnetization in some Appalachian limestones. *Geophys. Res. Lett.*, 12, No. 12, pp. 805-808.
- Kent, D.V. and Opdyke, N.D., 1978. Paleomagnetism of Devonian Catskill red beds: evidence for motion of coastal New England - Canadian Maritime region relative to cratonic North America. *J. Geophys. Res.*, 83, pp. 4441-4450.

Kindle, C.H. and Whittington, H.B., 1958. Stratigraphy of the Cow Head region, western Newfoundland. Geol. Soc. Amer. Bull., 69, pp. 315-342.

Klappa, C.F., Opalinski, P.R. and James, N.P., 1980. Middle Ordovician Table Head Group of western Newfoundland: a revised stratigraphy. Can. J. Earth Sci., 17, pp. 1007-1019.

Knight, I., 1977. Cambro-Ordovician platformal rocks of the Northern Peninsula, Newfoundland. Mineral Development Division, Dept. of Mines and Energy, Government of Newfoundland and Labrador Report 77-6, 27p.

Knight, I., (1980). Cambro-Ordovician carbonate stratigraphy of western Newfoundland; sedimentation, diagenesis and zinc-lead mineralization; Summary of a paper given at 82nd Can. Inst. Mines Metall. Annual General Meeting, Toronto, 34p.

Larochelle, A., 1967. A re-examination of certain statistical methods in paleomagnetism. Geol. Surv. Canada Paper, 67-18.

Larson, E.E. and Mutschler, F.E., 1971. Anomalous paleomagnetic pole from isotopically dated Cambro-Ordovician intrusives in Colorado. Geol. Soc. Amer. Bull., 82, pp. 1657-1666.

- Larson, E.E., Patterson, P.E., Curtis, G., Drake, R. and Mutschler, F.E., 1985. Petrologic, paleomagnetic, and structural evidence of a Paleozoic rift system in Oklahoma, New Mexico, Colorado and Utah. *Geol. Soc. Amer. Bull.*, 96, pp. 1364-1372.
- Levesque, R.J., 1977. Stratigraphy and sedimentology of Middle Cambrian to Lower Ordovician shallow water carbonate rocks, western Newfoundland. Unpublished M.Sc. thesis, Memorial University of Newfoundland, 276p.
- Levesque, R.J., James, N.P. and Stevens, R.K., 1977. Facies anatomy of Cambro-Ordovician shelf carbonates, Northern Maritime Appalachians: *Geol. Soc. Amer. Abst. with Programs*, 9, p. 293-294.
- Lochman-Balk, C., 1938. Middle and Upper Cambrian faunas from western Newfoundland. *J. Paleontol.*, 12, pp. 461-477.
- Lock, B.E., 1969. The Lower Paleozoic geology of western White Bay, Newfoundland. Unpublished Ph.D. Thesis, Cambridge University, England, 343p.
- Lock, B.E., 1972. Lower Paleozoic history of a critical area; eastern margin of the St. Lawrence platform in White Bay, Newfoundland, Canada. 24th International Geological Congress, Montreal, Section 6, pp. 310-324.
- Lowrie, W. and Heller, F., 1982. Magnetic properties of marine limestones. *Rev. Geophys. Space Phys.*, 20, pp. 171-192.

- Lynnes, C.S. and Van der Voo, R., 1984. Paleomagnetism of the Cambro-Ordovician McClure Mountain alkali complex, Colorado. *Earth Planet. Sci. Lett.*, 71, pp. 163-172.
- McCabe, C., Freeman, R., Peacor, D.R., Scotese, C.R. and Van der Voo, R., 1983. Diagenetic magnetite carries ancient yet secondary remanence in some Paleozoic sedimentary carbonates, *Geology*, 11, pp. 221-223.
- McCabe, C., Van der Voo, R. and Ballard, M.M.; 1984. Late Paleozoic remagnetization of the Trenton Limestone. *Geophys. Res. Lett.*, 11, pp. 979-982.
- McCabe, C., Van der Voo, R., Wilkinson, B.H. and Devaney, K., 1985. A Middle/Late Silurian paleomagnetic pole from limestone reefs of the Wabash Formation, Indiana. *J. Geophys. Res.*, 90, pp. 2959- 2965.
- McElhinny, M.W., 1973. *Paleomagnetism and Plate Tectonics*. Cambridge Univ. Press, London, 357p.
- McElhinny, M.W. and Opdyke, N.D., 1973. Remagnetization hypothesis discounted: A paleomagnetic study of the Trenton Limestone, New York State. *Geol. Soc. Amer. Bull.*, 84, pp. 3697-3708.
- McFadden, P.L. and Jones, D.L., 1981. The fold test in paleomagnetism. *Geophys. J.R. Astron. Society*, 67, pp. 53-58.
- McKerrow, W.S. and Ziegler, A.M., 1972. Paleozoic oceans. *Nature Phys. Sci.*, 240, pp. 92-94.
- Morel, P. and Irving, E., 1978. Tentative paleocontinental maps for the Early Phanerozoic and Proterozoic. *J. Geology*, 86, pp. 535-561.

- Murthy, G.S., 1971. The paleomagnetism of diabase dikes from the Grenville Province. *Can. J. Earth Sci.*, 8, pp. 802-812.
- Murthy, G.S., 1983. Paleomagnetism of the Uppermost member of the Long Point Formation, western Newfoundland. *Geol. Assoc. Canada, Newfoundland Section, 1983 Annual Spring Meeting (Abstract)*, St. John's.
- Murthy, G.S., 1985. Paleomagnetism of certain constituents of the Bay St. George sub-basin, western Newfoundland. *Phys. Earth Planet. Interiors*, 39, pp. 89-107.
- Murthy, G.S. and Rao, K.V., 1976. Paleomagnetism of Steel Mountain and Indian Head anorthosites from western Newfoundland. *Can. J. Earth Sci.*, 13, pp. 75-83.
- Nowlan, G.S., 1974. Conodonts from the Cow Head Group, western Newfoundland. Unpublished M.Sc. thesis, Memorial University of Newfoundland, 183p.
- Nowlan, G.S. and Barnes, C.R., 1985. Thermal maturation of Paleozoic strata in eastern Canada from conodont color alteration index (CAI) data with implications for burial history, tectonic evolution, hotspot tracks and mineral and hydrocarbon potential. *Geol. Surv. Canada Bull.*, 367 (In press).
- O'Brien, F.H.C., 1975. The stratigraphy and paleontology of the Clam Bank Formation, and the upper part of the Long Point Formation of the Port au Port Peninsula, on the west coast of Newfoundland. Unpublished M.Sc. thesis, Memorial University of Newfoundland, 156p.

- Palmer, H.C. and Hayatsu, A., 1975. Paleomagnetism and K-Ar dating of some Franklin lavas and diabases, Victoria Island. *Can. J. Earth Sci.*, 12, pp. 1439-1447.
- Pratt, B.R., 1979. The St. George Group (Lower Ordovician), western Newfoundland: Sedimentology, diagenesis and cryptalgal structures. Unpublished M.Sc. thesis, Memorial University of Newfoundland, 254p.
- Proko, M.S. and Hargraves, R.B., 1973. Paleomagnetism of the Beemerville (New Jersey) complex. *Geology*, 1, pp. 185-186.
- Pullaiah, G., Irving, E., Buchan, K.L. and Dunlop, D.J., 1975. Magnetization changes caused by burial and uplift. *Earth Planet. Sci. Lett.*, 28, pp. 133-143.
- Rao, K.V. and Deutsch, E.R., 1976. Paleomagnetism of the Lower Cambrian Bradore sandstones and the rotation of Newfoundland. *Tectonophysics*, 33, pp. 337-357.
- Robertson, W.A. and Baragar, W.R.A., 1972. The petrology and paleomagnetism of the Coronation Sills. *Can. J. Earth Sci.*, 9, pp. 123-140.
- Rodgers, J., 1965. Long Point and Clam Bank Formations, western Newfoundland. *Proc. Geol. Assoc. Canada*, 16, pp. 83-94.
- Rodgers, J. and Neale, E.R.W., 1963. Possible Taconic klippen in western Newfoundland, *Am. J. Science*, 261, pp. 713-730.

- Roy, J.L., Tanczyk, E. and Lapointe, P., 1983. The paleomagnetic record of the Appalachians. In "Regional Trends in the Geology of the Appalachian-Caledonian-Hercynian-Mauritanide Orogen". Edited by P.E. Schenk, D. Reidel Publishing Co., pp. 11-26.
- Schillereff, S. and Williams, H., 1979. Geology of the Stephenville map area, Newfoundland. In Current Research, Part A., Geol. Surv. Canada, Paper 79-1A, pp. 327-332.
- Schuchert, C. and Dunbar, C.D., 1934. Stratigraphy of Western Newfoundland. Geol. Soc. Amer. Memoir, 1, 123p.
- Scotese, C.R., Van der Voo, R. and McCabe, C., 1982.
- Paleomagnetism of the Upper Silurian and Lower Devonian carbonates of New York State: Evidence for secondary magnetizations residing in magnetite. Phys. Earth Planet. Interiors, 30, pp. 385-395.
- Seguin, M.K., 1976. Reconnaissance paleomagnetic investigation of the ophiolitic complex, Thetford Mines, Asbestos, Quebec. Tectonophysics, 34, pp. 231-243.
- Seguin, M.K., 1979. Paleomagnetism of the Thetford Mines ophiolites, Quebec. J. Geomag. Geoelect., 31, pp. 103-113.
- Seguin, M.K. and Michaud, C., 1985. The Becancour-Yamaska Area, Quebec: A paleomagnetic study. J. Geomag. Geoelect., 37, pp. 895-912.

- Sloss, L.L., 1963. Sequences in the cratonic interior of North America. Bull. Geol. Soc. Amer., 74, pp. 93-113.
- Stevens, R.K., 1970. Cambro-Ordovician flysch sedimentation and tectonics in west Newfoundland and their possible bearing on a proto-Atlantic ocean. Geol. Assoc. Canada, Special Paper No. 7, pp. 165-177.
- Stouge, S., 1981. Cambrian-Middle Ordovician stratigraphy of Salmon River region, southwest Hare Bay, Great Northern Peninsula. Mineral Development Division, Dept. of Mines and Energy, Govt. Newfoundland and Labrador Report 81-1, pp. 1-16.
- Tarling, D.H., 1983. Paleomagnetism. Chapman and Hall, London, 379p.
- Van der Voo, R., French, R.B. and Williams, D.W., 1976. Paleomagnetism of the Wilburns Formation and the Late Cambrian paleomagnetic field for North America. J. Geophys. Res., 81, pp. 5633-5638.
- Van der Voo, R. and French, R.B., 1977. Paleomagnetism of the Late Ordovician Juniata Formation and the remagnetization hypothesis. J. Geophys. Res., 82, pp. 5796-5802.
- Vincenz, S.A., Yaskawa, K. and Ade-Hall, J.M., 1975. Origin of the magnetization of the Wichita Mountain granites, Oklahoma. Geophys. J. R. Astron. Soc., 42, pp. 21-48.

- Watson, G.S., 1956.. Analysis of dispersion on a sphere.
Monthly Notices, R. Astron. Soc. Geophys. Suppl., 7,
pp. 153-159.
- Watts, D.R. and Van der Voo, R., 1979. Paleomagnetic
results from the Ordovician Moccasin, Bays, and
Chapman Ridge Formations of the Valley and Ridge
Province eastern Tennessee. J. Geophys. Res., 84, pp.
645-655.
- Watts, D.R., Van der Voo, R. and French, R.B., 1980a.
Paleomagnetic investigation of the Cambrian Waynesboro
and Rome Formations of the Valley and Ridge Province
of the Appalachian Mountains. J. Geophys. Res.; 85,
pp. 5331-5343.
- Watts, D.R., Van der Voo, R. and Reeve, S.C., 1980b.
Cambrian paleomagnetism of the Llano uplift, Texas.
J. Geophys. Res., 85, pp. 5316-5330.
- Wegener, A., 1929. The Origin of Continents and Oceans
(Translation). Dover Publications, New York, Transl.
1966.
- Whittington, H.B. and Kindle, C.H., 1969. Cambrian and
Ordovician stratigraphy of western Newfoundland. In
"North Atlantic Geology and Continental Drift", Edited
by M. Kay, Amer. Assoc. Petrol. Geologists, Memoir 12,
pp. 655-664.
- Williams, H., 1979. Appalachian orogen in Canada. Can. J.
Earth Sci., 16, pp.792-807.

- Williams, H., 1980. Structural telescoping across the Appalachian orogen and the minimum width of the Iapetus Ocean. In "The Continental Crust and its Mineral Deposits", Edited by D.W. Strangway. Geol. Assoc. Canada Special Paper 20, pp. 421-440.
- Williams, H. and Stevens, R.K., 1974. The ancient continental margin of eastern North America. In "The Geology of Continental Margins". Edited by C.A. Burk and C.L. Drake. Springer-Verlag, New York, N.Y., pp. 781-796.
- Williams, H., James, N.P. and Stevens, R.K., 1985. Humber Arm Allochthon and nearby groups between Bonne Bay and Portland Creek, western Newfoundland. Current Research, Part A, Geol. Surv. Canada Paper 85-1A, pp. 399-406.
- Wilson, J.T., 1966. Did the Atlantic close and then reopen? *Nature*, 211, pp. 676-681.
- Wisniowiecki, M.J., Van der Voo, R., McCabe, C. and Kelly, W.C., 1983. A Pennsylvanian paleomagnetic pole from the mineralized Late Cambrian Bonneterre Formation, southeast Missouri. *J. Geophys. Res.*, 88, pp. 6540-6548.
- Zijderveld, J.D.A., 1967. A.C. demagnetization of rocks: analysis of results. In "Methods in Paleomagnetism", Edited by D.W. Collinson, K.M. Creer and S.K. Runcorn, Elsevier, Amsterdam.

APPENDIX A

TECHNIQUES

A.1 Sample preparation

Oriented hand samples only were collected from the rock exposures discussed in the present study. The samples were oriented by means of a magnetic compass. Drill cores of 2.3-2.4 cm diameter were prepared in the laboratory and were cut into cylindrical specimens, typically 2.1 cm in height. Usually two to four specimens were prepared from each hand sample.

A.2 Remanence measurement

All remanence measurements of specimens were performed on a cryogenic magnetometer made by CTF Industries, Port Coquitlam, B.C. This is a two-axis device which measures the two orthogonal components - horizontal and vertical - of magnetic moment. The two detecting units (SQUID sensors and superconducting pick-up coils) require temperatures $\leq 30^{\circ}\text{K}$ for their operation and are surrounded by a superconducting magnetic shield. The shield and detecting assembly in turn are housed in a 30-litre, superinsulated (liquid nitrogen-free) Dewar flask containing liquid helium (boiling point -4.2°K). The entire unit is enclosed in a 3-layered μ -metal shield to produce a nearly field-free space inside. The residual internal field is "frozen" into the internal shield at the time it becomes superconducting;

actual residual field values in the space to be occupied by a rock specimen were observed to be of the order of 50 nT or less. The observed maximum noise level is of the order of $5 \times 10 \text{ Am}^2$, which is an order of magnitude less than the moment of the holder ($3 \text{ to } 5 \times 10^{-11} \text{ Am}^2$) used in all the measurements.

The measurement procedure involves rotating the specimen in successive 90° steps about a vertical axis between measurements and repeating the procedure with the specimen turned upside down. This yields 4 values each of the x- and y- components, and 8 values of the z-component. This output is transferred to an on-line computer which prints out the results in terms of declination, inclination and x, y, z components, and the resultant magnetic moment.

Because the NRM of carbonates in the present study is very weak ($\sim 10^{-8}$ to 10^{-10} Am^2 in moment), it can become an appreciable proportion of the total measured moment in the more weakly magnetic specimens. Therefore it was routinely subtracted from the resultant moment in each remanence measurement of a rock specimen. In order to detect any changes in holder moment due to contamination from rock particles, the moment was regularly remeasured, usually after 5 to 8 remanence determinations; the new holder moment value was then applied to the next set of measurements. If any significant increase in holder moment was observed, the holder was then cleaned in soap and warm water, the moment remeasured and the measurements were

continued as outlined above. The vectorial subtraction of the holder moment produced a significant change in the resultant direction only when the magnetization was reduced to a very low value as a result of demagnetizing specimens having a low NRM. In such cases, the reliability of the observed direction was checked by a repeated remanence measurement. In the case of most specimens giving a stable direction, correction for the holder moment either produced no change or a barely significant change ($< 3^\circ$) in the resultant direction.

A.3 Alternating field (AF) demagnetization

AF demagnetization was carried out using a Schonstedt GSD-1 demagnetizer. This is a single axis solenoid which can produce a peak alternating field of 100 mT. The residual field inside the center of the demagnetizing coil is 50 nT. The normal procedure is to demagnetize the NRM of the sample along three perpendicular directions in turn and then measure the corresponding components of residual magnetization with the magnetometer. Unless otherwise specified in the text, the following steps were chosen for the treatment: 5, 10, 15, 20, 25, 30, 40, 50, 60, 80 and 100 milliteslas (mT). A spurious component of magnetization was induced in a number of specimens at 60 mT and above in the AF demagnetizer. It is not known what caused this spurious magnetization, and the AF results from specimens where it was observed were not used.

A.4 Thermal demagnetization

Thermal demagnetization was done using a Schonstedt TSD-1 thermal demagnetizer. In this model, a magnetic field-free space in the specimen region is maintained by three layers of mu-metal shields surrounding the furnace and six layers of mu-metal shields surrounding the cooling chamber. The residual field inside the cooling chamber is less than 5 nT.

Generally the following temperature steps were chosen throughout this study for the treatment of at least one specimen from each site: 100°, 200°, 300°, 350°, 400°, 450°, 500°, 530°, 560°, 590°, and 680°C. While all the samples of the St. George and Table Head Groups from Port au Port Peninsula were treated according to the above schedule, a slightly modified schedule was adopted for the treatment of a majority of samples in the rest of the rock formations. This modification meant the exclusion of the 100° and 200°C steps and the inclusion of 250, 330, 370 and 420°C steps in the treatment schedule. This modified schedule was adopted only after the detailed demagnetizations of at least one specimen per site had been done. It was observed that the two lower temperature steps (100 and 200°C) led to the removal of only a steep viscous component. Also, the detailed initial results had shown that many specimens lost their entire magnetization in the range 300-400°C. Therefore closer temperature steps were inserted for treating the rest of

the specimens to test the stability of direction in that temperature range.

A.5 Statistical analysis

Throughout the present investigation, Fisher's (1953) statistical analysis was used. In this analysis each direction of magnetization is represented by a vector of unit length and there is no weighting as a function of the intensity of magnetization. It is assumed that these vectors, when regarded as points on a unit sphere, will be distributed with probability density $P(\theta)$, given by

$$P(\theta) = \frac{K}{4\pi \sinh k} \exp(K \cos \theta)$$

where θ is the angle between the direction of a sample and the mean direction of the population. The parameter K is called the precision parameter and determines the dispersion of points. If $K = 0$ they are uniformly distributed and the directions are random. When K is large, the points are confined to a small area of the sphere around the true mean direction and the distribution tends to conform to a two-dimensional Gaussian distribution. In such cases the precision parameter is in effect the invariance or the reciprocal of the variance in all directions.

For a sample of N points dispersed about a common centre, Fisher showed that the best estimate (l, m, n) of the position of this centre (the mean direction) is the

vector sum of the N individual directions (l_i, m_i, n_i), i.e.,

$$l = \frac{1}{R} \sum_i l_i, \quad m = \frac{1}{R} \sum_i m_i, \quad n = \frac{1}{R} \sum_i n_i$$

where (l, m, n) are the direction cosines of the mean direction and R is the vector sum of N vectors given by

$$R^2 = (\sum l_i)^2 + (\sum m_i)^2 + (\sum n_i)^2$$

where $i = 1, 2, \dots, N$.

In paleomagnetic studies the direction of magnetization of a rock sample is specified by the declination D , measured clockwise from true north, and the inclination I , measured positively downwards from the horizontal. This direction may be specified by its three direction cosines as follows:

$$\text{north component } (l) = \cos D \cos I$$

$$\text{east component } (m) = \sin D \cos I$$

$$\text{down component } (n) = \sin I$$

The declination, D_m and inclination, I_m , of the mean direction are given by

$$\tan D_m = \frac{\sum m_i}{\sum l_i}$$

and

$$\sin I_m = \frac{1}{R} \sum n_i$$

The best estimate k of the precision parameter is given, for $k > 3$, by

$$k = \frac{N-1}{N-R}$$

The accuracy of the mean direction obtained from N vectors with resultant R is expressed as the semi-angle of a cone about the observed mean within which the true mean lies with any given probability $(1-P)$: for $k > 3$

$$\cos \alpha_{(1-P)} = 1 - \frac{N-R}{R} \left[\left(\frac{1}{P} \right)^{\frac{1}{N-1}} - 1 \right]$$

P is normally taken to be 0.05. This means that there is a 95% probability that the observed mean is within α° of the true mean (the 'circle of confidence').

APPENDIX B

SAMPLING LOCALITIES AND DIRECTIONS OF MAGNETIZATION -
PORT AU PORT GROUP

B.1 Sampling localities

March Point Formation

Location: $48^{\circ} 30.5' N$, $59^{\circ} 7.9' W$ (Sites MP1-5).

The outcrop is on the south shore of the Port au Port Peninsula, 1 km west of the village of Degras. The beds are gently dipping north. Total stratigraphic thickness covered for the above five sites is ~ 30 meters.

Tilt correction:

Values of strike and dip of the bedding, as listed below, are required to make this correction. The convention followed is that the down-dip direction is 90° clockwise from the quoted strike direction. In the tilt correction, the beds containing the magnetization vector are restored to their presumed original horizontal position through a simple rotation about the strike by the amount of dip. In the listing below each pair of strike and dip values is based on a number of measurements taken on the bedding plane. The site names are the same as given in Figures 2.3-2.4.

<u>Sites</u>	<u>Strike,</u>	<u>Dip</u>	<u>Sites</u>	<u>Strike,</u>	<u>Dip</u>
MP1	263°	13°N	MP4	272°	11°N
MP2	261°	12°N	MP5	275°	10°N
MP3	273°	11°N			

Petit Jardin Formation:

Locations: 48° 31.1'N, 58° 51.8'W (Sites CC1-10)

50° 38.9'N, 57° 14.7'W (Sites PC23-24)

Sites CC1-10 (See Figure 2.3) were sampled from the outcrop at Campbells Cove on the south shore of the Port au Port Peninsula, about 3 km east of Picadilly Junction. The rocks are exposed on the shore to the west and east of the only creek to flow into the sea at this locality. Sites CC1-4 were sampled from the eastern side and CC5-10 from the western side of the creek. The stratigraphic thickness covered was 1 m and 16 m respectively. Sites PC 23-24 (See Figure 2.4) are in the Port au Choix area. The outcrop is in a quarry at the Port au Choix turn-off from the Viking trail, 4-5 km due east of Port Saunders. The samples were taken from the western side of the quarry. The stratigraphic thickness covered for the two sites is 2 m.

Tilt correction:

<u>Sites</u>	<u>Strike,</u>	<u>Dip</u>	<u>Sites</u>	<u>Strike,</u>	<u>Dip</u>
CC1	270°	14°N	CC4	272°	14°N
CC2	273°	15°N	CC5-10	249°	18°NW
CC3	277°	17°N	PC23-24	146°	7°SW

B.2 Detailed directions of magnetization

In the following pages, NRM directions at 20°C and the directions after each step of thermal demagnetization are given for those specimens from which a characteristic direction was obtained (Tables 3.1-3.2 and 3.4-3.5). Site names "March Point", "Camp Cove" in the following listing correspond to MP and CC sites respectively of the above discussion. The directions are given before correcting for the tilt. Where applicable in the tables below, "360°C" should be read "370°C".

APPENDIX B

DETAILED SPECIMEN DIRECTIONS

SITE: MARCH POINT-1 SPEC#: MP1-1

TEMP	DEC	INC	J(R/M)	J/JN
20	+157.8	+ 74.7	4.77E-4	01.00
100	+164.2	+ 55.7	3.39E-4	00.71
200	+165.8	+ 51.2	2.89E-4	00.50
300	+169.6	+ 45.3	2.23E-4	00.46
350	+169.1	+ 44.2	1.53E-4	00.32
400	+167.1	+ 39.7	8.98E-5	00.18
450	+160.9	+ 34.2	6.93E-5	00.14
500	+160.3	+ 40.5	5.59E-5	00.11
530	+146.0	+ 57.6	4.44E-5	00.09
560	+231.9	+ 71.2	2.62E-5	00.05
590	+ 43.6	+ 50.2	3.93E-5	00.08

SITE: MARCH POINT-1 SPEC#: MP2-A

20	+130.1	+ 84.2	2.94E-4	01.00
300	+164.9	+ 57.3	4.71E-5	00.16
350	+155.8	+ 70.0	3.25E-5	00.11
400	+264.8	+ 30.6	6.31E-6	00.02
450	+262.7	+ 46.7	1.73E-5	00.06
500	+227.8	- 13.6	2.24E-5	00.07

SITE: MARCH POINT-1 SPEC#: MP3-A

20	+358.8	+ 69.9	6.87E-4	01.00
300	+107.9	+ 56.0	4.71E-5	00.06
350	+105.1	+ 41.9	3.45E-5	00.05
400	+ 3.6	+ 48.8	1.34E-5	00.01
450	+ 34.6	+ 76.4	2.08E-5	00.03
500	+240.4	+ 22.8	1.57E-5	00.02

SITE: MARCH POINT-1 SPEC#: MP4-A

20	+154.0	+ 65.5	2.34E-4	01.00
300	+175.8	+ 17.6	7.43E-5	00.31
350	+185.9	+ 14.8	6.63E-5	00.28
400	+174.7	+ 17.1	2.64E-5	00.11
450	+178.3	+ 12.3	3.24E-5	00.13
500	+197.2	+ 19.0	2.25E-5	00.09

APPENDIX B

DETAILED SPECIMEN DIRECTIONS

SITE: MARCH POINT-1 SPEC#: MP5-A

TEMP	DEC	INC	J(A/M)	J/JN
20	+244.1	+ 79.0	2.56E-4	01.00
300	+300.5	+ 79.5	6.07E-5	00.23
350	+274.7	+ 73.6	4.56E-5	00.17
400	+303.7	+ 54.9	1.47E-5	00.05
450	+330.0	+ 38.2	8.39E-6	00.03
500	+259.5	+ 44.1	1.23E-5	00.04

SITE: MARCH POINT-2 SPEC#: MP6-B

20	+ 42.9	+ 84.4	6.23E-4	01.00
100	+147.4	+ 78.5	3.49E-4	00.56
200	+154.0	+ 73.9	2.61E-4	00.41
300	+154.6	+ 69.8	2.04E-4	00.32
350	+167.1	+ 80.1	1.30E-4	00.20
400	+130.6	+ 77.5	3.93E-5	00.06
450	+350.3	+ 84.1	2.99E-5	00.04
500	+235.2	+ 60.2	6.18E-6	00.00
530	+338.2	+ 63.4	8.52E-6	00.01
560	+315.2	+ 19.1	7.14E-6	00.01
590	+355.0	- 13.8	1.13E-5	00.01

SITE: MARCH POINT-2 SPEC#: MP7-B

20	+118.1	+ 89.2	2.74E-4	01.00
300	+194.7	+ 66.9	4.20E-5	00.15
350	+183.2	+ 51.0	2.89E-5	00.10
400	+203.5	+ 45.8	1.10E-5	00.04
450	+ 6.9	+ 74.3	1.96E-5	00.07
500	+ 7.8	- 30.2	2.94E-5	00.10

SITE: MARCH POINT-2 SPEC#: MP9-B

20	+181.9	+ 80.9	1.38E-4	01.00
300	+159.1	+ 58.0	1.87E-5	00.13
350	+125.9	+ 52.0	1.38E-5	00.09
400	+ 11.5	+ 58.4	4.50E-6	00.03
450	+189.6	+ 45.3	7.57E-6	00.05
500	+244.0	- 2.7	1.11E-5	00.08

APPENDIX B

DETAILED SPECIMEN DIRECTIONS

SITE: MARCH POINT-3 SPEC#: MP12-1

TEMP	DEC	INC	J(A/M)	J/JN
20	+131.6	+ 68.5	2.07E-4	01.00
300	+147.0	+ 38.8	3.57E-5	00.17
350	+145.2	+ 28.1	3.05E-5	00.14
400	+129.3	- 30.8	4.60E-6	00.02
450	+ 66.8	- 43.3	1.37E-5	00.06
500	+310.9	- 57.8	7.84E-5	00.37

SITE: MARCH POINT-3 SPEC#: MP13-1

20	+ 80.1	+ 65.6	2.59E-4	01.00
300	+131.8	+ 48.3	3.31E-5	00.12
350	+111.9	+ 49.3	2.62E-5	00.10
400	+335.5	+ 83.6	1.99E-5	00.07
450	+286.0	+ 16.0	1.95E-5	00.07
500	+285.4	- 20.5	7.36E-5	00.28

SITE: MARCH POINT-3 SPEC#: MP14-1

20	+112.6	+ 72.9	4.77E-4	01.00
300	+139.5	+ 50.5	1.11E-4	00.23
350	+148.5	+ 42.5	1.01E-4	00.21
400	+143.0	+ 41.2	5.06E-5	00.10
450	+125.8	+ 37.8	5.20E-5	00.10
500	+347.6	+ 3.1	2.68E-5	00.05

SITE: MARCH POINT-3 SPEC#: MP15-2

20	+ 25.3	+ 70.9	4.27E-4	01.00
300	+310.9	+ 87.8	5.81E-5	00.13
350	+279.3	+ 78.7	4.67E-5	00.10
400	+ 38.0	+ 57.1	3.23E-5	00.07
450	+ 8.7	+ 6.6	1.24E-5	00.02
500	+336.9	+ 46.6	2.68E-5	00.06

APPENDIX B

DETAILED SPECIMEN DIRECTIONS

SITE: MARCH POINT-4 SPEC#: MP16-1

TEMP	DEC	INC	J(R/M)	J/JN
20	+ 26.2	+ 62.4	2.03E-3	01.00
100	+ 17.5	+ 63.7	1.09E-3	00.53
200	+ 33.0	+ 43.6	3.67E-4	00.18
300	+ 39.1	+ 11.0	2.01E-4	00.09
350	+ 36.5	- 11.8	1.72E-4	00.09
400	+ 28.4	- 34.3	1.35E-4	00.06
450	+ 23.2	- 35.8	8.87E-5	00.04
500	+348.2	- 75.3	1.41E-4	00.06
530	+350.4	- 33.2	4.23E-5	00.02
560	+269.2	+ 29.8	1.27E-4	00.06
590	+ 11.1	+ 45.5	2.07E-4	00.10

SITE: MARCH POINT-4 SPEC#: MP19-A

20	+113.5	+ 68.8	1.02E-3	01.00
300	+152.8	+ 46.0	1.97E-4	00.19
350	+154.4	+ 41.4	1.52E-4	00.14
400	+143.3	+ 38.5	8.40E-5	00.08
450	+ 88.4	+ 55.6	2.16E-5	00.02
500	+342.1	+ 27.9	4.09E-5	00.03

SITE: MARCH POINT-4 SPEC#: MP20-1

20	+113.6	+ 73.1	7.80E-4	01.00
300	+ 90.8	+ 76.4	5.18E-5	00.06
350	+157.2	+ 50.0	5.01E-5	00.06
400	+113.2	+ 51.9	1.38E-5	00.01
450	+112.2	+ 75.8	5.42E-5	00.06
500	+331.9	+ 19.5	6.82E-5	00.03

SITE: MARCH POINT-5 SPEC#: MP21-B

20	+ 35.3	+ 76.4	5.96E-4	01.00
100	+ 2.2	+ 71.6	3.74E-4	00.62
200	+ 9.2	+ 74.2	2.01E-4	00.33
300	+ 11.3	+ 77.1	1.11E-4	00.18
350	+357.1	+ 80.5	5.74E-5	00.09
400	+279.2	+ 83.4	2.38E-5	00.03
450	+287.3	+ 47.5	2.37E-5	00.03
500	+279.6	- 21.1	1.85E-5	00.03
530	+236.5	+ 58.9	1.10E-4	00.18
560	+262.1	+ 42.6	5.98E-5	00.10
590	+318.2	- 4.3	1.63E-4	00.27

APPENDIX B

DETAILED SPECIMEN DIRECTIONS

SITE: MARCH POINT-5 SPEC#: MP22-2

TEMP	DEC	INC	J(A/M)	J/JN
20	+ 38.2	+ 73.6	3.04E-4	01.00
300	+ 17.5	+ 40.3	5.11E-5	00.16
330	+ 8.7	+ 34.7	3.16E-5	00.10
350	+ 10.4	+ 52.8	1.61E-5	00.05
400	+351.6	+ 40.6	1.21E-5	00.03
420	+349.3	+ 12.9	2.16E-5	00.07
450	+ 14.0	+ 41.5	1.07E-5	00.03

SITE: MARCH POINT-5 SPEC#: MP23-1

20	+ 33.8	+ 76.7	2.98E-4	01.00
300	+156.0	+ 55.4	5.81E-5	00.19
330	+166.9	+ 56.7	4.12E-5	00.13
350	+159.8	+ 53.6	3.63E-5	00.12
400	+191.0	+ 58.7	2.29E-5	00.07
420	+188.0	+ 81.8	1.03E-5	00.03
450	+330.9	+ 45.4	7.21E-5	00.24

SITE: MARCH POINT-5 SPEC#: MP25-2

20	+ 72.9	+ 74.5	2.71E-4	01.00
300	+ 26.8	+ 76.1	5.27E-5	00.19
330	+ 10.2	+ 78.0	4.44E-5	00.16
350	+ 45.4	+ 79.4	3.74E-5	00.13
400	+ 41.5	+ 41.9	1.80E-5	00.06
420	+358.9	+ 23.9	2.08E-5	00.07
450	+345.6	+ 52.0	5.46E-6	00.02

SITE: CAMP COVE-3 SPEC#: CC9-2

20	+356.3	+ 88.3	1.41E-4	01.00
100	+353.9	+ 82.4	6.93E-5	00.49
200	+341.6	+ 77.4	3.33E-5	00.23
300	+353.8	+ 60.6	2.11E-5	00.14
350	+330.0	+ 54.8	1.36E-5	00.09
400	+ 38.7	+ 62.0	1.10E-5	00.07
450	+350.5	+ 44.5	2.81E-5	00.19
500	+355.1	- 64.5	1.71E-4	01.21
530	+352.1	+ 7.1	1.03E-4	00.73
560	+ 30.7	- 41.6	8.06E-5	00.57

APPENDIX B

DETAILED SPECIMEN DIRECTIONS

SITE: CAMP COVE-4 SPEC#: CC16-A

TEMP	DEC	INC	J(R/M)	J/JN
20	+204.2	+ 78.0	2.42E-4	01.00
300	+188.6	+ 20.2	3.31E-5	00.13
330	+171.7	+ 1.5	3.00E-5	00.12
350	+192.6	- 10.7	2.65E-5	00.10
400	+181.2	- 2.1	3.28E-5	00.13
420	+193.1	- .3	1.13E-5	00.04
450	+170.1	- 12.0	1.61E-5	00.06

SITE: CAMP COVE-5 SPEC#: CC17-2

20	+ 29.9	+ 81.3	8.48E-4	01.00
100	+ 94.8	+ 83.2	4.88E-4	00.57
200	+112.4	+ 82.6	3.38E-4	00.39
300	+139.8	+ 82.3	1.62E-4	00.19
350	+158.7	+ 80.1	8.82E-5	00.10
400	+165.5	+ 67.0	3.29E-5	00.03
450	+175.4	+ 42.4	2.76E-5	00.03
500	+176.0	+ 54.3	1.78E-5	00.02
530	+291.3	- 79.1	2.01E-5	00.02
560	+266.1	+ 11.5	1.57E-5	00.01
590	+ 1.8	+ 13.9	6.80E-5	00.08

SITE: CAMP COVE-5 SPEC#: CC18-A

20	+320.0	+ 74.2	5.63E-4	01.00
300	+171.9	+ 23.1	5.58E-5	00.09
330	+178.1	+ 19.8	5.46E-5	00.09
350	+171.2	+ 20.7	4.13E-5	00.07
360	+171.8	+ 22.9	3.45E-5	00.06
400	+169.3	+ 25.5	3.02E-5	00.05
420	+175.2	+ 22.2	2.86E-5	00.05
450	+175.7	+ 24.0	2.66E-5	00.04
500	+203.2	+ 19.1	1.05E-5	00.01
530	+204.6	+ 29.4	1.33E-5	00.02
560	+346.3	- 50.7	8.51E-6	00.01
590	+358.8	+ 12.2	1.35E-5	00.02

APPENDIX B

DETAILED SPECIMEN DIRECTIONS

SITE: CAMP COVE-5 SPEC#: CC19-1

TEMP	DEC	INC	J(R/M)	J/JN
20	+162.0	+ 35.3	5.52E-4	01.00
300	+159.8	- 8.3	2.92E-4	00.52
330	+158.6	- 8.3	2.49E-4	00.45
350	+157.3	- 8.6	2.03E-4	00.36
360	+156.7	- 7.4	1.69E-4	00.30
400	+157.8	- 7.2	1.47E-4	00.26
420	+156.1	- 8.8	1.34E-4	00.24
450	+160.5	- 7.2	1.16E-4	00.20
500	+159.9	- 14.6	5.50E-5	00.09
530	+144.4	+ 5.6	4.00E-5	00.07
560	+138.5	- 31.9	2.37E-5	00.04
590	+ 60.5	- 63.2	2.12E-5	00.03

SITE: CAMP COVE-5 SPEC#: CC20-B

20	+177.4	+ 34.5	1.18E-3	01.00
300	+178.9	- 3.7	7.79E-4	00.66
330	+178.1	- 2.5	6.60E-4	00.55
350	+178.2	- 1.3	5.36E-4	00.45
360	+177.5	+ .7	4.46E-4	00.37
400	+178.2	+ 2.6	3.63E-4	00.30
420	+177.5	+ 2.3	3.64E-4	00.30
450	+176.6	+ 5.1	3.09E-4	00.26
500	+178.5	+ 15.3	1.86E-4	00.15
530	+196.3	+ 30.6	1.53E-4	00.12
560	+189.1	+ 37.3	9.36E-5	00.07
590	+184.9	+ 53.6	6.15E-5	00.05

SITE: CAMP COVE-5 SPEC#: CC21-A

20	+306.8	+ 78.0	8.48E-4	01.00
300	+176.6	+ 20.1	1.03E-4	00.12
330	+175.5	+ 15.1	8.25E-5	00.09
350	+180.9	+ 14.3	7.58E-5	00.08
360	+175.7	+ 22.5	5.13E-5	00.06
400	+166.2	+ 20.2	4.41E-5	00.05
420	+170.9	+ 20.3	4.84E-5	00.05
450	+178.5	+ 24.1	4.61E-5	00.05
500	+174.3	+ 39.9	2.24E-5	00.02
530	+177.7	+ 82.6	1.52E-5	00.01
560	+321.9	+ 43.3	2.11E-5	00.02
590	+ 36.4	+ 26.3	2.14E-5	00.02

APPENDIX B

DETAILED SPECIMEN DIRECTIONS

SITE: CAMP COVE-6 SPEC#: CC22-2

TEMP	DEC	INC	J(K/M)	J/JN
20	+ 49.4	+ 79.5	9.31E-4	01.00
100	+ 91.2	+ 74.6	5.44E-4	00.58
200	+107.9	+ 72.6	4.17E-4	00.44
300	+116.1	+ 70.8	2.44E-4	00.26
350	+129.0	+ 69.9	1.25E-4	00.13
400	+145.0	+ 60.9	5.06E-5	00.05
450	+144.8	+ 67.0	3.79E-5	00.04
500	+141.4	+ 47.2	2.19E-5	00.02
530	+340.6	- 48.9	2.51E-5	00.02
560	+321.7	- 56.4	1.51E-5	00.01
590	+355.3	+ 11.6	2.67E-5	00.02

SITE: CAMP COVE-6 SPEC#: CC23-1

20	+161.7	+ 45.3	4.02E-4	01.00
300	+171.1	- 9.0	2.21E-4	00.54
330	+170.7	- 7.8	1.85E-4	00.46
350	+172.0	- 10.6	1.59E-4	00.39
360	+170.6	- 9.0	1.23E-4	00.30
400	+172.7	- 9.0	1.02E-4	00.25
420	+173.3	- 11.1	9.74E-5	00.24
450	+172.0	- 9.3	8.43E-5	00.20
500	+173.2	- 6.9	5.27E-5	00.13
530	+151.9	- 5.7	2.47E-5	00.06
560	+204.4	- 14.2	1.33E-5	00.03
590	+ 1.0	+ 36.9	1.05E-5	00.02

SITE: CAMP COVE-6 SPEC#: CC24-2

20	+130.4	+ 80.1	2.00E-4	01.00
300	+125.2	+ 68.5	3.17E-5	00.15
330	+106.5	+ 58.1	2.30E-5	00.11
350	+105.7	+ 58.2	1.72E-5	00.08
360	+153.8	+ 43.6	1.12E-5	00.05
400	+147.0	+ 51.7	7.92E-6	00.03
420	+145.9	+ 59.7	5.33E-6	00.02
450	+145.4	+ 48.5	4.36E-6	00.02
500	+117.4	+ 53.4	3.91E-6	00.01

APPENDIX B

DETAILED SPECIMEN DIRECTIONS

SITE: CAMP COVE-6 SPEC#: CC25-A

TEMP	DEC	INC	J(A/M)	J/JN
20	+105.4	+ 83.6	2.11E-4	01.00
300	+124.3	+ 70.9	2.53E-5	00.12
330	+127.8	+ 50.7	2.19E-5	00.10
350	+130.3	+ 49.2	1.39E-5	00.06
360	+181.3	+ 35.7	9.31E-6	00.04
400	+276.7	+ 73.5	1.05E-5	00.04
420	+183.0	+ 22.5	9.33E-6	00.04
450	+265.3	+ 65.3	6.76E-6	00.03
500	+253.2	+ 69.9	8.12E-6	00.03

SITE: CAMP COVE-6 SPEC#: CC26-B

20	+162.4	+ 23.5	3.93E-4	01.00
300	+168.5	- 8.9	1.84E-4	00.46
330	+167.6	- 9.8	1.46E-4	00.37
350	+166.4	- 8.3	1.28E-4	00.32
360	+166.9	- 8.6	8.90E-5	00.22
400	+164.1	- 9.7	7.56E-5	00.19
420	+164.1	- 9.6	7.05E-5	00.17
450	+163.2	- 6.8	5.35E-5	00.13
500	+164.1	- 10.6	3.98E-5	00.10
530	+ 90.9	+ 30.5	1.37E-5	00.03
560	+119.7	- 60.7	8.03E-6	00.02
590	+ 10.7	+ 21.0	5.25E-5	00.13

SITE: CAMP COVE-7 SPEC#: CC27-B

20	+ 21.7	+ 66.6	9.83E-4	01.00
100	+ 19.0	+ 66.1	7.20E-4	00.73
200	+ 20.3	+ 68.6	5.21E-4	00.52
300	+ 19.7	+ 71.6	3.01E-4	00.30
350	+ 20.3	+ 81.2	1.33E-4	00.13
400	+111.1	+ 85.5	4.83E-5	00.04
450	+ 59.6	+ 87.9	2.56E-5	00.02
500	+ 14.4	+ 74.8	2.03E-5	00.02
530	+345.3	+ 62.3	9.13E-6	00.00
560	+300.2	+ 6.1	1.04E-5	00.01
590	+339.2	+ 15.4	1.41E-5	00.01

APPENDIX B

DETAILED SPECIMEN DIRECTIONS

SITE: CAMP COVE-7 SPEC#: CC29-1

TEMP	DEC	INC	J(A/M)	J/JN
20	+152.4	+ 82.2	1.31E-4	01.00
300	+140.7	+ 58.4	2.40E-5	00.18
330	+135.2	+ 60.8	2.18E-5	00.16
350	+158.4	+ 54.1	1.72E-5	00.13
360	+162.7	+ 34.0	1.35E-5	00.10
400	+157.8	+ 29.7	6.99E-6	00.05
420	+125.7	+ 48.9	4.43E-6	00.03
450	+146.6	+ 52.3	6.35E-6	00.04
500	+331.6	- 42.3	1.27E-5	00.09
530	+346.4	+ 2.6	2.17E-5	00.16

SITE: CAMP COVE-7 SPEC#: CC30-A

20	+276.3	+ 84.5	7.69E-4	01.00
300	+164.8	- .6	1.39E-4	00.18
330	+160.7	- 1.8	1.22E-4	00.15
350	+167.5	- 2.1	1.10E-4	00.14
360	+163.0	+ .5	9.30E-5	00.12
400	+161.4	+ .3	7.29E-5	00.09
420	+162.5	- 1.0	6.37E-5	00.08
450	+166.7	+ 1.6	6.44E-5	00.08
500	+174.7	+ 12.3	3.39E-5	00.04
530	+164.6	+ 15.4	3.58E-5	00.04
560	+176.2	+ 39.3	2.46E-5	00.03
590	+170.2	+ 72.3	1.59E-5	00.02

SITE: CAMP COVE-7 SPEC#: CC31-B

20	+125.2	+ 73.9	2.31E-4	01.00
300	+165.1	+ 18.9	6.10E-5	00.26
330	+164.5	+ 22.5	6.01E-5	00.26
350	+167.7	+ 24.7	4.91E-5	00.21
360	+170.1	+ 15.0	4.81E-5	00.20
400	+157.5	+ 23.5	3.48E-5	00.15
420	+150.4	+ 16.8	2.44E-5	00.10
450	+137.8	+ 15.9	2.50E-5	00.11
500	+199.9	- 1.6	1.08E-5	00.04
530	+193.3	+ 28.2	9.31E-6	00.04
560	+301.9	- 48.9	4.06E-5	00.17
590	+328.9	- 69.3	7.91E-5	00.34

APPENDIX B

DETAILED SPECIMEN DIRECTIONS

SITE: CAMP COVE-8 SPEC#: CC32-B

TEMP	DEC	INC	J(A/M)	J/JN
20	+136.2	+ 79.2	7.97E-4	01.00
100	+155.6	+ 54.7	4.87E-4	00.51
200	+160.0	+ 39.4	4.10E-4	00.51
300	+161.2	+ 22.2	3.26E-4	00.40
350	+160.1	+ 5.7	2.55E-4	00.31
400	+163.5	- 4.4	2.38E-4	00.29
450	+161.2	- 6.0	1.65E-4	00.20
500	+161.7	- 4.1	9.92E-5	00.12
530	+156.2	+ 22.9	3.12E-5	00.03
560	+149.0	+ 14.1	1.66E-5	00.02
590	+ 85.0	+ 18.3	1.60E-5	00.02

6

SITE: CAMP COVE-8 SPEC#: CC33-A

20	+128.2	+ 86.2	6.80E-4	01.00
300	+135.9	+ 45.0	1.09E-4	00.16
330	+138.8	+ 37.8	9.46E-5	00.13
350	+144.5	+ 30.0	8.15E-5	00.11
360	+136.1	+ 33.1	4.05E-5	00.05
400	+139.0	+ 29.1	3.41E-5	00.05
420	+138.5	+ 33.0	3.46E-5	00.05
450	+139.7	+ 27.5	3.29E-5	00.04
500	+102.8	+ 15.4	1.42E-5	00.02
530	+ 95.2	+ 45.8	1.73E-5	00.02
560	+ 51.0	+ 37.1	4.12E-5	00.06
590	+ 19.6	+ 31.8	3.38E-5	00.04

SITE: CAMP COVE-8 SPEC#: CC34-A

20	+157.8	+ 63.2	7.99E-4	01.00
300	+166.6	- 2.1	4.78E-4	00.59
330	+168.6	- 3.3	4.43E-4	00.55
350	+171.9	- 4.0	4.16E-4	00.52
360	+172.3	- 4.7	3.71E-4	00.46
400	+171.6	- 4.1	2.51E-4	00.31
420	+171.3	- 4.7	2.31E-4	00.28
450	+170.1	- 3.3	2.27E-4	00.28
500	+169.7	- 12.4	1.71E-4	00.21
530	+160.1	- 6.3	1.06E-4	00.13
560	+139.6	- 27.0	5.31E-5	00.06
590	+120.3	+ 35.5	6.07E-5	00.07

APPENDIX B

DETAILED SPECIMEN DIRECTIONS

SITE: CAMP COVE-8 SPEC#: CC35-A

TEMP	DEC	INC	J(A/M)	J/JN
20	+164.1	+ 47.8	2.91E-3	01.00
300	+164.5	- 9.5	2.11E-3	00.72
330	+162.9	- 9.2	1.79E-3	00.61
350	+163.5	- 9.1	1.69E-3	00.59
360	+162.5	- 8.7	1.40E-3	00.47
400	+164.3	- 7.8	9.00E-4	00.31
420	+162.5	- 7.2	8.39E-4	00.28
450	+162.6	- 6.9	8.48E-4	00.29
500	+164.8	- 6.4	6.07E-4	00.20
530	+161.9	- 6.2	4.79E-4	00.16
560	+155.1	- 7.6	1.44E-4	00.04
590	+150.6	- 5.8	7.21E-5	00.02

SITE: CAMP COVE-9 SPEC#: CC37-A

20	+192.2	+ 84.3	9.79E-4	01.00
100	+183.2	+ 71.3	5.55E-4	00.56
200	+182.2	+ 63.3	3.72E-4	00.37
300	+178.7	+ 55.2	1.79E-4	00.18
350	+171.7	+ 39.5	7.98E-5	00.08
400	+164.1	+ 19.5	4.85E-5	00.04
450	+155.0	+ 41.4	2.48E-5	00.02
500	+227.6	+ 27.3	6.59E-6	00.00
530	+318.3	- 72.9	1.13E-5	00.01
560	+270.2	- 58.0	2.42E-5	00.02
590	+334.9	- 20.4	3.67E-5	00.03

SITE: CAMP COVE-9 SPEC#: CC38-1

20	+341.5	+ 79.2	3.70E-3	01.00
300	+172.6	+ 7.9	5.72E-4	00.15
330	+171.3	+ 8.8	4.89E-4	00.13
350	+171.6	+ 9.1	4.96E-4	00.13
360	+168.6	+ 10.2	4.40E-4	00.11
400	+170.6	+ 13.7	3.62E-4	00.09
420	+173.0	+ 15.7	3.33E-4	00.08
450	+171.5	+ 14.4	3.35E-4	00.09
500	+172.4	+ 17.5	2.99E-4	00.08
530	+168.5	+ 20.8	2.52E-4	00.06
560	+167.8	+ 26.4	1.52E-4	00.04
590	+138.1	+ 15.1	9.86E-5	00.02

APPENDIX B

DETAILED SPECIMEN DIRECTIONS

SITE: CAMP COVE-9 SPEC#: CC39-A

TEMP	DEC	INC	J(A/M)	J/JN
20	+ 87.4	+ 74.3	3.75E-4	01.00
300	+161.2	+ 6.9	6.37E-5	00.16
330	+156.1	+ 1.5	4.40E-5	00.11
350	+165.5	+ 2.0	4.99E-5	00.13
360	+159.4	+ 3.9	3.71E-5	00.09
400	+165.6	- 8.0	2.66E-5	00.07
420	+164.9	+ 5.3	2.43E-5	00.06
450	+171.7	- 13.3	1.43E-5	00.03
500	+218.7	- 85.5	6.72E-6	00.01
530	+321.5	- 10.7	1.31E-5	00.03

SITE: CAMP COVE-9 SPEC#: CC40-1

20	+168.8	+ 33.4	4.40E-4	01.00
300	+167.0	- 16.8	2.89E-4	00.65
330	+167.6	- 18.0	2.31E-4	00.52
350	+168.6	- 16.3	2.09E-4	00.47
360	+168.8	- 16.9	1.97E-4	00.44
400	+169.1	- 16.8	1.64E-4	00.37
420	+168.3	- 16.0	1.51E-4	00.34
450	+169.3	- 16.8	1.06E-4	00.24
500	+160.0	- 9.2	5.44E-5	00.12
530	+145.9	- 7.7	2.40E-5	00.05
560	+273.1	- 58.9	3.65E-5	00.03

SITE: CAMP COVE-9 SPEC#: CC41-A

20	+ 24.3	+ 71.7	2.75E-4	01.00
300	+178.3	+ 58.6	3.16E-5	00.11
330	+206.8	+ 54.4	2.58E-5	00.09
350	+170.2	+ 31.7	2.63E-5	00.09
360	+178.3	+ 39.0	2.11E-5	00.07
400	+184.5	+ 31.3	1.77E-5	00.06
420	+180.5	+ 36.8	1.82E-5	00.06
450	+181.5	+ 47.5	1.18E-5	00.04
500	+318.5	+ 78.3	1.07E-5	00.03
530	+248.4	- 51.3	6.15E-6	00.02

APPENDIX B

DETAILED SPECIMEN DIRECTIONS

SITE: CAMP COVE-10 SPEC#: CC42-R

TEMP	DEC	INC	J(R/M)	J(JN)
20	+194.0	+ 74.1	1.09E-3	01.00
100	+199.0	+ 31.0	7.63E-4	00.70
200	+185.1	+ 17.8	6.88E-4	00.63
300	+192.3	+ 12.5	5.19E-4	00.47
350	+175.5	+ 8.3	3.58E-4	00.32
400	+177.9	+ 3.7	3.25E-4	00.29
450	+176.6	+ 10.0	2.29E-4	00.21
500	+191.2	+ 12.5	1.97E-4	00.17
530	+181.2	+ 20.5	1.20E-4	00.11
560	+196.9	+ 16.3	9.95E-5	00.09
590	+207.9	+ 26.9	6.11E-5	00.05

SITE: CAMP COVE-10 SPEC#: CC43-R

20	+172.0	+ 21.7	1.06E-3	01.00
300	+177.5	- 5.2	7.59E-4	00.71
330	+176.1	- 6.3	7.22E-4	00.68
350	+176.2	- 6.0	6.53E-4	00.61
360	+177.1	- 5.7	6.17E-4	00.58
400	+177.0	- 5.7	5.60E-4	00.52
420	+175.6	- 5.2	5.03E-4	00.47
450	+175.6	- 4.7	4.41E-4	00.41
500	+175.0	+ 3.7	2.35E-4	00.22
530	+174.3	+ 7.1	1.93E-4	00.17
560	+185.3	+ 41.3	5.66E-5	00.05
590	+320.3	+ 36.7	7.62E-5	00.07

SITE: CAMP COVE-10 SPEC#: CC44-1

20	+154.1	+ 29.8	1.07E-3	01.00
300	+154.4	- 12.8	6.73E-4	00.62
330	+155.4	- 12.6	6.53E-4	00.61
350	+155.1	- 12.2	6.27E-4	00.58
360	+157.0	- 12.6	5.75E-4	00.53
400	+154.6	- 11.7	5.27E-4	00.49
420	+155.0	- 11.5	4.52E-4	00.42
450	+155.8	- 11.9	4.13E-4	00.38
500	+154.5	- 6.8	2.49E-4	00.23
530	+153.7	- 6.5	2.14E-4	00.20
560	+151.9	- 6.5	1.09E-4	00.10
590	+178.9	- 6.4	2.64E-5	00.02

APPENDIX B

DETAILED SPECIMEN DIRECTIONS

SITE: CAMP COVE-10 SPEC#: CC45-A

TEMP	DEC	INC	J(R/M)	J/JN
20	+353.5	+ 79.4	1.47E-3	01.00
300	+158.8	+ .6	1.99E-4	00.13
330	+159.5	+ 1.3	1.88E-4	00.12
350	+152.0	+ 1.7	1.88E-4	00.12
360	+161.7	+ 2.8	1.62E-4	00.11
400	+158.8	+ 1.1	1.47E-4	00.09
420	+159.4	+ 3.2	1.25E-4	00.08
450	+157.9	+ 2.7	1.22E-4	00.08
500	+153.5	+ 12.3	7.08E-5	00.04
530	+152.4	+ 4.0	6.21E-5	00.04
560	+158.7	- 2.8	4.68E-5	00.03
590	+ 12.0	+ 1.0	6.39E-5	00.04

SITE: CAMP COVE-10 SPEC#: CC46-1

20	+105.7	+ 85.7	5.03E-4	01.00
300	+169.2	- 2.5	1.13E-4	00.22
330	+172.7	- 5.2	1.05E-4	00.21
350	+163.2	- 4.3	1.23E-4	00.24
360	+165.5	- 7.1	1.01E-4	00.20
400	+166.3	- 4.2	8.53E-5	00.16
420	+168.4	- 4.4	7.79E-5	00.15
450	+168.4	- 3.8	5.85E-5	00.11
500	+179.4	+ 1.1	4.30E-5	00.08
530	+179.0	+ 6.5	4.07E-5	00.08
560	+182.3	- 11.3	2.09E-5	00.04
590	+313.7	- 13.6	5.31E-5	00.10

SITE: PC-23 SPEC#: PC 111-A

20	+ 30.8	+ 57.3	2.52E-3	01.00
100	+ 9.9	+ 61.2	1.74E-3	00.69
200	+355.4	+ 36.3	3.13E-4	00.12
250	+ .6	- 7.8	1.76E-4	00.06
300	+ 3.2	- 23.1	1.47E-4	00.05
330	+ 8.3	- 24.6	1.38E-4	00.05
350	+ 1.2	- 34.0	1.22E-4	00.04
360	+ 5.3	- 36.7	1.27E-4	00.05
400	+359.8	- 39.7	1.05E-4	00.04
420	+ .8	- 36.4	8.69E-5	00.03
450	+ .4	- 46.8	4.18E-5	00.01
500	+328.4	+ 27.9	1.67E-5	00.00

APPENDIX B

DETAILED SPECIMEN DIRECTIONS

SITE: PC-23 SPEC#: PC 112-A

TEMP	DEC	INC	J(R/M)	J/JN
20	+ 56.9	+ 61.0	3.30E-3	01.00
100	+ 39.8	+ 67.8	2.45E-3	00.64
200	+ 3.7	+ 26.7	4.60E-4	00.12
250	+ 1.9	- 10.0	3.24E-4	00.08
300	+ .9	- 29.9	3.11E-4	00.08
330	+ 1.7	- 33.2	2.88E-4	00.07
350	+357.0	- 33.6	3.04E-4	00.07
360	+ .9	- 34.3	2.53E-4	00.06
400	+ 6.1	- 37.4	2.19E-4	00.05
420	+358.7	- 37.1	1.92E-4	00.05
450	+355.5	- 41.4	1.23E-4	00.03
500	+315.3	+ .8	3.22E-5	00.00

SITE: PC-23 SPEC#: PC 112-1-A

20	+ 62.8	+ 72.9	2.13E-3	01.00
100	+ 31.3	+ 79.4	1.53E-3	00.71
200	+ 2.8	+ 70.2	4.04E-4	00.18
250	+ 1.7	+ 65.1	2.34E-4	00.10
300	+355.8	+ 52.7	1.29E-4	00.06
330	+343.3	+ 33.5	6.53E-5	00.03
350	+331.7	+ 25.2	5.82E-5	00.02
360	+339.5	+ 14.9	5.53E-5	00.02
400	+324.4	- 6.3	5.52E-5	00.02
420	+342.5	- 6.3	2.87E-5	00.01
450	+345.8	+ 28.9	7.22E-5	00.03

SITE: PC-23 SPEC#: PC 113-A

20	+ 60.1	+ 78.9	2.00E-3	01.00
100	+345.6	+ 76.8	1.33E-3	00.66
200	+330.3	+ 60.9	3.37E-4	00.16
250	+334.8	+ 46.8	1.81E-4	00.09
300	+343.2	+ 32.0	1.12E-4	00.05
330	+341.9	+ 8.6	6.90E-5	00.03
350	+336.3	+ 15.2	7.55E-5	00.03
360	+354.8	+ 5.4	6.62E-5	00.03
400	+310.5	- 11.0	5.53E-5	00.02
420	+344.1	- 7.0	2.93E-5	00.01
450	+348.0	+ 7.1	3.07E-5	00.01

APPENDIX B

DETAILED SPECIMEN DIRECTIONS

SITE: PC-23 SPEC#: PC 114-A

TEMP	DEC	INC	J(R/M)	J/JN
20	+ 37.9	+ 86.0	2.29E-3	01.00
100	+334.2	+ 76.7	1.50E-3	00.65
200	+353.3	+ 54.8	3.88E-4	00.16
250	+356.5	+ 40.9	2.33E-4	00.10
300	+358.1	- .2	1.35E-4	00.05
330	+ 4.2	- 17.1	1.26E-4	00.05
350	+ 1.1	- 20.4	1.30E-4	00.05
360	+ 2.1	- 19.5	1.07E-4	00.04
400	+356.8	- 36.9	5.76E-5	00.02
420	+ 3.7	- 29.8	4.76E-5	00.02
450	+358.2	- 16.6	3.52E-5	00.01

SITE: PC-23 SPEC#: PC 115-1

20	+ 69.7	+ 70.3	3.40E-3	01.00
100	+ 11.3	+ 71.5	2.30E-3	00.67
200	+343.6	+ 53.8	6.58E-4	00.19
250	+340.7	+ 38.8	4.13E-4	00.12
300	+342.8	+ 5.8	2.47E-4	00.07
330	+342.9	- 3.9	2.40E-4	00.07
350	+344.1	- 18.9	2.32E-4	00.06
360	+343.9	- 20.2	2.06E-4	00.06
400	+346.2	- 30.7	1.26E-4	00.03
420	+346.9	- 29.4	8.63E-5	00.02
450	+342.6	- 26.8	5.96E-5	00.01

SITE: PC-24 SPEC#: PC 116-A

20	+ 38.3	+ 74.1	2.96E-3	01.00
100	+358.2	+ 79.9	2.15E-3	00.72
200	+335.6	+ 65.3	5.32E-4	00.17
250	+335.9	+ 60.9	3.47E-4	00.11
300	+341.6	+ 52.6	1.56E-4	00.05
330	+339.1	+ 46.8	1.32E-4	00.04
350	+336.6	+ 46.6	1.22E-4	00.04
360	+339.3	+ 40.1	9.04E-5	00.03
400	+338.7	+ 26.2	5.04E-5	00.01
420	+343.4	+ 42.6	3.82E-5	00.01
450	+332.1	+ .3	2.43E-5	00.00

APPENDIX B

DETAILED SPECIMEN DIRECTIONS

SITE: PC-24 SPEC#: PC 117-A

TEMP	DEC	INC	J(R/M)	J/JN
20	+ 35.5	+ 59.5	4.31E-3	01.00
100	+ 29.2	+ 67.1	2.97E-3	00.60
200	+356.0	+ 68.6	6.99E-4	00.16
250	+350.9	+ 67.2	4.94E-4	00.11
300	+330.9	+ 57.9	1.55E-4	00.03
330	+324.5	+ 56.4	1.59E-4	00.03
350	+334.9	+ 58.3	1.58E-4	00.03
360	+332.0	+ 52.4	1.46E-4	00.03
400	+326.5	+ 49.6	7.02E-5	00.01
420	+337.8	+ 43.3	5.79E-5	00.01
450	+300.8	+ 26.3	3.27E-5	00.00

SITE: PC-24 SPEC#: PC 118-A

20	+ 15.3	+ 68.0	3.36E-3	01.00
100	+350.2	+ 71.6	2.18E-3	00.64
200	+333.3	+ 69.6	5.14E-4	00.15
250	+325.5	+ 66.9	3.62E-4	00.10
300	+330.5	+ 58.3	1.47E-4	00.04
330	+335.9	+ 48.8	1.27E-4	00.03
350	+338.2	+ 56.5	1.15E-4	00.03
360	+335.3	+ 46.7	1.04E-4	00.03
400	+339.8	+ 46.6	6.04E-5	00.01
420	+329.9	+ 34.8	4.49E-5	00.01
450	+321.1	+ 22.2	3.28E-5	00.00

SITE: PC-24 SPEC#: PC 119-B

20	+ 58.2	+ 68.1	3.11E-3	01.00
100	+ 23.2	+ 73.6	1.94E-3	00.62
200	+356.3	+ 59.8	3.51E-4	00.11
250	+355.3	+ 49.2	2.49E-4	00.07
300	+354.0	+ 22.1	9.86E-5	00.03
330	+351.7	+ 10.5	8.93E-5	00.02
350	+354.1	+ 3.9	9.08E-5	00.02
360	+349.1	- 7.1	8.61E-5	00.02
400	+343.5	- 21.6	4.44E-5	00.01
420	+340.3	+ 6.2	4.51E-5	00.01
450	+332.3	- 21.7	2.64E-5	00.00

APPENDIX B

DETAILED SPECIMEN DIRECTIONS

SITE: PC-24 SPEC#: PC 120-C

TEMP	DEC	INC	J(R/M)	J/JN
20	+ 67.4	+ 69.4	3.36E-3	01.00
100	+ 18.2	+ 70.7	2.04E-3	00.50
200	+344.8	+ 66.3	4.33E-4	00.12
250	+340.1	+ 61.7	3.42E-4	00.10
300	+342.3	+ 58.2	2.10E-4	00.06
330	+337.3	+ 56.8	1.49E-4	00.04
350	+343.1	+ 51.0	1.26E-4	00.03
360	+342.9	+ 35.1	9.32E-5	00.02
400	+344.2	+ 44.1	5.13E-5	00.01
420	+323.2	+ 26.8	4.70E-5	00.01
450	+317.9	+ 36.4	4.53E-5	00.01

APPENDIX C

SAMPLING LOCALITIES AND DIRECTIONS OF MAGNETIZATION -
ST. GEORGE GROUP

C.1 Sampling localities:

Isthmus Bay Formation:

Locations: 48° 32.6'N, 58° 44.3'W (Sites IB1-5)

50° 47.7'N, 57° 4.7'W (Sites PC1-4)

50° 45.6'N, 57° 9.7'W (Sites PC5-6

and PC5A-6A)

Sites IB1-5 are from an outcrop called "The Gravels", located about 2 km west of the Isthmus on the south shore of the Port au Port Peninsula. The other two localities listed above are in the Great Northern Peninsula. Sites PC1-4 were sampled from diagenetic dolostones exposed about 7.5 km south of Doctor's Brook. According to a proposed revised stratigraphy (I. Knight, personal comm.), this exposure belongs to the Watts Bight Formation which is Lower Tremadoc (Lowest Ordovician) in age. Sites PC5-6 and PC5A-6A were sampled from the interbedded limestone and syngenetic dolostone strata exposed at Oldman's Cove, about 1 km north of Eddies Cove West. This belongs to the Boat Harbour Formation of the proposed revised stratigraphy, and is Middle to Late Tremadoc in age (I. Knight, pers. comm.). Samples were taken from both the limestone and dolostone beds.

Tilt correction and stratigraphic thickness:

<u>Sites</u>	<u>Strike,</u>	<u>Dip</u>	<u>Approx. thickness</u>
IB1-5	245°,	17°NW	5.5 m
PC1-4	237°,	5°NW	3.5 m
PC5, 6, 5A, 6A	0°,	0°	4 m

Catoche Formation:

Locations: 48° 30.8'N, 59° 0.3'W (Sites PH1-5)
 50° 43.2'N, 57° 22.1'W (Sites PC7-11)
 50° 43.0'N, 57° 22.5'W (Sites PC12-14)

Sites PH1-5 are located about 6.5 km from Picadilly Junction on the southshore of the Port au Port Peninsula and characterize the Middle, mainly subtidal limestones of the St. George Group. Sites PC7-11 are limestones and Sites 12-14 are diagenetic dolostones, both located close to the town of Port au Choix in the Northern Peninsula.

Tilt correction and stratigraphic thickness:

<u>Sites</u>	<u>Strike,</u>	<u>Dip</u>	<u>Approx. thickness</u>
PH1-5	236°,	12°NW	7 m
PC7-14	137°,	5°SW	3 m (PC7-11); 8.5 m (PC12-14)

Aguathuna Formation:

Locations: 48° 33.7'N, 58° 46.3'W (Sites AQL-4)
 50° 22.5'N, 57° 31.7'W (Sites PC19-22)

Sites AQL-4 are exposed in a quarry 2 km west of The Gravels along the north coast of the Port au Port Peninsula. In this locality, in addition to the Aguathuna Formation, Middle Ordovician (Table Point Formation) and

Mississippian (Codroy Group) strata, all separated by unconformities, are exposed. Strata belonging to the Aguathuna Formation represent the upper dolomite beds of the St. George Group, overlain unconformably by the dark limestones of the Table Point Formation.

Sites PC19-22 were sampled at Table Point in the Northern Peninsula (Figures 2.1, 2.4), about 6.3 km north of Bellburns where a creek flows into the ocean. Here about 500 m of continuous shoreline section representing the upper part of the St. George, and of lower parts of the Table Head are exposed.

Tilt correction and stratigraphic thickness:

<u>Sites</u>	<u>Strike,</u>	<u>Dip</u>	<u>Approx. thickness</u>
AQ1-4	274°,	18°N	13 m
PC19-22	130°,	11°SW	12 m

C.2 Detailed directions of magnetization

Thermal demagnetization results after each demagnetization step are listed below for those specimens from which characteristic component(s) were isolated and were discussed in Chapter 5. The listing scheme is the same as under Appendix B.2.

APPENDIX C

DETAILED SPECIMEN DIRECTIONS

SITE: IB1 SPEC#: IB1-B

TEMP	DEC	INC	J(A/M)	J/JN
20	+160.8	+ 42.1	3.80E-4	01.00
100	+169.9	+ 5.1	3.01E-4	00.79
200	+174.5	- 2.9	3.12E-4	00.82
300	+176.2	- 5.5	2.69E-4	00.70
350	+175.4	- 6.2	2.49E-4	00.65
400	+178.3	- 8.5	1.88E-4	00.49
450	+176.1	- 6.9	1.64E-4	00.43
500	+179.4	- 7.5	1.29E-4	00.33
530	+179.5	- 6.3	1.17E-4	00.30
560	+182.7	- 6.4	1.02E-4	00.26
590	+169.0	- 5.8	6.06E-5	00.15
620	+163.4	+ 11.9	4.65E-5	00.12
650	+328.4	+ 65.5	7.30E-6	00.01
680	+245.0	+ 14.2	2.22E-5	00.05

SITE: IB1 SPEC#: IB2-A

20	+174.1	+ 54.6	1.67E-4	01.00
100	+171.6	+ 47.7	1.30E-4	00.77
200	+170.2	+ 10.4	1.36E-4	00.81
300	+172.9	+ .1	1.19E-4	00.71
350	+172.8	- 2.2	1.11E-4	00.66
400	+166.0	- 23.0	5.05E-5	00.30
450	+172.4	- 16.5	3.84E-5	00.22
500	+180.2	- 20.7	2.96E-5	00.17
530	+164.5	- 24.8	4.34E-5	00.25
560	+186.4	- 39.3	2.12E-5	00.12
590	+187.7	- 7.4	3.62E-5	00.21
620	+217.8	- 35.2	2.08E-5	00.12
650	+ 1.1	- 38.3	5.00E-6	00.02
680	+ 65.5	+ 5.3	1.50E-5	00.09

APPENDIX C

DETAILED SPECIMEN DIRECTIONS

SITE: IB1 SPEC#: IB3-C

TEMP	DEC	INC	JCR/M	J/JN
20	+145.8	+ 71.2	3.02E-4	01.00
100	+158.6	+ 19.5	1.07E-4	00.35
200	+166.8	- 6.9	1.09E-4	00.35
300	+166.7	- 14.5	1.07E-4	00.35
350	+165.6	- 15.6	9.94E-5	00.32
400	+168.4	- 17.6	7.69E-5	00.25
450	+171.1	- 17.5	6.51E-5	00.21
500	+170.4	- 7.3	4.97E-5	00.16
530	+171.1	- 19.9	5.05E-5	00.16
560	+174.7	- 15.8	4.64E-5	00.15
590	+164.2	- 30.0	4.83E-5	00.15
620	+163.2	- 26.1	3.19E-5	00.10
650	+156.0	- 36.0	4.70E-5	00.15
680	+187.7	+ 28.1	2.07E-5	00.06

SITE: IB1 SPEC#: IB4-A

20	+165.0	+ 41.1	8.79E-5	01.00
100	+179.5	+ 8.9	9.80E-5	01.11
200	+183.7	- 2.7	1.04E-4	01.18
300	+190.9	- 8.6	9.39E-5	01.06
350	+180.1	- 9.5	8.81E-5	01.00
400	+194.6	- 15.8	6.97E-5	00.79
450	+182.6	- 13.1	6.00E-5	00.68
500	+186.6	- 14.4	3.35E-5	00.38
530	+187.5	- 14.5	3.96E-5	00.45
560	+179.8	- 15.4	3.79E-5	00.42
590	+191.0	- 5.1	2.57E-5	00.29
620	+212.5	- 41.5	3.15E-5	00.35
650	+190.2	+ 40.2	1.06E-5	00.12
690	+ 48.5	+ 75.1	9.41E-6	00.10

APPENDIX C

DETAILED SPECIMEN DIRECTIONS

SITE: IB1 SPEC#: IB7-2.

TEMP	DEC	INC	J(A/M)	J/JN
20	+136.8	+ 53.4	9.44E-5	01.00
100	+152.0	+ 28.7	7.90E-5	00.83
200	+156.2	+ 15.0	7.84E-5	00.83
300	+156.2	+ 10.5	6.97E-5	00.73
350	+156.9	+ 9.3	5.35E-5	00.61
400	+159.9	+ 5.4	4.46E-5	00.47
450	+158.0	+ 7.3	3.20E-5	00.33
500	+156.1	+ 7.2	1.57E-5	00.16
530	+162.9	+ 4.5	1.44E-5	00.15
560	+161.7	+ 1.7	1.47E-5	00.15
590	+224.5	- 55.2	6.43E-6	00.06

SITE: IB1 SPEC#: IB8-1

20	+174.0	+ 7.2	3.15E-4	01.00
100	+173.4	- 3.8	3.50E-4	01.10
200	+174.8	- 7.6	3.47E-4	01.09
300	+173.2	- 9.1	2.87E-4	00.90
350	+175.1	- 8.1	2.17E-4	00.58
400	+174.4	- 7.8	1.37E-4	00.43
450	+173.9	- 5.2	6.31E-5	00.19
500	+174.3	- 14.2	2.77E-5	00.08
530	+179.6	- 8.7	1.78E-5	00.05
560	+184.0	- 27.8	1.34E-5	00.04
590	+320.0	- 3.1	2.19E-6	00.00

SITE: IB3 SPEC#: IB9-C

20	+ 14.8	+ 90.2	5.13E-4	01.00
100	+146.9	+ 53.9	9.65E-5	00.18
200	+158.2	- 19.8	5.11E-5	00.11
300	+159.1	- 37.7	8.42E-5	00.16
350	+165.9	- 33.2	5.26E-5	00.10
400	+163.3	- 44.0	6.45E-5	00.12
450	+167.7	- 51.5	4.90E-5	00.09
500	+172.3	- 55.9	4.23E-5	00.08
530	+158.8	- 70.1	3.94E-5	00.07
560	+212.6	- 84.9	3.05E-5	00.05
590	+313.6	- 71.8	1.15E-5	00.02
620	+346.3	- 69.0	1.55E-5	00.03

APPENDIX C

DETAILED SPECIMEN DIRECTIONS

SITE: IB3 SPEC#: IB11-A

TEMP	DEC	INC	J(A/M)	J/JN
20	+ 16.6	+ 77.0	4.78E-4	01.00
100	+150.6	+ 54.8	1.34E-4	00.27
200	+163.7	+ 10.1	9.75E-5	00.20
300	+163.4	+ 1.5	9.41E-5	00.19
350	+164.8	- .7	8.16E-5	00.17
400	+166.5	+ 4.4	6.60E-5	00.13
450	+163.6	+ 4.7	4.37E-5	00.09
500	+165.3	+ 9.2	3.72E-5	00.07
530	+161.9	+ 20.0	2.90E-5	00.06
560	+165.6	+ 21.3	1.53E-5	00.03
590	+355.5	+ 63.6	9.12E-6	00.01
620	+349.8	+ 40.1	6.98E-6	00.01

SITE: IB4 SPEC#: IB13-A

20	+127.7	+ 66.1	2.71E-4	01.00
100	+162.2	+ 38.6	1.91E-4	00.70
200	+163.3	+ 27.8	1.68E-4	00.62
300	+166.4	+ 13.3	1.59E-4	00.58
350	+170.8	+ 10.9	1.52E-4	00.55
400	+170.1	+ 3.0	1.28E-4	00.47
450	+170.7	+ 6.2	1.12E-4	00.41
500	+173.1	+ 5.2	7.63E-5	00.28
530	+171.4	+ 6.6	7.12E-5	00.26
560	+349.9	+ 22.3	1.29E-5	00.04
590	+180.5	+ 2.5	4.18E-5	00.15
620	+168.6	- .1	3.23E-5	00.11

SITE: IB4 SPEC#: IB14-C

20	+151.9	+ 71.9	1.93E-4	01.00
100	+154.5	+ 52.0	1.25E-4	00.64
200	+167.0	+ 14.0	1.18E-4	00.61
300	+168.8	+ 3.0	1.05E-4	00.54
350	+169.2	+ .1	1.03E-4	00.53
400	+171.5	- 9.1	4.60E-5	00.23
450	+172.6	- 5.4	2.77E-5	00.14
500	+178.6	- 5.6	3.25E-5	00.16
530	+179.4	- 11.7	3.95E-5	00.20
560	+187.3	- 18.5	3.81E-5	00.19
590	+144.6	+ 26.3	2.73E-5	00.14
620	+196.5	- 10.8	1.97E-5	00.10
650	+212.8	+ 70.5	1.50E-5	00.07
680	+168.3	- 38.4	1.58E-5	00.08

APPENDIX C

DETAILED SPECIMEN DIRECTIONS

SITE: IB4 SPEC#: IB15-C

TEMP	DEC	INC	J(A/M)	J/JN
20	+ 36.9	+ 58.0	3.03E-4	01.00
100	+ 65.0	+ 65.4	1.27E-4	00.42
200	+110.8	+ 49.3	6.35E-5	00.20
300	+136.0	+ 7.6	4.67E-5	00.15
350	+144.9	+ 1.3	3.99E-5	00.13
400	+139.1	- 18.1	3.31E-5	00.10
450	+139.9	- 6.9	2.61E-5	00.09
500	+139.5	- 26.4	6.92E-6	00.02
530	+175.3	- 15.5	3.99E-6	00.01

SITE: IB4 SPEC#: IB16-1

20	+ 17.2	+ 67.4	5.68E-4	01.00
100	+ 83.0	+ 71.0	1.82E-4	00.32
200	+112.4	+ 66.6	1.18E-4	00.20
300	+134.5	+ 36.6	6.18E-5	00.10
350	+138.4	+ 31.0	5.66E-5	00.09
400	+138.8	+ 31.0	3.85E-5	00.06
450	+153.6	+ 21.1	2.97E-5	00.05
500	+182.6	- 38.6	7.55E-6	00.01
530	+198.1	+ 68.3	6.47E-6	00.01

SITE: IB4 SPEC#: IB16A-1

20	+ 27.1	+ 76.1	3.12E-4	01.00
100	+138.3	+ 74.2	1.17E-4	00.37
200	+151.8	+ 60.7	8.29E-5	00.26
300	+156.4	+ 46.9	5.91E-5	00.18
350	+162.5	+ 39.2	4.63E-5	00.14
400	+155.5	+ 34.8	3.02E-5	00.09
450	+170.3	+ 37.2	1.95E-5	00.06
500	+159.8	+ 57.6	1.20E-5	00.03
530	+152.2	+ 90.9	7.71E-6	00.02
560	+182.6	+ 36.3	2.67E-6	00.00

APPENDIX C

DETAILED SPECIMEN DIRECTIONS

SITE: IB5 SPEC#: IB17-A

TEMP	DEC	INC	J(A/M)	J/JN
20	+143.7	+ 48.1	1.10E-3	01.00
100	+150.9	+ 33.5	8.90E-4	00.90
200	+160.1	+ 21.9	8.59E-4	00.77
300	+162.9	+ 16.0	8.16E-4	00.73
350	+164.6	+ 14.5	7.30E-4	00.66
400	+164.1	+ 13.5	6.30E-4	00.57
450	+166.5	+ 12.6	3.59E-4	00.32
500	+166.4	+ 5.0	4.66E-5	00.04
530	+173.6	- 2.7	2.31E-5	00.02
560	+175.6	- 29.5	1.61E-5	00.01
590	+180.6	- 24.3	2.00E-5	00.01
620	+ 45.6	- 69.5	1.71E-5	00.01
650	+274.6	- .6	2.85E-5	00.02

SITE: IB5 SPEC#: IB19-A

20	+130.4	+ 65.4	9.80E-4	01.00
100	+148.4	+ 43.0	7.23E-4	00.73
200	+153.3	+ 22.1	6.93E-4	00.70
300	+154.2	+ 16.7	6.31E-4	00.64
350	+154.6	+ 17.1	5.10E-4	00.52
400	+154.1	+ 16.4	3.17E-4	00.32
450	+155.7	+ 20.2	4.15E-5	00.04
500	+163.7	+ 17.7	3.48E-5	00.03
530	+193.4	+ 37.9	1.89E-5	00.01
560	+185.2	+ 32.6	8.14E-6	00.00

SITE: IB5 SPEC#: IB19-A

20	+118.1	+ 54.1	1.09E-3	01.00
100	+138.7	+ 35.5	8.46E-4	00.78
200	+144.3	+ 22.3	7.89E-4	00.72
300	+148.1	+ 17.1	7.65E-4	00.70
350	+147.7	+ 15.2	6.58E-4	00.60
400	+148.9	+ 15.0	5.46E-4	00.50
450	+152.3	+ 14.6	2.88E-4	00.26
500	+158.7	+ 15.7	6.56E-5	00.06
530	+166.1	+ 7.2	4.74E-5	00.04
560	+155.4	+ 8.1	-2.24E-5	00.02
590	+143.7	+ .5	1.89E-5	00.01
620	+142.3	+ 59.5	3.11E-5	00.02
650	+335.9	- 19.2	1.33E-5	00.01

APPENDIX C

DETAILED SPECIMEN DIRECTIONS

SITE: IB5 SPEC#: IB20-B

TEMP	DEC	INC	J(A/M)	J/JN
20	+129.2	+ 49.2	1.24E-3	01.00
100	+142.0	+ 36.8	1.09E-3	00.87
200	+147.6	+ 23.6	1.06E-3	00.85
300	+149.4	+ 18.0	9.98E-4	00.80
350	+150.2	+ 18.5	8.15E-4	00.65
400	+151.2	+ 18.7	6.48E-4	00.52
450	+151.2	+ 21.3	2.53E-4	00.20
500	+157.6	+ 39.4	6.45E-5	00.05
530	+147.2	+ 48.3	5.16E-5	00.04
560	+147.6	+ 50.4	4.70E-5	00.03
590	+171.6	+ 55.7	4.53E-5	00.03
620	+128.0	+ 35.9	5.88E-5	00.04
650	+ 18.3	+ 19.0	1.03E-5	00.00

SITE: PH1 SPEC#: PH2-1

20	+ 70.7	+ 72.7	5.43E-4	01.00
100	+120.1	+ 64.8	1.94E-4	00.35
200	+148.0	+ 18.2	8.71E-5	00.16
300	+153.7	- 14.2	9.83E-5	00.18
350	+157.9	- 10.5	9.57E-5	00.17
400	+165.9	- 6.2	7.02E-5	00.12
450	+163.4	- 7.1	5.11E-5	00.09
500	+162.3	- 9.9	4.08E-5	00.07
530	+165.4	- 2.9	3.38E-5	00.06
560	+190.4	- 20.8	9.78E-6	00.01
590	+ 26.1	- 71.4	1.13E-5	00.02

SITE: PH1 SPEC#: PH4-A

20	+117.3	+ 71.1	4.15E-4	01.00
100	+ 99.9	+ 66.2	2.37E-4	00.57
200	+113.2	+ 42.6	1.01E-4	00.24
300	+123.2	+ 6.0	7.58E-5	00.18
350	+132.3	+ 9.1	6.66E-5	00.16
400	+134.6	+ 16.9	2.93E-5	00.07
450	+ 79.8	+ 30.4	4.62E-6	00.01
500	+359.3	+ 34.2	4.15E-6	00.01
530	+ 1.4	- 6.2	4.55E-6	00.01
560	+ 36.9	- 55.4	8.13E-6	00.01
590	+ 10.0	+ 43.4	2.01E-5	00.04

APPENDIX C

DETAILED SPECIMEN DIRECTIONS

SITE: PH2 SPEC#: PH5-1

TEMP	DEC	INC	J(A/M)	J/JN
20	82.8	+ 82.1	1.37E-4	01.00
100	+139.0	+ 55.5	8.90E-5	00.47
200	+147.3	+ 32.3	6.61E-5	00.35
300	+149.3	+ 22.5	4.93E-5	00.26
350	+149.8	+ 26.3	4.07E-5	00.21
400	+149.5	+ 25.3	2.29E-5	00.12
450	+152.0	+ 50.9	1.05E-5	00.05
500	+ 52.2	+ 78.7	3.91E-6	00.02
530	+153.8	+ 67.8	6.35E-6	00.03
560	+127.9	+ 12.0	4.38E-6	00.02
590	+358.4	- 21.6	4.64E-6	00.02

SITE: PH2 SPEC#: PH7-1

20	+ 64.0	+ 82.0	2.56E-4	01.00
100	+148.0	+ 70.0	1.42E-4	00.55
200	+155.0	+ 43.0	9.90E-5	00.38
300	+156.0	+ 22.0	8.40E-5	00.32
350	+160.0	+ 23.0	3.72E-5	00.14
400	+164.0	+ 15.0	6.49E-5	00.25
450	+168.0	+ 35.0	2.08E-5	00.08
500	+175.0	+ 75.0	7.85E-6	00.03

SITE: PH2 SPEC#: PH8-A

20	+107.2	+ 58.6	7.09E-4	01.00
100	+124.4	+ 56.7	4.92E-4	00.69
200	+136.3	+ 34.9	3.59E-4	00.50
300	+141.2	+ 20.0	3.33E-4	00.46
350	+143.8	+ 19.6	3.09E-4	00.43
400	+145.0	+ 19.6	2.60E-4	00.36
450	+145.6	+ 21.1	1.41E-4	00.19
500	+148.7	+ 18.1	2.35E-5	00.03
530	+101.3	+ 40.1	9.94E-6	00.01
560	+ 18.8	+ 37.0	1.29E-5	00.01
590	+353.9	+ 52.4	9.17E-6	00.01

APPENDIX C

DETAILED SPECIMEN DIRECTIONS

SITE: PH3 SPEC#: PH9-1

TEMP	DEC	INC	J(R/M)	J/JN
20	+120.6	+ 68.5	1.74E-4	01.00
100	+143.8	+ 52.9	1.04E-4	00.59
200	+160.7	+ 27.4	8.04E-5	00.46
300	+161.5	+ 15.9	6.12E-5	00.35
400	+161.5	+ 16.0	2.82E-5 ⁰	00.16
450	+170.0	+ 16.5	1.42E-5	00.08
500	+129.6	- 47.3	2.39E-6	00.01

SITE: PH3 SPEC#: PH9-1

20	+120.6	+ 68.5	1.74E-4	01.00
100	+143.8	+ 52.9	1.04E-4	00.59
200	+160.7	+ 27.4	8.04E-5	00.46
300	+161.5	+ 15.9	6.12E-5	00.35
400	+161.5	+ 16.0	2.82E-5	00.16
450	+170.0	+ 16.5	1.42E-5	00.08
500	+129.6	- 47.3	2.39E-6	00.01

SITE: PH3 SPEC#: PH10-B

20	+ 99.3	+ 68.2	2.15E-4	01.00
100	+101.1	+ 65.7	1.39E-4	00.64
200	+125.5	+ 58.2	9.62E-5	00.44
300	+131.6	+ 43.2	6.46E-5	00.30
350	+129.5	+ 34.3	5.08E-5	00.23
400	+125.1	+ 32.6	3.27E-5	00.15
450	+124.9	+ 37.8	2.02E-5	00.09
500	+ 66.0	+ 52.7	6.42E-6	00.02

SITE: PH3 SPEC#: PH11-1

20	+ 78.7	+ 76.2	2.63E-4	01.00
100	+ 75.9	+ 73.1	1.87E-4	00.71
200	+105.0	+ 60.8	1.30E-4	00.49
250	+119.0	+ 54.2	9.97E-5	00.37
300	+124.5	+ 39.1	8.83E-5	00.33
350	+132.0	+ 30.4	6.74E-5	00.25
400	+129.9	+ 22.3	5.07E-5	00.19
450	+138.8	+ 69.8	2.41E-6	00.00
500	+137.2	+ 86.0	4.97E-6	00.01

APPENDIX C

DETAILED SPECIMEN DIRECTIONS

SITE: PH3 SPEC#: PH12-2

TEMP	DEC	INC	J(A/M)	J/JN
20	+141.2	+ 67.2	2.08E-4	01.00
100	+147.7	+ 70.6	1.43E-4	00.68
200	+149.7	+ 60.8	9.10E-5	00.43
300	+150.5	+ 45.6	6.52E-5	00.31
350	+150.9	+ 34.3	5.13E-5	00.24
400	+145.3	+ 33.8	3.59E-5	00.17
450	+156.2	+ 38.6	1.91E-5	00.09
500	+ 30.7	+ 64.0	5.39E-6	00.02

SITE: PH4 SPEC#: PH13-1

20	+135.2	+ 53.9	2.88E-4	01.00
100	+135.4	+ 50.9	2.13E-4	00.73
200	+145.3	+ 38.6	1.64E-4	00.56
300	+144.4	+ 25.7	1.32E-4	00.45
350	+147.8	+ 20.3	1.07E-4	00.37
400	+143.9	+ 21.0	6.62E-5	00.22
450	+144.9	+ 24.0	5.00E-5	00.17
500	+167.7	+ 46.3	6.65E-6	00.02

SITE: PH4 SPEC#: PH14-2

20	+190.1	+ 62.7	2.16E-4	01.00
100	+162.1	+ 55.1	1.53E-4	00.70
200	+149.1	+ 34.1	1.22E-4	00.56
300	+145.2	+ 19.7	1.06E-4	00.49
350	+149.7	+ 21.2	9.18E-5	00.42
400	+147.3	+ 22.0	5.83E-5	00.27
450	+148.2	+ 22.5	3.85E-5	00.17
500	+144.4	+ 40.5	8.83E-6	00.04
530	+129.3	+ 69.6	5.67E-6	00.02

SITE: PH4 SPEC#: PH15-2

20	+137.6	+ 68.7	2.20E-4	01.00
100	+139.8	+ 57.8	1.60E-4	00.72
200	+146.1	+ 36.9	1.25E-4	00.56
250	+141.5	+ 27.6	1.10E-4	00.49
300	+140.6	+ 18.3	1.05E-4	00.47
350	+141.1	+ 22.0	8.13E-5	00.36
400	+140.7	+ 18.5	6.22E-5	00.28
450	+138.8	+ 16.7	4.46E-6	00.02
500	+180.0	+ 85.4	2.19E-6	00.00

APPENDIX C

DETAILED SPECIMEN DIRECTIONS

SITE: PH4 SPEC#: PH16-B

TEMP	DEC	INC	J(R/M)	J/JN
20	+142.9	+ 55.2	2.42E-4	01.00
100	+128.9	+ 51.8	1.80E-4	00.74
200	+131.1	+ 38.7	1.33E-4	00.54
300	+136.7	+ 28.1	1.08E-4	00.44
350	+140.6	+ 24.2	8.43E-5	00.34
400	+139.8	+ 25.6	4.29E-5	00.17
450	+135.0	+ 33.3	2.12E-5	00.08
500	+ 79.7	+ 47.9	7.89E-6	00.03
530	+ 8.1	+ 78.7	4.25E-6	00.01

SITE: PH5 SPEC#: PH17-B

20	+134.2	+ 55.1	2.37E-4	01.00
100	+141.5	+ 40.7	1.47E-4	00.61
200	+143.2	+ 30.4	1.20E-4	00.50
300	+143.5	+ 13.1	9.51E-5	00.40
350	+148.3	+ 13.0	9.25E-5	00.39
400	+148.2	+ 11.9	7.32E-5	00.30
450	+150.0	+ 9.4	4.13E-5	00.17
500	+161.5	- 1.7	8.27E-6	00.03
530	+173.5	- 1.4	4.83E-6	00.02

SITE: PH5 SPEC#: PH18-A

20	+122.2	+ 38.5	1.79E-3	01.00
100	+132.1	+ 31.1	1.31E-3	00.72
200	+138.1	+ 18.4	1.12E-3	00.62
300	+142.2	+ 7.9	1.02E-3	00.56
350	+142.9	+ 7.4	9.79E-4	00.54
400	+144.5	+ 6.3	8.79E-4	00.49
450	+145.1	+ 5.8	5.54E-4	00.30
500	+150.7	+ .9	1.10E-4	00.06
530	+150.8	+ 1.5	5.53E-5	00.03

APPENDIX C

DETAILED SPECIMEN DIRECTIONS

SITE: PH5 SPEC#: PH19-3

TEMP	DEC	INC	J(A/M)	J/JN
20	+108.6	+ 53.0	1.97E-3	01.00
100	+129.9	+ 43.1	1.46E-3	00.73
200	+138.6	+ 25.9	1.21E-3	00.61
250	+140.4	+ 15.2	1.14E-3	00.57
300	+142.1	+ 10.8	1.09E-3	00.55
350	+145.3	+ 10.1	9.35E-4	00.47
400	+145.1	+ 10.0	6.21E-4	00.31
450	+150.2	+ 10.0	7.57E-5	00.03
500	+136.7	- 30.9	5.93E-6	00.00

SITE: PH5 SPEC#: PH20-1

20	+106.3	+ 48.2	1.66E-3	01.00
100	+130.9	+ 38.0	1.25E-3	00.75
200	+139.8	+ 21.5	1.11E-3	00.67
300	+144.8	+ 11.1	1.05E-3	00.63
350	+146.0	+ 9.3	9.81E-4	00.59
400	+149.0	+ 9.3	8.12E-4	00.49
450	+150.3	+ 6.2	2.95E-4	00.17
500	+160.8	+ 3.9	7.67E-5	00.04
530	+156.8	- 9.2	4.16E-5	00.02
560	+133.5	+ 3.0	2.69E-5	00.01

SITE: AQ1 SPEC#: AQ1-B

20	+130.9	+ 77.2	4.72E-4	01.00
100	+143.0	+ 69.4	2.80E-4	00.59
200	+150.9	+ 46.7	1.65E-4	00.34
300	+161.0	+ 30.0	1.31E-4	00.27
350	+157.9	+ 27.7	9.27E-5	00.19
400	+158.9	+ 23.9	5.06E-5	00.10
450	+153.2	+ 17.0	3.49E-5	00.07
500	+160.2	+ 3.0	9.96E-6	00.02
530	+168.8	+ 21.1	6.95E-6	00.01
560	+163.8	+ 24.5	4.02E-6	00.00

APPENDIX C

DETAILED SPECIMEN DIRECTIONS

SITE: AQ1 SPEC#: AQ2-A

TEMP	DEC	INC	J(A/M)	J/JN
20	+108.0	+ 50.1	6.61E-4	01.00
100	+102.5	+ 65.9	3.99E-4	00.60
200	+153.2	+ 49.4	1.86E-4	00.28
300	+160.1	+ 31.6	1.28E-4	00.19
350	+159.4	+ 27.1	1.26E-4	00.19
400	+154.7	+ 31.1	8.00E-5	00.12
450	+157.2	+ 45.5	1.36E-5	00.02
500	+125.5	+ 72.9	6.88E-6	00.01

SITE: AQ1 SPEC#: AQ3-B

20	+ 9.2	+ 72.8	1.38E-4	01.00
100	+ 19.4	+ 70.6	1.01E-4	00.72
200	+157.7	+ 58.4	4.43E-5	00.32
300	+155.6	+ 35.1	2.37E-5	00.17
350	+155.9	+ 32.0	2.46E-5	00.17
400	+149.0	+ 24.9	1.40E-5	00.10
450	+150.6	- 1.2	9.33E-6	00.06
500	+118.0	- 47.1	5.07E-6	00.03
530	+206.2	+ 41.6	6.55E-6	00.04
560	+247.8	+ 1.9	7.55E-6	00.05
590	+237.3	+ 60.3	1.29E-5	00.09

SITE: AQ1 SPEC#: AQ4-D

20	+100.7	+ 52.0	4.83E-4	01.00
100	+ 87.8	+ 58.8	3.26E-4	00.57
200	+136.0	+ 36.7	1.68E-4	00.34
300	+144.5	+ 23.3	1.55E-4	00.32
350	+145.5	+ 21.1	1.49E-4	00.30
400	+143.8	+ 19.0	1.12E-4	00.23
450	+147.2	+ 15.8	3.42E-5	00.07
500	+157.8	- 13.1	1.31E-5	00.02
530	+165.1	+ .2	8.51E-6	00.01
560	+ 48.5	+ 32.9	5.27E-6	00.01
590	+268.2	+ 17.4	5.97E-6	00.01

APPENDIX C

DETAILED SPECIMEN DIRECTIONS

SITE: AQ2 SPEC#: AQ5-A

TEMP	DEC	INC	J(A/M)	J/JN
20	+125.6	+ 46.2	6.53E-4	01.00
100	+138.2	+ 43.7	5.29E-4	00.80
200	+153.2	+ 26.4	4.90E-4	00.75
300	+155.7	+ 23.7	4.50E-4	00.69
350	+155.8	+ 22.3	4.40E-4	00.67
400	+159.1	+ 22.5	3.34E-4	00.51
450	+157.2	+ 25.8	9.11E-5	00.13
500	+168.4	+ 30.0	2.12E-5	00.03
530	+166.7	+ 27.0	2.14E-5	00.03
560	+181.4	+ 40.7	1.77E-5	00.02
590	+188.5	+ 23.6	1.78E-5	00.02
620	+200.1	- 58.8	1.50E-5	00.02

SITE: AQ2 SPEC#: AQ6-C

20	+156.4	+ 38.3	6.31E-4	01.00
100	+163.1	+ 25.8	5.31E-4	00.84
200	+164.0	+ 13.9	4.92E-4	00.77
300	+163.4	+ 9.8	4.93E-4	00.78
350	+165.1	+ 8.2	4.29E-4	00.67
400	+167.6	+ 4.5	2.73E-4	00.43
450	+174.2	- .3	1.86E-4	00.29
500	+176.3	- 3.0	1.46E-4	00.23
530	+178.6	- 5.7	1.45E-4	00.22
560	+177.3	- 4.0	1.04E-4	00.16
590	+169.3	- .8	9.18E-5	00.14
620	+106.7	- 81.0	5.25E-6	00.00

SITE: AQ2 SPEC#: AQ8-C

20	+144.3	+ 40.9	6.82E-4	01.00
100	+143.1	+ 42.4	5.02E-4	00.73
200	+152.2	+ 26.4	4.58E-4	00.67
300	+154.2	+ 23.7	3.91E-4	00.57
350	+155.7	+ 22.9	3.40E-4	00.49
400	+157.1	+ 22.5	2.39E-4	00.35
450	+157.3	+ 41.6	3.70E-5	00.05
500	+130.9	+ 35.0	3.31E-6	00.00

APPENDIX C

DETAILED SPECIMEN DIRECTIONS

SITE: AQ3 SPEC#: AQ9-A

TEMP	DEC	INC	J(A/M)	J/JN
20	+133.8	+ 34.5	1.10E-3	01.00
100	+143.3	+ 37.2	8.10E-4	00.73
200	+146.9	+ 29.3	7.30E-4	00.66
300	+151.3	+ 21.5	6.45E-4	00.58
350	+153.4	+ 21.1	4.61E-4	00.41
400	+154.2	+ 24.5	9.40E-5	00.08
450	+158.3	+ 27.1	5.53E-5	00.05
500	+182.2	+ 38.5	8.88E-6	00.00
530	+204.1	+ 68.1	3.34E-6	00.00

SITE: AQ3 SPEC#: AQ10-1

20	+150.2	+ 28.9	1.24E-3	01.00
100	+148.9	+ 30.7	9.02E-4	00.72
200	+147.4	+ 24.3	8.35E-4	00.67
300	+155.2	+ 18.2	7.58E-4	00.61
350	+155.1	+ 17.7	5.81E-4	00.47
400	+154.0	+ 19.4	1.61E-4	00.13
450	+158.2	+ 20.5	1.04E-4	00.08
500	+143.3	+ 28.8	1.18E-5	00.00
530	+165.6	+ 57.1	3.49E-6	00.00

SITE: AQ3 SPEC#: AQ11-A

20	+138.4	+ 50.7	9.98E-4	01.00
100	+143.2	+ 42.5	7.69E-4	00.77
200	+143.3	+ 29.6	6.90E-4	00.69
300	+146.5	+ 23.7	6.53E-4	00.66
350	+148.6	+ 22.2	4.97E-4	00.50
400	+148.2	+ 28.8	1.53E-4	00.15
450	+149.7	+ 25.4	8.81E-5	00.06
500	+116.3	+ 25.8	5.37E-6	00.00
530	+ 14.5	+ 66.7	7.85E-6	00.00
560	+ 88.1	+ 49.2	3.65E-6	00.00

APPENDIX C

DETAILED SPECIMEN DIRECTIONS

SITE: AQ3 SPEC#: AQ12-B

TEMP	DEC	INC	J(A/M)	J/JN
20	+135.3	+ 35.0	1.35E-3	01.00
100	+147.9	+ 35.6	1.05E-3	00.77
200	+149.9	+ 28.2	9.86E-4	00.73
300	+154.1	+ 21.7	9.18E-4	00.68
350	+152.2	+ 21.1	7.47E-4	00.55
400	+153.6	+ 21.0	2.96E-4	00.21
450	+155.8	+ 23.5	1.68E-4	00.12
500	+156.3	+ 42.3	2.40E-5	00.01
530	+ 1.6	- 16.7	8.48E-6	00.00

SITE: AQ4 SPEC#: AQ13-A

20	+136.9	+ 46.3	1.28E-4	01.00
100	+150.3	+ 41.0	9.51E-5	00.74
200	+157.0	+ 29.1	8.03E-5	00.62
300	+161.9	+ 19.5	7.27E-5	00.56
350	+162.1	+ 11.3	6.14E-5	00.47
400	+155.1	+ 14.3	3.47E-5	00.27
450	+161.5	+ 11.5	2.91E-5	00.22
500	+161.3	+ 10.0	1.74E-5	00.13
530	+149.8	+ 24.7	9.24E-6	00.07
560	+102.9	- 1.5	7.23E-6	00.05
590	+135.0	- 23.5	8.83E-6	00.06
620	+ 18.9	- 54.9	9.52E-6	00.07

SITE: AQ4 SPEC#: AQ15-B

20	+141.1	+ 67.0	1.36E-4	01.00
100	+155.3	+ 36.3	7.94E-5	00.58
200	+156.9	+ 23.6	6.41E-5	00.47
300	+155.4	+ 21.6	5.31E-5	00.38
350	+160.0	+ 20.3	3.96E-5	00.29
400	+154.2	+ 30.0	1.91E-5	00.13
450	+167.8	+ 25.7	1.65E-5	00.12
500	+166.3	+ 18.4	1.01E-5	00.07
530	+135.0	+ 25.9	6.32E-6	00.04
560	+150.6	+ 14.3	7.30E-6	00.05
590	+ 74.1	+ 57.6	7.73E-6	00.05
620	+215.0	+ 15.1	5.63E-6	00.04

APPENDIX C

DETAILED SPECIMEN DIRECTIONS

SITE: AQ4 SPEC#: AQ16-C

TEMP	DEC	INC	J(R/M)	L/JN
20	+150.0	+ 74.3	1.41E-4	01.00
100	+155.8	+ 37.6	7.69E-5	00.54
200	+157.8	+ 10.6	7.41E-5	00.52
300	+153.9	+ 10.9	6.56E-5	00.46
350	+161.8	+ 11.1	3.79E-5	00.26
450	+161.0	+ 9.7	1.73E-5	00.12
500	+137.1	+ 3.4	5.97E-6	00.04
530	+ 10.5	- 24.6	1.88E-6	00.01
560	+150.4	- 3.6	7.46E-6	00.05
590	+124.7	+ 5.2	5.91E-6	00.04

SITE: PC1 SPEC#: PC1-1

20	+358.1	+ 81.8	3.75E-4	01.00
100	+ 5.1	+ 67.3	2.60E-4	00.69
200	+ 19.3	+ 47.9	1.03E-4	00.27
300	+ 12.7	- 1.2	6.42E-5	00.17
350	+ 10.1	- 2.8	6.08E-5	00.16
400	+ 8.9	+ 26.1	2.38E-5	00.06
450	+ 11.5	+ 29.1	1.72E-5	00.04
500	+ 4.3	+ 66.0	5.10E-6	00.01

SITE: PC1 SPEC#: PC3-A

20	+ 22.8	+ 67.5	7.78E-4	01.00
300	+ 27.7	- 5.9	1.25E-4	00.16
350	+ 31.0	+ 7.3	6.69E-5	00.08
400	+ 35.7	+ 29.7	3.00E-5	00.03
450	+ 56.6	+ 60.7	1.51E-5	00.01

SITE: PC1 SPEC#: PC4-A

20	+ 1.9	+ 70.2	8.40E-4	01.00
300	+ 26.0	- 19.5	1.50E-4	00.17
350	+ 24.2	- 18.4	9.92E-5	00.11
400	+ 32.8	- 25.8	2.75E-5	00.03
450	+ 33.7	- 6.8	1.43E-5	00.01

APPENDIX C

DETAILED SPECIMEN DIRECTIONS

SITE: PC2 SPEC#: PC6-1

TEMP	DEC	INC	J(A/M)	J/JN
20	+ 1.1	+ 65.7	5.96E-4	01.00
100	+ 3.7	+ 59.9	4.73E-4	00.79
200	+ 12.1	+ 33.5	1.99E-4	00.33
300	+ 14.2	- 20.0	1.35E-4	00.22
350	+ 8.6	- 21.7	1.29E-4	00.21
400	+ 25.0	+ 3.1	3.52E-5	00.05
450	+ 32.0	+ 11.8	1.71E-5	00.02
500	+ 9.1	+ 61.3	5.60E-6	00.00

SITE: PC2 SPEC#: PC8-A

20	+ 23.5	+ 79.0	5.91E-4	01.00
300	+ 5.4	- 25.0	1.94E-4	00.32
350	+ .3	- 26.6	1.67E-4	00.28
400	+342.2	- 25.6	7.92E-5	00.13
450	+ 5.6	+ 4.5	4.75E-5	00.08

SITE: PC2 SPEC#: PC9-A

20	+ .7	+ 58.7	4.36E-4	01.00
300	+ 3.8	- 14.3	1.37E-4	00.28
350	+ 2.2	- 14.1	9.82E-5	00.20
400	+357.1	+ 2.9	3.26E-5	00.06
450	+ 4.5	+ 29.1	2.62E-5	00.05

SITE: PC2 SPEC#: PC10-A

20	+356.8	+ 60.5	4.77E-4	01.00
300	+ 16.0	- 9.4	1.05E-4	00.21
350	+ 17.8	- 5.6	6.07E-5	00.12
400	+ 24.1	+ 20.7	2.47E-5	00.05
450	+ 45.2	+ 39.9	2.26E-5	00.04

APPENDIX C

DETAILED SPECIMEN DIRECTIONS

SITE: PC3 SPEC#: PC11-B

TEMP	DEC	INC	J(R/M)	J/JN
20	+ 9.9	+ 69.1	9.65E-4	01.00
100	+ 16.9	+ 59.2	7.19E-4	00.74
200	+ 29.5	+ 42.9	2.96E-4	00.29
300	+ 34.1	- 10.5	1.56E-4	00.16
350	+ 28.3	- 17.1	1.50E-4	00.15
400	+ 57.4	+ 25.0	4.89E-5	00.05
450	+ 75.2	+ 40.7	3.03E-5	00.03
500	+ 49.8	+ 78.9	1.51E-5	00.01

SITE: PC3 SPEC#: PC13-B

20	+ 9.4	+ 65.9	4.48E-4	01.00
300	+ 15.0	- 30.1	9.47E-5	00.21
350	+ 9.8	- 25.0	7.54E-5	00.16
400	+ 11.9	- 22.4	3.24E-5	00.07
450	+ 15.8	- 27.2	1.06E-5	00.02

SITE: PC3 SPEC#: PC14-A

20	+ 35.6	+ 56.6	4.54E-4	01.00
300	+ 27.8	- 34.9	1.36E-4	00.30
350	+ 19.0	- 29.9	9.92E-5	00.21
400	+ 31.4	- 14.2	3.43E-5	00.07
450	+ 60.3	- 2.8	9.28E-6	00.02

SITE: PC3 SPEC#: PC15-2

20	+ 64.4	+ 76.0	1.03E-3	01.00
300	+ 29.0	- 23.2	1.57E-4	00.15
350	+ 26.9	- 21.3	1.26E-4	00.12
400	+ 47.9	- 11.8	4.24E-5	00.04
450	+ 81.8	+ 4.1	2.04E-5	00.01

SITE: PC4 SPEC#: PC18-A

20	+352.9	+ 67.7	6.87E-4	01.00
300	+ 18.1	- 27.7	1.42E-4	00.20
350	+ 15.7	- 26.5	9.83E-5	00.14
400	+ 25.3	- 14.7	3.35E-5	00.04
450	+ 38.9	+ .3	1.26E-5	00.01

APPENDIX C

DETAILED SPECIMEN DIRECTIONS

SITE: PC4 SPEC#: PC19-2

TEMP	DEC	INC	J(A/M)	J/JN
20	+ 28.8	+ 59.5	3.96E-4	01.00
300	+ 8.1	- 43.0	1.26E-4	00.32
350	+ 2.4	- 39.1	8.16E-5	00.21
400	+ 3.3	- 28.7	4.37E-5	00.11
450	+ 9.0	- 13.8	2.24E-5	00.05

SITE: PC4 SPEC#: PC20-A

20	+326.4	+ 70.8	1.15E-3	01.00
300	+ 31.4	- 17.2	1.69E-4	00.14
350	+ 36.2	- 14.5	1.04E-4	00.09
400	+ 39.0	- 16.5	5.55E-5	00.04
450	+ 32.5	- 17.7	2.28E-5	00.01

SITE: PC5 SPEC#: PC21-A

20	+ 51.8	+ 75.3	9.05E-4	01.00
100	+ 7.1	+ 68.2	6.12E-4	00.67
200	+ 4.6	+ 61.8	1.91E-4	00.21
300	+ 21.2	- 2.2	5.06E-5	00.05
350	+ 24.5	- 21.9	5.95E-5	00.06
400	+ 28.0	- 18.7	3.84E-5	00.04
450	+ 50.6	- 7.8	1.25E-5	00.01
500	+ 64.1	- 12.3	6.04E-6	00.00

SITE: PC5 SPEC#: PC25-B

20	+183.2	+ 87.6	1.70E-3	01.00
300	+349.6	+ 31.0	1.70E-4	00.10
350	+359.1	+ 6.8	1.33E-4	00.07
400	+ 3.2	- 10.1	9.05E-5	00.05
450	+ 20.0	- 9.8	2.82E-5	00.01

APPENDIX C

DETAILED SPECIMEN DIRECTIONS

SITE: PC7 SPEC#: PC31-2

TEMP	-DEC	INC	J(R/M)	J/JN
20	+ 12.1	+ 68.7	2.18E-3	01.00
100	+ 6.4	+ 65.2	1.34E-3	00.61
200	+355.6	+ 60.4	4.50E-4	00.20
300	+354.7	- 13.8	6.76E-5	00.03
350	+357.9	- 53.2	9.12E-5	00.04
400	+ 3.5	- 69.2	7.70E-5	00.03
450	+351.6	- 67.0	2.56E-5	00.01
500	+ 58.4	- 17.9	2.76E-5	00.01

SITE: PC7 SPEC#: PC33-R

20	+341.8	+ 82.3	2.15E-3	01.00
300	+341.4	+ 35.7	6.94E-5	00.03
350	+331.7	- 19.0	5.07E-5	00.02
400	+344.8	- 39.9	2.97E-5	00.01
450	+326.7	- 28.6	3.92E-5	00.01

SITE: PC7 SPEC#: PC35-A

20	+215.6	+ 83.2	2.02E-3	01.00
300	+353.8	+ 39.8	7.96E-5	00.03
350	+344.5	- 29.0	5.56E-5	00.02
400	+355.4	- 37.8	4.78E-5	00.02
450	+349.2	+ 1.1	1.46E-5	00.00

SITE: PC8 SPEC#: PC36-B

20	+344.5	+ 66.6	1.81E-3	01.00
100	+342.8	+ 61.2	1.08E-3	00.59
200	+338.9	+ 48.1	3.99E-4	00.22
300	+342.4	- 22.2	1.31E-4	00.07
350	+342.8	- 52.4	1.46E-4	00.09
400	+347.5	- 61.8	1.29E-4	00.07
450	+328.1	- 67.4	4.07E-5	00.02
500	+ 15.3	- 78.4	3.36E-5	00.01

APPENDIX C

DETAILED SPECIMEN DIRECTIONS

SITE: PC8 SPEC#: PC37-A

TEMP	DEC	INC	J(A/M)	J/JN
20	+163.0	+ 83.7	2.67E-3	01.00
300	+ 4.2	- 14.6	1.01E-4	00.03
350	+358.8	- 54.5	1.89E-4	00.07
400	+349.2	- 47.3	1.21E-4	00.04
450	+339.7	- 27.6	6.68E-5	00.02

SITE: PC8 SPEC#: PC39-1

20	+298.0	+ 81.0	2.24E-3	01.00
300	+ 6.0	- 17.9	1.23E-4	00.05
350	+ 17.0	- 53.3	1.70E-4	00.07
400	+ 24.2	- 31.8	1.69E-4	00.07
450	+ 15.9	- 45.5	7.27E-5	00.03

SITE: PC11 SPEC#: PC51-A

20	+291.2	+ 85.9	1.50E-3	01.00
100	+352.1	+ 78.5	1.01E-3	00.63
200	+338.7	+ 69.9	3.03E-4	00.18
300	+348.5	+ 28.4	5.93E-5	00.03
350	+343.0	- 35.4	6.03E-5	00.03
400	+345.2	- 45.6	7.45E-5	00.04
450	+352.1	- 23.9	2.39E-5	00.01
500	+357.8	+ 16.0	2.94E-5	00.01
530	+359.5	+ 32.6	2.13E-5	00.01

SITE: PC11 SPEC#: PC52-B

20	+ 15.6	+ 83.0	3.27E-3	01.00
300	+356.4	+ 8.7	1.37E-4	00.04
350	+357.0	- 31.6	1.46E-4	00.04
400	+352.4	- 42.7	6.70E-5	00.02
450	+345.6	- 39.1	3.36E-5	00.01

SITE: PC11 SPEC#: PC53-A

20	+ 8.5	+ 81.5	2.59E-3	01.00
300	+ .7	+ 27.1	1.36E-4	00.05
350	+359.8	- 37.0	1.45E-4	00.05
400	+357.3	- 33.7	1.00E-4	00.03
450	+358.5	- 16.0	6.07E-5	00.02

APPENDIX C

DETAILED SPECIMEN DIRECTIONS

SITE: PC11 SPEC#: PC54-B

TEMP	DEC	INC	J(A/M)	J/JN
20	+ 3.8	+ 81.9	2.89E-3	01.00
300	+349.1	+ 69.7	9.89E-5	00.03
350	+325.6	- 51.8	1.42E-4	00.04
400	+309.1	- 45.9	1.14E-4	00.03
450	+299.3	- 27.2	8.69E-5	00.03

SITE: PC11 SPEC#: PC55-1

20	+251.1	+ 83.6	1.63E-3	01.00
300	+304.4	+ 47.2	4.43E-5	00.02
350	+339.4	- 49.6	9.83E-5	00.06
400	+338.1	- 55.4	1.18E-4	00.07
450	+337.3	- 47.9	6.67E-5	00.04

SITE: PC12 SPEC#: PC56-A

20	+317.1	+ 71.6	8.17E-4	01.00
100	+314.8	+ 67.7	5.72E-4	00.70
200	+311.8	+ 61.7	3.04E-4	00.37
300	+320.4	+ 54.4	1.39E-4	00.17
350	+329.8	+ 21.7	1.12E-4	00.13
400	+317.0	- 23.4	1.39E-4	00.16
450	+326.6	- 1.8	5.89E-5	00.07
500	+316.0	- 49.8	1.25E-5	00.01

SITE: PC13 SPEC#: PC62-B

20	+ 27.3	+ 70.6	9.24E-4	01.00
300	+ 21.7	- 34.0	1.10E-4	00.11
350	+348.6	- 36.7	9.85E-5	00.10
400	+337.6	- 22.0	4.15E-5	00.04
450	+ 2.8	+ 23.1	1.89E-5	00.02

SITE: PC13 SPEC#: PC63-B

20	+ 25.4	+ 80.5	8.90E-4	01.00
300	+ 11.5	- 10.6	8.29E-5	00.09
350	+354.2	- 32.7	8.78E-5	00.09
400	+340.9	- 8.8	5.35E-5	00.06
450	+334.9	+ 10.3	3.65E-5	00.04

APPENDIX C

DETAILED SPECIMEN DIRECTIONS

SITE: PC14 SPEC#: PC68-B

TEMP	DEC	INC	J(R/M)	J/JN
20	+ 32.4	+ 75.1	7.34E-4	01.00
300	+353.6	- 25.9	8.69E-5	00.11
350	+345.8	- 21.6	7.62E-5	00.10
400	+323.5	+ 4.8	1.38E-5	00.01
450	+296.5	+ 13.5	1.93E-5	00.02

SITE: PC14 SPEC#: PC70-A

20	+131.3	+ 79.5	3.74E-4	01.00
300	+ 37.9	- 57.8	9.66E-5	00.25
350	+ 20.0	- 50.0	8.46E-5	00.22
400	+ 62.4	- 56.5	4.22E-5	00.11
450	+ 73.1	- 24.9	1.24E-5	00.03

SITE: PC19 SPEC#: PC92-A

20	+258.3	+ 81.7	1.13E-3	01.00
300	+358.2	- 4.2	6.04E-5	00.05
350	+340.0	- 25.2	4.52E-5	00.04
400	+ 3.1	- 48.8	4.08E-5	00.03
450	+ 6.7	- 27.6	2.64E-5	00.02

SITE: PC19 SPEC#: PC93-1

20	+ 24.6	+ 79.2	1.02E-3	01.00
300	+ .2	- 15.1	6.39E-5	00.06
350	+354.2	- 57.3	4.46E-5	00.04
400	+347.3	- 51.1	5.03E-5	00.04
450	+ 1.7	- 26.8	4.16E-5	00.04

SITE: PC19 SPEC#: PC94-A

20	+ 5.4	+ 78.6	1.44E-3	01.00
300	+354.4	+ 60.5	9.23E-5	00.06
350	+354.2	+ 23.0	4.80E-5	00.03
400	+354.6	- 28.3	3.63E-5	00.02
450	+ 10.3	- 4.5	1.99E-5	00.01

APPENDIX C

DETAILED SPECIMEN DIRECTIONS

SITE: PC19 SPEC#: PC95-1

TEMP	DEC	INC	J(R/M)	J/JN
20	+ 49.4	+ 79.2	8.34E-4	01.00
300	+ 30.6	- 17.5	5.66E-5	00.06
350	+ 23.3	- 37.5	4.95E-5	00.05
400	+ 18.5	- 44.1	4.29E-5	00.05
450	+ 24.1	- 35.2	1.60E-5	00.01

SITE: PC20 SPEC#: PC98-A

20	+ 69.0	+ 80.0	1.08E-3	01.00
300	+ 9.3	- 42.0	3.63E-5	00.03
350	+358.1	- 51.9	4.34E-5	00.04
400	+ 13.9	- 40.1	1.09E-5	00.01
450	+309.7	- 20.9	2.63E-5	00.02

SITE: PC20 SPEC#: PC99-A

20	+ 7.3	+ 81.5	1.21E-3	01.00
300	+ 9.5	- 13.7	9.01E-5	00.07
350	+ 7.2	- 31.5	9.35E-5	00.07
400	+ 9.0	- 42.2	5.79E-5	00.04
450	+349.5	- 5.9	5.71E-5	00.04

SITE: PC20 SPEC#: PC100-A

20	+355.1	+ 79.3	1.38E-3	01.00
300	+ 9.5	+ 3.2	1.21E-4	00.08
350	+ 13.2	- 20.3	1.01E-4	00.07
400	+ 13.8	- 34.2	6.07E-5	00.04
450	+ .1	+ 2.9	3.83E-5	00.02

SITE: PC21 SPEC#: PC101-A

20	+ 22.2	+ 74.9	9.79E-4	01.00
100	+ 2.7	+ 66.2	6.95E-4	00.70
200	+ 2.9	+ 60.4	2.43E-4	00.24
300	+ 30.1	+ 27.7	7.18E-5	00.07
350	+ 25.9	- 10.1	4.03E-5	00.04
400	+ 25.6	- 42.3	5.10E-5	00.05
450	+ 34.0	- 7.0	2.68E-5	00.02
500	+ 58.5	+ 20.2	1.28E-5	00.01

APPENDIX C

DETAILED SPECIMEN DIRECTIONS

SITE: PC21 SPEC#: PC102-A

TEMP	DEC	INC	J(A/M)	J/JN
20	+ .9	+ 88.4	1.28E-3	01.00
300	+ 23.0	+ 30.0	1.04E-4	00.06
350	+ 17.5	+ 7.4	7.84E-5	00.06
400	+ 9.6	- 35.5	4.15E-5	00.03
450	+ 26.7	+ 8.2	1.12E-5	00.00

SITE: PC-21 SPEC#: PC103-A

20	+346.7	+ 70.2	1.03E-3	01.00
300	+359.0	- 24.0	1.08E-4	00.10
350	+ 3.2	- 30.5	1.28E-4	00.12
400	+ 1.8	- 41.9	7.85E-5	00.07
450	+321.9	- 18.1	5.26E-5	00.05

SITE: PC21 SPEC#: PC104-A

20	+318.4	+ 78.0	8.25E-4	01.00
300	+ 19.2	+ 1.2	5.59E-5	00.06
350	+ 8.8	- 23.8	4.44E-5	00.05
400	+ 22.4	- 40.4	3.91E-5	00.04
450	+ 12.6	+ 49.7	2.49E-5	00.03

SITE: PC22 SPEC#: PC106-2.

20	+ 30.4	+ 76.5	7.24E-4	01.00
100	+ 8.4	+ 73.5	5.25E-4	00.72
200	+ 22.9	+ 71.8	2.12E-4	00.29
300	+ 22.5	+ 52.4	7.63E-5	00.10
350	+ 21.8	- 3.3	2.69E-5	00.03
400	+ 21.3	- 43.5	3.64E-5	00.05
450	+ 14.5	- 24.7	2.47E-5	00.03
500	+345.2	- 10.6	2.72E-5	00.03

SITE: PC22 SPEC#: PC107-A

20	+343.5	+ 64.6	9.51E-4	01.00
300	+332.3	- 60.3	4.49E-4	00.47
350	+332.0	- 62.3	3.63E-4	00.38
400	+334.2	- 64.6	2.06E-4	00.21
450	+322.0	- 64.8	2.77E-5	00.02

APPENDIX C

DETAILED SPECIMEN DIRECTIONS

SITE: PC22 SPEC#: PC108-R

TEMP	DEC	INC	J(A/M)	J/JN
20	+ 9.4	+ 80.4	8.43E-4	01.00
300	+ 13.1	- 46.6	2.03E-4	00.24
350	+ 12.5	- 46.4	1.81E-4	00.21
400	+ 19.1	- 46.7	7.39E-5	00.08
450	+ 30.3	- 31.7	3.22E-5	00.03
500	+ 56.3	- 3.0	2.87E-5	00.03

SITE: PC22 SPEC#: PC109-R

20	+ 10.2	+ 86.4	9.44E-4	01.00
300	+ 51.4	- 36.6	7.54E-5	00.08
350	+ 63.2	- 26.5	6.47E-5	00.07
400	+ 89.4	+ 30.8	4.09E-5	00.04
450	+119.5	+ 49.9	5.08E-5	00.06
500	+127.9	+ 59.9	3.16E-5	00.03

SITE: PC22 SPEC#: PC110-1

20	+271.0	+ 86.2	7.68E-4	01.00
300	+359.9	- 18.9	2.43E-5	00.03
350	+ 23.4	- 27.5	2.49E-5	00.03
400	+ 4.7	- 27.1	3.02E-5	00.03
450	+ 1.4	- 27.9	1.70E-5	00.02
500	+ 38.4	- 10.6	1.44E-5	00.01

APPENDIX D

SAMPLING LOCALITIES AND DIRECTIONS OF MAGNETIZATION -

TABLE HEAD GROUP

D.1 Sampling localities

Table Point Formation:

Locations: 48° 33.7'N, 58° 46.3'W (Sites AQ5-8)

50° 21.7'N, 57° 32.3'W (Sites PC15-18)

50° 42.8'N, 57° 23.7'W (Sites PC25-26)

50° 42.2'N, 57° 21.6'W (Sites PC27)

50° 31.9'N, 57° 23.6'W (Sites PC28-30)

Sites AQ5-8 were sampled from the Table Head Group, unconformably overlying the St. George Group at Aguathuna quarry in the Port au Port Peninsula. This locality has already been discussed in Section C.1. Sites PC15-18 were sampled from Table Head strata at Table Point (Figures 2.1, 2.4), also discussed in Section C.1.

Sites PC25-26 are exposed at Black Point in the Point Riche Peninsula, about 2-3 km along the shore from the Point Riche Lighthouse. At this locality the dolostones of the uppermost St. George Group and overlying limestones of the Table Point Formation are exposed. Only the limestones were sampled. Site PC27 was sampled near Gargamelle Cove and PC28-30 at River of Ponds, both in the Great Northern Peninsula.

Tilt correction and stratigraphic thickness:

<u>Sites</u>	<u>Strike,</u>	<u>Dip</u>	<u>Approx. thickness</u>
AQ5-8	267°,	15°N	3 m
PC15-18	130°,	11°SW	5.5 m
PC25-26	93°,	5°S	3 m
PC27	114°,	5°SW	4 m
PC28-30	46°,	5°SE	6 m

Table Cove Formation:

Location: 48° 35.5'N, 58° 55.3'W (Sites WB1-3)

These sites were sampled from a quarry in the West Bay, 1.75 km west of Picadilly Park along the north coast of the Port au Port Peninsula. The outcrop consists of interbedded limestones and shales. The average strike and dip of the beds are 259°, 11°NW. A 2 m thick stratigraphic section was covered by all the above three sites.

Cape Cormorant Formation:

Location: 48° 32.8'N, 59° 12.3'W (Sites ML1-7)

This exposure is located along the beach west of the town of Mainland on the west coast of Port au Port Peninsula. Two formations, Cape Cormorant and the overlying Mainland sandstone, are exposed at this locality. The Cape Cormorant Formation comprises carbonate breccia beds 0.1 to 0.3 m thick and interbedded shales. Total thickness of the stratigraphic section for the sampled sites was 50 m.

Tilt correction:

<u>Sites</u>	<u>Strike,</u>	<u>Dip</u>	<u>Sites</u>	<u>Strike,</u>	<u>Dip</u>
ML1	252°,	57°NW	ML5	238°,	52°NW
ML2	245°,	50°NW	ML6	240°,	50°NW
ML3	242°,	49°NW	ML7	234°,	50°NW
ML4	244°,	45°NW			

D.2 Detailed directions of magnetization

Results after each thermal demagnetization step of those specimens listed in Table 6.1 are listed in the following pages. The listing scheme is the same as described under Appendix B.2. Where applicable in the tables shown below, "360°C" should be read "370°C".

APPENDIX D

DETAILED SPECIMEN DIRECTIONS

SITE: AQ5 SPEC#: AQ17-C

TEMP	DEC	INC	J(R/M)	J/JN
20	+149.0	+ 66.0	1.11E-4	01.00
100	+151.0	+ 73.0	7.50E-5	00.67
200	+153.0	+ 33.0	6.14E-5	00.55
300	+155.0	+ 37.0	4.49E-5	00.40
350	+154.0	+ 38.0	3.39E-5	00.30
400	+152.0	+ 39.0	2.47E-5	00.22
450	+ 33.0	+ 66.0	8.18E-6	00.07

SITE: AQ5 SPEC#: AQ18-A

20	+149.0	+ 66.0	9.29E-5	01.00
100	+144.0	+ 84.0	5.78E-5	00.62
200	+162.0	+ 59.0	4.53E-5	00.48
300	+158.0	+ 44.0	3.25E-5	00.34
350	+156.0	+ 47.0	2.62E-5	00.28
400	+159.0	+ 35.0	2.34E-5	00.25
500	+ 96.0	+ 55.0	2.65E-6	00.02

SITE: AQ5 SPEC#: AQ19-A

20	+ 99.9	+ 70.0	1.61E-4	01.00
100	+140.7	+ 76.3	10.0E-5	00.62
200	+157.3	+ 60.2	8.23E-5	00.51
300	+157.3	+ 49.3	5.52E-5	00.34
350	+157.1	+ 61.2	3.82E-5	00.23
400	+163.4	+ 39.8	3.86E-5	00.24
450	+179.0	+ 55.9	2.12E-5	00.13
500	+158.9	+ 72.5	1.27E-5	00.07
530	+288.1	+ 81.6	8.66E-6	00.05
560	+264.9	+ 28.9	3.80E-6	00.02
590	+117.8	+ 51.6	3.62E-6	00.02

APPENDIX D

DETAILED SPECIMEN DIRECTIONS

SITE: AQ5 SPEC#: AQ20-A

TEMP	DEC	INC	J(A/M)	J/JN
20	+129.2	+ 69.0	8.34E-5	01.00
100	+126.9	+ 62.9	5.57E-5	00.66
200	+137.6	+ 38.7	3.38E-5	00.40
300	+147.5	+ 30.6	2.89E-5	00.34
350	+155.8	+ 23.8	2.21E-5	00.26
400	+149.9	+ 30.7	1.56E-5	00.18
450	+155.5	+ 30.6	1.57E-5	00.18
500	+147.6	+ 48.7	6.86E-6	00.08
530	+126.3	+ 13.7	3.79E-6	00.04
560	+135.0	+ 53.5	3.25E-6	00.03

SITE: AQ6 SPEC#: AQ21-B

20	+ 6.8	+ 34.4	3.08E-5	01.00
100	+346.2	+ 70.1	8.20E-6	00.26
200	+171.6	+ 42.0	7.91E-6	00.25
300	+172.1	+ 23.1	5.44E-6	00.17
350	+162.9	+ 24.9	7.06E-6	00.22
400	+162.1	+ 25.7	8.53E-6	00.27
450	+164.6	+ 20.6	7.72E-6	00.25
500	+166.2	+ 19.3	4.17E-6	00.13

SITE: AQ6 SPEC#: AQ23-A

20	+ 51.3	+ 61.4	6.21E-5	01.00
100	+ 78.8	+ 84.5	3.43E-5	00.55
200	+143.0	+ 43.4	3.13E-5	00.50
300	+145.6	+ 34.2	2.56E-5	00.41
350	+142.2	+ 26.8	2.31E-5	00.37
400	+142.4	+ 24.5	2.09E-5	00.33
450	+148.1	+ 33.1	1.19E-5	00.19
500	+143.1	+ 28.2	6.39E-6	00.10
530	+ 55.5	- 56.0	2.84E-6	00.04

APPENDIX D

DETAILED SPECIMEN DIRECTIONS

SITE: AQ8 SPEC#: AQ29-A

TEMP	DEC	INC	J(A/M)	J/JN
20	+127.2	+ 60.2	4.84E-4	01.00
100	+138.2	+ 51.3	3.81E-4	00.78
200	+144.1	+ 43.7	3.38E-4	00.69
300	+144.9	+ 33.3	2.83E-4	00.58
350	+145.5	+ 33.0	2.41E-4	00.49
400	+146.5	+ 32.3	1.85E-4	00.38
450	+152.7	+ 33.7	8.07E-5	00.16
500	+115.1	+ 23.5	1.16E-4	00.23
530	+ 55.0	+ 17.6	1.29E-4	00.26
560	+332.6	+ 60.8	7.04E-5	00.14
590	+343.0	+ 64.1	8.05E-5	00.16
620	+ 80.8	+ 36.2	3.74E-5	00.07

SITE: AQ8 SPEC#: AQ30-A

20	+131.0	+ 63.5	5.38E-4	01.00
100	+147.7	+ 51.3	4.49E-4	00.83
200	+154.1	+ 41.6	4.10E-4	00.76
300	+154.0	+ 33.3	3.61E-4	00.66
350	+154.4	+ 32.3	3.02E-4	00.56
400	+155.4	+ 32.1	2.36E-4	00.43
450	+174.2	+ 19.2	8.04E-5	00.14
500	+155.9	+ 28.1	7.46E-5	00.13
530	+180.5	+ 56.2	3.42E-5	00.06
560	+ 28.8	+ 43.6	5.24E-5	00.09
590	+199.0	+ 2.1	4.85E-5	00.09
620	+153.1	- 25.0	1.75E-5	00.03

SITE: AQ8 SPEC#: AQ32-1

20	+151.6	+ 55.1	5.12E-4	01.00
100	+156.0	+ 42.4	4.30E-4	00.84
200	+156.1	+ 33.9	3.86E-4	00.75
300	+161.3	+ 24.7	3.19E-4	00.62
350	+153.9	+ 26.6	2.29E-4	00.44
400	+160.8	+ 28.9	1.92E-4	00.37
450	+152.6	+ 38.3	8.50E-5	00.16
500	+138.2	+ 9.9	2.33E-5	00.04
530	+ 80.6	- 42.5	5.83E-5	00.11
560	+337.4	+ 36.8	6.04E-5	00.11
590	+293.7	- 62.7	5.31E-5	00.10
620	+ 89.7	- 13.4	2.88E-5	00.05

APPENDIX D

DETAILED SPECIMEN DIRECTIONS

SITE: WB1 SPEC#: WB1-1

TEMP	DEC	INC	J(A/M)	J/JN
20	+153.6	+ 39.0	1.59E-3	01.00
100	+154.5	+ 38.3	1.39E-3	00.87
200	+153.4	+ 32.8	1.31E-3	00.82
300	+159.9	+ 29.8	1.14E-3	00.71
350	+158.0	+ 29.8	1.04E-3	00.65
400	+157.9	+ 30.9	3.60E-4	00.22
450	+154.7	+ 38.1	1.45E-4	00.09
500	+140.2	- 31.4	1.20E-4	00.07
530	+ 31.9	- 9.8	8.90E-5	00.05
560	+215.5	+ 8.5	8.89E-5	00.05

SITE: WB1 SPEC#: WB2-A

20	+142.0	+ 41.8	1.31E-3	01.00
100	+148.5	+ 36.5	1.21E-3	00.92
200	+153.7	+ 31.4	1.18E-3	00.90
300	+155.1	+ 27.8	1.09E-3	00.83
350	+154.7	+ 28.0	9.91E-4	00.75
400	+155.2	+ 27.7	5.28E-4	00.40
450	+154.2	+ 26.4	2.01E-4	00.15
500	+299.2	+ 1.6	1.58E-5	00.01
530	+334.5	+ 30.7	1.18E-4	00.09
560	+ .6	- 53.2	8.02E-5	00.06

SITE: WB1 SPEC#: WB3-1

20	+145.0	+ 39.9	1.40E-3	01.00
100	+150.2	+ 38.0	1.20E-3	00.86
200	+153.4	+ 32.3	1.12E-3	00.80
300	+155.2	+ 27.9	1.05E-3	00.74
350	+153.9	+ 28.9	9.55E-4	00.68
400	+155.7	+ 27.9	6.34E-4	00.45
450	+155.0	+ 28.7	2.29E-4	00.16
500	+ 36.1	- 10.1	5.42E-5	00.03
530	+347.3	- 3.8	6.51E-5	00.04
560	+316.7	+ 1.4	1.09E-4	00.07

APPENDIX D

DETAILED SPECIMEN DIRECTIONS

SITE: WB1 SPEC#: WB4-2

TEMP	DEC	INC	J(A/M)	J/JN
20	+139.7	+ 47.3	1.32E-3	01.00
100	+148.8	+ 44.2	1.13E-3	00.85
200	+153.1	+ 34.8	9.67E-4	00.73
300	+152.6	+ 30.4	9.00E-4	00.68
350	+150.9	+ 30.1	7.41E-4	00.55
400	+152.9	+ 37.4	1.68E-4	00.12
450	+176.0	+ 39.7	5.31E-5	00.04
500	+ 90.6	+ 34.0	1.22E-4	00.09
530	+282.0	+ 24.6	1.36E-4	00.10
560	+238.2	- 72.3	1.12E-4	00.08
590	+292.8	+ 6.3	5.15E-4	00.38

SITE: WB2 SPEC#: WB5-1

20	+138.5	+ 41.8	1.27E-3	01.00
100	+139.4	+ 41.0	1.09E-3	00.85
200	+144.3	+ 35.9	9.89E-4	00.77
300	+145.8	+ 30.9	9.19E-4	00.72
350	+144.7	+ 30.5	8.47E-4	00.66
400	+144.4	+ 30.1	6.07E-4	00.47
450	+143.9	+ 29.7	2.32E-4	00.18
500	+232.7	+ 48.5	4.69E-5	00.03
530	+ 72.6	+ 78.3	8.32E-5	00.06
560	+338.8	- 63.2	8.91E-5	00.07

SITE: WB2 SPEC#: WB6-1

20	+132.6	+ 47.6	1.07E-3	01.00
100	+141.4	+ 44.7	9.41E-4	00.88
200	+147.5	+ 36.3	8.81E-4	00.82
300	+147.9	+ 30.9	8.22E-4	00.76
350	+149.5	+ 30.4	7.40E-4	00.69
400	+148.9	+ 30.0	4.89E-4	00.45
450	+155.2	+ 30.9	1.61E-4	00.15
500	+358.1	+ 51.3	6.34E-5	00.05
530	+ 87.9	+ 16.4	8.53E-5	00.07
560	+302.1	+ 77.8	6.01E-5	00.05

APPENDIX D

DETAILED SPECIMEN DIRECTIONS

SITE: WB2 SPEC#: WB7-1

TEMP	DEC	INC	J(R/M)	J/JN
20	+151.0	+ 38.2	1.38E-3	01.00
100	+152.3	+ 36.9	1.13E-3	00.81
200	+153.4	+ 30.6	1.02E-3	00.73
300	+151.0	+ 26.6	9.34E-4	00.67
350	+155.0	+ 26.8	7.56E-4	00.55
400	+154.1	+ 26.6	4.21E-4	00.30
450	+153.6	+ 28.5	1.03E-4	00.07
500	+356.2	- 6.2	1.23E-4	00.08
530	+314.8	+ 63.8	1.62E-4	00.11
560	+332.9	+ 4.3	1.62E-4	00.11

SITE: WB2 SPEC#: WB8-A

20	+141.0	+ 47.9	1.12E-3	01.00
100	+149.4	+ 40.8	1.04E-3	00.92
200	+153.5	+ 31.5	9.64E-4	00.86
300	+152.1	+ 27.1	9.15E-4	00.81
350	+152.0	+ 26.4	7.85E-4	00.70
400	+151.7	+ 30.1	2.81E-4	00.25
450	+150.4	+ 26.6	7.91E-5	00.07
500	+142.2	- 3.0	7.64E-5	00.06
530	+300.0	+ 71.0	1.46E-4	00.13
560	+194.1	+ 37.5	1.88E-4	00.16
590	+ 6.1	+ 11.4	2.27E-4	00.20

SITE: WB3 SPEC#: WB9-A

20	+146.1	+ 36.5	1.73E-3	01.00
100	+152.6	+ 33.6	1.61E-3	00.92
200	+154.9	+ 28.9	1.55E-3	00.89
300	+154.7	+ 26.4	1.36E-3	00.78
350	+153.9	+ 25.8	1.06E-3	00.61
400	+153.8	+ 28.9	2.21E-4	00.12
450	+151.8	+ 28.6	1.66E-4	00.09
500	+ 19.2	- 1.6	8.40E-5	00.04
530	+ 84.5	+ 25.9	7.00E-5	00.04
560	+221.1	+ 24.2	1.54E-4	00.08

APPENDIX D

DETAILED SPECIMEN DIRECTIONS

SITE: WB3 SPEC#: WB10-B

TEMP	DEC	INC	J(A/M)	J/JN
20	+148.0	+ 38.3	1.37E-3	01.00
100	+150.9	+ 34.4	1.25E-3	00.91
200	+153.4	+ 28.5	1.16E-3	00.84
300	+153.9	+ 24.1	1.07E-3	00.78
350	+156.0	+ 24.3	8.92E-4	00.65
400	+155.7	+ 24.4	2.57E-4	00.18
450	+153.9	+ 25.7	2.09E-4	00.15
500	+ 95.2	- 53.3	4.15E-5	00.03
530	+156.8	+ 37.8	1.23E-4	00.09
560	+248.7	- 72.8	1.26E-4	00.09

SITE: WB3 SPEC#: WB11-A

20	+137.9	+ 39.5	1.54E-3	01.00
100	+143.3	+ 35.7	1.45E-3	00.94
200	+146.9	+ 29.7	1.41E-3	00.91
300	+149.8	+ 26.3	1.31E-3	00.85
350	+150.1	+ 25.7	1.12E-3	00.72
400	+151.2	+ 26.1	3.98E-4	00.25
450	+149.1	+ 26.8	3.16E-4	00.20
500	+ 53.9	+ 40.2	4.99E-5	00.03
530	+296.0	+ 33.5	1.41E-4	00.09
560	+199.8	+ 85.9	1.73E-4	00.11

SITE: WB3 SPEC#: WB12-B

20	+148.7	+ 53.0	1.28E-3	01.00
100	+145.2	+ 44.6	1.19E-3	00.92
200	+146.9	+ 35.5	1.12E-3	00.87
300	+148.2	+ 31.5	1.09E-3	00.84
350	+149.5	+ 31.0	9.54E-4	00.74
400	+150.9	+ 33.4	3.91E-4	00.30
450	+143.2	+ 33.4	9.17E-5	00.07
500	+231.1	+ 29.4	2.32E-4	00.18
530	+335.7	+ 35.6	2.24E-4	00.17
560	+111.5	+ 25.4	1.60E-4	00.12
590	+331.4	- 7.3	5.80E-5	00.04

APPENDIX D

DETAILED SPECIMEN DIRECTIONS

SITE: ML1 SPEC#: ML2-A

TEMP	DEC	INC	J(A/M)	J/JN
20	+ 72.1	+ 47.6	1.71E-4	01.00
300	+148.8	- 19.2	3.30E-5	00.19
350	+142.6	- 22.3	2.87E-5	00.16
400	+ 81.0	- 54.5	7.39E-6	00.04
450	+ 11.0	- 27.9	3.77E-5	00.22
500	+352.1	- 29.0	1.53E-4	00.89

SITE: ML1 SPEC#: ML3-A

20	+104.6	+ 49.7	1.48E-4	01.00
300	+123.2	- 3.4	4.80E-5	00.32
350	+150.5	- 41.5	4.02E-5	00.27
400	+167.5	- 17.5	3.42E-5	00.23
450	+166.4	- 46.0	2.06E-5	00.13
500	+349.7	- 11.7	6.44E-5	00.43

SITE: ML1 SPEC#: ML4-C

20	+ 79.7	+ 61.5	1.37E-4	01.00
300	+132.1	- 2.3	3.31E-5	00.24
330	+117.9	+ 2.6	3.31E-5	00.24
350	+139.2	- 16.1	3.13E-5	00.22
360	+141.1	- 6.4	3.57E-5	00.26
400	+138.5	- 30.7	2.73E-5	00.19
450	+110.4	- 7.0	2.03E-5	00.14

SITE: ML2 SPEC#: ML6-B

20	+ 71.8	+ 62.2	2.21E-4	01.00
300	+115.5	+ 4.3	5.00E-5	00.22
330	+122.4	- 13.8	5.58E-5	00.25
350	+134.2	- 26.6	5.00E-5	00.22
360	+119.0	- 19.7	4.56E-5	00.20
400	+128.1	- 31.9	3.33E-5	00.15
450	+144.9	- 24.7	3.42E-5	00.15
500	+321.2	- 20.4	3.48E-5	00.15

APPENDIX D

DETAILED SPECIMEN DIRECTIONS

SITE: ML2 SPEC#: ML6-C

TEMP	DEC	INC	J(A/M)	J/JN
20	+148.3	+ 53.8	1.60E-4	01.00
100	+145.8	+ 37.0	1.03E-4	00.64
200	+150.3	+ 4.9	7.55E-5	00.47
300	+159.4	- 21.8	7.92E-5	00.48
350	+154.3	- 23.9	7.12E-5	00.44
400	+143.0	- 24.8	4.14E-5	00.25
450	+149.0	- 28.2	3.54E-5	00.22
500	+114.3	- 43.5	2.16E-5	00.13

SITE: ML3 SPEC#: ML10-A

20	+ 11.1	+ 40.1	5.29E-4	01.00
300	+ 4.4	+ 21.7	2.60E-4	00.49
350	+352.4	+ 25.5	1.26E-4	00.23
400	+337.3	+ 30.9	4.91E-5	00.09
450	+ 3.3	+ 31.8	4.10E-5	00.07
500	+319.5	- 32.4	1.39E-5	00.02

SITE: ML3 SPEC#: ML10-C

20	+ 93.4	+ 56.7	1.39E-4	01.00
300	+135.4	- 13.3	2.98E-5	00.21
330	+140.4	- 27.0	3.14E-5	00.22
350	+130.1	- 32.4	2.81E-5	00.20
360	+132.7	- 46.5	1.57E-5	00.11
400	+128.7	- 25.5	1.96E-5	00.14
450	+258.4	- 73.3	1.46E-5	00.10
500	+338.3	- 15.3	3.13E-5	00.22

SITE: ML3 SPEC#: ML11-B

20	+ 69.8	+ 50.5	2.35E-4	01.00
300	+129.1	- 17.0	7.76E-5	00.33
350	+148.5	- 17.0	7.33E-5	00.31
400	+150.3	- 11.9	2.26E-5	00.09
450	+ 1.9	+ 24.1	4.73E-5	00.20
500	+ 20.0	- 27.3	7.28E-5	00.30

APPENDIX D

DETAILED SPECIMEN DIRECTIONS

SITE: ML3 SPEC#: ML11-C

TEMP	DEC	INC	J(A/M)	J/JN
20	+ 95.5	+ 66.2	1.58E-4	01.00
300	+162.5	- 45.8	2.76E-5	00.17
330	+155.3	- 19.0	5.73E-5	00.36
350	+157.8	- 42.0	4.62E-5	00.29
360	+189.9	- 69.7	2.38E-5	00.15
400	+ 88.1	- 47.2	2.20E-5	00.13
450	+303.8	+ 48.3	1.40E-5	00.08

SITE: ML4 SPEC#: ML14-B

20	+ 82.8	+ 61.6	1.33E-4	01.00
300	+120.7	- 25.2	2.64E-5	00.19
350	+129.1	- 7.7	1.82E-5	00.13
400	+126.2	+ 8.5	1.88E-5	00.14
450	+ 41.2	+ 11.0	1.98E-5	00.14
500	+232.6	- 16.2	3.91E-5	00.29

SITE: ML4 SPEC#: ML14-C

20	+189.6	+ 56.1	1.36E-4	01.00
300	+188.5	- 9.0	4.80E-5	00.35
330	+185.7	- 19.1	3.33E-5	00.24
350	+177.8	- 13.0	4.01E-5	00.29
360	+200.7	- 24.7	3.30E-5	00.24
400	+195.6	7 30.8	2.58E-5	00.18
450	+ 1.0	- .7	7.70E-6	00.05
500	+291.9	- 43.0	2.80E-5	00.20

SITE: ML5 SPEC#: ML17-1

20	+102.1	+ 62.6	1.62E-4	01.00
300	+125.4	+ 16.0	4.17E-5	00.25
330	+125.9	+ 12.9	3.98E-5	00.24
350	+ 45.0	+ 12.7	4.55E-5	00.28
360	+130.8	- 17.4	3.34E-5	00.20
400	+118.2	- 28.3	8.63E-6	00.05
450	+ 26.4	- 47.5	2.16E-5	00.13

APPENDIX D

DETAILED SPECIMEN DIRECTIONS

SITE: ML5 SPEC#: ML17-4

TEMP	DEC	INC	J(A/M)	J/JN
20	+ 85.0	+ 58.7	2.09E-4	01.00
300	+112.3	+ 22.5	4.89E-5	00.23
350	+111.5	+ 14.4	3.66E-5	00.17
400	+139.7	- 6.9	2.18E-5	00.10
450	+ 9.2	+ 41.0	1.18E-5	00.05
500	+ 42.0	- 39.2	1.35E-5	00.06

SITE: ML7 SPEC#: ML24-1

20	+118.7	+ 33.1	1.27E-4	01.00
300	+133.1	- 45.4	8.28E-5	00.65
350	+119.4	- 37.6	5.55E-5	00.43
400	+126.0	- 43.8	4.08E-5	00.32
450	+ 99.3	- 51.0	2.91E-5	00.22
500	+321.7	- 76.3	3.78E-5	00.29

SITE: ML7 SPEC#: ML24-2

20	+120.1	+ 70.4	7.72E-5	01.00
300	+146.1	- 28.4	3.38E-5	00.43
330	+131.4	- 39.3	4.02E-5	00.52
350	+141.9	- 51.6	4.97E-5	00.63
360	+135.2	- 50.9	5.18E-5	00.67
400	+145.8	- 39.0	5.29E-5	00.68
450	+212.9	- 12.8	3.65E-6	00.04

SITE: ML7 SPEC#: ML25-1

20	+116.8	+ 46.4	1.30E-4	01.00
300	+144.2	- 25.1	3.01E-5	00.23
350	+148.4	- 52.8	2.47E-5	00.18
400	+151.6	- 41.4	1.35E-5	00.10
450	+355.9	- 21.5	1.31E-5	00.10
500	+327.5	+ 16.4	4.42E-5	00.33

APPENDIX D

DETAILED SPECIMEN DIRECTIONS

SITE: ML7 SPEC#: ML25-2

TEMP	DEC	INC	J(R/M)	J/JN
20	+ 95.7	+ 69.7	1.17E-4	01.00
300	+113.2	- 10.2	4.04E-5	00.34
330	+115.5	- 27.8	4.00E-5	00.34
350	+119.6	- 18.4	3.45E-5	00.29
360	+143.8	+ 5.8	2.88E-5	00.24
400	+146.1	- 50.8	2.98E-5	00.25
450	+342.6	- 44.7	1.20E-5	00.10

SITE: ML7 SPEC#: ML27-1

- 20	+104.0	+ 49.5	1.35E-4	01.00
300	+117.1	- 19.0	4.80E-5	00.35
330	+121.6	- 13.2	4.04E-5	00.29
350	+115.0	- 20.9	4.62E-5	00.34
360	+132.2	- 22.9	3.04E-5	00.22
400	+140.8	- 23.6	2.40E-5	00.17
450	+ 3.8	+ 15.9	3.63E-5	00.26

SITE: ML7 SPEC#: ML27-2

20	+118.0	+ 41.1	1.04E-4	01.00
300	+142.6	- 54.5	3.51E-5	00.33
350	+111.3	- 41.0	2.73E-5	00.26
400	+121.2	- 29.9	1.61E-5	00.15
450	+ 16.9	- 20.7	1.97E-5	00.18
500	+345.5	- 17.0	4.13E-5	00.39

SITE: PC15 SPEC#: PC72-1

20	+ 79.8	+ 75.0	1.96E-3	01.00
300	+ 9.4	+ 42.0	7.33E-5	00.03
350	+ 20.6	- 22.3	4.79E-5	00.02
400	+ 16.1	- 48.8	4.16E-5	00.02
450	+ 25.8	+ 41.2	3.87E-5	00.01

SITE: PC15 SPEC#: PC73-1

20	+106.4	+ 71.7	1.31E-3	01.00
300	+ 23.7	+ 27.0	5.08E-5	00.03
350	+ 29.5	- 20.3	4.55E-5	00.03
400	+ 18.3	- 47.3	2.81E-5	00.02
450	+ 16.6	+ 23.1	3.98E-5	00.03

APPENDIX D

DETAILED SPECIMEN DIRECTIONS

SITE: PC15 SPEC#: PC74-2

TEMP	DEC	INC	J(A/M)	J/JN
20	+ 98.5	+ 80.8	1.20E-3	01.00
300	+ 14.7	- 30.4	7.25E-5	00.06
350	+ 11.0	- 48.3	8.50E-5	00.07
400	+ 16.7	- 55.9	6.79E-5	00.05
450	+ 13.3	+ 43.3	4.33E-5	00.03

SITE: PC15 SPEC#: PC75-2

20	+162.8	+ 75.0	1.50E-3	01.00
300	+ 44.2	+ 66.8	5.52E-5	00.03
350	+ 25.0	- 23.8	2.31E-5	00.01
400	+ 26.1	- 33.1	2.10E-5	00.01
450	+ 16.3	+ 49.5	5.59E-5	00.03

SITE: PC16 SPEC#: PC76-B

20	+ 57.4	+ 24.4	9.36E-5	01.00
100	+ 55.9	- 2.5	7.76E-5	00.92
200	+ 62.9	- 25.3	7.95E-5	00.84
300	+ 67.6	- 41.0	5.87E-5	00.62
350	+ 68.3	- 40.2	5.28E-5	00.56
400	+ 67.3	- 33.3	2.06E-5	00.22
450	+ 52.0	- 19.6	1.56E-5	00.16
500	+ 48.7	+ 10.7	8.40E-6	00.08
560	+ 24.8	- 3.0	7.71E-6	00.08
590	+ 81.4	+ 40.4	5.49E-6	00.05

SITE: PC16 SPEC#: PC77-1

20	+ 83.8	+ 72.5	9.21E-4	01.00
300	+ 60.3	+ 63.3	3.04E-5	00.13
350	+ 59.0	+ 44.5	1.72E-5	00.07
400	+ 68.0	+ 45.0	1.32E-5	00.05
450	+337.9	+ 10.9	3.08E-5	00.13

APPENDIX D

DETAILED SPECIMEN DIRECTIONS

SITE: PC17 SPEC#: PC81-2

TEMP	DEC	INC	J(R/M)	J/JN
20	+358.7	+ 75.3	3.06E-3	01.00
100	+337.6	+ 72.9	2.02E-3	00.66
200	+337.9	+ 69.5	7.49E-4	00.24
300	+341.1	+ 54.3	2.10E-4	00.06
350	+351.9	+ 30.6	1.12E-4	00.03
400	+340.7	- 51.7	1.18E-4	00.03
450	+358.8	- 35.9	6.04E-5	00.01
500	+256.3	- .8	2.82E-5	00.00

SITE: PC17 SPEC#: PC82-1

20	+ 47.6	+ 81.8	2.69E-3	01.00
300	+ 10.5	+ 14.8	1.29E-4	00.04
350	+ 10.2	- 22.7	1.37E-4	00.05
400	+ 11.5	- 43.6	8.55E-5	00.03
450	+ 19.0	- 39.4	4.88E-5	00.01

SITE: PC17 SPEC#: PC83-2

20	+349.4	+ 68.9	2.11E-3	01.00
300	+351.4	+ 24.3	8.92E-5	00.04
350	+352.2	- 31.8	8.85E-5	00.04
400	+ 3.9	- 52.8	7.82E-5	00.03
450	+359.7	- 48.5	3.39E-5	00.01

SITE: PC17 SPEC#: PC84-2

20	+339.4	+ 78.2	2.07E-3	01.00
300	+ 23.5	+ 48.8	6.40E-5	00.03
350	+ 22.3	- 24.8	5.98E-5	00.02
400	+ 19.0	- 51.2	7.13E-5	00.03
450	+ 17.7	- 41.7	3.96E-5	00.01

SITE: PC17 SPEC#: PC85-2

20	+ 20.5	+ 77.5	2.46E-3	01.00
300	+ 16.7	+ 19.5	1.12E-4	00.04
350	+ 14.8	- 22.2	1.02E-4	00.04
400	+ 13.5	- 51.1	9.71E-5	00.03
450	+ 25.5	- 26.8	3.28E-5	00.01

APPENDIX D

DETAILED SPECIMEN DIRECTIONS

SITE: PC18 SPEC#: PC90-1

TEMP	DEC	INC	J(A/M)	J/JN
20	+336.9	+ 84.5	2.14E-3	01.00
300	+ 47.8	+ 73.1	1.43E-4	00.06
350	+ 66.0	+ 74.3	8.61E-5	00.04
400	+ 52.9	+ 41.0	4.31E-5	00.02
450	+ 54.3	+ 40.2	4.11E-5	00.01

SITE: PC25 SPEC#: PC121-B

20	+107.5	+ 75.2	4.02E-3	01.00
300	+158.9	+ 47.1	5.01E-4	00.12
350	+160.5	+ 33.6	3.79E-4	00.09
400	+167.2	+ 11.2	2.23E-4	00.05
450	+170.4	+ 12.7	1.60E-4	00.03
500	+207.4	+ 39.5	3.64E-5	00.00

SITE: PC25 SPEC#: PC122-A

20	+119.2	+ 80.2	3.68E-3	01.00
300	+153.5	+ 21.0	3.53E-4	00.09
350	+149.3	+ 7.0	2.63E-4	00.07
400	+153.1	+ 5.9	2.07E-4	00.05
450	+152.6	+ 5.5	1.37E-4	00.03
500	+168.9	+ 33.0	2.90E-5	00.00

SITE: PC25 SPEC#: PC123-2

20	+ 32.0	+ 84.2	2.19E-3	01.00
300	+139.5	+ 72.2	2.08E-4	00.09
350	+134.4	+ 69.0	1.55E-4	00.07
400	+128.5	+ 65.6	7.29E-5	00.03
450	+140.5	+ 61.4	5.15E-5	00.02
500	+ 87.9	+ 80.2	2.87E-5	00.01

SITE: PC25 SPEC#: PC124-2

20	+343.2	+ 72.6	2.13E-3	01.00
300	+120.6	+ 79.3	2.39E-4	00.11
350	+123.7	+ 79.7	1.94E-4	00.09
400	+107.1	+ 78.3	9.20E-5	00.04
450	+118.6	+ 67.4	7.78E-5	00.03
500	+259.5	+ 51.3	2.25E-5	00.01

APPENDIX D

DETAILED SPECIMEN DIRECTIONS

SITE: PC25 SPEC#: PC125-A

TEMP	DEC	INC	J(R/M)	J/JN
20	+ 82.6	+ 84.4	2.57E-3	01.00
300	+148.5	+ 43.7	2.82E-4	00.10
350	+148.0	+ 35.7	2.23E-4	00.08
400	+148.2	+ 19.6	1.04E-4	00.04
450	+154.6	+ 19.5	8.06E-5	00.03
500	+ 85.7	- 9.6	2.73E-5	00.01

SITE: PC26 SPEC#: PC126-1

20	+ 63.1	+ 84.2	2.49E-3	01.00
100	+ 50.0	+ 82.6	1.67E-3	00.67
200	+110.3	+ 76.2	7.62E-4	00.30
300	+127.7	+ 60.4	3.75E-4	00.15
350	+135.2	+ 48.9	2.61E-4	00.10
400	+132.3	+ 47.6	1.87E-4	00.07
450	+123.9	+ 71.2	5.23E-5	00.02
500	+ 73.8	- 68.4	2.96E-5	00.01

SITE: PC26 SPEC#: PC127-1

20	+139.3	+ 76.9	2.37E-3	01.00
300	+139.3	+ 51.3	3.26E-4	00.13
350	+137.8	+ 45.2	2.49E-4	00.10
400	+143.1	+ 42.3	1.30E-4	00.05
450	+138.7	+ 45.9	7.87E-5	00.03
500	+174.1	+ 44.1	3.42E-5	00.01

SITE: PC26 SPEC#: PC128-A

20	+358.5	+ 77.0	2.14E-3	01.00
300	+167.5	+ 68.0	2.93E-4	00.13
350	+152.4	+ 66.0	2.42E-4	00.11
400	+151.5	+ 64.0	1.05E-4	00.04
450	+142.5	+ 56.4	1.05E-4	00.04
500	+230.2	+ 80.8	3.58E-5	00.01

APPENDIX D

DETAILED SPECIMEN DIRECTIONS

SITE: PC26 SPEC#: PC129-B

TEMP	DEC	INC	J(A/M)	J/JN
20	+ 50.1	+ 76.3	2.19E-3	01.00
300	+109.4	+ 72.2	3.57E-4	00.16
350	+114.9	+ 66.0	2.77E-4	00.12
400	+115.0	+ 64.2	1.15E-4	00.05
450	+133.0	+ 60.0	10.0E-5	00.04
500	+ 75.9	+ 54.0	3.97E-5	00.01

SITE: PC26 SPEC#: PC130-A

20	+341.2	+ 72.0	2.27E-3	01.00
300	+131.9	+ 74.7	2.97E-4	00.13
350	+130.3	+ 70.3	2.18E-4	00.09
400	+131.5	+ 69.7	8.37E-5	00.03
450	+141.7	+ 55.5	8.70E-5	00.03
500	+249.5	+ 18.8	3.02E-5	00.01

SITE: PC27 SPEC#: PC131-B

20	+355.7	+ 79.2	5.93E-4	01.00
100	+346.6	+ 79.3	4.89E-4	00.82
200	+354.2	+ 78.3	3.12E-4	00.52
300	+ 6.6	+ 75.2	1.52E-4	00.25
350	+ 17.0	+ 68.6	3.96E-5	00.06
400	+ 21.7	+ 66.2	3.50E-5	00.05
450	+ 30.6	+ 76.6	2.02E-5	00.03
500	+ 7.0	+ 58.1	1.65E-5	00.02

SITE: PC27 SPEC#: PC133-A

20	+ 59.6	+ 82.0	2.24E-4	01.00
300	+ 94.0	+ 64.0	3.14E-5	00.13
350	+110.7	+ 73.7	1.92E-5	00.08
400	+ 63.9	+ 53.6	1.05E-5	00.04
450	+163.9	+ 71.9	1.08E-5	00.04

SITE: PC27 SPEC#: PC135-A

20	+ 24.0	+ 80.9	4.61E-4	01.00
300	+ 56.7	+ 46.2	6.15E-5	00.13
350	+ 65.9	+ 43.7	4.91E-5	00.10
400	+ 81.1	+ 31.9	2.20E-5	00.04
450	+ 54.5	+ 31.2	1.51E-5	00.03

APPENDIX D

DETAILED SPECIMEN DIRECTIONS

SITE: PC28 SPEC#: PC137-1

TEMP	DEC	INC	J(A/M)	J/JN
20	+302.4	+ 76.8	7.55E-4	01.00
100	+314.5	+ 77.7	5.19E-4	00.68
200	+309.7	+ 78.6	2.93E-4	00.38
300	+325.4	+ 83.6	1.37E-4	00.18
350	+313.4	+ 79.6	7.82E-5	00.10
400	+ 76.5	+ 59.2	1.84E-5	00.02
450	+ 85.1	+ 72.0	1.60E-5	00.02
500	+ 63.2	+ 46.8	1.83E-5	00.02
530	+271.9	+ 47.4	5.72E-6	00.00

SITE: PC28 SPEC#: PC138-1

20	+331.1	+ 73.9	6.93E-4	01.00
300	+ 48.8	+ 63.1	7.21E-5	00.10
350	+ 30.2	+ 75.1	5.52E-5	00.07
400	+ 47.6	+ 32.4	9.54E-6	00.01
450	+ 84.9	+ 36.4	1.36E-5	00.01

SITE: PC28 SPEC#: PC139-1

20	+315.3	+ 73.8	6.48E-4	01.00
300	+352.6	+ 68.3	1.24E-4	00.19
350	+ .3	+ 61.6	1.07E-4	00.16
400	+ 25.4	+ 39.2	2.16E-5	00.03
450	+ 15.4	+ 44.2	2.39E-5	00.03

SITE: PC28 SPEC#: PC140-B

20	+121.0	+ 53.0	1.25E-3	01.00
300	+118.1	+ 38.2	3.05E-4	00.24
350	+117.0	+ 38.6	1.66E-4	00.13
400	+198.0	+ 78.7	2.16E-5	00.01
450	+202.2	+ 64.6	1.09E-5	00.00

SITE: PC29 SPEC#: PC142-1

20	+ 85.5	+ 75.7	1.07E-3	01.00
300	+ 44.7	+ 65.6	9.11E-5	00.08
350	+ 64.8	+ 66.1	7.63E-5	00.07
400	+ 65.4	+ 62.7	2.39E-5	00.02
450	+ 9.6	+ 69.4	2.14E-5	00.01
500	+ 76.1	- 19.7	1.13E-5	00.01

APPENDIX D

DETAILED SPECIMEN DIRECTIONS

SITE: PC29 SPEC#: PC143-A

TEMP	DEC	INC	J(A/M)	J/JN
20	+352.2	+ 72.4	5.86E-4	01.00
300	+ 94.6	+ 84.0	4.33E-5	00.07
350	+107.6	+ 76.4	2.58E-5	00.04
400	+112.8	+ 52.9	1.61E-5	00.02
450	+126.2	+ 62.2	1.98E-5	00.03

SITE: PC29 SPEC#: PC145-B

20	+338.7	+ 85.3	8.21E-4	01.00
300	+ 41.5	+ 68.2	2.97E-5	00.03
350	+ 57.9	+ 44.9	2.06E-5	00.02
400	+ 48.2	+ 48.0	2.20E-5	00.02
450	+122.7	+ 30.0	1.90E-5	00.02

SITE: PC30 SPEC#: PC146-A

20	+ 19.6	+ 76.5	1.73E-3	01.00
300	+ 10.0	+ 68.6	1.06E-4	00.06
350	+ 26.9	+ 56.2	4.54E-5	00.02
400	+ 66.0	+ 54.8	2.12E-5	00.01
450	+ 74.4	+ 45.1	1.78E-5	00.01

SITE: PC30 SPEC#: PC147-1

20	+ 7.4	+ 85.7	1.19E-3	01.00
300	+ 30.0	+ 82.8	8.36E-5	00.07
350	+ 57.9	+ 69.9	4.60E-5	00.03
400	+ 48.8	+ 66.0	1.61E-5	00.01
450	+105.2	+ 44.8	1.78E-5	00.01

SITE: PC30 SPEC#: PC149-2

20	+338.8	+ 82.4	8.29E-4	01.00
300	+261.7	+ 89.6	8.12E-5	00.09
350	+ 70.7	+ 84.6	4.64E-5	00.05
400	+114.4	+ 56.9	1.34E-5	00.01
450	+ 66.7	+ 78.9	9.25E-6	00.01

APPENDIX E

SAMPLING LOCALITY AND DIRECTIONS OF MAGNETIZATION -

LONG POINT GROUP

E.1 Sampling locality

Lourdes Limestone: 48° 41.1'N, 58° 53.5'W (Sites BD1-4)

An outcrop at Black Duck Brook, on the southeastern shore of the Long Point Peninsula, was sampled. The strata are exposed in seacliffs. The total stratigraphic thickness covered by the above 4 sites was 9 meters.

Tilt correction:

<u>Sites</u>	<u>Strike,</u>	<u>Dip</u>
BD1	220°,	40°NW
BD2	225°,	38°NW
BD3	223°,	43°NW
BD4	224°,	38°NW

E.2 Detailed directions of magnetization

Following are the directions of magnetization after each step of thermal demagnetization for those specimens listed in Table 7.1 from which a characteristic direction was computed. The listing scheme is the same as described under Appendix B.2. Where applicable in the tables below, "360°C" should be read "370°C".

APPENDIX E

DETAILED SPECIMEN DIRECTIONS

SITE: BD1 SPEC#: BD1-B

TEMP	DEC	INC	J(A/M)	J/JN
20	+ 90.6	+ 80.2	2.39E-4	01.00
300	+343.2	+ 24.7	1.24E-4	00.51
350	+257.8	+ 34.5	2.27E-5	00.09
400	+ 6.6	- 18.8	3.37E-5	00.14
450	+ 7.5	- 21.4	7.15E-5	00.29
500	+334.9	- 42.7	6.88E-5	00.28

SITE: BD1 SPEC#: BD1-D

20	+ 56.5	+ 75.1	2.07E-4	01.00
300	+350.7	+ 36.1	5.03E-5	00.24
330	+ 36.5	+ 62.0	6.30E-5	00.30
350	+ 73.7	+ 67.9	4.55E-5	00.21
360	+ 92.3	+ 59.9	4.42E-5	00.21
400	+134.3	+ 69.9	3.95E-5	00.19
450	+ 71.2	- 58.1	1.57E-5	00.07

SITE: BD2 SPEC#: BD6-D

20	+ 28.4	+ 84.3	1.61E-4	01.00
300	+ 22.4	+ 34.0	6.27E-5	00.33
330	+ 25.5	+ 31.8	7.12E-5	00.44
350	+ 18.3	+ 25.1	6.28E-5	00.38
360	+ 24.7	+ 20.4	5.49E-5	00.34
400	+ 21.8	+ 5.9	3.29E-5	00.20
450	+ 6.9	+ 32.4	4.65E-5	00.28

SITE: BD4 SPEC#: BD13-A

20	+ 2.9	+ 52.2	1.47E-4	01.00
300	+338.0	+ 25.0	6.78E-5	00.46
330	+341.7	+ 25.7	6.83E-5	00.46
350	+339.2	+ 18.4	6.29E-5	00.42
360	+339.5	+ 26.5	6.82E-5	00.46
400	+340.5	+ 31.6	6.90E-5	00.46
450	+321.0	+ 10.5	4.87E-5	00.33
500	+ .0	- 28.5	2.18E-4	01.48

APPENDIX E

DETAILED SPECIMEN DIRECTIONS

SITE: BD4 SPEC#: BD13-0

TEMP	DEC	INC	J(A/M)	J/JN
20	+ 8.3	+ 63.1	2.21E-4	01.00
300	+348.4	+ 52.3	9.51E-5	00.42
350	+347.3	+ 47.4	6.90E-5	00.31
400	+338.5	+ 49.6	4.21E-5	00.19
450	+350.2	+ 27.7	1.21E-4	00.54
500	+359.2	+ 31.3	1.98E-4	00.89

SITE: BD4 SPEC#: BD14-A

20	+338.7	+ 76.2	2.18E-4	01.00
100	+335.2	+ 64.2	1.54E-4	00.70
200	+334.2	+ 33.8	1.05E-4	00.48
300	+330.3	+ 50.9	9.45E-5	00.43
350	+346.8	+ 32.5	9.04E-5	00.41
400	+333.9	+ 35.8	7.04E-5	00.32
450	+345.4	- 13.9	1.11E-4	00.50
500	+350.2	- 13.3	1.35E-4	00.61

SITE: BD4 SPEC#: BD15-1

20	+333.6	+ 80.7	2.13E-4	01.00
300	+327.4	+ 23.6	8.18E-5	00.38
350	+331.5	+ 25.9	1.04E-4	00.48
400	+322.5	+ 22.4	9.88E-5	00.46
450	+355.2	+ 23.5	9.27E-5	00.43
500	+ 14.7	+ 26.7	1.22E-4	00.57

SITE: BD4 SPEC#: BD15-3

20	+ .3	+ 75.8	2.51E-4	01.00
300	+339.2	+ 9.7	8.49E-5	00.33
330	+345.3	+ 14.8	1.08E-4	00.42
350	+331.5	+ 10.0	8.92E-5	00.35
360	+333.3	+ 12.6	8.11E-5	00.32
400	+313.0	- .1	6.90E-5	00.27
450	+328.0	+ 25.6	9.32E-5	00.37
500	+344.0	- 40.9	1.22E-4	00.48

APPENDIX E

DETAILED SPECIMEN DIRECTIONS

SITE: BD4 SPEC#: BD17-B

TEMP	DEC	INC	J(R/M)	J/JN
20	+ 10.9	+ 77.1	4.99E-5	01.00
300	+341.6	+ 50.5	1.64E-5	00.32
350	+346.3	+ 24.6	1.19E-5	00.23
400	+265.1	+ 49.5	3.59E-6	00.07
450	+ 25.7	+ 10.5	9.95E-6	00.19
500	+ 36.0	+ 10.9	3.35E-5	00.67

SITE: BD4 SPEC#: BD17-C

20	+ 15.6	+ 65.5	5.13E-5	01.00
300	+ 3.2	+ 38.8	2.71E-5	00.52
330	+ .1	+ 29.9	2.54E-5	00.49
350	+352.5	+ 34.3	1.89E-5	00.36
360	+358.6	+ 29.5	1.70E-5	00.33
400	+ 4.9	+ 18.5	1.58E-5	00.30
450	+354.7	- .8	1.92E-5	00.37

APPENDIX F

STRUCTURAL CORRECTIONS AND DIRECTIONS OF MAGNETIZATION -

COW HEAD GROUP

F.1 Sampling locality

Cow Head Peninsula: $49^{\circ} 50.1'N$, $57^{\circ} 52.1'W$

F.2 Correction for plunging folds

In plunging folds, the axis of movement is the fold axis, which is not parallel to the strike of the beds on the limbs. To restore the beds to paleohorizontal, two components of rotation are required:

(1) The fold axis is rotated into a horizontal position through the angle of plunge. In this position the two limbs have the same strike, which is parallel to the fold axis. This process will change the apparent dip of each limb to a new dip value.

(2) The inclined planes of each limb are then restored to horizontality by rotating about the strike through the (new) dip values, as in the case of the non-plunging fold.

For the above two-step correction to the magnetization vectors the following steps were undertaken to determine the angle of plunge (items a-d, below) and then the bedding correction (items e-g).

(a) All the strike and dip measurements on the bedding were plotted as great circles and as poles on a Wulff's net (Figure 8.2a, poles are not shown)..

(b) All the poles were averaged separately for the two limbs, using Fisher's statistics.

(c) The strike and dip of each limb was determined, corresponding to the mean pole calculated in (b). This gives the in situ orientation of the limbs which was found to be as follows:

	<u>Strike,</u>	<u>Dip</u>
Eastern Limb	141°,	33°SW
Western Limb	47°,	58°SE

(d) Two great circles representing the strikes and dips of (c) were plotted on another stereogram (Figure 8.2b). From the point of intersection of the two great circles, the plunge angle = 30.5°, and the trend (fold axis) = S208W, were determined. Strictly speaking, this intersection should be the midpoint of the area of maximum density of the great circle intersections in Figure 8.2a. The intersection points in Figure 8.2a were subjected to Fisher's statistics and it was found that their mean position almost coincided with the intersection of the two great circles of Figure 8.2b.

(e) Next, the bedding was corrected for the plunge. The mean bedding pole for each limb was reoriented by rotating it through 30.5° along the fold axis (now S208W). The in situ magnetization vectors (Table 8.1) were now corrected for the plunge, using a horizontal axis striking 118°, and a dip of 30.5°SW.

(f) From the reoriented bedding poles in (e), the new

strike and dip angles of the two limbs were determined, corresponding to their non-plunging orientation (Fig.

8.2b). These are listed below:

	<u>Strike,</u>	<u>Dip</u>
Eastern Limb	208°,	12.5°NW
Western Limb	28°,	54°SE

(g) The plunge-corrected magnetization vectors in (e) were further corrected for the presumed horizontal position of the folded strata, by using the strikes and dips in (f).

The characteristic directions after structural correction given in Table 8.1 are the final values obtained after the two-step correction described in (e) and (g), above.

F.3 Detailed directions of magnetization

Directions after each thermal demagnetization step are listed below for those specimens for which characteristic directions are quoted in Tables 8.1 and 8.4. The listing scheme is the same as described under Appendix B.2. Sites "BB 14 East" and "BB 14 West" correspond to "Bed No. 14 East" and "Bed No. 14 West" of Table 8.4. All directions are before structural correction.

APPENDIX F

DETAILED SPECIMEN DIRECTIONS

SITE: CH4 SPEC#: CH14-C

TEMP	DEC	INC	J(OA/M)	J/JN
20	+ 75.0	+ 85.5	3.46E-4	01.00
100	+116.9	+ 83.1	2.42E-4	00.69
200	+139.2	+ 69.2	1.52E-4	00.43
300	+141.9	+ 44.5	9.03E-5	00.26
350	+139.5	+ 37.6	7.88E-5	00.22
400	+143.5	+ 42.5	4.32E-5	00.12
450	+ 45.5	- 5.8	3.82E-5	00.11
500	+106.3	+ 20.2	1.81E-4	00.52
530	+304.6	+ 68.8	2.96E-4	00.85
560	+202.6	+ 18.3	1.87E-4	00.54
590	+ 94.7	+ 8.6	1.71E-4	00.49
620	+165.0	- 66.5	5.03E-5	00.14

SITE: CH4 SPEC#: CH15-B

20	+100.5	+ 71.0	7.44E-4	01.00
100	+113.4	+ 71.9	5.71E-4	00.76
200	+126.8	+ 61.5	3.76E-4	00.50
300	+132.5	+ 48.1	2.74E-4	00.36
350	+134.9	+ 43.2	2.17E-4	00.29
400	+132.5	+ 46.5	1.59E-4	00.21
450	+138.5	+ 47.3	9.95E-5	00.13
500	+286.6	- 62.0	2.16E-6	00.00
530	+ 29.1	- 36.5	3.97E-5	00.05
560	+ 60.7	+ 1.6	3.40E-5	00.04

SITE: CH4 SPEC#: CH16-B

20	+ 5.5	+ 82.6	1.01E-3	01.00
300	+133.7	+ 57.5	2.56E-4	00.25
350	+133.7	+ 54.7	2.10E-4	00.20
400	+141.7	+ 54.8	1.51E-4	00.14
450	+140.7	+ 75.4	6.73E-5	00.06
500	+250.3	- 27.7	1.51E-4	00.14

SITE: CH4 SPEC#: CH17-A

20	+ 24.6	+ 80.0	1.12E-3	01.00
300	+123.8	+ 56.6	2.37E-4	00.21
350	+123.1	+ 50.9	1.38E-4	00.16
400	+126.7	+ 51.5	1.52E-4	00.13
450	+129.0	+ 73.9	5.83E-5	00.05
500	+ 52.1	+ 34.2	4.53E-5	00.04

APPENDIX F

DETAILED SPECIMEN DIRECTIONS

SITE: CH4 SPEC#: CH18-B

TEMP	DEC	INC	J(A/M)	J/JN
20	+108.9	+ 82.7	3.84E-4	01.00
300	+118.3	+ 47.6	1.20E-4	00.31
350	+121.4	+ 46.0	9.21E-5	00.23
400	+117.5	+ 52.2	5.83E-5	00.15
450	+178.0	+ 62.5	3.26E-5	00.08
500	+260.9	+ 38.8	3.58E-4	00.93

SITE: CH5 SPEC#: CH19-A

20	+ 49.1	+ 82.0	1.30E-3	01.00
100	+ 66.5	+ 82.2	9.39E-4	00.72
200	+116.6	+ 75.1	5.45E-4	00.41
300	+128.8	+ 62.2	3.68E-4	00.28
350	+131.1	+ 55.0	2.83E-4	00.21
400	+132.2	+ 54.9	1.98E-4	00.15
450	+134.1	+ 57.3	1.31E-4	00.10
500	+300.7	- 52.6	2.84E-5	00.02
530	+244.6	- 17.1	4.05E-5	00.03
560	+296.3	- 85.7	5.49E-5	00.04

SITE: CH5 SPEC#: CH20-1

20	+202.7	+ 77.8	1.72E-3	01.00
100	+207.9	+ 71.5	1.47E-3	00.85
200	+207.5	+ 63.5	1.16E-3	00.67
300	+206.8	+ 57.7	9.91E-4	00.57
350	+206.3	+ 55.3	8.57E-4	00.49
400	+209.2	+ 52.6	6.26E-4	00.36
450	+209.7	+ 53.2	4.14E-4	00.23
500	+159.2	+ 15.4	1.11E-5	00.00
530	+132.8	+ 24.4	5.39E-5	00.03
560	+138.6	- 89.6	4.65E-5	00.02

SITE: CH5 SPEC#: CH21-A

20	+ 47.1	+ 73.3	1.15E-3	01.00
300	+ 82.9	+ 44.4	3.64E-4	00.31
350	+ 83.1	+ 42.3	3.19E-4	00.27
400	+ 84.4	+ 53.5	1.49E-4	00.12
450	+ 80.4	+ 52.0	9.81E-5	00.08
500	+217.1	- 60.8	5.59E-5	00.04

APPENDIX F

DETAILED SPECIMEN DIRECTIONS

SITE: CH5 SPEC#: CH22-A

TEMP	DEC	INC	J(R/M)	J/JN
20	+102.7	+ 76.7	2.01E-3	01.00
300	+123.3	+ 52.8	8.58E-4	00.42
350	+122.6	+ 51.1	7.62E-4	00.37
400	+122.3	+ 51.2	6.40E-4	00.31
450	+125.9	+ 55.5	2.54E-4	00.12
500	+ 75.4	+ 30.6	4.80E-5	00.02

SITE: CH5 SPEC#: CH23-B

20	+116.6	+ 74.2	9.90E-4	01.00
300	+133.1	+ 37.7	3.89E-4	00.39
350	+131.7	+ 36.3	3.05E-4	00.30
400	+135.4	+ 40.0	2.10E-4	00.21
450	+121.8	+ 23.7	9.39E-5	00.09
500	+200.6	- 19.5	6.65E-5	00.06

SITE: CH6 SPEC#: C 24-B

20	+104.3	+ 77.1	5.93E-4	01.00
100	+103.0	+ 76.0	4.97E-4	00.82
200	+109.2	+ 72.9	3.37E-4	00.56
300	+119.6	+ 73.7	2.24E-4	00.37
350	+119.8	+ 78.1	1.46E-4	00.24
400	+112.3	+ 81.6	9.04E-5	00.15
450	+120.8	+ 80.8	4.97E-5	00.08
500	+165.2	+ 71.5	3.36E-5	00.05
530	+355.8	+ 50.5	2.51E-5	00.04
560	+353.8	+ 1.8	7.71E-5	00.13

SITE: CH6 SPEC#: CH25-B

20	+323.9	+ 86.9	9.29E-4	01.00
100	+358.3	+ 79.1	6.16E-4	00.66
200	+357.0	+ 82.7	3.49E-4	00.37
300	+237.7	+ 88.4	1.94E-4	00.20
350	+204.9	+ 88.1	1.53E-4	00.16
400	+203.1	+ 86.1	1.12E-4	00.12
450	+ 2.3	+ 57.2	2.90E-5	00.03
500	+ 14.3	+ 2.4	3.73E-5	00.04
530	+123.6	- 72.5	6.32E-5	00.06
560	+319.7	+ 10.3	5.62E-5	00.06
590	+ 96.0	+ 39.8	2.69E-5	00.02
620	+119.3	- 23.0	9.25E-5	00.09

APPENDIX F

DETAILED SPECIMEN DIRECTIONS

SITE: CH6 SPEC#: CH26-B

TEMP	DEC	INC	J(R/M)	J/JN
20	+332.9	+ 79.8	1.30E-3	01.00
300	+338.1	+ 89.7	2.95E-4	00.22
350	+137.5	+ 88.2	2.18E-4	00.16
400	+276.1	+ 87.5	1.17E-4	00.08
450	+331.8	+ 72.5	7.09E-5	00.05
500	+ 10.0	- .6	3.05E-5	00.02

SITE: CH6 SPEC#: CH27-B

20	+12.6	+ 87.5	9.02E-4	01.00
300	+173.6	+ 65.1	2.85E-4	00.31
350	+169.3	+ 64.7	2.21E-4	00.24
400	+174.1	+ 70.5	1.20E-4	00.13
450	+302.4	+ 74.4	4.74E-5	00.05
500	+241.3	+ 76.8	6.69E-5	00.07

SITE: CH6 SPEC#: CH28-1

20	+329.9	+ 83.8	4.40E-4	01.00
300	+285.2	+ 79.1	1.69E-4	00.38
350	+288.1	+ 75.6	1.30E-4	00.29
400	+284.7	+ 72.4	9.45E-5	00.21
450	+296.5	+ 63.3	4.96E-5	00.11
500	+287.8	+ 62.6	3.30E-5	00.07

SITE: CH7 SPEC#: CH29-1

20	+ 34.6	+ 74.3	7.35E-4	01.00
100	+ 29.0	+ 71.6	5.62E-4	00.76
200	+ 28.7	+ 73.7	3.89E-4	00.52
300	+ 27.7	+ 79.3	2.00E-4	00.27
350	+ 23.8	+ 75.8	1.52E-4	00.20
400	+ 17.0	+ 76.0	1.19E-4	00.16
450	+346.3	+ 82.4	6.43E-5	00.08
500	+ 18.5	+ 75.3	3.56E-5	00.04
530	+165.1	- 14.0	3.26E-5	00.04
560	+107.8	+ 88.9	1.76E-4	00.23
590	+333.5	- 15.7	1.80E-4	00.24
620	+ 37.6	+ 68.2	1.88E-4	00.25

APPENDIX F

DETAILED SPECIMEN DIRECTIONS

SITE: CH7 SPEC#: CH30-1

TEMP	DEC	INC	J(A/M)	J/JN
20	+351.7	+ 76.5	9.97E-4	01.00
100	+340.2	+ 71.5	8.27E-4	00.92
200	+324.3	+ 70.6	6.46E-4	00.64
300	+316.9	+ 68.5	4.77E-4	00.47
350	+315.5	+ 66.5	4.35E-4	00.43
400	+314.5	+ 66.0	4.05E-4	00.40
450	+314.9	+ 66.5	1.76E-4	00.17
500	+316.5	+ 77.1	9.34E-5	00.08
530	+296.0	- 50.3	8.62E-5	00.08
560	+313.7	- 29.6	4.62E-5	00.04
590	+307.6	- 5.0	1.46E-4	00.14
620	+310.2	+ 32.4	4.65E-5	00.04

SITE: GH7 SPEC#: CH31-B

20	+342.6	+ 68.2	1.03E-3	01.00
300	+309.3	+ 68.1	5.06E-4	00.49
350	+312.6	+ 67.7	4.57E-4	00.44
400	+316.9	+ 66.4	3.75E-4	00.36
450	+321.5	+ 64.0	1.67E-4	00.16
500	+279.6	+ 63.7	6.31E-5	00.06
530	+339.1	+ 44.2	4.08E-5	00.03
560	+241.1	- 56.8	3.50E-5	00.03

SITE: CH7 SPEC#: CH32-1

20	+340.3	+ 73.6	9.69E-4	01.00
300	+319.3	+ 83.8	3.81E-4	00.39
350	+313.0	+ 83.5	2.97E-4	00.30
400	+309.4	+ 83.0	2.31E-4	00.23
450	+327.6	+ 78.6	1.12E-4	00.11
500	+337.7	+ 78.7	6.69E-5	00.06

SITE: CH7 SPEC#: CH33-A

20	+312.0	+ 72.1	1.17E-3	01.00
300	+279.6	+ 69.7	5.27E-4	00.44
350	+277.5	+ 68.3	4.18E-4	00.35
400	+272.4	+ 65.5	3.45E-4	00.29
450	+278.0	+ 69.5	1.63E-4	00.13
500	+292.1	+ 70.3	7.32E-5	00.06

APPENDIX F

DETAILED SPECIMEN DIRECTIONS

SITE: CH12 SPEC#: CH54-A

TEMP	DEC	INC	J(A/M)	J/JN
20	+ 82.0	+ 74.8	2.90E-4	01.00
100	+ 92.7	+ 75.5	2.45E-4	00.84
200	+ 96.9	+ 75.1	1.97E-4	00.67
300	+ 89.4	+ 76.0	8.40E-5	00.28
350	+ 88.6	+ 71.1	6.24E-5	00.21
400	+ 65.6	+ 70.9	2.68E-5	00.09
450	+ 79.2	+ 68.3	1.96E-5	00.06
500	+337.7	+ 54.0	1.46E-5	00.05
530	+333.1	+ 58.8	7.65E-5	00.26
560	+ 9.1	+ 84.4	7.03E-5	00.24
590	+ 37.9	- 40.4	1.78E-4	00.61
620	+304.6	- 68.9	7.15E-5	00.24

SITE: CH12 SPEC#: CH55-A

20	+ 56.4	+ 67.3	2.07E-4	01.00
100	+ 70.9	+ 67.3	1.53E-4	00.74
200	+ 73.9	+ 68.4	1.01E-4	00.48
300	+ 74.3	+ 57.4	5.20E-5	00.25
350	+ 77.4	+ 49.9	4.13E-5	00.19
400	+ 83.2	+ 37.4	2.81E-5	00.13
450	+ 70.0	+ 33.8	3.73E-5	00.18
500	+155.1	+ 40.0	2.90E-5	00.14
530	+286.5	- 6.3	6.78E-5	00.32
560	+328.1	+ 80.0	1.52E-5	00.07
590	+248.4	- 55.1	7.17E-5	00.34
620	+ 86.6	- 32.1	3.26E-5	00.15

SITE: CH12 SPEC#: CH58-B

20	+ 2.7	+ 71.5	2.00E-4	01.00
300	+ .1	+ 72.8	8.90E-5	00.44
350	+359.1	+ 68.0	5.09E-5	00.25
400	+ 1.3	+ 58.1	3.06E-5	00.15
450	+ 18.3	+ 49.6	3.25E-5	00.16
500	+ 63.0	+ 26.6	6.14E-5	00.30

APPENDIX F

DETAILED SPECIMEN DIRECTIONS

SITE: BB14 EAST SPEC#: C1-A

TEMP	DEC	INC	J(A/M)	J/JN
20	+ 50.8	+ 83.2	7.02E-5	01.00
100	+ 46.6	+ 75.5	6.36E-5	00.90
200	+ 49.2	+ 76.1	4.64E-5	00.66
300	+ 63.1	+ 66.5	2.96E-5	00.42
350	+ 48.3	+ 46.9	1.56E-5	00.22
400	+ 36.3	+ 48.2	1.40E-5	00.19
450	+ 37.9	+ 49.0	9.66E-6	00.13
500	+ 48.1	+ 55.7	6.70E-6	00.09
530	+344.7	+ 60.4	3.60E-6	00.05
560	+339.5	- 5.9	3.03E-6	00.04
590	+216.7	+ 30.5	2.23E-6	00.03

SITE: BB14 EAST SPEC#: C3-B

20	+ 18.7	+ 72.0	1.84E-4	01.00
100	+ .4	+ 76.8	1.24E-4	00.67
200	+357.3	+ 76.2	8.94E-5	00.48
300	+ 3.7	+ 73.8	5.61E-5	00.30
350	+331.0	+ 73.8	2.99E-5	00.16
400	+346.4	+ 73.2	2.28E-5	00.12
450	+338.2	+ 51.1	1.29E-5	00.07
500	+311.9	+ 3.8	9.80E-6	00.05
530	+352.4	+ 6.3	1.70E-5	00.09
560	+ 7.3	- 16.4	1.10E-5	00.05
590	+334.4	- 2.6	2.86E-5	00.15

SITE: BB14 EAST SPEC#: C4-A

20	+ 48.5	+ 63.7	7.21E-4	01.00
100	+ 43.5	+ 60.8	5.50E-4	00.76
200	+ 49.0	+ 56.7	4.19E-4	00.58
300	+ 51.8	+ 54.1	2.72E-4	00.37
350	+ 48.8	+ 60.2	1.09E-4	00.15
400	+ 35.0	+ 67.6	8.21E-5	00.11
450	+ 58.2	+ 54.3	2.87E-5	00.03
500	+270.8	+ 64.6	1.33E-5	00.01
530	+253.1	- 24.4	9.57E-6	00.01
560	+182.1	- 83.6	2.30E-5	00.03
590	+316.4	- 30.3	3.02E-5	00.04

APPENDIX F

DETAILED SPECIMEN DIRECTIONS.

SITE: BB14 EAST SPEC#: C10-B

TEMP	DEC	INC	J(A/M)	J/JN
20	+145.4	+ 81.8	2.81E-4	01.00
300	+135.5	+ 79.9	1.09E-4	00.38
350	+140.7	+ 80.9	9.52E-5	00.33
400	+117.2	+ 77.9	5.85E-5	00.20
450	+136.1	+ 78.6	3.66E-5	00.13
500	+164.1	+ 79.0	2.85E-5	00.10
530	+ 79.8	+ 61.9	2.22E-5	00.07

SITE: BB14 EAST SPEC#: C11-A

20	+ 43.5	+ 62.6	1.18E-4	01.00
300	+ 45.0	+ 21.5	5.33E-5	00.45
350	+ 40.4	+ 23.7	4.69E-5	00.39
400	+ 47.1	+ 5.4	4.73E-5	00.40
450	+ 31.7	+ 14.7	3.11E-5	00.26
500	+ 35.9	+ 1.6	3.67E-5	00.31
530	+ 43.1	+ 6.3	3.48E-5	00.29

SITE: BB14 EAST SPEC#: C14-A

20	+ 35.0	+ 54.9	1.23E-4	01.00
300	+ 41.8	+ 58.2	3.54E-5	00.28
350	+ 52.2	+ 65.3	2.52E-5	00.20
400	+ 27.2	+ 49.8	1.79E-5	00.14
450	+ 27.8	+ 59.0	1.92E-5	00.15
500	+ .9	+ 15.6	2.97E-5	00.24
530	+ 19.2	+ 62.9	9.52E-6	00.07

SITE: BB14 EAST SPEC#: C15

20	+ 15.4	+ 70.4	2.96E-4	01.00
300	+ 8.4	+ 65.8	9.89E-5	00.33
350	+ 7.8	+ 66.9	7.33E-5	00.24
400	+ 23.1	+ 67.3	3.01E-5	00.10
450	+ 33.6	+ 58.4	2.77E-5	00.09
500	+ 19.0	+ 47.8	2.58E-5	00.08
530	+342.3	+ 44.2	9.56E-6	00.03

APPENDIX F

DETAILED SPECIMEN DIRECTIONS

SITE: BB14 EAST SPEC#: C16-1

TEMP	DEC	INC	J(A/M)	J/JN
20	+107.0	+ 77.4	6.71E-5	01.00
300	+ 74.5	+ 73.0	2.01E-5	00.41
350	+131.4	+ 73.0	1.92E-5	00.29
400	+ 72.8	+ 66.9	1.82E-5	00.27
450	+121.8	+ 76.3	1.36E-5	00.20
500	+117.1	+ 48.6	1.07E-5	00.15
530	+ 64.1	+ 40.9	5.34E-6	00.07

SITE: BB14 EAST SPEC#: C17-A

20	+ 19.3	+ 54.5	1.20E-4	01.00
300	+ 24.3	+ 51.1	4.92E-5	00.40
350	+ 20.6	+ 56.4	3.95E-5	00.32
400	+ 20.1	+ 56.2	2.94E-5	00.24
450	+ 37.7	+ 48.2	2.08E-5	00.17
500	+333.0	- 35.9	5.46E-5	00.45
530	+ 24.8	+ 43.7	5.41E-5	00.45

SITE: BB14 EAST SPEC#: C18-B

20	+268.5	- 68.7	1.75E-3	01.00
300	+268.2	- 69.9	1.18E-3	00.67
350	+268.3	- 69.4	9.54E-4	00.54
400	+266.0	- 70.0	6.65E-4	00.38
450	+265.0	- 69.3	5.83E-4	00.33
500	+263.9	- 68.3	2.92E-4	00.16
530	+247.7	- 71.2	7.42E-5	00.04

SITE: BB14 EAST SPEC#: C19-A

20	+254.6	- 68.3	1.45E-4	01.00
300	+212.2	- 75.9	8.50E-5	00.58
350	+205.8	- 81.2	5.80E-5	00.40
400	+147.6	- 80.2	3.39E-5	00.23
450	+153.3	- 77.1	2.43E-5	00.16
500	+ 98.2	- 45.9	9.95E-6	00.06
530	+ 76.8	- 9.4	1.68E-5	00.11

APPENDIX F

DETAILED SPECIMEN DIRECTIONS

SITE: BB14 EAST SPEC#: C20-1

TEMP	DEC	INC	J(R/M)	J/JN
20	+348.3	- 23.6	2.16E-4	01.00
300	+341.2	- 27.2	1.13E-4	00.52
350	+346.3	- 28.4	6.77E-5	00.31
400	+354.6	- 21.3	3.89E-5	00.17
450	+355.0	- 12.6	2.42E-5	00.11
500	+358.5	- 10.7	1.90E-5	00.08
530	+ 98.0	+ 16.2	5.91E-5	00.27

SITE: BB14 WEST SPEC#: B1-1

20	+269.8	+ 24.8	5.35E-4	01.00
100	+267.5	+ 10.4	5.52E-4	01.03
200	+262.5	- 7.3	5.33E-4	00.99
300	+261.0	- 12.2	5.31E-4	00.99
350	+259.8	- 14.5	4.90E-4	00.91
400	+260.7	- 15.4	3.94E-4	00.73
450	+262.5	- 16.7	2.40E-4	00.44
500	+264.3	- 50.7	4.73E-5	00.08
530	+282.1	+ 29.8	2.18E-5	00.04
560	+290.8	+ 83.8	3.79E-5	00.07
590	+285.9	+ 34.8	4.73E-5	00.08

SITE: BB14 WEST SPEC#: B6-2

20	+ 32.5	+ 78.7	5.68E-4	01.00
300	+ 35.2	+ 77.9	1.30E-4	00.22
350	+ 56.0	+ 79.2	9.78E-5	00.17
400	+ 36.5	+ 84.5	4.82E-5	00.08
450	+359.4	+ 70.2	3.67E-5	00.06
500	+ 84.3	+ 49.8	2.24E-5	00.03

SITE: BB14 WEST SPEC#: B7-A

20	+148.9	+ 88.3	3.33E-4	01.00
300	+221.6	+ 86.4	1.27E-4	00.38
350	+232.4	+ 88.0	1.04E-4	00.31
400	+142.6	+ 86.2	5.21E-5	00.15
450	+129.6	+ 83.4	3.71E-5	00.11
500	+148.9	+ 77.9	2.44E-5	00.07

APPENDIX F

DETAILED SPECIMEN DIRECTIONS

SITE: BB14 WEST SPEC#: B8-2

TEMP	DEC	INC	J(A/M)	J/JN
20	+ 88.8	+ 80.2	3.35E-4	01.00
300	+ 90.8	+ 80.5	1.38E-4	00.41
350	+ 85.9	+ 80.8	1.17E-4	00.34
400	+ 75.3	+ 83.1	5.66E-5	00.16
450	+ 84.3	+ 76.8	3.97E-5	00.11
500	+ 41.4	+ 82.8	3.54E-5	00.10

SITE: BB14 WEST SPEC#: B9-2

20	+359.9	+ 75.6	5.68E-4	01.00
300	+299.2	+ 82.5	1.46E-4	00.25
350	+282.2	+ 84.0	1.15E-4	00.20
400	+332.2	+ 76.2	6.26E-5	00.11
450	+ 29.8	+ 62.3	5.70E-5	00.10
500	+350.0	- 3.5	3.27E-5	00.05
530	+336.4	+ 66.9	1.18E-4	00.20
560	+287.2	+ 11.6	1.91E-4	00.33

SITE: BB14 WEST SPEC#: B10-2

20	+ 56.7	+ 57.4	2.30E-4	01.00
300	+ 54.8	+ 18.0	4.96E-5	00.21
350	+ 70.1	+ 6.7	5.34E-5	00.23
400	+ 77.3	- 3.5	4.47E-5	00.19
450	+ 71.5	- 3.1	2.18E-5	00.09
500	+ 42.7	- 3.8	2.71E-5	00.11
530	+349.9	+ 2.6	3.42E-5	00.14
560	+350.5	- 13.8	7.47E-5	00.32

SITE: BB14 WEST SPEC#: B12-A

20	+290.8	+ 79.0	3.79E-4	01.00
300	+271.1	+ 77.6	2.21E-4	00.58
350	+276.3	+ 74.7	1.68E-4	00.44
400	+269.3	+ 72.9	1.21E-4	00.31
450	+271.2	+ 71.5	8.55E-5	00.22
500	+252.7	+ 75.7	7.31E-5	00.19
530	+257.7	+ 80.0	5.57E-5	00.14
560	+229.3	+ 54.7	1.41E-5	00.03

APPENDIX F

DETAILED SPECIMEN DIRECTIONS

SITE: BB14 WEST SPEC#: B13-A

TEMP	DEC	INC	J(R/M)	J/JN
20	+287.8	+ 61.1	4.84E-4	01.00
300	+287.0	+ 60.7	1.58E-4	00.32
350	+291.2	+ 68.0	9.78E-5	00.20
400	+299.3	+ 65.3	7.95E-5	00.16
450	+302.1	+ 62.5	5.85E-5	00.12
500	+310.0	+ 68.5	3.47E-5	00.07
530	+308.3	+ 12.6	2.41E-5	00.04
560	+284.8	- 55.6	2.19E-5	00.04

SITE: BB14 WEST SPEC#: B14-2

20	+155.2	+ 62.9	4.95E-5	00.00
300	+149.4	- 18.4	1.26E-5	00.25
350	+147.9	- 2.5	1.84E-5	00.37
400	+144.8	- 8.5	1.29E-5	00.26
450	+175.8	- 1.6	1.90E-5	00.38
500	+294.9	- 9.4	3.67E-6	00.07

SITE: BB14 WEST SPEC#: B15-A

20	+287.8	+ 72.2	9.22E-4	01.00
300	+283.1	+ 72.3	3.41E-4	00.36
350	+271.4	+ 70.6	1.96E-4	00.21
400	+269.9	+ 72.5	1.20E-4	00.13
450	+267.9	+ 65.2	8.95E-5	00.09
500	+296.2	+ 78.0	6.13E-5	00.06
530	+289.1	+ 62.1	4.66E-5	00.05
560	+260.0	+ 73.9	3.18E-5	00.03

SITE: BB14 WEST SPEC#: B16-1

20	+273.3	- 69.4	7.08E-4	01.00
300	+285.9	- 78.2	3.95E-4	00.55
350	+304.7	- 82.7	2.66E-4	00.37
400	+331.2	- 81.1	1.36E-4	00.19
450	+320.0	- 80.8	9.48E-5	00.13
500	+302.0	- 77.4	6.76E-5	00.09
530	+316.6	- 76.1	5.87E-5	00.08
560	+307.0	- 72.3	4.45E-5	00.06

APPENDIX F

DETAILED SPECIMEN DIRECTIONS

SITE: BB14 WEST SPEC#: B17-A

TEMP	DEC	INC	J(A/M)	J/JN
20	+356.4	+ 84.2	6.71E-4	01.00
300	+ 11.6	+ 81.8	2.65E-4	00.39
350	+ 29.4	+ 78.3	1.92E-4	00.28
400	+ 49.1	+ 78.7	8.52E-5	00.12
450	+ 49.6	+ 81.4	5.68E-5	00.08
500	+ 15.5	+ 77.9	5.00E-5	00.07
530	+ 5.2	+ 71.5	4.29E-5	00.06
560	+215.0	+ 63.8	6.63E-5	00.09

SITE: BB14 WEST SPEC#: B18-A

20	+297.7	+ 80.4	5.50E-4	01.00
300	+300.6	+ 85.1	3.02E-4	00.54
350	+296.1	+ 79.4	2.07E-4	00.37
400	+320.6	+ 81.6	1.16E-4	00.21
450	+303.2	+ 88.0	9.29E-5	00.16
500	+258.5	+ 82.5	6.89E-5	00.12
530	+270.7	+ 80.3	5.16E-5	00.09
560	+263.2	+ 74.0	3.06E-5	00.05

SITE: BB14 WEST SPEC#: B20-1

20	+ 37.1	+ 63.1	5.61E-4	01.00
300	+ 43.3	+ 55.0	2.33E-4	00.41
350	+ 43.5	+ 53.4	1.15E-4	00.20
400	+ 50.0	+ 53.2	8.07E-5	00.14
450	+ 36.7	+ 57.7	6.19E-5	00.11
500	+ 26.2	+ 45.2	5.12E-5	00.09
530	+ 30.6	+ 53.3	3.32E-5	00.05
560	+ 27.1	- 17.9	1.41E-5	00.02

